SEARCHING FOR ORDER IN BODY CLOCKS

Circadian Rhythms and Redox Balance

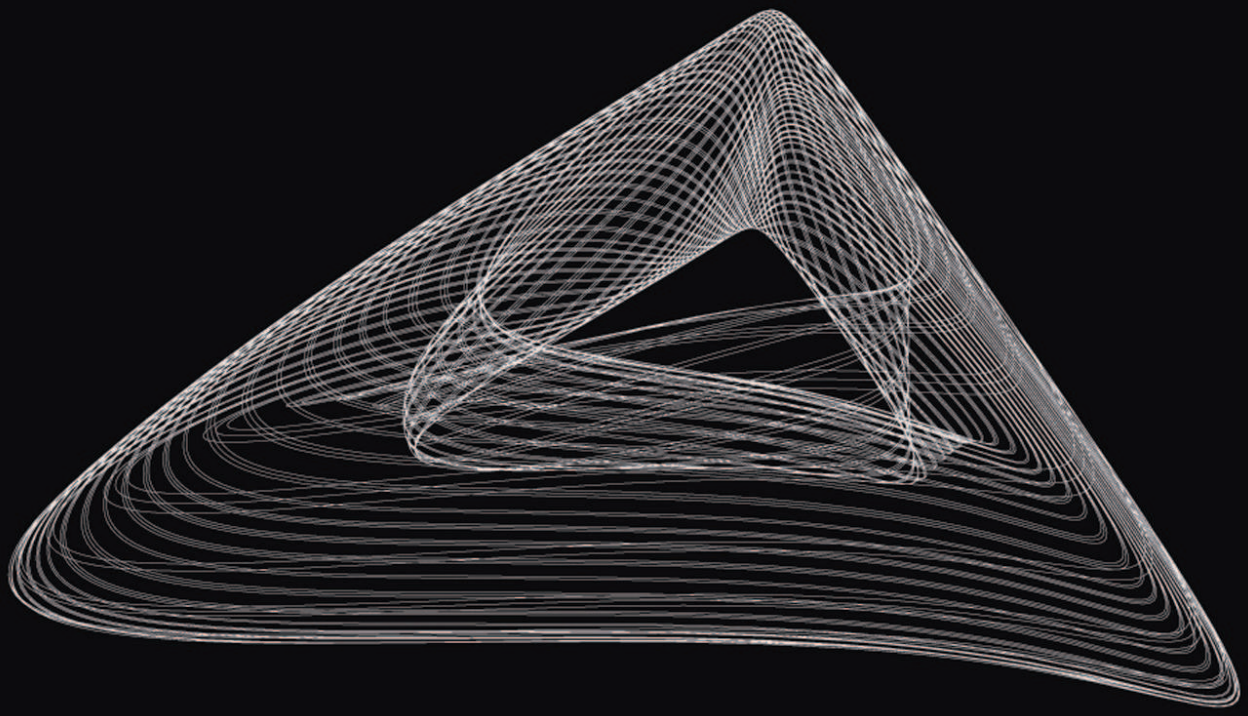

Marta del Olmo Somolinos

λογος

Searching for Order in Body Clocks

Circadian Rhythms and Redox Balance

Marta del Olmo Somolinos

Logos Verlag Berlin

Bibliographic information published by Die Deutsche Bibliothek

Die Deutsche Bibliothek lists this publication in the Deutsche Nationalbibliografie; detailed bibliographic data is available in the Internet at http://dnb.d-nb.de.

Cover design by: Marta del Olmo Somolinos and Aina Akua Casals Frempong. It illustrates a network of desynchronized feedback loops within a mammalian mathematical model of the circadian clockwork. It shows how beauty can arise even in the darkest of places, and how complexity can generate richness in unexpected ways.

ISBN 978-3-8325-5406-4

Logos Verlag Berlin GmbH
Georg-Knorr-Str. 4, Geb. 10,
12681 Berlin
Tel.: +49 (0)30 / 42 85 10 90
Fax: +49 (0)30 / 42 85 10 92
http://www.logos-verlag.de

Abstract

Biological timing is a necessity in all living organisms. Mammalian physiology and behavior are organized around the day/night cycle and is regulated by the coordinated action of cell-autonomous circadian clocks that exist throughout the body. Single cell circadian oscillators are organized into tissue networks which are further hierarchically arranged to constitute the mammalian circadian timing system. At the core of the molecular clockwork are multiple coupled transcription-translation feedback loops that generate cell-autonomous and self-sustained circadian rhythms in gene expression to ultimately orchestrate physiology and metabolism. Disruption of circadian timekeeping by genetic or environmental perturbations can lead to metabolic dysregulation. But metabolic regulation is not a mere output of the circadian system. Conversely, nutrient energy and redox levels can signal back to cellular clocks to reinforce circadian rhythmicity and to adapt physiology to temporal tissue-specific needs.

While gene expression cycles are essential for the temporal coordination of normal physiology, evidence suggests that rhythms in metabolism and redox balance are cell-intrinsic phenomena, which regulate gene expression cycles reciprocally, but can persist in their absence. This is illustrated by the discovery of self-autonomous rhythms in peroxiredoxin oxidation in red blood cells, which do not have nuclei and thus cannot oscillate according to the transcription-translation feedback loop paradigm. Although increasing evidence supporting the crosstalk of metabolic, redox and transcriptional circadian timing systems has accumulated over the last years, the mechanistic details that mediate this interaction remain to be elucidated.

Here, we provide additional evidence for the role of metabolism in regulating the core clock. We identified genes involved in energetic and redox pathways which are essential for the robustness of cellular timekeepers to temperature fluctuations. We developed the first computational model for circadian redox oscillations to understand how cellular redox balance might adjust circadian rates in response to perturbations, and thus convey timing information to the core transcriptional oscillator. We show that coupling our novel redox model with models of the transcriptional clockwork results in 1:1 synchronization, supporting robustness of the models. Understanding how redox and circadian cycles are mutually coupled together will be of great importance to gain insights into how basic timekeeping mechanisms are integrated into cellular physiology. Such knowledge might highlight new ways by which functional consequences of circadian timekeeping can be explored in the context of human health and disease.

Zusammenfassung

Die zeitliche Koordination biologischer Prozesse ist eine Grundvoraussetzung für alle lebenden Organismen. Die Rhythmik physiologischer Vorgänge und des Verhalten von Säugetieren folgt Licht/Dunkel-Rhythmen und wird durch die Koordination zellautonomer circadianer Uhren gesteuert. Dazu sind circadiane Oszillatoren einzelner Zellen in Gewebenetzwerken organisiert, die in hierarchischer Interaktion wiederum das circadiane Zeitmesssystem in Säugetieren bilden. Im Kern stehen hierbei verschiedene transkriptionelle Rückkopplungsschleifen, die zellautonome und selbsterhaltende circadiane Genexpressionsrhythmen generieren, um letztlich physiologische Prozesse, wie den Metabolismus, zyklisch zu regulieren. Störungen der inneren Uhr durch äussere Einflusse oder durch genetische Defekte können zu metabolischer Dysregulation führen. Weiterhin, werden metabolische Prozesse nicht nur durch die circadiane Uhr gesteuert, sondern können auch auf die zellulären Uhren rückwirken und damit circadiane Rhythmen verfestigen, sowie eine physiologische Adaptation an gewebespezifische Anforderungen ermöglichen.

Während rhythmische Genexpressionszyklen weithin als essenziell für die zeitliche Kontrolle physiologischer Prozesse erachtet werden, gibt es Hinweise darauf, dass Stoffwechsel- und Redoxoszillationen zwar reziprok mit Genexpressionszyklen interagieren, aber unabhängig von der circadianen Genexpression aufrecht erhalten werden können. Dies wurde insbesondere durch die Entdeckung selbsterhaltender circadianer Rhythmen der Peroxiredoxin-Oxidation in roten Blutkörperchen verdeutlicht, welche aufgrund des fehlenden Zellkerns keine transkriptionellen Rückkopplungsschleifen aufweisen. Jedoch sind mechanistische Zusammenhänge der Wechselwirkungen zwischen metabolischen und transkriptionellen Rhythmen bisher und trotz dieser jüngsten Entdeckungen weitgehend unverstanden.

In dieser Arbeit präsentieren wir Ergebnisse, die zeigen, dass der Stoffwechsel den Kernmechanismus der zellulären inneren Uhr direkt beeinflusst. Wir haben metabolisch- und redox-relevante Gene identifiziert, die für die Aufrechterhaltung robuster circadianer Oszillationen bei Temperaturfluktuationen essenziell sind. Des Weiteren präsentieren wir das erste mathematische Modell für circadiane Redoxoszillationen auf dessen Grundlage wir die Wechselwirkungen zwischen Redoxgleichgewicht und innerer Uhr untersuchen. Wir zeigen, dass das von uns entwickelte Redoxmodell mit Modellsimulationen transkriptioneller Rhythmen im 1:1 Verhältnis synchronisiert werden kann, wodurch die Robustheit der Rhythmen verstärkt wird. Erkenntnisse über Interaktionen metabolischer und circadianer Oszillationen leisten einen wichtigen Beitrag zum Verständnis der Integration grundlegender biologischer Rhythmen in die zelluläre Physiologie, insbesondere wichtiger Stoffwechselprozesse. Weiterhin, tragen diese Erkenntnisse letztlich dazu bei, die Entwicklung metabolischer Krankheiten besser zu verstehen und die Gesundheit des Organismus zu erhalten.

A la familia que no he elegido,
pero que sin duda habría.
A mis padres, Cristina y Alfonso,
por guiarme,
y enseñarme el valor de la ciencia.

Y a la familia que sí he elegido.
A, Anna, Irene, Carla,
por estar cuando hay arco iris
pero también bajo la lluvia.
Y a Gianmarco,
por entrenarme y hacer *fácil*
el rudo oficio de la distancia.

Table of Contents

Abbreviations

A Activation switch

ACTH Adrenocorticotropic hormone

ADP Adenosine diphosphate

AMP Adenosine monophosphate

AMPK AMP-activated protein kinase

Aqp Aquaporin

ASPS Advanced sleep phase syndrome

ATP Adenosine triphosphate

a.u. Arbitrary unit

bHLH Basic helix-loop-helix

BMAL1 Brain and Muscle ARNT-Like 1

CK1δ Casein kinase 1δ

CK1ϵ Casein kinase 1ϵ

CLOCK Circadian Locomotor Output Cycles Kaput

CO Carbon monoxide

CO_2 Carbon dioxide

CRE cAMP response element

CRY1 Cryptochrome 1

CRY2 Cryptochrome 2

CSP-1 Conidial separation-1

Cys Cysteine

DNA Deoxyribonucleic acid

DSPS Delayed sleep phase syndrome

dsRNA Double stranded RNA

FASPS Familial advanced sleep phase syndrome

FDR False discovery rate

FEO Food entrainable oscillator

FRH FRQ-interacting RNA helicase

FRQ Frequency

H_2O_2 Hydrogen peroxide

HAT Histone acetyl transferase

I/L Inactivation-Leakage switch

ipRGC Intrinsically photosensitive retinal ganglion cell

LD Light-dark cycle

LL Constant light

luc Luciferase

MAPK Mitogen-activated protein kinase

MASCO Methamphetamine-sensitive circadian oscillator

MCTQ Munich chronotype questionnaire

miRNA Micro RNA

mRNA Messenger RNA

MSH Melanocyte-stimulating hormone

NAD Nicotinamide adenine dinucleotide

NADP Nicotinamide adenine dinucleotide phosphate

NAMPT Nicotinamide phosphorybosyltransferase

ODE Ordinary differential equation

PAS Per Arnt Single-minded

PER1 Period 1

PER2 Period 2

PER3 Period 3

PPAR Peroxisome proliferator-activated receptors

PRC Phase-response curve

PRX Peroxiredoxin

RBC Red blood cell

RNA Ribonucleic acid

RNAi RNA interference

RORE Retinoic acid-related orphan receptor response element

ROS Reactive oxygen species

RT-PCR Real time polymerase chain reaction

SCN Suprachiasmatic nucleus

SD Standard deviation

shRNA Short-hairpin RNA

siRNA Small interfering RNA

SIRT1 Sirtuin 1

SRE Serum response element

Srx Sulfiredoxin

Trx Thioredoxin

TTFL Transcription-translation feedback loop

U-2 OS Human bone osteosarcoma cells

UV Ultraviolet

WC-1 White collar 1

WC-2 White collar 2

WCC White collar complex

Symbols

A Amplitude

A_1 Active (reduced) Prx3 (Prx3-SH)

A_2 **(or A)** Active (but partially oxidized) Prx3 (Prx3-SOH)

b Damping rate

D_1 Danger 1 (mitochondrial H_2O_2)

D_2 Danger 2 (cytosolic H_2O_2)

F Zeitgeber amplitude (or strength)

I Inactive Prx3 (Prx3-SO_2H)

Q_{10} Temperature coefficient

R Rescuer (mitochondrial Srx)

S Cytosolic Srx

ϵ Twist

ϕ Intrinsic phase

Φ Zeitgeber phase

Ψ Phase of entrainment

λ Amplitude relaxation rate

τ Intrinsic period

T Zeitgeber period

"That's not right! That's not even wrong!"

Wolfgang Pauli

Charité Campus Mitte, Berlin

:

1

Circadian Clocks: An Overview

At the heart of our universe is a steady, insistent beat. The sound of cycles in sync. It pervades nature at every scale, from the nucleus to the cosmos. Even our bodies are symphonies of rhythm.

– Steven Strogatz, Sync: How order emerges from chaos in the universe, nature, and daily life

Chronobiology is concerned with the timing of biological events in individual organisms, especially repetitive or cyclical phenomena. The mechanisms underlying the timekeeping of biological systems, as well as the potential consequences of their failure, are among the issues addressed in this field. In its broadest sense, chronobiology includes all research areas focusing on biological timing, including high-frequency cycles (e.g., hormone secretion occurring in distinct pulses throughout the day), daily cycles (e.g., activity and rest cycles), and monthly or annual cycles (e.g., reproductive cycles in some species). Among these interrelated areas of chronobiology, the work in this PhD thesis focuses on one frequency domain: the daily cycles known as circadian rhythms. Although virtually all life forms including bacteria, fungi, plants, insects, fish, mice and humans, exhibit circadian rhythms, this thesis primarily focuses on the mammalian system. Other organisms are discussed in cases in which they have contributed to the understanding of the mammalian system, particularly in studies of the molecular genetic makeup of the timekeeping system.

One does not have to look at many living organisms before noticing that a lot of their behavior and physiology is temporally organized in periodic patterns. And perhaps we should not be too surprised by the relationship between organisms and the daily light-dark cycle. Life on Earth began some 3 billion years ago, and it evolved under cyclic light-dark conditions due to our planet's rotation. This means that there have

been about a trillion dawns and dusks, and such predictable daily rhythms have exposed nearly all living beings to the constant repetition of light and dark. Correspondingly, the behavioral physiology of most organisms has adapted to such daily oscillations. But rhythmicity in behavior and physiology is not a mere response to the 24 h changes in the physical environment imposed by the Earth turning around its axis but, instead, arises from an exquisitely accurate internal timekeeping system within the organism, that times daily events ranging from sleep and wakefulness in humans to photosynthesis in plants. This timekeeping system or biological clock allows the organism to anticipate and prepare for the changes in the physical environment that are associated with day and night, thereby ensuring that the organism does "the right thing" at the right time of the day. The biological clock also provides internal temporal organization and ensures that internal changes take place in coordination with one another.

The evolutionary "legacy" of internal time and circadian organization across species, including humans, has stimulated further thoughts on integrated circadian physiology for individual and public health. What effect do abrupt changes, such as making the night into day, and the widely-available man-made light since the industrialization, have on our ancient health-promoting systems? How is health affected by conflicts between rhythmic internal and external phenomena? Because often modern society forces us to live against our internal rhythm (jet lag, shift work, social responsibilities, etc.), medical implications of circadian disruption are gaining public recognition. Chronobiology has evolved into a very interdisciplinary research field, interacting with other fields such as medicine (sleep medicine, geriatrics, endocrinology, space medicine), sociology, ecology, or applied mathematics, among others.

1.1 A Chronology of Chronobiology

Already in the 18$^{\text{th}}$ century both Jean-Jacques d'Ortous de Mairan and Carl Linnaeus marked the dawn of chronobiology. In his flower clock, Linnaeus developed a garden plan that would take advantage of several plants that open and close their flowers at particular times of the day to accurately indicate the time [1]. Conversely, De Mairan's observations in 1729 were devoid of light-dark influence. Until his "experiment in a cupboard", the assumption was that leaves in the *Mimosa pudica* plant opened in the day due to sunlight and closed at night due to darkness. But even when he exposed the plant to total darkness, the opening and closing of the leaves continued. Both discoveries suggested that an intrinsic timekeeper must be present for the plants to respond to light/dark and non-light/dark influences. From here, it took more than 200 years before Nathaniel Kleitman and his student Bruce Richardson performed a month-long study and camped out ~30 m underground in Mammoth Cave, a location devoid of natural light, to investigate intrinsic timekeepers in humans [2]. With no environmental time cues, they attempted to switch to a 28 h sleep-wake cycle. Regardless of the day length,

~24 h body temperature rhythms were observed, indicating that the ~24 h rhythmicity is not dependent on the environmental light-dark cycle. In addition, two decades before the Mammoth Cave expedition, one peculiar observation prepared the ground for identifying melatonin – now considered one of the body's key time messengers. Namely, when McCord and Allen fed bovine pineal gland materials to *Rana pipiens* tadpoles, they observed larger viscera and a dose-dependent skin lightening [3]. When investigating vitiligo-like disruptions in skin pigmentation in the 1950s, Lerner *et al.* followed up on these observations to discover that a pineal compound (melatonin) was causing melanin granules in frog melanocytes to aggregate and their skin to lighten [4].

In order to describe falsifiable concepts for interpretable research, it is necessary to agree on unambiguous terminology. And so, for chronobiology to emerge as a discipline by its own, the use of terms had to be solidified. In 1951, the German chronobiologist Jürgen Aschoff termed external or environmental time cues "Zeitgeber" (from German, "time-giver"). These environmental factors were named "synchronizers" by Franz Halberg *et al.* [5] and "entrainment agents" by Colin Pittendrigh and Serge Daan [6] but the three terms are synonymous. In 1959, Halberg proposed the term "circadian" - deriving from Latin: "circa" (about) and "dies" (day) [7]. Ehret, in the early 70s, coined "chronotype" as the behavioral manifestation of the underlying circadian rhythms of a myriad of physical processes, which captures a biological trait regarding when individuals tend to be awake or asleep [8]. Already in 1959, Halberg emphasized what is still true today: "one of the difficulties in correlating the various views and opinions on how periodic biological phenomena are established and maintained lies in the confusion of terms used" [7]. In this regard, the 1960 Cold Spring Harbor Symposium: Biological Clocks, Vol. XXV, proved a landmark event bringing together the modern fathers of chronobiology and laying down laws "for future investigations, and providing stimulating seeds and feeds for the nascent field" [9].

In the last 90 years there was a surge in chronobiological research. An important figure and co-founder of modern chronobiology was Erwin Bünning. In the early 1930s, he demonstrated that periods of biological rhythms are inheritable in bean plants [10]. This finding led to a paradigm shift from the "hourglass hypothesis", describing biological rhythms as entirely driven by external light-dark cycles, towards the "Bünning hypothesis". Bünning proposed that rhythmicity derives from endogenous biological rhythms, which synchronize to photoperiodic stimuli, and that such light stimuli trigger photoinductive responses during certain phases of the circadian cycle [11]. In the 1960s, Aschoff *et al.* followed up the landmark experiment by Kleitman with observation of humans in underground bunkers. Ultimately, they concluded that human volunteers had endogenously generated circadian sleep-wake cycles [12].

Paved by the earlier work, Axelrod was awarded the Nobel Prize in 1970 for his work investigating melatonin and the pineal gland. It had taken Lerner *et al.* no less than 250 000 bovine pineal glands to ultimately characterize the "chemical expression

of darkness" [13]. Axelrod clarified relationships between melatonin, tryptophan, and serotonin, which all follow circadian rhythms [14]. Today we know that melatonin rhythms serve both as a clock and calendar [15].

One new era for research in chronobiology came with the discovery of the first clock mutants in the fruit fly *Drosophila melanogaster* in 1971 and in Syrian hamsters *Mesocricetus auratus* in 1988 [16, 17]. The former led the discovery of the *period* gene [16], which was later isolated and characterized as the first clock gene by Jeffrey Hall, Michael Rosbash, and Michael Young in the 1980s [18], work of which won the Nobel award in 2017 for the discoveries of molecular mechanisms controlling the circadian rhythm. Regarding the latter, Ralph and Menaker discovered that a single gene mutation, called *tau* mutation, affected the circadian period in hamsters [17]. These breakthroughs in understanding the molecular basis of circadian rhythms made chronobiology develop into an independent field of research, based on the concept that single clock genes act as drivers of endogenous biological rhythms [17]. Considerable frustration ensued as researchers sought to isolate the equivalent clock genes in mammals. But finally, in 1994, Vitaterna *et al.* identified the first mammalian clock gene in mice, which they termed "Circadian Locomotor Output Cycles Kaput" (CLOCK), by a mutagenesis screening [19]. Similar to the phenotype of *Drosophila* harboring the *period* mutation, they showed that mutation of the *Clock* gene resulted in aberrant or even arrhythmic behavior of mice [19]. Since the discovery of the *Clock* gene in mice, the list of circadian clock genes identified in mammals has grown in a remarkably short period of time, and the concept of self-sustained transcription-translation feedback loops (TTFL) emerged as the central mechanism of circadian rhythm generation [20]. This introduced a new paradigm in chronobiology, namely that, despite differences in their molecular components, circadian clocks in all organisms use the same molecular design principle for the generation of self-sustained rhythms.

Besides their molecular makeup, entrainment (i.e., adaptation of period and phase) of circadian rhythms to environmental light-dark cycles constitutes a fundamental feature of circadian biology. In the 1960s, Aschoff and Pittendrigh were studying entrainment of circadian clocks to environmental Zeitgebers and they redefined Bünning's concept of synchronization between internal and external rhythms [21]. As Daan described, entrainment is an essential characteristic for circadian clock systems that "requires the sensitivity of endogenous oscillators towards particular environmental cues, as well as insensitivity towards others" [22]. In agreement with words from the Argentinian novelist Julio Cortázar "time is born in the eyes", adaptation to photic information was thought to occur via the eyes and a downstream light-sensitive machinery. In 1972, Moore and Lenn discovered a projection from the retina to the suprachiasmatic nucleus (SCN) of the anterior hypothalamus [23], a region that had previously been shown to be involved in sleep-wake cycle and rhythm regulation [23, 24]. In the same year, the SCN was shown to be essential for hormone, activity and feeding rhythms by a series of SCN-lesioning experiments carried out by Moore, Eichler and Zucker.

These experiments laid the foundations for the recognition of the SCN as the master pacemaker in mammals. In the early 1990s, Ralph and Menaker showed very elegantly that transplantation of *tau* mutant SCN into SCN-ablated wild-type animals inflicted the donor's rhythm on the host; namely, they gained the homozygous mutant's 20 h sleep-wake cycle instead of wild-type 24 h [25]. This confirmed the SCN as the site of the master mammalian circadian pacemaker.

However, research from the last decades has shown that photic cues are not the only signals that can entrain endogenous clocks and, since Aschoff's and Pittendrigh's initial studies, a number of photic as well as non-photic entrainment studies have been performed. Of particular interest nowadays are conflicting Zeitgeber signals that impinge at the organismic level, which have been associated to pathologies and to disruption of the endogenous circadian clock, but this will be addressed in Section 1.5.

With the increasingly developing techniques of molecular and cell biology of the 1990s and early 2000s, we are now able to track circadian rhythms at the organism, tissue and even single cell level, and we can identify and quantify oscillating transcripts or proteins in cells. A milestone in chronobiology was the finding that almost 10% of all genes are transcribed rhythmically and in a cell-autonomous and tissue-specific manner [26–31]. Moreover, real-time bioluminescence and fluorescence imaging of circadian reporter genes and proteins have helped to show that single cell oscillators exhibit cell-autonomous rhythms and that rhythms persist even when tissues or cells are cultivated *ex vivo* or *in vitro* [32, 33]. The current laboratory techniques have even allowed to discover and propose mechanisms driving circadian clocks that are independent of the TTFL. For example, the circadian clock in cyanobacteria is driven by three proteins, namely KaiA, KaiB and KaiC, that follow cyclic phosphorylation patterns [34]. In 2005, Nakajima *et al.* showed in a series of remarkable experiments that the cyanobacterial clock can be reconstituted in a test tube if the three clock proteins are incubated with ATP [35]. Moreover, in 2011, O'Neill and Reddy showed that ~24 h redox cycles drive circadian rhythms in red blood cells, which do not have a nucleus and thus cannot rely on TTFL rhythms [36]; and that such rhythms are conserved among all kingdoms of life [37]. New questions emerge from these findings: how essential are TTFL components for circadian timekeeping? Are there different models for circadian rhythm generation that evolved differently? How many clocks are there and, can they potentially have conflicting sources of information to sense a single time of day?

Winning the Nobel Prize for circadian biology undoubtedly represented a landmark in the field of chronobiology. But nevertheless, unsolved important question still remain. How is circadian time relayed throughout the day? How are health and disease linked with circadian organization? How can we translate chronobiological insights to fight disease?

1.2 Properties of Circadian Rhythms

De Mairan's observations already illustrate one critical feature of circadian rhythms: their self-sustained nature. Strictly speaking, a diurnal rhythm should not be called circadian until it has been shown to persist under constant environmental conditions and thereby can be distinguished from those rhythms that are simply a response to 24 h environmental changes. Daily rhythms in hormone release, body temperature, blood pressure or sleep-wake cycles can be called circadian processes, because they occur under natural conditions in an organism but also continue to cycle under laboratory conditions devoid of external time-giving cues (Figure 1.1A). Circadian rhythms that are expressed in the absence of any 24 h signals from the external environment (e.g., under constant light or constant darkness) are called free-running. In the same lines, the free-running period of an organism is the period of its inner clock in the absence synchronizing cues from cyclic changes in the environment.

A second characteristic feature of circadian rhythms is that these cycles persist with a free-running period of close to, but not exactly, 24 h [38]. The chronobiology community accepts rhythms with a period of 24±4 h as circadian. Pittendrigh suggested that the slight deviation from a 24 h cycle might provide a means for the internal timekeeping system to be continuously aligned by and aligned to the light-dark (or any other environmental) cycle [39]. This continuous adjustment results in great precision in controlling the timing, or phase, of the expressed rhythms, and allows the circadian system to reset its rhythm by Zeitgebers each day to avoid falling out of phase with external time. From an evolutionary perspective, it seems that the ability of clocks to be aligned to environmental cycles has been under strong selection [40], probably even more than the intrinsic clock's period. As of today, there is no clear answer to whether a clock with a period different than 24 h is easier to align to external cues than a 24 h clock, as Pittendrigh had suggested.

A third characteristic property of circadian rhythms is their ability to be synchronized, or entrained, by external Zeitgebers such as the light-dark cycle. Thus, although circadian rhythms can persist in the absence of external timing cues, normally such cues are present and the rhythms are aligned to them. Accordingly, if a shift in external cues occurs (e.g., following travel across time zones), the rhythms will be aligned to the new Zeitgeber (Figure 1.1B). This alignment is called entrainment. In more specific terms, entrainment is the adjustment of the period τ of the circadian system such that it equals the period T of the Zeitgeber. When entrainment occurs, the system adopts a specific phase-relationship with the Zeitgeber's phase, and this phase difference is known as phase of entrainment Ψ [22].

Initially, it was unclear whether entrainment was achieved by modulating the rate of cycling (i.e., whether the cycle was shortened or lengthened until it was aligned to

the new cues and then reverted to its original length) or by discrete "resetting" events. Experiments resulting from this debate led to fundamental findings. It was discovered that the organism's response to light (i.e., whether a cycle advances, is delayed or remains unchanged) differs depending on the phase in the cycle at which it is presented [39]. Exposure to light during the early part of the individual's "normal" dark period generally results in a phase delay, but, on the other hand, light exposure at the late part of the individual's normal dark period generally results in a phase advance. This difference in responses can be represented by a phase-response curve (PRC, Figure 1.1C). These curves show that, although the amplitude of a perturbation applied to an oscillation can be quickly "neutralized", phase changes persist [41]. Moreover, such changes in phase usually depend strongly on the phase of the cycle at which the pulse is given [22, 38, 39]. PRCs can be analytically calculated from mathematical models [41, 42], and they can be used to predict the way in which an organism will entrain not only to shifts in the light-dark cycles, but also to more unusual light cycles, such as non-24 h cycles or different light:dark ratios. Moreover, they are able to explain another interesting feature of oscillators, namely that specific perturbations of a given strength and at a certain phase of the cycle might "stop" the oscillator. Such "phase singularities" were predicted by Winfree [43] and are often discussed in the context of circadian rhythms [44] but also importantly in cardiology [45].

Not only the timing of light exposure, but also the light intensity (i.e., the amplitude or "strength" of the Zeitgeber) can modulate the period when organisms are left in constant light. Exposure to brighter light intensities can lengthen the period in some species and shorten it in other species, a phenomenon that has been dubbed "Aschoff's rule" [40]. Graphically, entrainment can be represented by Arnold tongues – triangular regions on a "Zeitgeber period – Zeitgeber strength" plane that predict the degree of entrainment of the oscillator in response to an external cycling cue (Figure 1.1D) [46–48]. Ultimately, both mechanisms of entrainment appear to be aspects of the same thing, because the consequences of Aschoff's rule can be predicted or explained by the Arnold tongues or the phase-response curves to light.

The light-dark cycle is clearly the major Zeitgeber for all organisms. Nevertheless, other factors such as social interactions, activity or exercise, feeding-fasting schedules, and even temperature, can also modulate the phase of an oscillation. The influence of temperature in circadian rhythms is particularly interesting because changes in temperature can affect the phase of a cycle without substantially altering the rate (period) of the circadian oscillation [49]. This means that, in response to a temperature pulse, the circadian cycle might start at an earlier- or later-than-normal time but still have the same length. On the one hand, this ability of the internal clock's pacemaker to compensate for changes in temperature is critical for its ability to predict and adapt to environmental changes, since a clock that speeds up and slows down as temperature changes would not be useful. On the other hand, this so called temperature-compensation property also is rather puzzling, because most biochemical processes are accelerated or

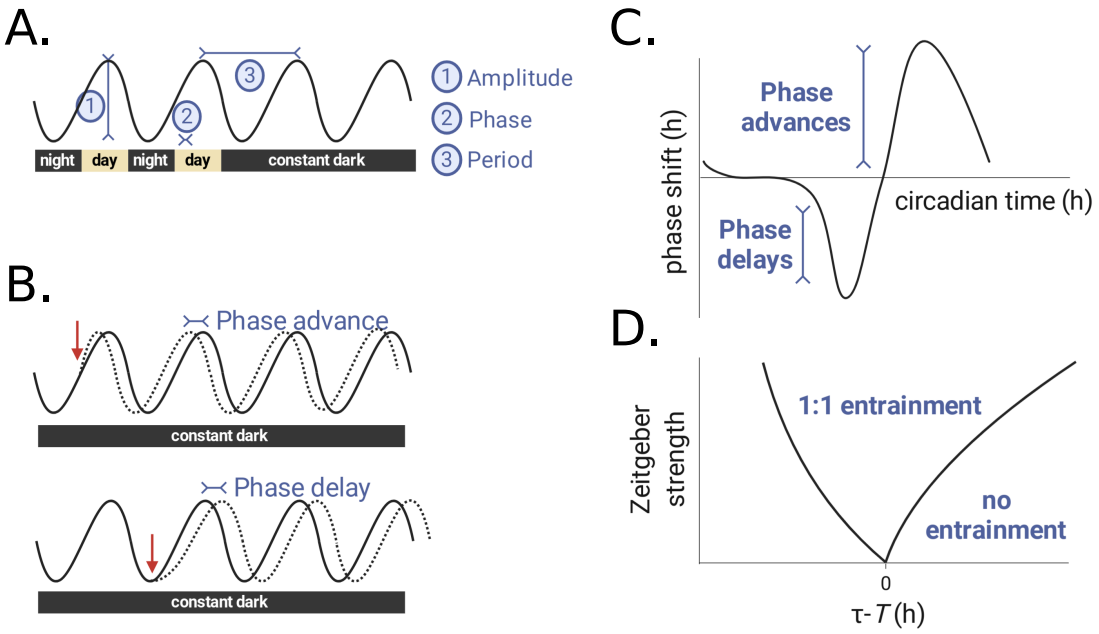

Figure 1.1: Properties of circadian rhythms. (**A**) Parameters of circadian rhythms. A representative circadian rhythm is depicted, in which the level of a particular measure (e.g., blood hormone levels, activity levels, etc.) varies with time. The difference between peak and trough values of the oscillation is the *amplitude* of the rhythm. The timing of a reference point in the cycle (e.g., the peak) relative to a fixed event (e.g., beginning of the night phase) is the *phase*. The time interval between phase reference points (e.g., two peaks) is the *period*. (**B**) Resetting the circadian rhythm. The effects of a rhythm-resetting signal (red arrow), such as exposure to light, can shift the rhythm (dashed line) either back (upper panel) or ahead (lower panel), depending on when the signal is presented. In case of phase advances, the peak levels are reached earlier than they would be had the rhythm not been shifted. In the case of phase delays, peak levels are reached later. The black solid line shows how cycling would appear if the rhythm remained unchanged. (**C**) Scheme of a phase-response curve. Virtually all species show phase-dependent resetting responses to external Zeitgeber cues, which can be expressed as a phase-response curve. (**D**) Scheme of an Arnold tongue. The period T and the intensity of the Zeitgeber can modulate the entrainment response of organisms to periodic Zeitgebers. For T values close to the intrinsic oscillator period ($\tau - T \sim 0$), low Zeitgeber strengths can entrain a self-sustained oscillator. For bigger $\tau - T$ differences, higher Zeitgeber strengths (amplitudes) are required to achieve entrainment.

slowed by temperature changes. Ultimately, this riddle gave researchers an insight into the nature of the internal clock, even before the first clock genes were identified: the fact that circadian rhythms have a genetic basis. They hypothesized that a gene expression program would be more resistant to temperature alteration than, for example, a simple biochemical reaction [50].

From an evolutionary perspective, temperature compensation seems logical. If circadian clocks function as reliable timekeeping systems, then their frequency should be essentially resistant to environmental fluctuations (such as temperature), on one hand, but also to fluctuations within the cell, on the other. Cells and multicellular organisms inherently have to cope with a number of sources of intracellular noise, including coordination of metabolic pathways, variation in transcription and translation rates or changes in the ATP/ADP ratio [51–54]. Thus, it has been speculated that compensation against temperature and metabolic changes might be part of a larger

compensatory phenomenon which maintains the frequency of the clock within a narrow range upon perturbation of the oscillator's internal or external milieu [55]. Chapter 2 addresses these concepts.

A last property that will be further addressed in Section 1.4 also provides an important landmark of the rhythms' makeup: the ubiquity of such rhythms in nature, from eubacteria to eukaryotes. Circadian rhythms exist in a broad array of biological processes and organisms, with similar properties and even similar phase-response curves [56]. Even unicellular organisms such as algae or the dinoflagellate *Gonyaulax*, and highly complex mammals, standing very far from each other in the phylogenetic tree, show pretty much the same rhythms.

The simple model depicted in Figure 1.2 has been the key metaphor in biological clock research for the past 40 years or more. The uppermost question in chronobiology has been to translate such a conceptual model into biological structures and processes. Where is the clock? Is it produced by individual cells or does it emerge from a hierarchical network? Unlike homeostatic systems, which seek to return to and stay at a fixed point, how can a set of biochemical reactions produce a regular self-sustained rhythm at the cellular level that can persist in constant conditions? How can this process be synchronized with the solar and other cyclic cues and why is the clock not altered by temperature? How can a biological system, where temperature-dependent biochemical reactions usually occur in fractions of a second, generate remarkably precise oscillations, with particularly long periods, of 24 h? And how is the time information of this rhythm communicated throughout the body?

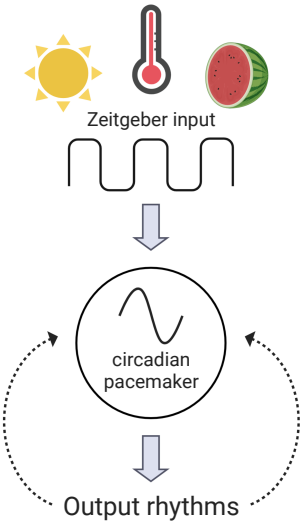

Figure 1.2: Simplified scheme of circadian clock systems. Circadian clock systems consist of a network of input pathways that integrate external Zeitgeber timing cues, the central oscillator (pacemaker) and output pathways. Central oscillators generate the endogenous rhythm and must be able to synchronize to environmental Zeitgebers (e.g., light) via input pathways. Consequently, pacemakers drive output pathways (e.g., physiology, behavior) and clock-controlled activities by synchronizing downstream oscillators. Additionally, intertwined positive and negative feedback loops (dashed lines) influence the interaction of the output pathways with the pacemaker. Figure modified from [57].

1.3 The Mammalian Circadian System

The rhythmic processes of an animal, plant or bacterium are governed by environmental time cues (e.g., fluctuations in light intensity and temperature), an internal

circadian timing system, and the interaction between the timekeeping system and the environmental time signals (Figure 1.2). In the last two decades, we have come to appreciate the underlying mechanisms of the mammalian circadian clock at the molecular, cellular, network and organismic levels. Although the field pioneered with discoveries in *Drosophila*, owing to remarkable similarities of the circadian pacemaker system between mammals and *Drosophila*, the understanding of mammalian clock mechanisms has advanced rapidly.

1.3.1 Organization of the mammalian circadian system

In mammals, the circadian timing system is composed of virtually as many clocks as there are cells, since most cells harbor self-sustained and cell-autonomous circadian oscillations [58]. Single cell circadian oscillators are organized into tissue networks which are then hierarchically arranged to constitute the mammalian circadian clock system (Figure 1.3). While the control of locomotor activity, cognition, and behavior resides in central oscillators, that mainly transduce light information so that opaque organisms tick in phase with the external light-dark cycles, oscillators in the periphery modulate physiological and metabolic functions of peripheral tissues.

The master pacemaker in mammals is located in the suprachiasmatic nucleus (SCN), a bilateral cluster of neurons which are located in a region at the base of the brain called the anterior hypothalamus. The role of the SCN as the master clock was demonstrated by a series of landmark discoveries that started in the 1970s. Back then, early work on mammalian rhythms used rhythmic behavior as a readout of the clock. Researchers found that endocrine and behavioral rhythms could be disrupted and abolished if the SCN was damaged [59, 60]. Moreover, the rhythms could be restored in SCN-lesioned animals upon transplantation of a healthy SCN, and it was shown that the restored rhythms exhibited the clock properties (i.e., the period and phase of the rhythm) of the donor rather than of the host [25]. The discovery of the SCN as the site of primary regulation of circadian rhythmicity in mammals gave researchers a focal point for their studies: if one wanted to understand 24 h timekeeping, one needed to study the clock in the SCN. By the same time, Reppert and his team cultured cells from neonatal rat SCN on fixed microelectrode arrays, and recorded spontaneous action potentials (spikes) from individual SCN neurons for days and weeks. The spike frequency from individual SCN neurons showed prominent circadian rhythms in firing rate, showing that the SCN is comprised of a large population of autonomous, single-cell circadian oscillators [61]. In other words, the basic oscillation lay within individual cells and was not the product of a network of cells within the SCN. The finding that individual SCN neurons, isolated from all other cells, show near 24 h rhythms in electrical activity indicated that the basic mechanisms that generate this internal day must be product of intracellular molecular mechanisms.

A new era for photoreception research arrived with understanding that the eye is a dual sense organ. In 1991, Foster *et al.* showed that mice with hereditary retinal disorders, despite loss of image-forming visual photoreceptors, could respond to light signals [62]. It was later demonstrated that intrinsically photosensitive retinal ganglion cells (ipRGCs) contain the photopigment melanopsin and contribute critically to circadian (non-image-forming) vision [63]. In 2007, non-rod, non-cone photoreceptors were demonstrated in two humans with rare eye diseases. They had no rods or cones but intact ipRGCs and photoentrainment proved possible [64]. Hattar *et al.* illustrated "hardware" connections of ipRGCs to the SCN and further architecture and projections throughout the brain [65, 66]. Thus, it was demonstrated that not only does the SCN act as a master clock, but it also receives direct photic input from light-dark cycles. Photic cues are transformed into biochemical signals in the SCN and induce time-dependent phase resetting of the central pacemaker. Consequently, the organism entrains to such external rhythms, so that internal and environmental time coincide.

More recently, gene expression studies and the development of circadian gene and protein reporter methods have allowed chronobiologists to find that circadian rhythms persist in isolated lungs, livers, fibroblasts as well as primary and immortalized cells grown in culture dishes *in vitro* without receiving direct input from the SCN [58, 67, 68]. These observations indicate that most cells and tissues of the mammalian organism may be capable of modulating their activity on a circadian basis; and this is further supported by transcriptomic studies that have shown that the expression of almost 10% of all genes in peripheral tissues is regulated rhythmically (despite small overlap between tissues) [28, 31, 58, 69]. Nevertheless, such findings to not diminish the central role played by the SCN. Especially if one takes into consideration the fact that the SCN oscillates robustly under constant conditions for long periods of time, whereas rhythms of peripheral tissue explants *ex vivo* and *in vitro* dampen over time [67]. Although the SCN does not force rhythmicity on all organs and cells of the body, it acts instead like the conductor of an orchestra. It produces a rhythmic signal, from which the various component parts of the orchestra (peripheral tissues) take a reference cue and align their rhythmicity accordingly. The result is the coordination of the entire 24 h temporal organization of cells, tissues and the whole mammalian organism. This implied that peripheral clocks might be "inferior" to that of the central pacemaker [67]. Indeed, the SCN coordinates time information with peripheral clocks by neuronal and hormonal signals, which act as synchronizing agents to establish the physiologically required phase relationships among them [70–72]. This way, some of the SCN output pathways serve as input pathways for peripheral tissues [58].

But, like always in biology, the picture is more complex than it seems, and peripheral tissues have been shown to exchange timing information with each other and to impact the SCN clock as well [73, 74] (Figure 1.3). In the last years, a number of studies have shown that non-pacemaker peripheral tissues can also entrain to non-photic input signals independently of the SCN. The liver clock, for example, unlike the SCN, is

particularly sensitive to resetting by feeding. Hepatic rhythms of clock gene and protein expression rapidly shift their phase to follow the timing of a scheduled meal [75, 76]. Similarly, behaviorally arrhythmic mice display rhythms in many transcripts (including a number of transcripts involved in metabolic processes) when fed in regular 24 h intervals [77], and liver rhythms persist in liver-specific clock (but otherwise clockless) mice [78]. Taken together, these results indicate that the SCN might not be necessary to sustain rhythmicity, at least in the liver. Still, the SCN seems to be required for the orchestration of all body clocks in order to coordinate rhythmic physiological outputs among the different tissues.

Nevertheless, specific tissue clocks regulate some of the most prominent physiological functions in each organ. For example, in kidney, the circadian clock modulates blood flow, glomerular filtration rate and ion and water excretion [74]. In the pancreas, excretion of both insulin and glucagon is under circadian control, whereas in the muscle, respiration and autophagy (processes that enable robust energy production) follow circadian rhythmicity [74]. There are a manifold of clock-controlled hormones that regulate physiology across the organism: glucagon, insulin, triiodothyronine, TRH, TSH, renin, angiotensin, leptin or ghrelin, among others (reviewed in [74]). It seems likely that these peripheral outputs, in turn, become circadian timekeeping cues that are transmitted to the other clocks throughout the body, likely ultimately feeding back into the SCN. Therefore, the mammalian circadian system can be seen as a web of interconnected oscillators. Feedback loops, both among peripheral and central clocks and among endogenous rhythms and exogenous Zeitgebers, indeed exist but are not well understood to date (Figure 1.3).

In short, the current paradigm of mammalian circadian organization is as follows: although the central pacemaker is located in the SCN, the discovery of clock genes has led to the realization that the capacity for circadian gene expression is widespread throughout the body, and that thus mammals have subsidiary clocks in every somatic cell [32, 33, 58, 68, 79]. The central clock in the SCN is synchronized to geophysical time mainly by photic cues. Changes in light intensity at dawn and dusk are perceived by the retina and transmitted by electrical signals to SCN neurons. In turn, the SCN coordinates circadian physiology and behavior by using neuronal and humoral signals that synchronize local clocks within cells of most organs and tissues. Conversely, tissue signals representing the internal environment return information to the central clock (Figure 1.3), thus resulting in a network of interconnected oscillators. To date, it is commonly accepted in circadian research that synchronization among tissues exists, but there are open questions such as why are there differences in phases and amplitudes among tissues [31, 80–82], what are the roles of intrinsic tissue-specific clocks, what is the relevance of the SCN as a driving force in tissues (compared to the intrinsic tissue clocks), among others, that remain to be answered.

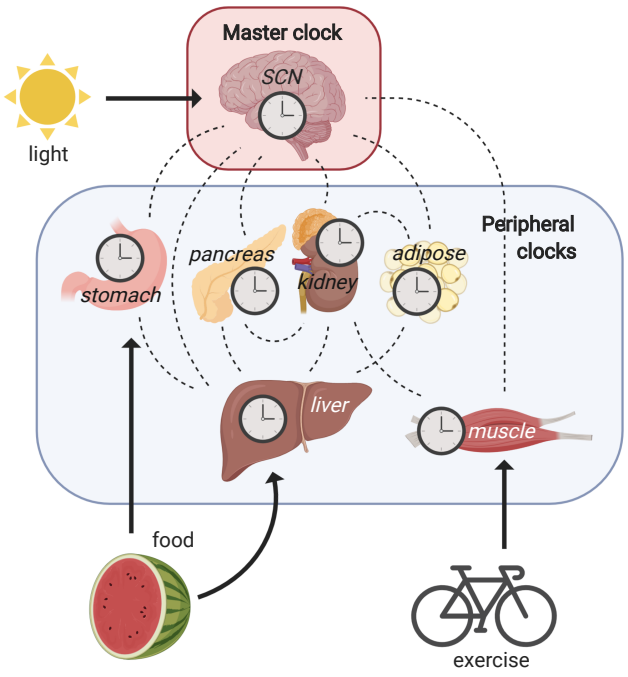

Figure 1.3: Organization of the mammalian circadian timing system. Circadian clocks are found in virtually all mammalian cells. The master clock is located in the SCN of the brain and synchronizes peripheral body clocks via direct and indirect pathways (dashed lines). The SCN is sensitive to and resets the clock in response to light. Other Zeitgebers, like food or exercise, have a major influence in liver or skeletal muscle, respectively, and can feed back to the central clock and to other peripheral tissue clocks. Figure modified from [73].

To conclude, and to make the picture slightly more complicated: it is not entirely true that, in the absence of the SCN, the system becomes disorganized, activity becomes non-rhythmic and peripheral tissues and cells drift out of phase. Mammals have at least two striking exceptions to this phenomenon. They are referred to, in the circadian community, as the food-entrainable oscillator (FEO) [83, 84] and the methamphetamine-sensitive circadian oscillator (MASCO) [85]. Scheduled restricted feeding and chronic administration of the psychostimulant drug methamphetamine can drive rhythms of circadian periodicity in various physiological functions, including sleep-wakefulness, feeding, drinking, body temperature as well as autonomic nervous functions, even in SCN-lesioned animals [86, 87].

1.3.2 The molecular clock machinery in mammals

To date, up to 20 genes and their protein products have been linked to the generation of circadian rhythms. At the heart of the molecular clockwork is a feedback cycle of gene expression, commonly referred to as a negative transcription-translation feedback loop (TTFL). In very simple lines, the outline of the pacemaker consists of the following sequence of events: clock genes are transcribed and their mRNAs are translated into proteins; proteins interact to form complexes, which translocate from the cytoplasm into the nucleus to repress transcription of the clock genes; the inhibitory clock protein complexes are then degraded, and the core clock genes are once again free to make their mRNA and hence fresh protein, and so a new cycle starts again. This negative feedback loop generates ~24 h rhythms, which encode the biological day. But in biology the picture is never so simple, and to produce this 24 h rhythmicity in mammals requires

a complex mechanism involving a manifold of clock genes, proteins, phosphorylation events, protein complexes and degradation or nuclear translocation events.

The first known mammalian clock gene, *Clock* was cloned in 1997 [88], which was soon followed by the cloning of the clock genes *Period1* (*Per1*) [89] and *Bmal1* [90]. The genes *Clock* and *Bmal1* encode bHLH-PAS proteins (basic helix-loop-helix; *Per-Arnt-Single-minded*, named after proteins in which the domains were first characterized) that form the positive limb of the feedback circuit (reviewed in [91]). BMAL1 interacts with CLOCK in a large complex [92] and binds to E-box enhancer elements upstream of its target genes. This set of activated genes includes members of the negative limb of the feedback loop including *Per* (*Per1*, *Per2* and *Per3*) and *Cry* (*Cry1* and *Cry2*) genes [88, 93, 94]. The resulting Per and Cry proteins form a large macromolecular complex [92] and translocate to the nucleus, where they interact with the CLOCK:BMAL1 complex to inhibit enhancer activity [92, 94] (Figure 1.4). One cycle of this negative feedback loop takes about 24 h, thus generating circadian rhythmicity. *Dec1* and *Dec2* are two other bHLH elements of an interlocking feedback loop found to repress CLOCK:BMAL1-induced transactivation at E-boxes [95]. MyoD or HIF-1α, also bHLH proteins, have been found to positively regulate BMAL1 expression and activity, respectively [96, 97].

The CLOCK:BMAL1 complex also initiates the transcription of a second feedback loop which acts in coordination with the loop described above. This involves the E-box mediated transcription of the orphan nuclear receptor genes *Nr1d1/2* and *Rora/b* [98–100]. Nr1d1 (RevErb) and Ror proteins compete for retinoic acid-related orphan receptor response element (RORE) binding sites within the promoter of *Bmal1* where Ror proteins activate *Bmal1* transcription and RevErb proteins inhibit it [98–100] (Figure 1.4). This loop was originally acknowledged as an accessory loop due to the subtle phenotypes observed in mice with individual null alleles of any of these genes. Nevertheless, inducible double knockout strategies that allow the deletion of the *Nr1d1/2* genes in adult mice (traditional double-knockouts have been shown to be lethal during development) have revealed that the RevErb proteins are necessary for normal period regulation of circadian behavioral rhythmicity [101]. Moreover, computational studies have shown that the Ror-BMAL1-RevErb loop, even in the absence of Pers and Crys, can function as an independent oscillator, and that *in silico* overexpression of RevErbα and RevErbβ results in the loss of oscillations [102]. In addition, a repressilator motif containing regulated expression of *Cry1*, *Per2* and *RevErb*α has been identified as a core element of the mammalian oscillator, and is sufficient to generate 24 rhythmicity [103]. Taken together, these findings highlight the role of RevErb proteins in the generation and regulation of 24 h rhythmicity.

A separate set of genes which regulate D-box elements in promoters of clock genes make up additional transcriptional loops. These include genes in the HLF family, Dbp and E4BP4 (or Nfil3) [104–106] (Figure 1.4). Although no genes, or even gene families, in these D-box accessory loops are required for clock function, they may serve to confer

robustness to the core oscillations and to add precision to the period [98, 107]. Such combination of interlocked and synergistic molecular loops is thought to be advantageous in terms of providing stability as well as fine-tuning circadian periodicity. Moreover, it has been proposed that the three known binding elements together provide the necessary delay to cycle at near 24 h: E-box in the morning, D-box in the day, and RORE elements in the evening [107].

Other enhancer elements have been shown to regulate clock gene expression in response to external Zeitgebers directly. For example, *Per1* and *Per2* expression is induced in response to light or serum via activation of the c-AMP response elements (CRE) or serum response elements (SRE), respectively, present in their promoter regions (Figure 1.4) [68, 108–110].

In circadian clocks, a particularly long delay between the induction of clock gene expression and its later repression is necessary to get 24 h rhythms. In the absence of this long delay, the changing levels of protein and transcripts would otherwise settle in a fixed point (also referred to as homeostasis in the literature) [111–113]. The detailed mechanisms that result in such lengthy delays are not well understood to date, but delays can be (partially) achieved by a number of "intermediate steps" between gene expression and repression, including phosphorylation of proteins, translocation to nucleus or clock protein degradation, among other post-translational events. Degradation of clock proteins is required to terminate the repression phase and thus, a new cycle of transcription restarts. The first mammal identified as a circadian mutant was the *tau* mutant hamster which displayed a free-running period of 20 h, compared to a wild-type free-running period of 24 h [17]. This shortened period resulted from a mutation in the enzyme casein kinase 1ϵ (CK1ϵ), a kinase that phosphorylates Per proteins [114]. A second casein kinase, CK1δ, was later found to also phosphorylate Pers. It was shown that the CK1δ/ϵ-mediated phosphorylation targets Per proteins for ubiquitination by βTrCP and consequent degradation by the proteasome [115–118]. Similar to Pers, mutant animals with unusual free-running periods (although longer than the wild-types in these cases) led to elucidation of the degradation pathways of Cry proteins. Fbxl3 was found to polyubiquitinate Cry proteins, thus targeting them for proteasomal degradation [119]. These findings, together with computational studies [102], highlight the key role of stability and degradation rates of clock proteins in settling the period of the clock.

Because of the interlocked nature of its various elements, it is perhaps not surprising that so many aspects of the circadian clock can be ablated without abrogation of the clock function. In this regard, clock gene redundancy seems to be an important factor in mammalian circadian rhythmicity. It has been shown that single knockouts of most integral clock genes do not completely disrupt behavioral rhythmicity due to the apparent functional redundancy of paralogs. Three independent null alleles of *Per1* yielded mice with free-running periods 0.5 – 1 h shorter than wild-types, but a loss of *Per2* produced mice with a 1.5 h period reduction [121–124] (although the behavior of the *Per2* null

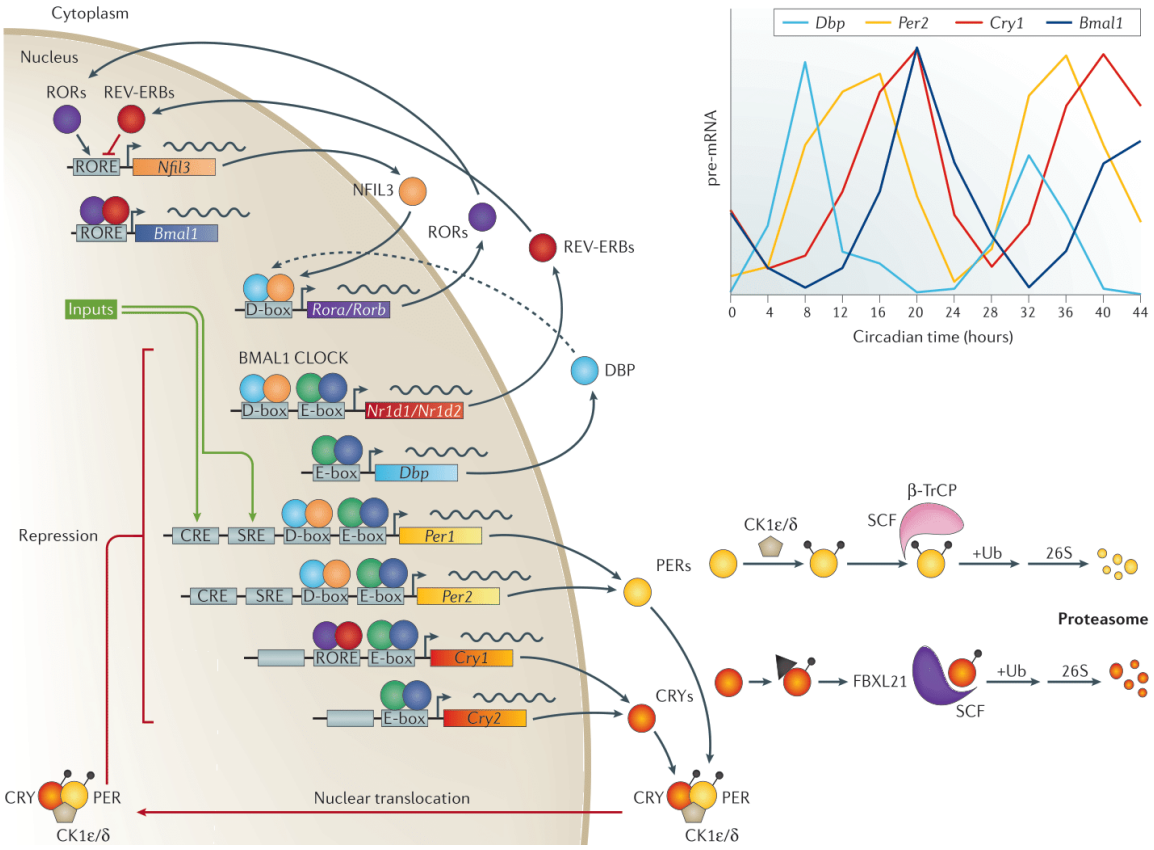

Figure 1.4: The circadian gene network in mammalian cells, with synergistic feedback loops. The transcription factors CLOCK and BMAL1 drive the E-box dependent expression of target genes, including *Pers, Crys, RevErbs (Nr1d1/2), Rors, Dbp* (E-box sites not shown for all genes, but see [120]). In one of the feedback loops (frequently termed "core feedback loop" in the literature), Per and Cry protein products form complexes and suppress their own transcription by inhibiting the CLOCK:BMAL1 complex. The stability of Per and Cry is regulated by CK1 and E3 ubiquitin ligase pathways (βTrCP, Fbxl3). In a second feedback loop, RevErbα/β and Rorα/β competitively repress and activate *Bmal1* transcription, respectively, by binding to its RORE promoter elements. A third accessory feedback loop is generated by *Nfil3* (whose expression is regulated by RevErbs and Rors) and *Dbp*, which competitively regulate the expression of clock genes via modulation of their D-box promoter elements. More feedback loops and regulatory interactions exist, but for the sake of simplicity are omitted from the illustration. Figure modified from [108].

mice only remained rhythmic for less than a week before becoming arrhythmic [123, 124]). Knockout alleles of the *Cry* paralogs produced opposite effects. *Cry1*$^{-/-}$ mice ran 1 h shorter than wild type mice, while *Cry2*$^{-/-}$ mice ran 1 h longer [125–127]. At the molecular level, it was shown that when one gene of a family is lost or reduced, the expression of a paralog of that gene is increased to partially compensate. This way, a reduction in *Per1* or *Cry1* produced an increase in *Per2* or *Cry2*, respectively [128]. At the behavioral level, it seems that at least one member of each family is critical for circadian rhythmicity, as *Per1,2*$^{-/-}$ mice and *Cry1,2*$^{-/-}$ mice display no circadian behavioral rest/activity cycles under standard experimental conditions [123–127]. These results, taken in combination with theoretical simulations [129], suggest that genetic redundancy provides resiliency to maintain clock function and renders mammalian clocks more robust against the effects of genetic damage to single elements. Over the last

years, however, this has been a matter of debate, since molecular studies have shown that SCN slices from *Cry1,2*$^{-/-}$ mouse neonates continue to exhibit approximately ~20 h PER2::LUC rhythms [130], despite having been previously described as arrhythmic, and that rhythms in PER2 gene and protein expression may persist even in the absence of CRY proteins in cell culture [131].

To further complicate the picture, there is a need for chromatin remodeling for the cyclic transcriptional activity. This is achieved by a combination of clock-specific and ubiquitous histone-modifying proteins, and can be observed in the rhythmic acetylation/deacetylation of histones (H3 and H4) and multiple clock target genes [120, 132]. The CLOCK protein itself possesses a histone acetyl transferase (HAT) domain which is necessary for the rescue of rhythms in *Clock* mutant fibroblasts [133]. Deacetylation takes place, in part, due to recruitment by Per1 of histone deacetylase complexes to CLOCK:BMAL1-bound DNA. SIRT1 also regulates deacetylation of histone H3 at the promoters of circadian genes and, interestingly, this deacetylase is sensitive to NAD^+ levels [134, 135]. This is interesting considering that the NAD^+:NADH ratio has been shown to regulate the ability of CLOCK:BMAL1 to bind DNA *in vitro* [136]. These observations shed some light on the important role of metabolism in regulating the transcriptional state, and therefore the phase, of the clock. The link between the clock and metabolism will be further addressed in the next chapters.

1.3.3 Non transcriptional rhythms

In some specific examples, 24 h rhythms are generated without transcription or translation, and thus the paradigm of the TTFL being required for circadian rhythm generation comes into conflict. In cyanobacteria, 24 h rhythms of phosphorylation of the KaiC protein are observed when the proteins KaiA, KaiB, and KaiC are isolated in a test tube in the presence of ATP [35]. The auto-phosphorylation and dephosphorylation of KaiC is mediated by KaiA and KaiB, respectively [137–139]. Later, circadian rhythms which are independent of transcription were discovered in the algae *Ostreococcus tauri*. In this organism, transcription stops in the absence of light, but 24 h oxidation cycles of the antioxidant proteins peroxiredoxins continue in constant darkness [140].

Hints that transcription-independent processes exist also in the mammalian circadian clock come from several studies. The surprising discovery that rhythmic transcription of *Bmal1, Cry1 and Cry2* [131, 141, 142] is not necessary for circadian clock function in mammalian cells, and that the mammalian cellular clock is particularly resilient to attenuation of transcription [53], suggests that mechanisms other than the TTFL are involved in generating oscillations. Perhaps the most striking demonstration of a transcription-independent circadian rhythm in mammals comes from the report of daily oscillations in human red blood cells of the oxidation of peroxiredoxins (PRX) [36], a protein that eliminates reactive oxygen species from the cell. In liver cells, expression

of PRX is circadian [143], but this is not possible in mature erythrocytes because they have no nucleus. Rhythms in PRX oxidation are also temperature-compensated and entrainable to temperature cycles, thus fulfilling the necessary attributes of true circadian clocks [36]. Moreover, the peroxiredoxin oscillators are remarkably conserved among all phyla that have been examined [37]. It should be noted, however, that in nucleated cells the transcriptional clock influences the cytoplasmic peroxiredoxin clock [36]. Rhythms in PRX oxidation and the crosstalk with the TTFL is precisely the subject of study of this PhD thesis and will be addressed in more detail in the next chapters.

It is thus tempting to speculate on the existence of further molecular circadian rhythms that can persist without the transcriptional oscillator left to be discovered, and on how the communication between these and transcriptional molecular clocks might reveal a whole new level of regulation of circadian functions within a single cell.

1.4 Conservation of Circadian Rhythms

The evolutionary biologist Theodosius Dobzhansky posited that "nothing in biology makes sense except in the light of evolution" [144]. This doctrine applies well to circadian rhythms, which can be traced back to the earliest life forms. Circadian clocks are ubiquitous in eukaryotes and also found in eubacteria among cyanobacteria. This ubiquity suggests that circadian clocks somehow enhance reproductive fitness, and thus they must have conferred organisms the presumed benefit of selective advantage. Nevertheless, as of today, there has been no rigorous test of this postulation.

Winfree posits some thoughts on why circadian clocks might have evolved in life. He argues that "in an alternating environment that intrudes forcibly into a cell's internal affairs, the cell would, in principle, need no additional clock" [43]. Nevertheless, it could improve itself by optimizing the transfer from one predominant metabolic activity to the next one, and thus it would economize waste, anticipate changes and bridge them slowly. Impelled by selection to gather more and more "fail-safe backups" to ensure the efficient state transition, Winfree says that "the cell might surprise itself to discover, 3.5 billion years later, when some scientist first puts it into constant conditions, that it shuffles its way through almost the same cycle" [43].

1.4.1 The Big Bang of circadian clocks

Some scientists believe that circadian clocks may have evolved at the time of the Great Oxidation Event 2.5 billion years ago [145] in order to drive detoxification of reactive oxygen species (ROS). This is the suggestion of a study from the groups of O'Neill and Reddy [37]. They show that peroxiredoxin (PRX) enzymes that scavenge the toxic by-products of oxygen respiration such as hydrogen peroxide, are conserved markers of

circadian rhythms, cycle with ~24 h rhythmicity and exist across all kingdoms of life [37].

The Great Oxidation Event resulted in a catastrophic change in the Earth's ecology that led to the loss of many anaerobic life forms and facilitated the development of aerobic metabolism [146, 147]. Cyanobacteria, the most ancient organisms with functional clocks, are thought to have evolved at around this time. Rising oxygen levels, attributed to the ability of photosynthetic cyanobacteria to use water as the main electron donor, are thought to have created a strong selective pressure on anaerobes to evolve defense systems that could deal with this harsh oxidizing environment. Driven by the day-night cycle, diurnal rhythms in oxygen or ROS of a biological origin, as well as ROS directly generated by UV radiation, could have potentially driven the co-evolution of circadian and redox systems so that processes sensitive to ROS would anticipate, and be buffered against, harmful oxidative stress. Thus, rhythms of oxygen consumption/generation and ROS production driven by the solar cycle, would have led to the evolution of a metabolic protoclock [37, 148, 149].

Evidence for circadian oscillations in redox pathways were documented in the early days of chronobiology, during the pre-genomic era. Before any of the clock genes were discovered, rhythms in $NADP^+$:NADPH were demonstrated in plant seedlings kept in constant darkness [150]. Studies performed in rodents also showed that key redox couples such as glutathione and $NADP^+$:NADPH displayed diurnal variation in their oxidation status in the liver [151, 152]. Although these oscillations might be a result of feeding schedules, it was later found that glutathione levels in platelets kept *in vitro* [153, 154] and in blood serum [155] also display diurnal variation, implying that the redox balance of blood somehow resonates with the day-night cycles. Such redox rhythms might work in parallel with the canonical genetic mechanism to keep circadian time. An unanswered question is how redox homeostasis relays timing information to the clock. These matters will be discussed in the next chapters.

An alternative explanation to the origin of circadian clocks, however, is that they may have evolved to cope with UV radiation from the sun. The products of *Cry* genes possess strong sequence homology with photolyases, a family of primitive enzymes that repair UV-damaged DNA in response to light [156]. This conservation suggests that these ancestors of the Cry timekeepers linked the maintenance of genomic integrity with exposure to the sun, and thus helped counteracting the damaging effects of UV on DNA [157, 158]. In *Drosophila* and plants, Cry homologs function as blue light photoreceptors and directly connect light exposure with molecular clocks [159–161]. In mammalian organisms, however, both the photolyase and photoreceptor properties appear to have been lost [162].

Despite the huge complexity of metazoans, core components of this evolutionary clock toolset are highly conserved. This concept is exemplified by PRX antioxidant

enzymes and CRY proteins, whose nucleotide and protein sequence appears conserved in many kingdoms of life. It appears that, instead of synthesizing entirely new genes *de novo*, evolution has "repurposed" master regulatory factors to accommodate selective pressures of individual organisms.

1.4.2 Segregation of incompatible processes

Period and phase adaptation (i.e., entrainment) to environmental cycles guarantees the temporal coordination of behavior and physiology with external conditions [21]. In these lines, circadian clocks seem to have promoted fitness by allowing organisms to organize their behavior and physiology in order to increase the likelihood of finding food or mating, or to avoid predators and harmful environmental conditions [163]. The advantage of tuning an organism's metabolism to the alternating day-night cycles is most evident in the case of plants and other photosynthetic organisms which perform oxygenic photosynthesis during the light phase [164]. Even the primitive *Synechococcus* species of cyanobacteria has a ~24 h clock. These unicellular organisms must conduct two essential metabolic processes for growth: nitrogen fixation and photosynthesis. Problematically, the enzymatic machinery that fixes nitrogen is highly sensitive to molecular oxygen, which is copiously produced as a function of photosynthesis during the light phase. To resolve this conflict, some species of cyanobacteria can segregate these two processes to different times of the day, with photosynthesis occurring during the light phase and nitrogen fixation during the dark phase [165, 166]. Moreover, the cyanobacterial clock prevents DNA replication during daylight under the harmful UV rays of the sun and increases organism survival and reproductive fitness [167–169].

As with the cyanobacterial circadian cycle, which seems to have evolved to enable incompatible metabolic processes to occur harmoniously within the confines of a cell that lacks organelles, the eukaryotic circadian cycle has an important role in optimizing metabolic output via temporal compartmentalization. Spatial compartmentalization by organelles is essential to the highly specialized functions of eukaryotic cells. Temporal dynamics of this compartmentalization represent a further refinement of this adaptation [170]. At the single cell level, organelles serve as specialized compartments that are dedicated to executing specific metabolic functions. Mitochondria represent the site of oxidative phosphorylation, peroxisomes perform fatty-acid oxidation and the endoplasmatic reticulum facilitates protein oxidation. By confining in time particular reactions within organelles, different biochemical reactions are isolated from the bulk environment and can proceed under locally optimized conditions. This way, for example, concurrent activation of certain anabolic and catabolic pathways that would result in futile cycles of some metabolites, is avoided. Also, similarly to cyanobacteria, DNA replication is favored at times when DNA-damaging agents like UV light or endogenous ROS production are low [170]. In complex metazoan animals, this spatial

compartmentalization also occurs at a more macroscopic levels within tissues and organs [29, 170, 171] and thus, the liver can be gluconeogenic when other organs are glycolytic.

In summary, circadian rhythms seem to provide both intrinsic and extrinsic advantages. Firstly, by the increased fitness that is provided by the alignment of internal period and phase to the environment, and secondly, by the selective advantage that comes from synchronization of internal processes and coordination of rhythmic biological function.

1.4.3 How to measure fitness?

Parameters such as longevity, growth and developmental rate have been studied to try to elucidate if clocks represent an evolutionary advantage among organisms [149]. In some cases, these parameters are improved when organisms are maintained on light-dark (LD) cycles with periods that resonate optimally with the free-running period of the endogenous circadian clock [172–178]. For example, the longevity of insects was reported to be maximal in LD cycles that most closely matched that of the free-running period [172–174]. Moreover, one study in a simulated field condition suggested that arrhythmic ground squirrels are more susceptible to predation [179], and that eastern chipmunks with surgically ablated SCN exhibited significantly higher mortality rates when released into their natural habitats compared to sham-operated and intact controls [180]. Since these parameters do not directly assess the fitness of an organism, a more appropriate way to evaluate the adaptive significance of circadian programs would be to examine the reproductive fitness of organisms under different LD cycles or of mutants whose clockwork is altered.

More recent studies that support the concept of adaptive advantage of circadian clocks were performed by the Johnson laboratory in 2004. Using cyanobacterial strains with different clock properties growing in competition with each other, they found that those strains with a functional clock defeated clock-disrupted strains in rhythmic environments [169]. Moreover, in competition experiments they showed that cyanobacterial strains compete most effectively in rhythmic environments when the frequency of their internal clock is similar to that of the environmental cycle [169]. Similarly, in pitcher-plant mosquitoes, individuals raised in a non-resonant LD cycle had significantly lower fecundity [181], and in *Drosophila*, loss-of-function mutations in canonical clock genes resulted in both decreased sperm quality in males and reduced production of oocytes in females [182, 183]. Similar results have been obtained with hamsters [184], mice [185] and ants [186]. Taken together, these results strongly suggest that a close match (i.e., resonance) between the endogenous circadian period and exogenous environmental cycles promotes individual fitness.

1.5 Time for Chronomedicine

Previous sections have discussed the importance of the synchrony of an organism with both its external and internal environments. If a nocturnal rodent were to venture from its burrow in the middle of the day, it would be an exceptionally easy prey for other animals. Similarly, a lack of synchrony with the internal environment seems to lead to health problems also in humans. Until we turned our nights into days and we began to jet-travel across multiple time zones, we were largely unaware that our bodies also measure internal time, driven by the circadian clock. Yet, the striking impairment of our abilities in the early hours in the morning or late hours at night soon reminds us that we are slaves of our biology.

1.5.1 Clock in modern societies

For millions of years, evolution installed in us a powerful internal clock programmed to adapt and thrive under the selective pressures of food scarcity, seasonal changes in sunlight availability, and variable range of temperature exposure. And although this highly fine-tuned system was sufficient for many thousands of years, we have rapidly developed living conditions in our societies that likely exceed the adaptive limitations of our circadian programming. Nowadays, with the introduction of fast food restaurants, cheap and calorically dense meals are accessible at almost any time of the day. The trend is even more detrimental to human health considering the growing population of shift workers, more regular travel across time zones, social jet lag, and almost constant exposure to artificial light pollution, which is 50 to 1 000 times less bright than outdoor lighting. Moreover, most people work, recreate, and reside in indoor conditions where heating and cooling systems maintain a constant ambient environment. This, in combination with the largely sedentary lifestyle our societies live in, represents a great contrast to the realities with which our ancestors were frequently faced (Figure 1.5).

It is not a coincidence that these radical adjustments in nutrition, light, or temperature are correlated with dramatic increases in the rates of obesity, diabetes, cardiovascular disease, depression, and many types of cancer [188–198]. In mouse models, misalignment of feeding time with endogenous clock time contributes to diet-induced obesity [199, 200]. Moreover, the reverse is also true, and alignment of feeding and activity through restriction of food access to the night time protects rodents from fatty liver [201]. Similar strategies to control eating time might likewise improve human metabolic health. It has indeed been suggested by population analyses that individuals subjected to shift work, where internal clocks and external light-dark cycles are repeatedly misaligned, are associated with greater incidence of breast cancer [202], obesity [195] and metabolic disease [194]. In addition, exposure to blue light at night with electronic

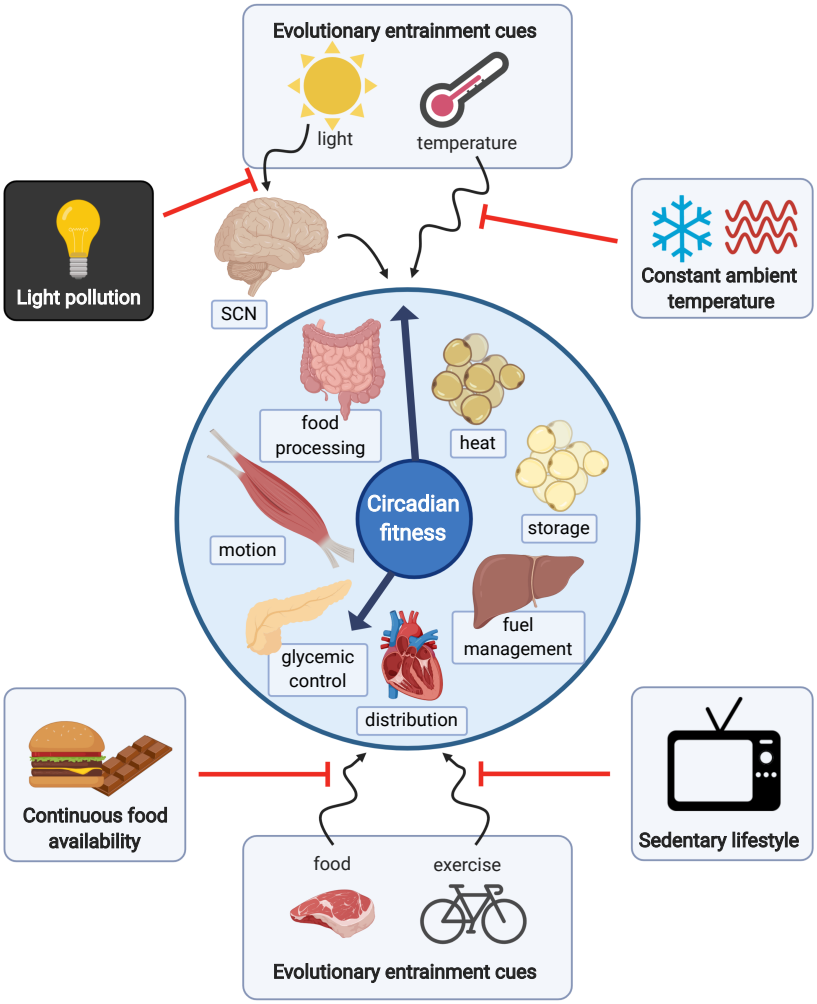

Figure 1.5: Impact of modern environments on evolutionarily programmed circadian functions. Sunlight, temperature, physical activity and food intake serve as basic entraining cues (Zeitgebers), that coordinate tissue-specific circadian processes to cumulatively define the whole organism physiology. Light acts to reset the master clock in SCN each day, which then relays signaling to peripheral tissues. Evolutionarily fine-tuned, tissue-specific circadian processes are depicted, including heat production by brown adipose; energy storage by white adipose; fuel source management between carbohydrate and lipid substrates in the liver; distribution or circulation of blood-borne factors, hormones, and metabolites by the heart; control of blood glucose levels by the pancreas; capacity for movement and activity by skeletal muscle, and food processing and nutrient extraction by the gut and microbiome. A combination of light pollution from artificial light sources, sedentary lifestyles largely lacking physical activity, continuous access to high-caloric foods, and living conditions maintained at constant ambient temperature have all contributed to the disruption of circadian fitness. Figure modified from [187].

readers or tablets, and the misalignment between going to bed early on weekdays, but staying up late on weekends (referred to as social jet lag) may induce circadian disturbance similar to the effects of shift work [195, 203]. Roenneberg *et al.* posit that the risk of shift work disorder may be more widespread than anticipated from work schedules alone [195].

Modern lifestyle also impacts our entire sleep-activity behavior. There is a large variability in the way we organize our sleep and wakefulness during the 24 h day. In this regard, the concept of chronotype is important, this is, the manifestation of a

person's underlying circadian rhythms [204]. The chronotype is usually assessed by questionnaires that examine sleeping habits, and it shows a normal distribution ranging from very early chronotypes (larks) to very late chronotypes (owls) [204–207]. There is a clear association between chronotype and duration of sleep on work and free days. Late owls exhibit the largest difference in sleeping time between work days and free days. This group of people wake up earlier than their biological wake up time during the work days due to work schedule, resulting in social jet lag. Social jet lag has been defined as the difference between the social clock and biological clock [204], usually due to work and social constraints [208]. Since the circadian clock determines when people can fall asleep, people with later chronotypes often accumulate sleep debt during the work week to be compensated on free days, which may cause conflicting schedules with family members and friends, leading to social and psychological stress that may worsen sleep and even mood disorders [209].

Chronotype is also dependent on age. While it is usually early in childhood, it is then delayed as people mature, reaching the latest stage at the age of ~20 [206]. Interestingly, the peak of social jet lag is in teenage times [204]. Teenagers are forced to sleep far too short on week days and thus have to catch up in weekends. In this way, teenagers can be compared to shift workers suffering from similar problems, and not only accumulate a severe sleep deficit during the work week but also suffer from reduced sleep quality, decreased performance and day-time fatigue. The picture gets even more dramatic because social jet lag has also been positively correlated with increased risk of adverse endocrine, behavioral, cardiovascular and mental profiles in apparently healthy subjects, putting them at a higher risk of developing metabolic and neurodegenerative diseases as well as mood disorders [195, 209–211]. Such metabolic and mental health implications of mismatching clocks should be carefully considered in discussions of Daylight Savings Time as well as work and school start times [195].

In short, the consequences of industrialization have drastically reduced Zeitgeber strength in our daily lives, so that our clocks have become much later. Nevertheless, our social schedules have remained relatively early. The consequence is that we cannot fall asleep as early as we should, in order to fulfill our sleep requirements, but still, we have to get up early. More than 80% of the population in the MCTQ questionnaire uses an alarm clock during work days [207]; and the use of alarm clocks simply means that our biological sleeping time is not over yet. "We mistreat our sleep and circadian needs by simply ignoring the consequences of modern technology and modern decision", Roenneberg says [212].

1.5.2 Disrupted clocks at the molecular level

On the other side of the coin, some human disorders and diseases have been shown to occur as a consequence faulty circadian clocks. Patients with Delayed Sleep Phase

Syndrome (DSPS) and Advanced Sleep Phase Syndrome (ASPS) suffer from insomnia and hypersomnia that result from the misalignment of one's internal time and the desired sleep schedule [213]. Familial ASPS (FASPS) has been shown to co-segregate both with a mutation in PER2 and, independently, with a mutation in the PER2-phosphorylating kinase, CK1δ [214, 215]. Transgenic mice engineered to carry the same single amino acid change in PER2 observed in FASPS patients reproduce the human symptoms of a shortened period [216]. Though rare, familial cases of DSPS have also been described. Polymorphisms in the 3'-untranslated region of the *CLOCK* gene have been associated to the development of DSPS [217]. Another study reported that an amino acid substitution (S408N) in the *CK1*ϵ gene may play a protective role in the development DSPS.

In addition to sleep-related disorders, circadian clocks are also directly linked with feeding and cellular metabolism, and a number of metabolic complications may result from miscommunication between the circadian clock and metabolic pathways (for a detailed review, see [218]). For example, a loss-of-function mutation of *Bmal1* in pancreatic β cells can lead to hypoinsulinaemia and diabetes [219]. *Clock*$^{\Delta 19}$ mutant mice are hyperphagic and obese, and not only lose rhythms of core clock genes, but also have lower levels of orexin and ghrelin (two hormones known to regulate food intake) in the arcuate nucleus [220]. Although these mutations are likely not the end of the story, they give insights into the way molecular clocks affect human well-being.

1.5.3 Medicine's secret ingredient: time

Although sleep-wake cycles are an obvious output of circadian rhythmicity in mammals, the circadian clock governs rhythms within an organism far beyond the sleep-activity cycle. Body temperature, blood pressure, circulating hormones, metabolism, vascular tone, cerebral activity, urine excretion, cytokine release or cell cycle progression are all examples of physiological functions that also follow 24 h cycles [29, 221, 222]. The consequence of this is that a number of diseases display a circadian component. For example, heart attacks or asthmatic episodes are more likely to occur in the late evening or early morning, coinciding with the peaks in blood pressure or cytokine release [223, 224]. Also, susceptibility to UV light-induced skin cancer and chemotherapy treatments have been shown to vary greatly across the circadian cycle in mice [225, 226]. These connections stress the concept that the body is more susceptible to challenges (e.g., infections, toxins, injuries) at specific phases of the circadian cycle than at others. Most of all, it hints to "times of day" at which a given tissue might be metabolically more sensitive to targeted treatment modalities in the clinic. Moreover, oscillations in the expression and activity of multiple rate-limiting regulatory enzymes in critical metabolic pathways establish times at which targeted treatment could yield the greatest results.

These concepts are the foundations for a more specific field of study known as chronotherapy, in which time becomes a critical variable when it comes to studying the

effects of when a given treatment needs to be administered. The goal of chronotherapy is to ensure that, *in vivo*, the availability of a drug is timed to correspond with the rhythms of the disease and, thus, to optimize the therapeutic outcomes in order to yield the greatest efficacy while minimizing adverse effects (for a detailed review see [227]). In the field of immunology, for example, it is known that the number of leukocytes circulating in blood in mammals is under circadian control [228] and, in addition, it has been shown that the circadian clock of CD8 T cells modulates the response to vaccination [229]. These findings highlight the importance of the circadian system in the development of inflammatory diseases and pose a challenge for chronotherapy, that seeks to adjust time-tailored therapies to human patients. Moreover, a pioneer in the field of cancer chronotherapy is Francis Lévi, from the University of Warwick. Research from his team has shown that circadian timing can modify 2- to 10-fold the tolerability of anticancer medications in experimental models and in cancer patients (for a complete review see Lévi *et al.* [230]).

Over the past several decades, chronobiologists have faced the challenge of identifying molecular players, uncovering elusive mechanistic details, and deciphering regulatory networks to explain how time relates to processes relevant to normal physiology, disease onset and progression, and treatment outcome. Acquiring this knowledge has helped to overcome the view of the physiology of the human body as a relatively invariant (rather than dynamic) homeostatic unit.

1.6 Future Perspectives: Uchronia vs. Dyschronia

Overall, from a public health point of view, a promising approach to improve circadian-related health and performance may be to strive for Zeitgeber hygiene [231]. In other words, to strive to align the diverse Zeitgebers such as light, food, activities, and social factors such that they interact synergistically rather than antagonistically. A unifying concept that arises from all these observations is that circadian disruption may be thought of as a sustained environmental stressor leading to chronic conflicts between endogenous biologic cycles and the environment. Our 24 h clock was fixed in time before the advent of electric light, jet travel, blue light-emitting computer screens and 24/7 food availability. Thus, a big goal in circadian clock research nowadays is to explore tissue-specific circadian biology and to examine how circadian signals are relayed among tissues. Ultimately, as reviewed in [187], we, as chronobiologists, hope that these insights will help to identify areas of circadian metabolic control that could be targeted for novel therapeutic strategies to rewire specific clock-regulated pathways with minimal or no detriment to the core machinery.

As in many aspects of life, there is a great deal of truth in the proclamation that "timing is everything". Thus, it does not come as a surprise that this saying also applies to circadian biology. While circadian biology is still considered a young science, the

possibilities it presents are endless. It has waited decades to emerge but is now regarded as a complementary and inclusive scientific discipline capable of bridging systems biology, bioinformatics, computational modeling, molecular genetics, biochemistry, physiology, pharmacology, pathology, clinical research and ecology. Circadian research is, to date, at its highest level of interdisciplinary research and thus attracts researchers from a manifold of scientific backgrounds, making it an extremely enriching field.

1.7 Work Overview

This dissertation seeks to uncover mechanisms behind the dynamics of mammalian circadian oscillations, and how redox homeostasis relays timing information to the clock. Both wet laboratory experiments and dry computer simulations have been performed and will be presented in the next chapters.

The concept of "metabolic compensation" is addressed in Chapter 2. For a biological clock to function as a circadian pacemaker that confers a fitness advantage, its timing functions must be stable in response to both environmental (external) and metabolic (internal) fluctuations. Temperature compensation is a well-known property of the circadian clock. But recently, it was found that clocks are also resilient to a number of metabolic changes, including variation in transcription and translation rates or changes in the ATP/ADP ratio [51–54]. In these lines, we hypothesized that compensation against temperature and metabolic changes might be part of a larger compensatory phenomenon that maintains the robust frequency of circadian oscillators in response to a multitude of factors that could otherwise destabilize the clocks. A question that arose at this point is whether the circadian clockwork might be equipped with a sensor that adjusts and compensates the circadian period to changes in metabolic rates. In this regard, the novel peroxiredoxin (PRX) redox rhythms might be related to metabolic compensation, in that they might be a mechanism to respond to (and to compensate for) varying levels of ROS that are generated by fluctuations of metabolic rates that tend to vary over the daily cycle.

Because there is little knowledge on the mechanisms generating 24 h rhythms in the oxidation status of PRX proteins, it is helpful to perform modeling work in order to gain insights into the design principles of such oscillators. Since there was no previous model for redox rhythmicity, we opted for the design of a new minimal model which we published in [232]. Invoking Occam's razor, we typically prefer simple models over more complex ones and by these means, we avoid making more assumptions than those needed. Chapter 3 focuses on modeling these relatively novel redox oscillations, first from a deterministic point of view, and then assuming that cellular redox rhythms might behave like stochastic ensembles. We thus introduced a stochastic component and analyzed how ensembles of mitochondrial redox oscillators might act synergistically to produce a coherent cellular redox output.

The next challenge, presented in Chapter 4, was to address the emerging links between redox oscillations and the canonical TTFL, and to understand how coupling between the clock and redox rhythms might be achieved. Thus, we coupled our redox model to two pre-existing models of the canonical circadian clockwork [102, 233] and analyzed the conditions under which the two oscillators remain synchronized. However, the results presented here are the first steps of the project. We seek to further investigate whether additional coupling nodes between the redox and TTFL clocks might be relevant in different tissues, and what are the consequences that arise from such differences. Ultimately, we hope to be able to relate our theoretical findings to previously published experimental observations. However, experimental data will have to investigate whether redox oscillator properties differ among tissues.

Final considerations and future work regarding the interaction between metabolism, redox and the canonical clockwork are presented on Chapter 5. We discuss the key findings and the limitations of our work. Although the detailed mechanisms by which redox and circadian cycles couple to each other remain to be mechanistically elucidated, further research in this topic will undoubtedly contribute to the understanding of the basic mechanisms of cellular timekeeping and how they integrate into a coherent physiological output.

In this chapter that now finishes, I have chosen to give an overview of the history of chronobiology and to discuss the main findings over the last years, as well as the questions that remain unanswered. Readers that are not familiar with circadian clocks might therefore get an idea of where circadian biology lies nowadays. I have not given detailed reviews of the ideas behind our working hypotheses, namely what motivated us to think about metabolic compensation or to model redox oscillations and its interaction with the canonical TTFL clocks. Rather, I will focus on the most relevant findings to introduce our hypotheses and results in introductory sections within the next chapters.

Institute for Theoretical Biology, Berlin

2

Compensation in Circadian Clocks

2.1 Compensation in Circadian Clocks: A Brief Overview

There are three hallmarks of circadian clock-related rhythms that have been already discussed in Section 1.2: (i) they are free-running and will continue to oscillate with an approximate 24 h period in the absence of external stimuli, (ii) they are entrainable by external signals such as light, temperature or feeding cues, and (iii) in contrast with most metabolic processes that are strongly affected by changes in temperature, the overall periodicity is mostly unaffected by, or compensated to temperature changes within a physiological range [49, 55].

2.1.1 Temperature compensation: a well-known property of clocks

Many physiological processes are sensitive to temperature. At the biochemical level, the speed of reactions tends to increase two- to three-fold with a 10°C temperature rise [49] and the same occurs at the system level. For instance, cell growth and cell division accelerate with temperature, as shown by studies from NIH3T3 fibroblasts which report that cell cycle period decreases to one-third as the temperature rises by 10°C [234]. In contrast, circadian rhythms are robust to temperature and the oscillation period remains relatively constant in spite of temperature changes [49, 235], as illustrated in Figure 2.1A, where a decrease in temperature of 15°C lengthens the cyanobacterial period by only ~2 h. Obviously, a temperature change of this magnitude will have a major effect on the metabolic rates of an organism such as a cyanobacterium, which cannot regulate its temperature. Nevertheless, the timekeeper's circadian period is somehow surprisingly compensated to such a temperature step.

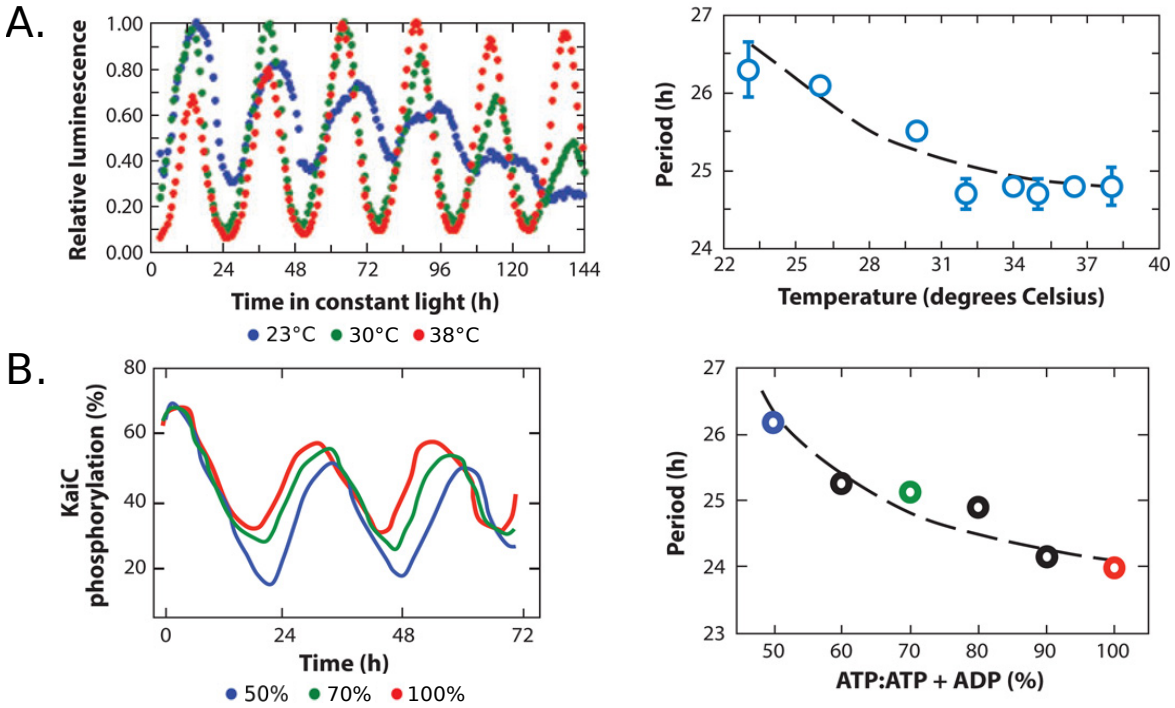

Figure 2.1: Circadian compensation to temperature and ATP:ADP variations. (**A**) *In vivo* bioluminescence rhythms with the *kaiBC* promoter-*luxAB* reporter at different temperatures in constant light conditions. Left panel: *in vivo* rhythms at 23°C, 30°C and 38°C in constant light conditions. Right panel: summary data for the period of the *in vivo* rhythm as a function of temperature over the range from 23°C to 38°C in constant light. (**B**) Rhythmic KaiABC *in vitro* reactions in buffers with various ATP:ADP ratios. Left panel: *in vitro* rhythms of KaiC phosphorylation at 100%, 70% and 50% ATP. Right panel: summary data for the period of the *in vitro* oscillation as a function of the ATP:ADP ratio. Figure adapted from [55].

The Q_{10} temperature coefficient is often used as a measure of the rate of change of a biological or chemical system as a consequence of increasing the temperature by 10°C [236], and it is defined as,

$$Q_{10} = \frac{R_2}{R_1}^{10^\circ/(T_2-T_1)} \tag{2.1}$$

where R is the rate and T is the temperature in degrees Celsius or Kelvin. For most biological systems, the Q_{10} value is between 2 and 3 but for temperature-compensated systems like the circadian clock, where the oscillator period is robust to changes in temperature, the consensus is that $0.85 < Q_{10} < 1.15$ [237].

From a biochemical perspective, explaining how the period of biological rhythms remains stable under varying temperatures in species with and without thermal homeostasis is not trivial. Proposed hypotheses for this temperature compensation property include the following:

1. The *critical reaction hypothesis* posits that there are critical reactions governing the circadian period, and that the period can be stable if these reactions are insensitive to temperature. This is supported by experimental evidence from cyanobacteria and mammals: the ATPase activity of KaiC, an essential component of the cyanobacterial circadian system, is temperature-insensitive [238], as well as the degradation rate of PER2, which has been extensively studied in the Ueda laboratory and is now known to be regulated by the temperature-insensitive CKIϵ/δ-dependent phosphorylation in mammalian cells [239, 240]. However, it still remains unclear how the circadian period can be maintained against temperature in a system in which not only the critical reactions, but also other reactions should affect the period.

2. The *balance hypothesis*, proposed by Hastings and Sweeney in 1957 [241], suggests that a balance between period-lengthening and -shortening reactions could lead to a stable period. Rouff, in his kinetic oscillator model [242], describes that increases in rate constants belonging to positive feedback reactions increase frequency, while increasing rate constants of negative feedback reactions will lower the frequency. Thus, for a certain set of activation energies, positive and negative feedback reactions will, due to their opposing effects in response to temperature, tend to compensate the influence of temperature on period length.

3. The *temperature-amplitude coupling hypothesis* proposes that as the temperature increases, the compensation mechanism may increase the amplitude of the oscillator to maintain a constant period [243, 244]. Supporting this hypothesis is data on the yeast metabolic cycle: this ultradian rhythm is stable under temperature variation and the amplitude increases at higher temperatures [244]. However, there is no further strong experimental evidence advocating for this hypothesis. For example, the amplitude of bioluminescence in the *Gonyaulax* circadian clock decreases with temperature [241].

The hypothetical mechanisms for temperature compensation mentioned above rise the question of whether any of them is the actual mechanism of temperature compensation for circadian rhythms. Nevertheless, they are not mutually exclusive and the mechanism might be a combination of hypotheses.

2.1.2 Metabolic compensation: hints to its existence

But, as was already pointed out by Pittendrigh and Caldarola in 1973, if circadian oscillations function as reliable frameworks to temporally organize cellular function, then their frequency (or period) should be essentially resistant to, on the one hand, fluctuations that they encounter in the environment and, on the other hand, to fluctuations within the cell (or within the organism for multicellular organisms) [55, 245]. Examples of sources of

intracellular noise that timekeepers have to cope with include cell division, coordination of metabolic pathways or fluctuations in the number of mRNA and protein molecules due to large variations in the rates of transcription, translation and degradation [246, 247]. On top of this, many environmental factors can create noise that could disrupt a non-resilient timer: temperature changes, light intensity changes, oxidation and redox status, nutrient availability, etc.

That light and temperature can significantly affect circadian period and phase has been known for more than 50 years [49], but only recently have investigators learned the extent of linkage between circadian clocks and metabolism [218, 221, 248, 249]. Most of the recent metabolism/clock investigations have studied how the clock regulates metabolism and the impact of metabolic feedback into the clock. However, not much attention has been paid to the realization of how profoundly these timekeepers are buffered against metabolic noise, and there are some clear empirical regularities in the oscillators' response to large changes in several variables other than temperature, such as ATP:ADP ratio, glucose concentration, transcription rates or redox balance [51–54]. The following four examples illustrate the similarities of an oscillator's response to metabolic and temperature changes. These results suggest that homeostasis of the period length might be a general property of circadian oscillations or, in other words, that there might be an underlying homeostatic mechanism that conserves the period within a narrow range upon perturbation of the oscillator's milieu.

The cyanobacterial clook keeps time despite decreases in ATP concentration

In contrast to the transcription-translation feedback loop mechanism characteristic of eukaryotic circadian clocks, the cyanobacterial oscillator is a post-translational oscillator comprised of three central proteins: KaiA, KaiB and KaiC. KaiC is an autokinase, autophosphatase and ATPase whose daily rhythms of phosphorylation and ATPase activity are key features of the timekeeping mechanism [138, 250]. The cyanobacterial clock is the only model clock that, so far, can be reconstituted *in vitro*: mixing KaiA, KaiB and KaiC with ATP results in an oscillation of KaiC phosphorylation with a periodicity of ~24 h [35].

Cyanobacteria are photoautotrophic microorganisms that derive its energy exclusively from photosynthesis and photophosphorylation, which can only occur in the light [55, 251]. Consequently, if cyanobacteria are transferred to darkness, ATP levels decline significantly, reaching levels as low as 50% ATP ($\frac{[ATP]}{[ATP]+[ADP]}$) after only 8 h [51]. But, surprisingly, cyanobacteria can still keep accurate circadian time and the rhythm in KaiC phosphorylation continues to operate in darkness for several days despite (i) the major impact of darkness on the cyanobacterial metabolism and (ii) the ATP requirement of the clock [51, 55, 251, 252].

The ATP:ADP ratio can be experimentally modulated in the *in vitro* oscillator to study the changes in period upon variations in energy charge. It has been shown that even the *in vitro* oscillator is relatively imperturbable in the face of metabolic changes: despite its central characteristic (ATP hydrolysis), the period of KaiABC rhythm lengthens by only 2 h when the percentage of ATP is reduced to 50% of the optimal concentration [51] (Figure 2.1B). These findings show that both *in vitro* and *in vivo*, the ATP-hydrolyzing cyanobacterial clock can compensate for major metabolic changes that deplete ATP levels.

How an energy-requiring timekeeping system can be buffered against dramatic changes in energy charge is perplexing, and reminds of the timekeeper's response to temperature changes in two aspects. First of all, the period of the *in vitro* oscillator is only slightly affected by a reduction in energy charge or by different constant temperatures (within a physiological range). This is well seen in Figure 2.1, where both reduction of the ATP to 50% of the optimal concentration and a temperature change from 38 to 23°C result in a period change of only ~2 h. Second, both acute temperature steps and manipulation of the nucleotide ratio can cause phase shifts and thus serve as entrainment cues in the purified protein oscillator [51, 253]. These striking similarities suggest that a compensatory mechanism might operate to conserve the period within a narrow range upon perturbation of their milieu.

Glucose compensation in *Neurospora crassa*

Metabolism enhances biochemical reaction rates such as trancription and translation in a rather general manner [254–256], and even moderate changes of expression rates could unbalance physiological processes and disturb cellular homeostasis. Surprisingly, the period of some circadian oscillators is relatively insensitive to changes in nutrients (e.g., glucose) and this is referred to as "nutrient compensation". This is exemplified in the clock of the eukaryotic fungus *Neurospora*, which has been shown to be compensated against changes in glucose levels [52, 257].

In *Neurospora crassa*, circadian timekeeping is sustained through interlocked negative and positive feedback loops [258]. The core transcription factor of the *Neurospora* clock, white collar complex (WCC), a heterodimer of the zinc-finger proteins WC-1 and WC-2, activates the transcription of the *frequency* (*frq*) gene [259, 260]. Then, translated frequency (FRQ) protein binds to FRQ-interacting RNA helicase (FRH) and CK1 [261], translocates into the nucleus, and suppresses its own transcription by inactivating WCC, closing the negative feedback loop [262, 263]. Simultaneously, FRQ promotes WC-1 accumulation in the cytoplasm, increasing the level of WCC and forming a positive feedback loop [258, 263].

Recently, the circadian clock-regulated developmental regulator, conidial separation-1 (*csp-1*), was shown to be a global transcription repressor under the direct control of WCC, and was found to regulate expression of ~800 metabolic and other genes [264]. CSP-1 was shown to repress the expression of *wc-1* by binding at its promoter regions in response to high glucose and other carbon sources [52]. Further experiments suggested that this additional negative feedback loop formed by CSP-1 maintains relatively similar abundance of WC-1 in a wide range of glucose concentrations in the growth medium. This results in a relatively constant circadian period as a function of glucose concentrations (referred to as "glucose compensation"), which counterbalances the overall increased translation efficiency at high glucose levels. In other words, the CSP-1 negative feedback loop compensates the clock against glucose-related changes of biochemical rates by reducing the rate of transcription of a large number of genes, including *wc-1* [52], and thus coordinates cellular metabolism with the circadian clock. In contrast, the glucose compensation was disrupted in *csp-1*^{ko} with decreasing period as glucose concentration was increased [52].

Compensation against variations in transcription rate

The timing mechanism in mammals, plants, flies and fungi is typically described by TTFLs. TTFL models revolve around the protein products of clock genes that periodically feed back to regulate their own expression and, from this simple principle, models have been expanded to encompass multiple, interlocked loops. However, there is an increasing number of anomalous observations that do not fit the standard TTFL molecular mechanism for some model organisms. These anomalies fall into two classes: observations of rhythmicity in the organism when transcription of clock genes is held constant (overexpression of the repressors CRY1/2 does not affect rhythmicity [141]), and rhythmicity in the organism when clock gene function is missing in knockout mutants (single knockouts of *Cry1* or *Cry2* are rhythmic in constant darkness [127] and *Cry1,2* double knockout animals show ~18 h rhythms when transferred from constant light to constant darkness [265]). Not least are the observations of circadian photosynthetic rhythms persisting in green algae after enucleation and hence in the absence of nuclear transcription [266], or the peroxiredoxin rhythms found in red blood cells [36]. Nevertheless, the focus of this section, however interesting it may be, is not to question the TTFL but more to argue in favor of circadian compensation as a homeostatic mechanism. Peroxiredoxin rhythms will be the subject of study in the next chapter.

The challenge of the TTFL is somehow linked to the clock's compensation against metabolic changes. If the TTFL were at the heart of the fine temporal control of circadian timekeeping, disruptions in transcription would be expected to affect rhythmicity. Dibner *et al.* [53] have clearly shown that the cellular oscillator is remarkably resilient to large-scale changes in global transcription. In their study, mouse fibroblasts were pre-treated

with well-known transcriptional inhibitors such as α-amanitin and actinomycin D. Following treatment, a reduction of >70% in total mRNA production was observed, and RT-PCR and western blots confirmed that clock gene expression was similarly affected. Surprisingly, the inhibitor treated cells remained rhythmic (albeit with lower amplitude) and with a period that shortened by only 2-3 h at 37°C [53]. These findings suggest, again, a robust compensatory response to a treatment that significantly alters cell metabolism.

Mammalian circadian period is robust against redox perturbations

The O'Neill laboratory has recently shown that the period of oscillations is essentially insensitive to perturbations in redox balance [54]. They incubated cells with a range of concentrations of the reducing agent 2-mercaptoethanol or with glucose oxidase (an enzyme that oxidizes glucose resulting in H_2O_2 production) and observed that the amplitude and phase of PER2 oscillations were sensitive to changes in redox balance, but that the period of oscillations was essentially insensitive to these "sledgehammer" treatments. Again, the ability of redox balance to elicit phase shifts and the robustness of the timekeeping system to redox perturbations remind of the temperature compensation phenomenon.

2.2 Hypothesis: Circadian Compensation

The striking similarities between temperature compensation and the examples discussed in the previous section support the forgotten 40-year old proposition that the universal property of circadian clocks (temperature compensation) might actually be a subset of a larger phenomenon which creates a general homeostasis of the period of circadian oscillators [245].

We hypothesized that (i) the processes underlying circadian temperature compensation may be shared with those that buffer the cell against metabolic changes (changes in ATP levels, glucose concentration, gross transcriptional activity or redox balance) observed in different organisms. (ii) These compensation responses might be related to each other and might be part of a larger circadian compensation/homeostasis phenomenon. Preliminary observations suggest that mutations in the *kaiABC* genes that suppress temperature compensation render the circadian system more sensitive to metabolic perturbations (Xu and Johnson, unpublished results). On this basis, we proposed the same idea but in the opposite direction, and thus hypothesized, together with Prof. Dr. Carl Johnson, that (iii) interfering with metabolism would render the timekeeping mechanism more sensitive to temperature changes.

The goal of this chapter was to analyze if this prediction is upheld in mammalian cells, using U-2 OS human bone osteosarcoma cells as a cell culture model system. To test this hypothesis, we performed an RNAi screen and knocked down different genes involved in essential cellular metabolic pathways. If temperature and metabolic compensation are part of the same phenomenon, knockdown of a metabolic gene would result in the loss of the temperature compensation property. Understanding how circadian oscillators are buffered against metabolic changes might aid in the efforts towards understanding temperature and circadian compensation. The molecular characterization of such mechanisms would likely constitute a major challenge and a major advance for circadian biology research.

A question that also came up was whether the novel PRX oxidation rhythm might be related to metabolic compensation, in that it might be a mechanism to respond to (and compensate for) varying levels of reactive oxygen species that are generated by fluctuations of metabolic rates that tend to vary over the daily cycle. We hypothesized that the circadian clockwork mechanism might be equipped with a metabolic sensor (perhaps ATP levels, redox status) that adjusts and compensates the circadian period to changes in intracellular metabolic rates.

2.3 Results: Towards a More General Concept of Circadian Compensation

We hypothesized that, if metabolic and temperature compensation are part of the same larger phenomenon, then interference with temperature compensation might render the circadian system more sensitive to metabolic perturbations (preliminary unpublished observations from Xu and Johnson suggest that this is true in cyanobacteria) and vice versa. To test whether this link actually exists, we performed a small scale RNAi screen and knocked down 78 metabolic genes in human osteosarcoma U-2 OS cells harboring a *Bmal1-luc* circadian reporter (see Table 6.1). The resulting oscillations after knockdown were compared at two different temperatures, namely 32°C and 39°C. If the initial hypotheses were true, a loss of temperature compensation would be expected upon knockdown of some of the metabolic genes.

Components of major metabolic pathways such as glycolysis, citric acid cycle, phosphate pentose pathway and oxidative phosphorylation were selected because of their role on modulating the rate of biochemical reactions and maintaining the energy and reductive state of the cell. Since NAD^+ has been shown to modulate CLOCK:BMAL1 activity directly and indirectly through SIRT1 [134–136], we also knocked down several members of the family of sirtuins as well as enzymes involved in the NAD salvage pathway. Moreover, motivated by the discovery of the peroxiredoxin (PRX) oxidation rhythms, we asked ourselves whether these oscillations might be a mechanism to compensate for

varying levels of ROS generated in response to fluctuating metabolic rates that vary diurnally, and whether they might serve to adjust circadian rate constants to changes in intracellular metabolic rates. For this reason, genes that play a role in PRX rhythms, together with other genes that maintain the redox state of the cell, were also selected for knockdown. In addition, since AMPK and the PPAR family of nuclear receptors have been proposed to integrate the mammalian clock with energy metabolism [267, 268], different AMPK subunits as well as PPAR isoforms were knocked down. The 78 genes and the number of constructs used for each genetic knockdown are shown in Table 6.1. A list with all the constructs used in this screen is provided in Suppl. Table S1 (additional file).

Luminescence of reporter cells was measured in a biolumicorder after successful knockdown and consequently, the data was processed and circadian parameters were extracted as described in Section 6.3. Raw data is shown in Appendix A (Suppl. Figures A.1, A.2). Mean and standard deviation (SD) values of oscillation amplitude, damping rate, period and phase in single wells are shown in Suppl. Tables S2 and S3 (provided as additional files). A plate-wise summary of the same circadian parameters is provided in Suppl. Figure A.3 and Suppl. Table A.1.

2.3.1 Knockdown of metabolic genes affects oscillation parameters

We first analyzed whether knockdown of our genes affected amplitude, damping rate or period of the oscillations. We found that some metabolic genes modulate the circadian clock in that, when they are knocked down, they result in a significant change (increase or decrease) in the mean oscillation amplitude, damping rate or period compared to the negative controls.

As siRNAs have well-described potential "off target" effects, we focused on genes where the RNAi constructs generated a consistent phenotype, either by resulting in a p-value <0.05 (t-test) compared to the negative controls, or by resulting in a mean parameter value with strong circadian phenotype defined by two or more standard deviations from the mean of the negative control parameter values (i.e. absolute value of z score or $|z|>2$). We decided to consider both criteria (p-value and z score) to determine hits as they both are informative but in different ways: p-values give information about the consistency of an effect and z scores, of the size of the effect.

We hypothesized that consistent changes in parameter values at both 32°C and 39°C (for instance, increase in the period length at both temperatures) indicated that the resultant phenotype is not reporter- or response element-specific, but rather reports an impact on clock function in our U-2 OS reporter cell system. However, even though overlaps of hits at both temperatures are interesting, they are not necessary. The results are depicted in Figures 2.2, 2.3, and 2.4 where blue and red points show RNAi constructs

that resulted in a p-value <0.05 or $|z|$>2, respectively (green dots are RNAi constructs that result in both p-value <0.05 and $|z|$>2).

Modulation of period

We found that knockdown of *CYBB, MDH2, OGDH, PDHA1* and *PRKAB1* resulted in oscillations with shorter periods at 32°C (p<0.05, t-test, or/and $|z|$>2). Moreover, silencing of *COX6B1, COX7B, GCK, IDH2, LONP1, PRX2, PRX3, SDHD, SUCLG1* produced oscillations with longer periods (p<0.05, t-test, or $|z|$>2). At 39°C, *HSP90AA1, IDH1, LDHC, MDH2, NAMPT, PDHA1, RRM2* and *SIRT1* were found as short period hits (p<0.05, t-test, or/and $|z|$>2) and *COX4I2, COX5A, COX7A1, CYBB, HK2, HSP90AB1, LONP1, RRM1, SUCLG2* and *TXN* as long period hits (p<0.05, t-test, or/and $|z|$>2). The results are illustrated in Figure 2.2. Worth pointing out are *LONP1*, a long period hit, and *MDH2* and *PDHA1*, short period hits at both temperatures.

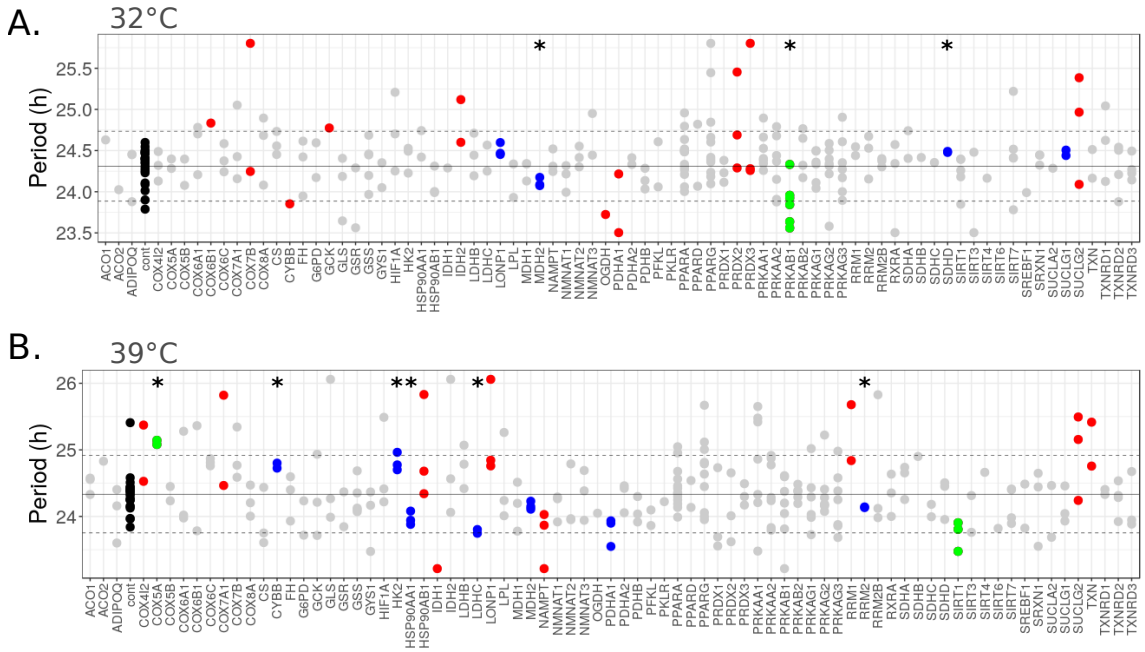

Figure 2.2: Metabolic genes that modulate oscillation period in *Bmal1-luc* U-2 OS cells at 32°C (A) and 39°C (B). Quantile-normalized data is represented here, since all plates were analyzed together to find putative hits. Depicted in black are the period values of the negative controls; in blue are those genes whose knockdown resulted in a mean period that was significantly different to the value of the non-silencing controls (p<0.05, t-test); in red, genes whose knockdown resulted in a mean period that was at least 2 SD away from that of the non-silencing controls ($|z|$>2); in green, genes for which the blue and red conditions were held true. Asterisks indicate hits at a FDR = 25%. The black horizontal lines depict the mean period value (continuous line) of the oscillations of cells transduced with non-silencing constructs ± 2 SD (dashed). n=1 single biological experiment with 2–14 shRNA constructs for each genetic knockdown.

Modulation of amplitude

Regarding genes that modulate the amplitude of the circadian clock compared to non-silencing controls, we found that, at 32°C, knockdown of *ADIPOQ, COX7A1, GSR, HK2, HSP90AB1, LPL, NMNAT1, NMNAT3, PRKAG2* and *TXNRD3* reduced the amplitude of the oscillation (p<0.05, t-test, *NMNAT3* also presented $|z|$>2). At the low temperature, we did not find any hits that resulted in an increased oscillation amplitude. At 39°C, knockdown of *COX6A1, COX7B, GYS1, IDH1, PRX1, PRKAB1, PRKAG1, RRM1, SDHB, SIRT3* and *TXN* resulted in a decreased oscillation amplitude, whereas knockdown of *MDH2* and *SUCLA2* increased the amplitude compared to the non-silencing controls (p<0.05, t-test, or/and $|z|$>2). There was no overlap between the amplitude hits at 32°C and 39°C. Figure 2.3 summarizes the results.

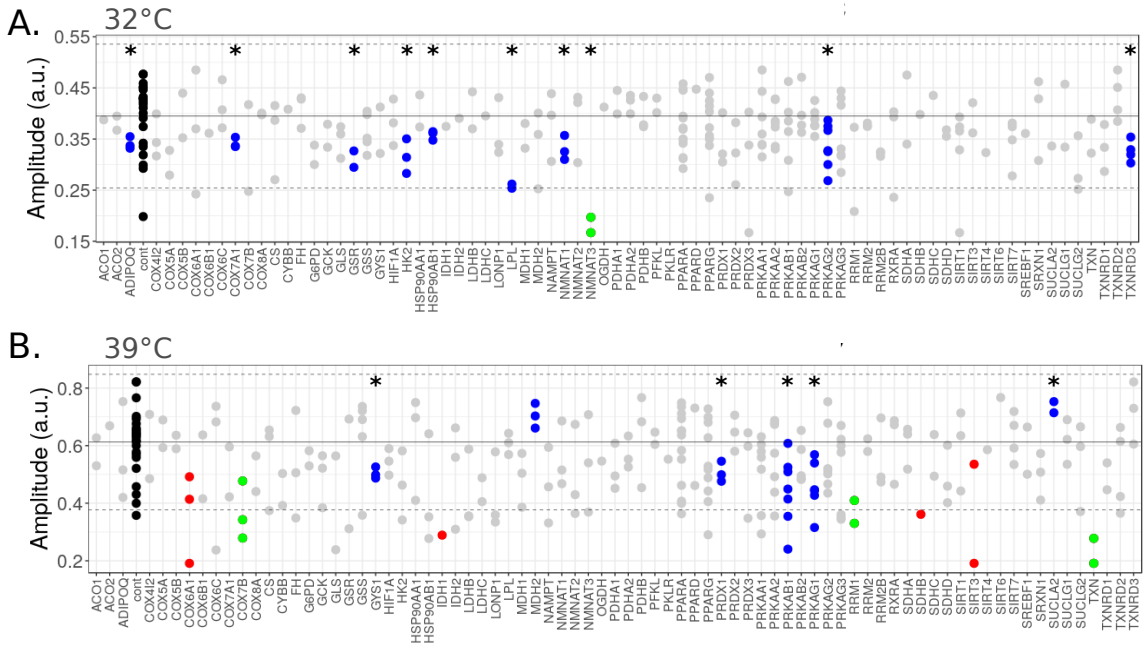

Figure 2.3: Metabolic genes that modulate oscillation amplitude in *Bmal1-luc* U-2 OS cells at 32°C (A) and 39°C (B). See caption of Figure 2.2 for details (on color-coding, lines, asterisks, etc.). n=1 single biological experiment with 2–14 shRNA constructs used for each genetic knockdown.

Modulation of damping rate

As for the damping of the oscillations, we found that, upon knockdown of *ACO2, COX4I2, COX6B1, CS, G6PD, HIF1A, HSP90AA1, HSP90AB1, IDH1, IDH2, LDHB, LONP1, LPL, MDH1, NMNAT3, PRX2, PRKAG1, PRKAG3, SDHD, SIRT3, SIRT7, TXNRD1* and *TXNRD3*, oscillations dampened faster at 32°C (p<0.05, t-test, or/and $|z|$>2). Oscillations were sustained longer over time at 32°C after knocking down *OGDH*. At 39°C, interference with *GSR, IDH1, LDHC, PDHA2* and *RRM1* expression resulted in faster-damping oscillations (p<0.05, t-test, or/and $|z|$>2); whereas knockdown of

COX5A and *OGDH* resulted in oscillations that were sustained longer over time (p<0.05, t-test). Knockdown of *OGDH* and *IDH1* resulted in the same phenotype in terms of damping at both temperatures. The results are shown in Figure 2.4.

A surprising observation was the overall higher oscillation amplitude of the reporter rhythms at 39°C (compare y axes in panels A and B from Figure 2.3), contrary to our initial expectation, since we *a priori* thought that the higher temperature would reduce transcriptional activity. Despite the higher amplitude rhythms, however, *Bmal1-luc* cells dampened faster at 39°C (Suppl. Figure A.3).

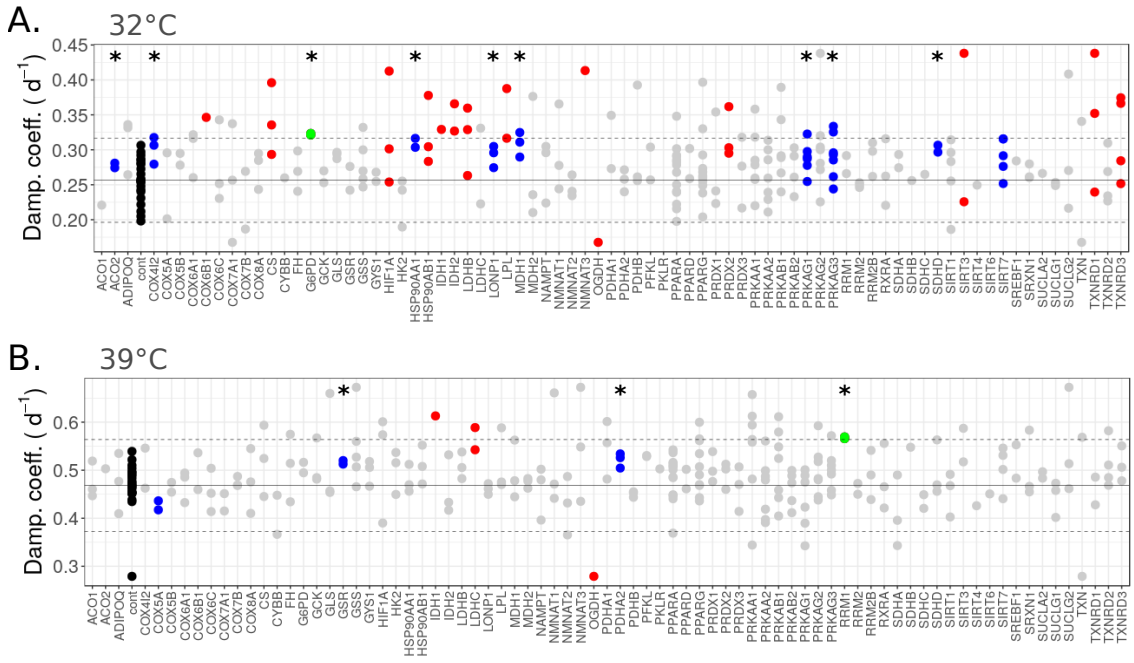

Figure 2.4: Metabolic genes that modulate damping rates of oscillations in *Bmal1-luc* U-2 OS cells at 32°C (A) and 39°C (B). See caption of Figure 2.2 for details (on color-coding, lines, asterisks, etc.). n=1 single biological experiment with 2–14 shRNA constructs for each genetic knockdown.

Setting a p-value threshold of 0.05 implies that there is a 5% chance that the result is a false positive and, in the same way, choosing an absolute z score value >2 as threshold also means that 5% of the observations are expected to lie more than two SD away from the mean just by chance. While 5% is acceptable for one test, if there are multiple tests performed on the data, like in our scenario, this 5% can result in a large number of false positives. There are a number of approaches to overcome the multiple testing problem and they all attempt to reduce the p-value threshold to a more reasonable value by assigning an "adjusted" p-value. Many traditional techniques such as the Bonferroni correction are very conservative in the sense that, while they reduce the number of false positives, they also reduce the number of true discoveries. False Discovery Rate-(FDR-) controlling procedures are less conservative and have a greater power to find truly significant results. The Benjamini-Hochberg procedure is a powerful tool that decreases the FDR [269]. It determines the adjusted p-values (referred to as q-values) for each test

but controlling the number of false discoveries in those tests that result in a discovery (i.e., a significant result). To control the FDR at any specified level, say 25%, one simply chooses the cases with q-value <0.25 as discoveries. The FDR-corrected q-values are also shown in Figures 2.2, 2.3 and 2.4, and hits at a FDR = 25% are indicated with asterisks.

To sum up, from this section we learned that some metabolic genes seem to be important in maintaining the period, amplitude or damping of the oscillations in *Bmal1-luc* cells. *LONP1, MDH2, PDHA1* and *SUCGL2* were found as common period hits at 32°C and 39°C and others, like *COX5A, HK2, SIRT1*, etc., showed a strong phenotype at one of the temperatures (Figure 2.2). We did not find any genes whose knockdown resulted in amplitude-effects at both temperatures, but we did find that knockdown of *LPL* or *TXNRD3* decreased and knockdown of *MDH2* increased the oscillation amplitude at 32°C and 39°C, respectively. As for the damping of the oscillation, we found that knockdown of *IDH1* and *OGDH* in *Bmal1-luc* U-2 OS cells resulted in oscillations that dampened faster or that were sustained longer over time, respectively, at both temperatures.

2.3.2 Knockdown of metabolic genes affects period compensation against temperature steps

Having found certain metabolic genes whose knockdown affected oscillation parameters, we next tested our main hypothesis. We analyzed the change of period with temperature to evaluate whether any of the genetic metabolic perturbations resulted in a greater sensitivity of our reporter cell system to temperature. If so, the slope of a period vs. temperature plot, after a specific knockdown, would change with respect to the slopes of the negative controls (which would have, in case of perfect temperature compensation, slope = 0). In order to account for the variability among plates and to be able to average the slopes of the non-silencing controls, we normalized the period values to the period at 32°C and determined the relative $\Delta\tau$ for each construct as follows,

$$\text{relative}\,\Delta\tau = \frac{\tau_{39^o\text{C}} - \tau_{32^o\text{C}}}{\tau_{32^o\text{C}}} \tag{2.2}$$

where τ represents the period of the oscillation. This new parameter serves as a proxy for the slope and thus is an indicator of how well the period of the system is compensated against temperature steps. In case of perfect compensation, we expect a relative $\Delta\tau$=0.

Again, we focused on genes where the RNAi constructs generated consistent phenotypes, this is, on genes where either the p-value of the t-test performed between the RNAi constructs targeting the same gene and the negative controls was <0.05; or where at least two constructs showed a z score >2 or <-2. The results are depicted in

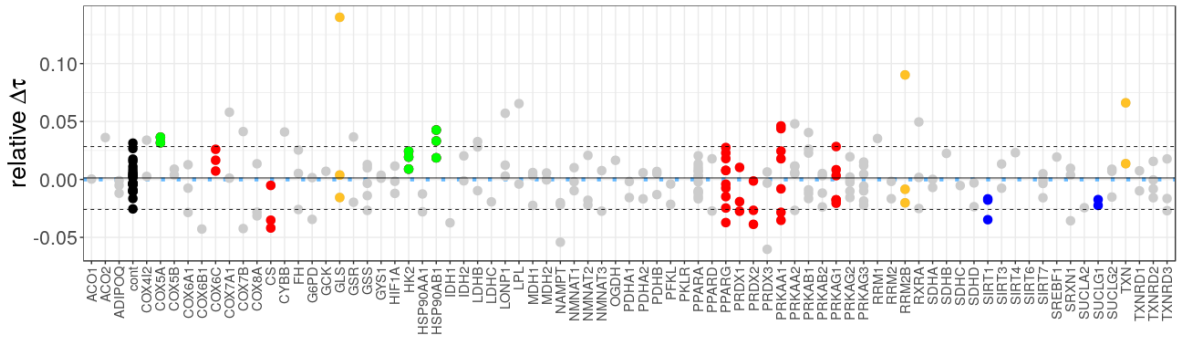

Figure 2.5: Knockdown of some metabolic genes resulted in the loss of the temperature compensation property in *Bmal1-luc* U-2 OS cells. Quantile-normalized data is represented here since all plates were analyzed together to find putative hits. Period sensitivity to temperature steps was calculated as shown in Equation 2.2. Depicted in yellow are genes that were potentially interesting because of the extreme phenotype observed for one of the constructs. The black horizontal lines depict the mean relative $\Delta\tau$ value of cells transduced with non-silencing constructs (continuous) ± 2 SD (dashed). The light blue dotted line indicates the situation of perfect compensation, where the period length at 32°C coincides with the one at 39°C. See caption of Figure 2.2 for further details (on color-coding, lines, etc.). n=1 single biological experiment with 2–14 shRNA constructs for each genetic knockdown.

Figure 2.5. The black horizontal line centered approximately at relative $\Delta\tau$=0 indicated that the period length of cells transduced with negative non-silencing controls did not change with temperature, suggesting that our reporter system seemed to be very well compensated against temperature changes.

The knockdown of *COX5A, COX6C, CS, HK2, HSP90AB1, PPARG, PRX1, PRX2, PRKAA1, PRKAG1, SIRT1* and *SUCLG1* resulted in a significant change in the period sensitivity to temperature as seen by the blue (p-value <0.05), red (at least two constructs reported a z score >2 or <-2) and green (both previous conditions met) points in Figure 2.5. Even though knockdown of *GLS, RRM2B* and *TXN* did not result in a significant change in the slope compared to the negative controls, they might also be interesting because of the extreme relative $\Delta\tau$ value observed for some of the constructs and, for this reason, they are marked in yellow in Figure 2.5. More specifically, the clock fastened at 39°C when *CS, PPARG, PRX1, PRX2, SIRT1* and *SUCLG1* were knocked down (as seen by lower values of relative $\Delta\tau$ compared to those the non-silencing controls), whereas it slowed down with temperature upon knockdown of *COX5A, COX6C, GLS, HK2, HSP90AB1, PRKAA1, RRM2B* and *TXN*. Suppl. Figure A.4A shows the detrended oscillations from each scenario and Suppl. Figures A.5 , the individual slopes of relative $\Delta\tau$.

The problem of multiple testing was again evident in this analysis. An interesting observation was that some of the hits that seemed to modulate the response of the circadian system to period compensation against temperature changes also played a role in maintaining the oscillator's period (as discussed in the previous Section 2.3.1). Because of this, we hypothesized that those genes where the knockdown had a significant effect in an oscillation parameter at one (or both) temperature(s) and on the response

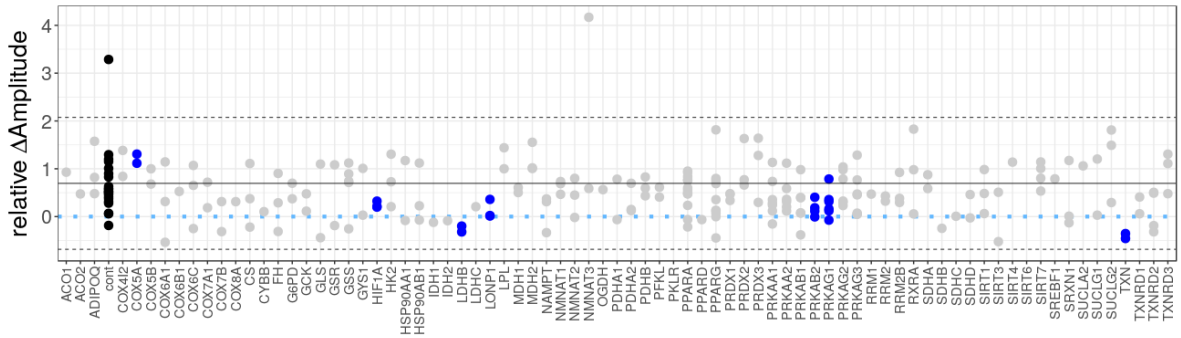

Figure 2.6: Amplitude seemed to increase in order to maintain a constant period upon temperature steps in *Bmal1-luc* cells, and interfering with the expression of some metabolic genes perturbs this amplitude response. Amplitude sensitivity to temperature steps was calculated as shown in Equation 2.2, but using the amplitude of the fit instead of the period. See caption of Figure 2.2 for details (on color-coding, lines, etc.). n=1 single biological experiment with 2–14 shRNA constructs for each genetic knockdown.

to temperature sensitivity were more likely to be true discoveries (although overlap purely by chance cannot be ruled out). Some candidates were *COX5A, HK2* (when knocked down, temperature compensation was partially lost and the clock ran slower at 39°C, which is consistent with the larger period observed at the high temperature, Figure 2.2B); *SIRT1* (the clock ran faster with temperature, consistent with the decrease in period length at 39°C observed when the gene was knocked down, Figure 2.2B) or *SUCLG1* (the clock ran faster at 39°C, consistent with the period lengthening at 32°C upon knockdown in *Bmal1-luc* cells, Figure 2.2A).

As explained in Section 2.1.1, the "temperature-amplitude coupling hypothesis" proposes that, as temperature increases, the compensation mechanism might increase the amplitude of the oscillator to maintain a constant period [243, 244]. Therefore, we next performed the same slope analysis but this time on the amplitude of the oscillation, and calculated relative ΔA with Equation 2.2. The results are depicted in Figure 2.6. The black horizontal line this time was at relative ΔA~0.70, indicating that the amplitude of the negative control oscillators increased with temperature while the period did not change (Suppl. Figure A.3). Taken together, the results from *Bmal1-luc* cells support the temperature-amplitude coupling hypothesis.

Interestingly, knockdown of some genes resulted in significant changes in the amplitude response to temperature compared to the negative controls. (i) Knockdown of *COX5A* resulted in a bigger amplitude increase with temperature (and also in a loss of period robustness against temperature). (ii) Although the amplitude of the oscillations upon knockdown *HIF1A, LONP1, PRKAB2* or *PRKAG1* slightly increased with temperature, the increase was significantly lower than the one observed in the negative controls. Lastly, (iii) knockdown of *LDHB* and *TXN* resulted in significant decreases of the oscillator amplitudes (relative ΔA<0), with the latter showing a loss of period robustness to temperature changes as well. Suppl. Figures A.4B and A.6 show the oscillations and the increase/decrease of relative ΔA with temperature in the hits.

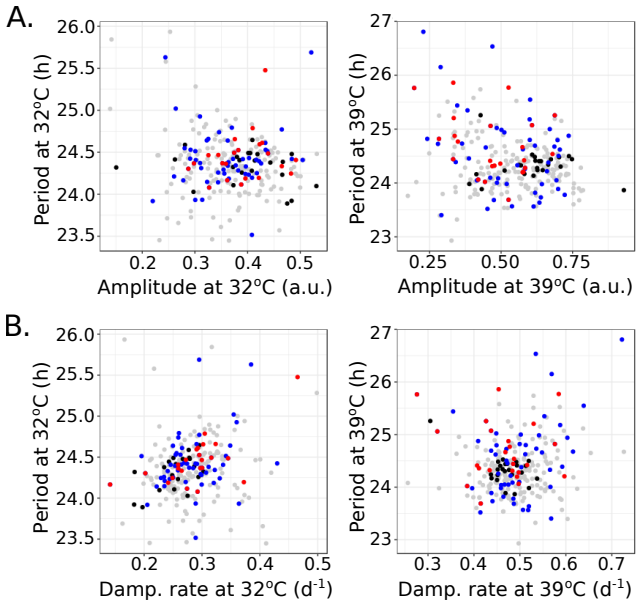

Figure 2.7: Relationship between amplitude or damping coefficient and period of the oscillation in *Bmal1-luc* cells. (**A**) Period values were plotted against amplitude values at 32°C (left) or 39°C (right panel). (**B**) Period values were plotted against damping coefficients at 32°C (left) or 39°C (right panel). Parameter values were estimated after detrending and fitting the raw data to Equation 6.2 with the ChronoStar V3.0 software, as described in Section 6.3. Values were quantile-normalized. Black: negative controls; blue: genes whose knockdown might have an effect on the period homeostasis upon temperature steps; red: genes whose knockdown might have an effect on the amplitude homeostasis upon temperature changes.

2.3.3 Low amplitude oscillations are associated with high period variability

Zhang *et al.* argue that low-amplitude traces usually exhibit poor curve fitting and generate inconsistent period length data [270]. Among theoreticians, the relationship between period and amplitude is known as "twist" [271]. We asked the question of whether there was any relationship between the period and amplitude (i.e., twist) or damping of the oscillation. We found that low amplitude oscillations generated more variability in period lengths, whereas the period of large amplitude oscillations was typically less variable, especially at 39°C (Figure 2.7A). The correlation between faster or slower damping and period variability was not so clear. Some fast-damping oscillations were also more variable in terms of period than those that were sustained longer in the time course and, typically, high values of damping coefficients were associated to higher period lengths (Figure 2.7B).

The circadian parameter values (period, amplitude damping rate) were obtained by fitting the oscillatory time series to an exponentially decaying sinusoidal equation as described in Section 6.3. Yet, we still checked whether there was any kind of period trend throughout the cycles of each individual time series. We found that the peak-to-peak distance was stable in the oscillatory time series and that the fits gave accurate estimates of the overall oscillation period (Appendix A and Suppl. Figures A.9, A.10).

2.3.4 Oscillation parameters differ in different reporter cells

The same experiments and analyses were done with U-2 OS cells harboring a second reporter, namely *Per2-luc*. *Per2-luc* oscillations were less robust than *Bmal1-luc* rhythms (Suppl. Figures A.1 and A.2). We found some overlaps in the effect of metabolic knockdown on oscillation parameters in *Bmal1-luc* and *Per2-luc* cells (Suppl. Figure

A.7). For example, knockdown of *LDHC* and *TXN* resulted in the same effect on period length at 39°C; knockdown of *MDH2* affected in a similar way the amplitude and period of the oscillation at 39°C in both reporter cells; and lastly interference with *COX5A* expression resulted in faster damping oscillations in both reporter cells at 39°C as well. However, to our surprise, we found that knockdown of some genes such as *COX5A* or *HSP90AB1* produced opposite period phenotypes in *Bmal1-luc* and *Per2-luc* cells. Regarding those genes whose knockdown resulted in a temperature compensation response, we observed interesting overlaps such as *PRX1* and *SUCLG1*.

Figure 2.8 shows the distributions of periods, amplitudes, damping rates and phases at 32 (blue) and 39°C (red) in both *Bmal1-luc* (top) and *Per2-luc* (bottom) reporter cells. Interesting and rather striking results, contrary to our expectations, were (i) the different period values of the negative controls observed in *Bmal1-luc* and *Per2-luc* cells, and (ii) the difference in period response to temperature steps in the reporter cells. Whereas the overall period did not change with temperature in *Bmal1-luc* cells (24.37±0.51 h at 39°C and 24.37±0.35 h at 32°C, mean±SD, Q_{10}=0.996), thus meaning that these cells are very well temperature-compensated, we observed that *Per2-luc* rhythms were 1 h slower at 32°C and ran significantly faster at 39°C (23.16±1.71 h at 39°C and 25.53±0.90 h at 32°C, mean±SD, p<0.00001, *t*-test; Q_{10}=1.15) (Figure 2.8B). The decrease in period length at 39°C in *Per2-luc* cells was an overall effect, meaning that even negative control cells ran faster at the high temperature (see Appendix A and Suppl. Figure A.11).

With regard to the phase of the oscillation, as expected, *Bmal1-luc* and *Per2-luc* rhythms oscillated in antiphase. *Bmal1-luc* oscillations peaked ~13 h after *Per2-luc* rhythms at 32°C, consistent with the phases of PER2 and BMAL1 observed in CircaDB [272]. Nevertheless, at 39°C, the bioluminescence bursts from *Bmal1-luc* cells occurred only ~7 h after the bursts from *Per2-luc* cells. In addition, the phase difference between the hot and the cold temperatures in both reporter cells was different: ~6 h in *Bmal1-luc* cells (probably because the bioluminescence recording was started ~6 h later), but ~9 h in *Per2-luc* cells. This observation, although rather surprising, agrees with experimental and computational results that argue that period shifts (like the one observed at the high temperature in *Per2-luc* cells) can induce even greater phase shifts [22, 273], and thus these results might also be interesting from a theoretical point of view.

In *Bmal1-luc* U-2 OS cells, the overall amplitude increased at the high temperature (0.54±0.14 a.u. at 39°C and 0.36±0.06 a.u. at 32°C, mean±SD, p<0.00001, Kolmogorov-Smirnov test and *t*-test) but, as mentioned before, the oscillations dampened faster (0.49±0.06 day^{-1} at 39°C and 0.28±0.04 day^{-1} at 32°C, mean±SD, p<0.00001, *t*-test). As for *Per2-luc* reporter cells, Figure 2.8B shows that the amplitude did not significantly change with temperature (0.21±0.07 a.u. at 39°C and 0.21±0.05 a.u. at 32°C, mean±SD). Opposite to *Bmal1-luc* cells, the mean damping coefficient decreased with temperature (0.63±0.22 day^{-1} at 39°C and 0.85±0.19 day^{-1} at 32°C, mean±SD p<0.00001, *t*-test).

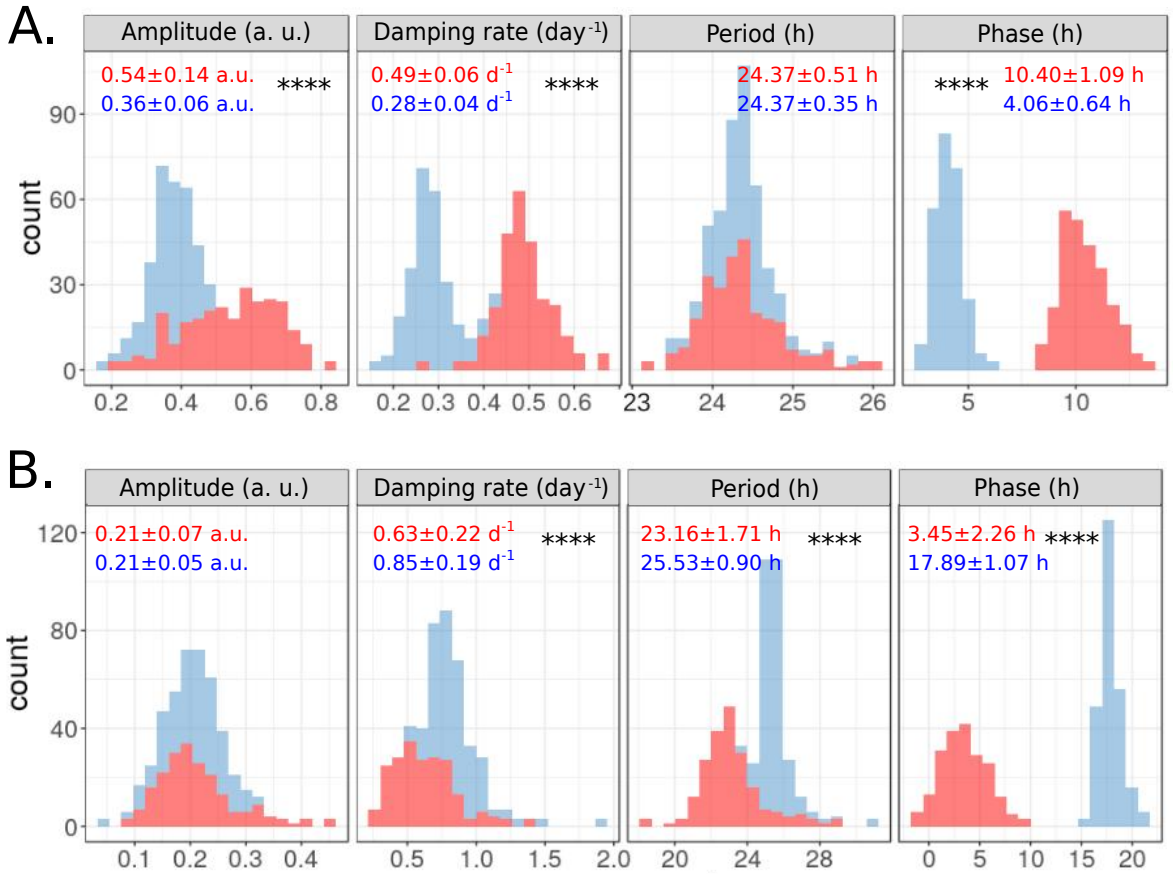

Figure 2.8: Distributions of the circadian parameter in *Bmal1-luc* (A) and *Per2-luc* (B) reporter cells at 32°C (blue) and 39°C (red). The parameter values of all three plates were pooled together in each histogram and hence, in order to account for plate-to-plate variation, quantile-normalized parameter values are represented here (after quality control and trend removal on raw data as described in Section 6.3). Mean±SD are shown in each panel, for $n = 288$ wells in 1 biological experiment. Asterisks denote p<0.00001, *t*-test. See main text for details.

The differences in periods, amplitudes and damping coefficients in the reporter cells were rather surprising. Since both *Bmal1-luc* and *Per2-luc* cells belong to the same U-2 OS cell line (despite different clonal lines), we would have expected (maybe naïvely) to find similar values in both reporters. Nevertheless, it is not the first time that different circadian parameters are observed in different reporters experimentally [274, 275]. As in [270], *Bmal1-luc* cells oscillated more robustly than *Per2-luc* cells (Suppl. Figure A.1). It should be remarked, however, that the results from *Per2-luc* cells at 32°C might not be very reliable, as the low values of GFP expression measured before bioluminescence recording suggest that the transduction might not have been fully successful.

2.4 Discussion

Temperature compensation has long been a defining characteristic of circadian oscillators. But a biological oscillator that functions as a reliable timekeeper should not only be stable to changes in temperature, but also to other environmental or metabolic

fluctuations. The rates at which biochemical systems operate are greatly affected by metabolite concentrations, and thus an accurate timekeeping machine should be capable to compensate for and adapt to the metabolic fluctuations it encounters. Given the number of studies dedicated to the link between clocks and metabolism, it is somehow surprising that this insight has not been subject of analysis. Nevertheless, studies on cyanobacteria, *Neurospora* and mammalian cells in culture have shown that cellular circadian clocks are resilient to changes in ATP, glucose or overall transcription rates, respectively [51, 53, 264].

In collaboration with Prof. Dr. Carl Johnson, we tested Pittendrigh's old proposition that temperature compensation is part of a larger phenomenon that also confers circadian oscillators robustness to metabolic changes. On the basis of this metabolic compensation proposition, we hypothesized that if resilience to temperature or metabolic fluctuations are part of the same phenomenon, then interfering with cellular metabolism would render the circadian system more sensitive to temperature perturbations. Our approach was to perturb metabolism via RNAi-mediated knockdown in a small scale screen. We knocked down a total of 78 genes involved in metabolically relevant pathways such as glycolysis (*HK, PFKL, PDH*, etc.), phosphate pentose pathway (G6PD), oxidative phosphorylation (subunits of the cytochrome c oxidase complex), NAD^+ production (*NAMPT, NMNAT1*), maintenance of the cellular redox state (peroxiredoxin or thioredoxin reductase isoforms), as well as genes whose products have been shown to integrate the clock with cellular metabolism and bioenergetics (sirtuins, PPARs and AMPK subunits).

2.4.1 Temperature compensation is modulated by metabolism

We found that several genes involved in cellular metabolism play a key role maintaining the period relatively robust to temperature steps. For example, knockdown of *PRX1, PRX2* and *TXN*, genes encoding antioxidant proteins, made the cell culture model system more sensitive to temperature changes (Figure 2.6). The NAD^+-dependent deacetlyase *SIRT1*, and several AMPK subunits (*PRKAA1* or *PRKAG1*) were also found to modulate the response to the temperature step (Figure 2.6). Although the list regulators of temperature compensation does not finish here, these are of particular interest because of their roles in modulating the clock. SIRT1 has been shown to control circadian clock gene expression through PER2 deacetylation [135] and AMPK transmits energy-dependent signals to the mammalian clock by driving phosphorylation and destabilization of CRY proteins. In addition, AMPK subunit, composition, subcellular localization and substrate phosphorylation are dependent on circadian time (for a complete review see [276]); and altered AMPK signaling has been identified as a mechanism leading to liver clock disruption in mathematical models [277]. As for the role of PRXs in the clock, it is becoming evident that there is a reciprocal interplay between PRX and the TTFL, as seen by the observations that *Arabidopsis* mutants lacking *prx* genes display TTFL rhythms that are altered in phase or amplitude [37]. Our results

add a level of complexity to this picture, in that these proteins not only regulate the clock, but might be the sensor by which cellular clocks adjust and compensate the period to changes in intracellular metabolic rates and extracellular fluctuations. Nevertheless, these results are preliminary, and although they confirm our initial predictions, they should be confirmed with genetic knockout or pharmacological perturbation studies.

We have also shown that the amplitude of oscillations seems to increase with temperature, supporting (*a priori*) the temperature-amplitude coupling hypothesis [243, 244]. Furthermore, knockdown of some metabolic genes which are involved in the same processes as mentioned before (e.g., *PRKAG1, TXN*) did not only interfere with period homeostasis, but also disturbed the oscillator's response to temperature in terms of amplitude (Figure 2.6). Nevertheless, one has to be careful in speculating about the temperature-amplitude coupling hypothesis. It cannot be ruled out that the dexamethasone stimulus used to synchronize the cells might have had a differential effect on the cell culture system at the higher temperature. In order to exclude dexamethasone-induced artifacts, the experiments should be done in single cells in the absence of synchronizing agents. Also related to the temperature-amplitude coupling hypothesis is the proposition that, if it were true, one would expect changes in amplitude if the model system loses its period compensation to temperature steps. This is true for some but not all knockdown phenotypes. For example, knockdown of *COX5A, PRKAG1* or *TXN* interferes with the period homeostasis and also disturbs the oscillator's response to temperature in terms of amplitude.

2.4.2 Metabolism regulates the mammalian clockwork

Studies over the last years have shown that metabolic regulation is not a mere output function of the circadian system. Rather, nutrient, energy and redox levels signal back to cellular clocks in order to reinforce circadian rhythmicity and to adapt physiology to temporal tissue-specific needs (for a detailed review on the crosstalk between metabolism and circadian clocks, see [74]). The results presented here support the role of metabolism in regulating the circadian clock. We identified several metabolic genes that control oscillation parameters. Among others, we found that *SIRT1* and *PRKAB1* (an AMPK subunit) control the period length (Figure 2.2). In addition, oscillation amplitude was decreased by knockdown of the AMPK subunits *PRKAAB1, PRKAG1, PRKAG2*, enzymes involved in NAD synthesis *NMNAT1, NMNAT3* and genes coding for proteins that maintain the cellular redox state (*PRX1, TXNRD3*) 2.3. These results highlight the role of metabolism in feeding into and regulating the circadian clockwork.

2.4.3 Does temperature increase damping?

The faster damping observed at the high temperature also deserves some discussion. The optimal temperature for the luciferase-luciferin reaction is 28°C and the reaction slows down perceptibly at higher temperatures (according to Sigma Aldrich's instructions), so the faster damping could be a result of an impaired luciferase activity. From a theoretical perspective, faster-damping oscillations might occur due to (i) weakly-coupled single-cell oscillators that decouple over time and/or (ii) high period heterogeneity in the cell population [278–282]. In these lines, weak coupling of oscillators at the high temperature might explain the faster damping but, if this is true, then dexamethasone-mediated amplitude increase is not likely to be the explanation of higher amplitude at high temperatures, and the support of the temperature-amplitude coupling hypothesis is then again plausible. Although the Takahashi and Kramer laboratories have proposed that there is a considerable heritability in oscillation period within the same cell line [283, 284], we cannot rule out a high period heterogeneity in the cell population at this stage, as this could also explain the faster damping. Computer simulations might help to differentiate these scenarios and might give hints to look for traces in the data.

2.4.4 Different reporters, different circadian parameters?

Another interesting, yet striking, observation was the different results obtained in both reporter cells. While *Bmal1-luc* cells were very well temperature-compensated, with a Q_{10} = 0.996, *Per2-luc* cells were more sensitive to variations in temperature, showing a Q_{10} = 1.15 (Figure 2.8). This number is still considered in the range of temperature compensation, although it stands in the upper limit (temperature compensation consensus for $0.85 < Q_{10} < 1.15$). A reason for such period changes could be different coupling strengths [281, 282] between cells at 32 or 39°C although if this were true, we would, in principle, expect the same coupling behavior in *Bmal1-luc* reporter cells. The distinct periods of the two reporter cells could be explained by different clonal lines. In order to confirm and validate that *Bmal1-luc* and *Per2-luc* reporters indeed display different periods, one would have to show oscillations in the same cell/cell culture and in the same experiment (ideally with reporters of different colors).

Nevertheless, these are not the first observations suggesting that different reporters might produce distinct results. Ono *et al.* reported differences in the circadian period of *Per1* and *Bmal1* rhythms in SCN slices from double-transgenic mice carrying reporters for both *Per1* and *Bmal1* expression, and they showed that the response of both rhythms to a light pulse was also different [274]. Moreover, Myung *et al.* also observed differences between periods and resistance to perturbations in mouse SCN explants expressing *Bmal1-ELuc* or those expressing PER2::LUC [275]. Theoretical studies propose that such dissociation of rhythms can occur when interlocked feedback loops (like the complex network in the mammalian circadian clockwork) "decouple" from each other [285, 286].

In fact, when dissociated rhythms (i.e., with two different frequencies) are plotted against each other, figures like the one from the cover of this dissertation emerge.

2.4.5 Concluding remarks

To summarize, in the present chapter we have analyzed the role that metabolic perturbations have on temperature compensation to try to elucidate if there is a common mechanism underlying both forms of compensation and if they are somehow intertwined. Preliminary unpublished results from the Johnson lab show that mutations that suppress the temperature compensation property in cyanobacterial circadian oscillations result in the oscillators being more sensitive to metabolic perturbations. We asked ourselves the opposite question, i.e., whether interference with metabolism via RNAi will render the model system more sensitive to temperature changes, and found that, for some metabolic perturbations, this indeed seems to be the case. We identified several genes that code for proteins involved in important metabolic pathways that might play a key role in maintaining the period relatively robust to temperature changes. Among these hits we found genes coding for PRX isoforms, AMPK subunits as well as members of the family of sirtuins. The results highlight the link between energy sensing, redox state and the circadian clock, which is nowadays a hot topic in chronobiology. These candidate genes might hint towards mechanisms by which the mammalian circadian clockwork senses and compensates for environmental and metabolic fluctuations. Thus, the link between temperature and metabolic compensation might reside in the mechanisms by which cells sense energy levels or redox state.

Of course, it is still an open question whether metabolic and temperature compensation are actually connected and whether the mechanisms underlying both forms of compensation are shared. Further studies are required to understand these processes and the phenotypes observed upon genetic knockdown should be reproduced and confirmed with experiments that interfere with metabolism in different ways. Pharmacological perturbation of metabolism could be a starting point. An interesting question that arises in the face of pharmacological perturbation experiments is whether the effects of drugs will have differential time-of-day effects. In this regard, it would be interesting to study metabolic phase-response curves and their relation to temperature compensation.

To close up, we have shown in this chapter that clocks might be equipped with metabolic sensors involving PRX, SIRT or AMPK pathways that might adjust circadian rates upon perturbations. Nevertheless, it remains to be understood how timekeeping systems are buffered against metabolic noise, but deciphering these mechanisms this will hopefully aid the efforts to understand temperature compensation.

Tempelhofer Feld

:

3

Modeling Circadian Redox Oscillations

3.1 Redox Oscillations: A Brief Overview

The approximate 24 h timing circuits that exist in all forms of life are believed to be organized through a transcription-translation feedback loop (TTFL) and additional regulatory interactions that derive from this primary rhythm-generating loop. However, accumulating evidence reinforces the notion that transcription-independent processes also contribute to, and can even generate circadian rhythmicity. These non-canonical oscillator mechanisms include the cyanobacterial KaiABC phosphorylation clock [35], or the circadian oxidation of peroxiredoxin (PRX) proteins [36]. The focus of this chapter are rhythms in peroxiredoxin oxidation. It is becoming evident that redox oscillations and TTFL rhythms regulate each other, but how the interaction of both oscillators cooperatively confers accurate timekeeping to organisms remains unknown, and will be addressed in the next chapter.

3.1.1 Redox homeostasis is central to life

For many years, the traditional view of oxidative stress was that the production of oxidant molecules was deleterious for the cell. It was thought that generation of reactive oxygen species (ROS) was unregulated and that their intracellular targets were random. However, today we know that this picture is two sided. On one hand, excessive oxidative stress can induce damage in biomolecules but, on the other hand, maintenance of a physiological level of oxidant challenge is essential in life processes through redox signaling [287]. Because aerobic metabolism is not entirely efficient, ROS are produced as inevitable by-products in what could be considered a trade off for the advantages

of metabolizing oxygen [288]. Mitochondrial respiration is a major source of ROS production. Approximately 2% of the electrons that pass through the mitochondrial electron transport chain "leak" and combine with oxygen to form unstable forms of the molecule known as reactive oxygen species (ROS) [289]. But not only mitochondria are big producers of ROS: other biochemical nanomachines such as the NADPH oxidase, used by neutrophils to engulf microorganisms, also result in the generation of these small reactive molecules [290].

As a central oxidant in redox homeostasis, hydrogen peroxide (H_2O_2) is membrane-permeable and has the highest stability among the physiologically relevant ROS [288, 291]. At physiological concentrations (in the range of nanomolar to low-micromolar), intracellular H_2O_2 can reversibly oxidize redox-sensitive cysteine (Cys) residues. It can act as a second messenger by oxidizing and inactivating such residues in active sites of cellular enzymes [292]. Phosphotyrosine phosphatases are a family of enzymes whose activity is regulated by the redox state. These enzymes contain an essential cysteinyl residue in their active site which, unless inactivated, executes a nucleophilic attack on phosphotyrosyl residue substrates [290, 293]. But the high reactivity of the catalytic Cys also predisposes the protein to inactivation via oxidation mediated by H_2O_2. Thus, this oxidant behaves as a redox-signaling molecule that provides the specificity in time and place which is required in signaling, thereby transmitting information about the cellular redox state to specific substrates, and ultimately regulating their activity [290, 293]. At higher concentrations, however, H_2O_2 oxidizes the glutathione pool and activates oxidative stress responses, both through a rapid rerouting of cellular metabolism and transcriptional responses [294–296]. Even higher concentrations of H_2O_2 can become toxic due to induction of single- and double-stranded DNA breaks, oxidative decarboxylation of α-ketoacids such as pyruvate, lipid peroxidation, or irreversible denaturation of proteins. To protect themselves from this barrage of ROS production, cells invest in antioxidant systems such as catalases, methionine sulfoxide reductases, glutathione peroxidases and peroxiredoxins [292]. But these antioxidant systems in turn require a steady state supply of reducing equivalents such as NAD(P)H and reduced glutathione.

In addition, a vast number of cellular processes are dependent on the local availability of appropriately reduced or oxidized redox cofactors. For example, anabolic routes are dependent on NAD^+ or FAD^+, and catabolic routes require NADPH [297]. Moreover, sirtuin-regulated deacetylation is dependent on NAD^+ [135, 298]. Another example of redox regulation is represented by eukaryotic compartmentalization. Some organelles, like the endoplasmatic reticulum or peroxisomes, exist in a more oxidized state than the cytosol or the nucleus. Thus, if a molecule is to be transported from a more reduced organelle to a more oxidized compartment, redox resources will inevitably be used to regulate this transport.

In summary, the pool of reducing and oxidizing equivalents in the intracellular milieu is constantly fluctuating to adapt to the cellular metabolic demands. When the exquisite regulation in redox homeostasis fails, cell death, apoptosis or necrosis is inevitable. In this regard, chronic oxidative stress and misregulation of redox balance underlie several theories of aging and, like circadian dysregulation, are associated with a large number of diseases including cancers, metabolic disorders and cardiovascular disease [299–301].

3.1.2 Biochemistry of peroxiredoxins

Peroxiredoxins (PRXs) are small (20-25 kDa) antioxidant enzymes that are ubiquitously expressed in virtually all aerobic organisms [302, 303]. The broad distribution of Prxs together with their high expression levels suggest that they are both an ancient and an important enzymatic family [302]. Peroxiredoxins, like catalases or glutathione peroxidases, catalyze the reduction reaction of H_2O_2 and other peroxides and maintain the cellular redox homeostasis. Prxs are classified by the number of Cys residues directly involved in catalysis: 2-Cys Prxs and 1-Cys Prxs [302]. Type 2-Cys Prxs are purely Cys-based peroxidase enzymes with no cofactor requirements, and they are divided into typical (mammalian Prx1-4) and atypical (Prx5) groups based on the catalytic mechanism.

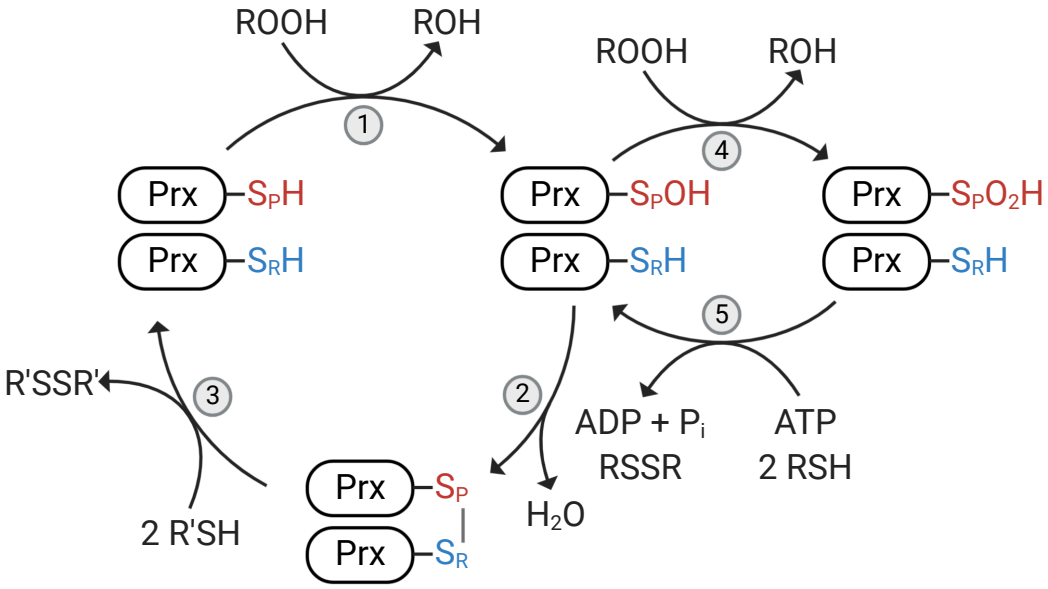

Figure 3.1: Catalytical cycle of typical 2-Cys Prxs. The peroxidatic catalytical cycle of typical 2-Cys Prxs involves three main reactions: 1 peroxidation of Cys_P by a peroxide, 2 resolution via disulfide bridge formation with Cys_R from a second subunit, and 3 recycling with the use of reducing equivalents. In some cases, the sulfenic intermediate (-SOH) enters the sulfinylation cycle in which the Cys_P-SOH, instead of condensing with Cys_R, is hyperoxidized by the peroxide into a sulfinic acid (-SO_2H) (reaction 4). Sulfinylated Prx can be reduced by an ATP dependent reduction by Srx (reaction 5). S_P and S_R denote the sulfur atoms of the peroxidatic and resolving cysteines, respectively. 2 R'SH in reaction 3 represents a thioredoxin-like protein or domain.

The enzymatic cycle of 2-Cys Prxs involves oxidation of free thiols (Cys-SH) from the peroxidatic Cys (Cys_P) by H_2O_2 to a sulfenic acid (Cys_P-SOH) with catalytic efficiencies in the order of $10^6 - 10^7\,M^{-1}s^{-1}$ [302, 303] (reaction 1 in Figure 3.1). The work of Rhee *et al.* has shown that the electrostatic environment surrounding Cys_P in the active site confers upon it a particularly low pK_a, in the order of 5 to 6 [304]. This means that the thiol group in the peroxidatic Cys_P exists mostly in the thiolate state (Cys_P-S^-). The low pK_a, in combination with the high Prx abundance (0.1-1% of total cellular protein) and the high selectivity, makes Prxs the primary sink for endogenously-produced peroxides like H_2O_2 [288, 290, 303, 304]. The oxidation of Cys_P is followed by conformational changes around its active site and subsequent condensation with the resolving Cys (Cys_R) from a second subunit (reaction 2 in Figure 3.1). The disulfide-linked homodimer can be reduced back by the thioredoxin-thioredoxin reductase system, ultimately consuming NADPH equivalents, and thus the catalytic cycle is completed [302] (reaction 3 in Figure 3.1).

In typical 2-Cys Prxs, however, a small fraction of the enzyme becomes catalytically inactivated through peroxide-mediated hyperoxidation of Cys_P to sulfinic ($-SO_2H$) or sulfonic ($-SO_3H$) acids (reaction 4 in Figure 3.1). This second oxidation occurs at a rate in the order of $10^4\,M^{-1}s^{-1}$, 100 – 1 000 times slower than the first oxidation. The sulfinic form has been demonstrated, in numerous contexts, to be reversibly reduced back to the sulfenic intermediate by sulfiredoxin (Srx), in a reaction that consumes ATP [304, 305] (reaction 5 in Figure 3.1).

3.1.3 A day in the life of peroxiredoxins

In 2011, O'Neill and Reddy published a paper that stunned the circadian community [36]. They discovered circadian rhythms of peroxiredoxin (PRX) oxidation in human red blood cells (RBCs) kept in culture. As mature mammalian red blood cells are devoid of nuclei, ribosomes and mitochondria, such cycles must have been generated independently of transcription, translation or oxidative phosphorylation processes. Moreover, and in contrast to the divergent evolution of the TTFL, it was shown one year later that these rhythms are conserved across all kingdoms of life [37] (although the quality of the antibody used to target the sulfinic acid in hyperoxidized Prx, and thus the reproducibility of results, has been a matter of debate over the last years). Rhee's laboratory then confirmed the existence of these rhythms in mouse RBCs and discovered that oxidation of PRX occurs to "clean" the erythrocyte from H_2O_2 generated as a result of hemoglobin auto-oxidation. Moreover, they showed that, instead of being reduced by the sulfiredoxin system, oxidized Prx is degraded by the 20S proteasome [306]. Thus, the cycles of hyperoxidized Prx in RBCs seem to reflect an oxidation-degradation cycle rather than a reversible redox cycle. The underlying mechanisms driving rhythmic cycles in peroxiredoxin and hemoglobin oxidation still need to be understood.

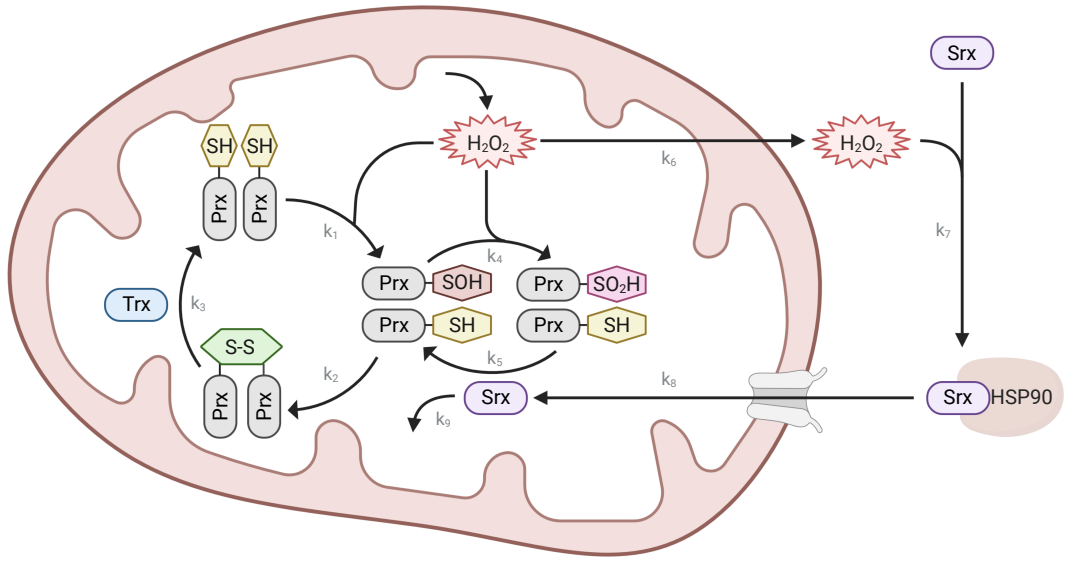

Figure 3.2: Model for mitochondrial Prx/Srx circadian redox oscillations. Model underlying daily oscillations of Prx-SO_2 and Srx levels in mitochondria from heart, brown adipose tissue and adrenal gland, as described by Kil *et al.* [307]. See main text for details.

The mechanism that generates circadian Prx redox rhythms in mammalian cells, however, seems to be different in different cell types. Unlike RBCs, sulfiredoxin (Srx) reduces hyperoxidized Prx in heart, adrenal gland and brown adipose tissue as described in Figure 3.1 [307]. Rhee's group showed that sulfiredoxin and Prx3 undergo antiphasic circadian oscillations in mitochondria from cardiac myocytes, adrenal gland cells and brown adipocytes [307]. In these major oxidative tissues, H_2O_2 production results in the oxidation and inactivation of the mitochondrial Prx3 isoform (reactions k_1 and k_4 from Figure 3.2). As the Prx3 pool becomes inactive, H_2O_2 accumulates inside mitochondria and the consequence is its overflow to the cytosol (k_6 in Figure 3.2). In the cytoplasm, H_2O_2 activates pathways to control its own production and among others, it stimulates Srx oxidation and intermolecular disulfide bridge formation with Hsp90 (reaction k_7). Hsp90 serves as a shuttle and directs Srx to mitochondria. Srx translocates into mitochondria, where it can reduce and reactivate hyperoxidized Prx3 (reaction k_5), constituting a negative feedback loop that enables a new cycle of Prx3 inactivation and H_2O_2 accumulation to start. Srx levels peak in mitochondria approximately 8 h after oxidized Prx3, and then decrease due to degradation by mitochondrial proteases (reaction k_9). Import to mitochondria and degradation determine the circadian oscillation of mitochondrial Srx. At the same time, mitochondrial Srx levels govern Prx3 activity and, consequently, mitochondrial H_2O_2 release.

Given the wide conservation of Prx proteins and their oxidation rhythms, it is likely that they emerged in evolution before the circadian TTFL. An important step is to now understand the crosstalk between the TTFL and Prx oscillations, as it is becoming

evident that a reciprocal interplay between the two exists. In one direction, embryonic fibroblasts from *Cry1,2*$^{-/-}$ mice display Prx rhythms with a longer period than those from wild type mice [36]. Moreover, in behaviorally arrhythmic *Drosophila* mutants and *N. crassa* mutants displaying a lengthened period, Prx rhythms persist but they are perturbed in phase. In the inverse direction, *Arabidopsis* mutants lacking *prx* genes show TTFL rhythms that are altered in phase or amplitude [36], and knockdown of specific PRX isoforms in human U-2 OS cells affects period length and amplitude of clock gene rhythms [270] (consistent with the results from Chapter 2). Moreover, acute treatment with high levels of extracellular oxidative stress has been shown to alter circadian rhythms in mammalian cells [54, 308, 309]. These observations bring us back to the recurring question of the interdependence of circadian and energetic systems, and how these processes communicate with each other. In summary, it seems that both clocks can run without each other, either the TTFL or the PRX system, but that for normal physiology, both need to operate. How endogenous H_2O_2 as well as Prx rhythms "communicate" with the canonical TTFL remains to be understood, and will be addressed in more detail in Chapter 4.

3.2 Aim: In Search of a Model for Redox Oscillations

This work is the first part of a wider analysis that seeks to uncover mechanisms behind the interaction between redox and TTFL rhythms from a computational perspective. As of today, there is little knowledge about quantitative details of the kinetic processes in the Prx/Srx oscillating system, and how they transmit timing information to the TTFL about the redox/energetic state of the cell. Moreover, how fast biochemical redox reactions result in 24 h rhythms is still unknown.

For this purpose, a first step in analyzing the crosstalk between Prx redox oscillations and canonical TTFL rhythms was to develop a mathematical model describing Prx/Srx oscillations, which is the focus of this chapter. We developed a robust simple, yet realistic model that explains the design principles behind the Prx/Srx circadian oscillating system. Part of the results shown in this Chapter have been published in [232]. But before jumping into the results of this project, I have chosen to give a short overview of how circadian clocks can be mathematically modeled, and what we can learn from such theoretical analyses.

3.3 How to Model Clocks? From Equations to Oscillations

Physiological rhythms are central to life. Some rhythms appear during certain phases in an individual's life, like the somite clock during embryonic development, and some others, like circadian clocks, are maintained throughout life [45]. Understanding the

mechanisms of physiological rhythms requires an approach that integrates mathematics and physiology. Of particular relevance is a branch of mathematics called nonlinear dynamics [45, 310]. Dynamics is the subject that deals with change, with systems that evolve in time. Whether the system in question settles down to an equilibrium, keeps repeating in cycles or does something more complicated, it is the theory of nonlinear dynamics what we use to analyze the behavior. The roots of nonlinear dynamics were set by Henri Poincaré at the end of the 19^{th} century, but have seen remarkable development over the past 50 years, especially in the application to biological systems.

The development of theoretical models in biology is not a recent field. Conceptual models were investigated, for example in population biology, long before the first genes were discovered. Nevertheless, with the molecular biology revolution of the 1980s, many new examples of gene regulatory or protein-interaction networks came to light. With so many feedback and feed-forward loops underlying complex dynamics of cellular processes, many questions became impossible to answer with intuitive reasoning. Thus, mathematical models gained popularity. Especially in the context of oscillations and clocks, which are the type of processes in which mathematical models give a good chance not only to describe them, but also to understand them. Through numerical simulations, models can highlight the role of key parameters in oscillations and can be used to predict the system's behavior in conditions that have not yet been experimentally tested. Mathematical models can also help in grasping the dynamic properties of molecular mechansims that are responsible for the generation of robust oscillations, both at the cellular and inter-cellular level. They even provide the tools to artificially construct biological networks that can aid in understanding the design principles in which oscillating biochemical systems are built upon. Elowitz and Leibler were pioneers on this and designed an oscillating network termed "repressilator" in *E. coli* [311].

3.3.1 Fundamentals of modeling: some important terms

Designing a model requires some understanding of the system of interest. It is necessary to gather and summarize information on what are the components and key interactions between them. Because biological systems are typically of great complexity, it is important to differentiate between essential and superfluous variables. In this sense, drawing a scheme of the system of interest is often helpful, even before formulating equations. Putting all the known information on a single picture helps us clarifying the nature of the interactions, and to order different molecular processes. Contrary to many expectations, this first step in the process of building a model is often the most laborious and time-consuming.

Although the mathematical and computer tools that are used to simulate models are standard, there is no consensus on how to construct a model. This always requires some considerations and assumptions. As modelers, there are some questions that naturally

arise when we have to write the equations. What are the key variables? How many equations should be considered? What kind of equations? Are all kinetic constants (model parameters) known? If not, how can we set them? Modelers have to make choices that depend, first of all, on the biological question we want to answer, but also on personal tastes and experiences. Simple generic models are useful to study general properties of circadian rhythms, such as coupling of large oscillator ensembles [279, 281] or the role of positive feedback loops in the generation of oscillations [312]. On the other hand, if the focus is to understand molecular details, more complex models with a larger number of variables are generated. A number of detailed models are now available for the circadian clock in mammals [102, 313–315], *Neurospora* [258, 316, 317] or *Drosophila* [318–320], among other organisms. The model, be it relatively simple, with only a few variables, or in contrast very complex, will be a precise representation of what we believe to be true. The modeler's task, as Tyson says, is "to determine whether it is a good or useful representation of that truth" [321].

Ordinary differential equations (ODEs)

Most circadian clock models are described with ordinary differential equations (ODEs). ODEs take the form

$$\frac{dx}{dt} = f(x, y, z...) \tag{3.1}$$

and they are often used to describe how a dynamical system changes over time [321]. The function $f(x, y, z...)$ describes the rate of change of a variable $x(t)$ as a function of (potentially) all the variables $x, y, z...$ that define the dynamical system. $f(x, y, z...)$ is typically a nonlinear function that depends on time-dependent variables $(x, y, z...)$ and on a number of time-independent parameters. For example, $x(t)$ might stand for mRNA or protein concentrations, whose evolution depends on parameters that have a physical interpretation, such as the rate of synthesis, degradation, modification, complex formation, transport, etc.

Using standard chemical mass action and enzymatic kinetics, we can convert the network diagram that we have drawn from the biological system into a set of ODEs. In such equations, concentrations of variables (i.e., the reactant species) are associated with rates of biochemical reactions (transcription, translation, degradation, phosphorylation, etc.). The equations can then be solved numerically, this is, by letting the computer work out the implications of the complex feedback and feed-forward loops in the network, without having to solve the system analytically.

One of the simplest and most famous ODE-based oscillator models is the one imagined by Goodwin [322]. In 1965, when Goodwin developed his model, the molecular mechanisms of circadian clocks were not yet known. He proposed the model as a generic biomolecular oscillator. The Goodwin model is based on a delayed negative feedback loop, where the final product of a 3-step chain of reactions inhibits the production of the first component (Figure 3.3A, B). This generic model can be seen as the minimal molecular model for circadian oscillations, as it accounts for the negative feedback exerted by PER and CRY proteins in their own genes. In the context of circadian rhythms, the model is interpreted as follows: a clock gene mRNA (x) produces a clock protein (y) that, in turn, activates a transcriptional inhibitor (z) that represses the synthesis of the x mRNA, closing the negative feedback loop. This simple generic model is still used today to describe fundamental properties of the core circadian oscillator [312, 323, 324], or the synchronization of an ensemble of coupled circadian oscillators [279, 325, 326].

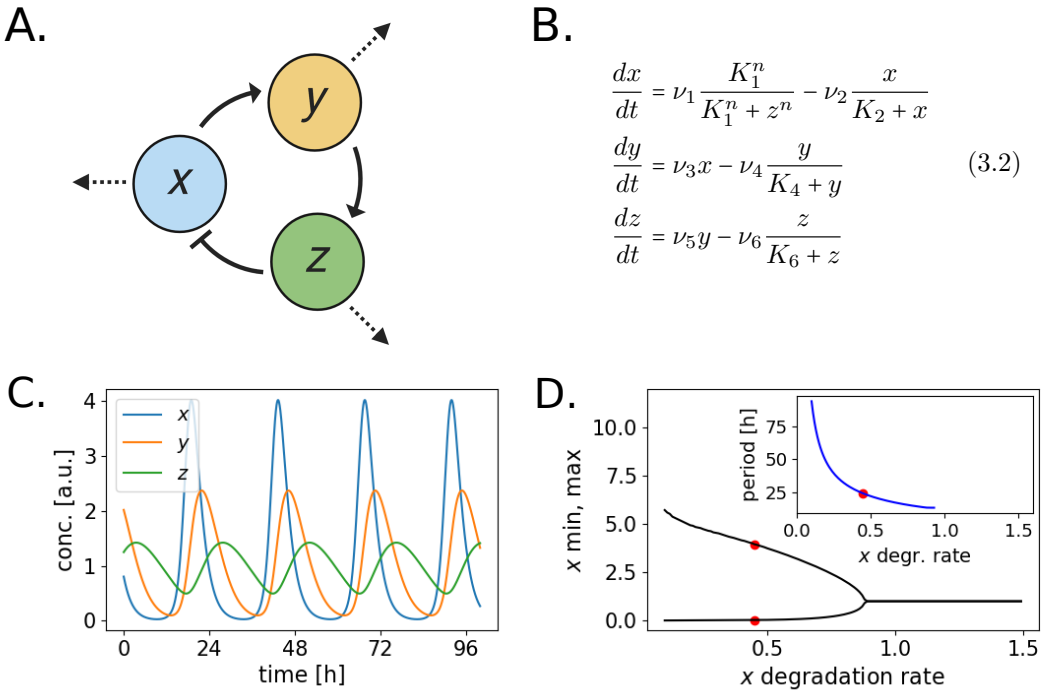

Figure 3.3: Goodwin model of self-sustained circadian oscillations. (**A**) Scheme of the model. (**B**) Equations of the model: the three variables account for a clock mRNA (x) that produces a clock protein (y) which activates a transcriptional inhibitor (z). Production reactions are modeled with mass action kinetics; degradation reactions are modeled assuming Michaelis Menten kinetics; repression is modeled with a Hill equation. (**C**) Limit cycle oscillations obtained by numerical integration of the equations in B for the following parameter values: ν_1=0.70 nM/h, ν_2=0.45 nM/h, ν_3=0.70 h^{-1}, ν_4=0.35 nM/h, ν_5=0.70 h^{-1}, ν_6=0.35 nM/h, K_1=1 nM, K_2=1 nM, K_4=1 nM, K_6=1 nM, n=7. (**D**) Bifurcation diagram as a function of the degradation rate of the clock mRNA x, ν_2. The diagram is built numerically by simulating the ODEs for each value of the control parameter ν_2 (degradation rate of x) and retaining the maximum and minimum values of the x oscillations (once the system has converged to its stable regime). Maximum and minimum values are plotted against the control parameter value. When the system converges to a stable steady state, maximum and minimum values are indistinguishable and a single point is plotted in the bifurcation diagram. Oscillations vanish at $\nu_2 = 0.85$. Inset: period of the oscillations as a function of ν_2. Red points indicate the default parameter value that produces 24 h circadian oscillations, $\nu_2 = 0.45$.

Limit cycles: Cooking recipe for oscillations

Most circadian clock models generate stable limit cycle oscillations. Limit cycles are isolated and closed trajectories characterized by a given period and amplitude [45, 310, 327]. Isolated means that neighboring trajectories are not closed, and they spiral either towards or away from the limit cycle. If all neighboring trajectories approach the limit cycle, we say the limit cycle is "stable" or "attracting". Thus, a small perturbation that pushes the system slightly out of a stable limit cycle will eventually dampen out, and the trajectory of the perturbed variable will be "attracted" back to the stable limit cycle. In nonlinear dynamical terms, stable limit cycles represent a type of attractor, since any perturbation will asymptotically return back to the limit cycle with time. Limit cycle oscillations, in this sense, ensure robustness to small perturbations in the environment.

For limit cycle oscillations to occur, the biological system of interest must fulfill a series of requirements that have been reviewed by many theoreticians, including Ferrell, Gonze and Tyson in [111, 113, 327]. Firstly, a negative feedback is necessary to carry the reaction network back to the point where the oscillation started. Second, the negative feedback signal must be sufficiently delayed in time so that reactions do not settle on a stable steady state. This time delay can be achieved by explicitly introducing time delays in the equations (the so called "delay-differential equations"), or by a long chain of reaction intermediates. The more variables in the loop, the longer the time delay will be, and the easier it is to generate oscillations. This explains why a Goodwin model with two variables (instead of 3) and a negative feedback loop does not oscillate, but the 3-ODE model does [113]. In addition, nonlinear kinetic processes must be present in the system to destabilize the steady state. Such nonlinear processes are also commonly referred to as switches [232, 258] or ultrasensitive processes [328–330], and they help to keep the system away from the stable steady state. Typically, phosphorylation, active transport and other enzymatic events are described by Michaelis Menten- or Hill-like kinetics, and this provides the necessary source of nonlinearity [331, 332]. And lastly, the system must be open; this is, it must be equipped with dissipative mechanims (e.g., degradation processes) and sources of energy (e.g., synthesis of mRNA or protein), so that oscillations that grow too large are dampened out, and oscillations that become too small are pumped up.

The equations of the Goodwin model and the limit cycle oscillations that result from it are shown in Figure 3.3. The negative feedback circuit shown in panel A is required to obtain self-sustained oscillations but, nevertheless, that is not sufficient: nonlinearities are needed. The original Goodwin model only contains one nonlinear term, given by the Hill equation which is used to model the z-mediated repression of x. Griffith demonstrated that the Hill coefficient had to be sufficiently high (n = 8) for the model to generate self-sustained oscillations [333]. But, since such high Hill coefficients are not biologically meaningful, Gonze modified the Goodwin model and included additional nonlinearities to reduce the need of high Hill coefficient [279]. In

the modified Goodwin model represented in Figure 3.3B, the nonlinearities come from the Hill term and from the Michaelian kinetics assumed for degradation processes [279].

Bifurcation diagrams

Another important concept that will appear in the next pages are bifurcation diagrams. The dynamics of a system greatly depend on parameter values. Unfortunately, kinetic rates and equilibrium constants are not measured experimentally in many cases, so this poses a challenge for constructing the model. Although a model with several parameters leads to a combinatorial number of possible parameter values, there are many constraints that fortunately allow us to narrow down the range of suitable values. In the context of circadian clocks, examples of such constraints might be given by the oscillation period (that needs to be circadian), by phase relationships of the variables (if known), effects of some mutations (assuming that we know which parameters are affected), some biochemical constants known from *in vitro* experiments, etc. The unknown parameters that have to be "guessed" should be chosen within realistic physiological ranges.

Usually, when a parameter value changes, the characteristics of the limit cycle also change. These changes can be illustrated on bifurcation diagrams. Novak and Tyson make the analogy of bifurcation diagrams being for modelers what signal-response curves are for experimentalists [321]. In a physiology experiment, biologists measure how some behavior of the cell (e.g., oscillation amplitude or period) depends on the value of an experimentally controlled signal (e.g., the concentration of a certain synchronizing factor in culture medium). The signal is held at a constant value until the response settles on a definitive value. Then, the signal is changed to a new value and the new response is recorded. A one-parameter bifurcation diagram illustrates the same concept. It shows how the final states of a mathematical model (e.g., maximum and minimum of oscillations, plotted in the y axis) depend on a control parameter in the model (plotted in the x axis). The manual exploration of the parameter space in bifurcation theory can give insights into the behavior of the model under different conditions and its sensitivity towards parameter changes.

Variation in parameter values can cause qualitative changes in the long-term behavior of the system. For example, the number of steady states or their stability properties can vary. The values at which such changes occur are called bifurcation points [310]. In the context of oscillations, Hopf bifurcations are the most important type of bifurcation point. They occur in dynamic systems when a periodic solution (limit cycle) arises from a stable steady state that loses its stability. Figure 3.3D shows the bifurcation diagram for the Goodwin model, as a function of the degradation rate of x. The plot shows, firstly, that oscillations disappear when the degradation rate is >0.85 nM/h. Moreover, it illustrates that both period and amplitude of mRNA oscillations decrease as its degradation rate increases. The model thus predicts that decreasing the degradation

rate should lead to oscillations with longer period. In this way, modeling can be used to predict the behavior of the system in conditions that might have not yet been tested experimentally.

3.3.2 Benefits of modeling

In the context of circadian rhythms, understanding the molecular basis of oscillations is much more than an exercise in experimental genetics or biochemistry. Oscillators have system-level characteristics (periodicity, coupling, robustness, entrainment...) that go beyond the properties of individual molecules or components, and that involve the full topology of the model network. Such ensemble properties can only be understood with the use of theoretical models. In the mammalian circadian clockwork, the use of mathematical models has been particularly helpful in the last years. Model-based predictions have been done regarding, for example, the necessity of noise and intercellular coupling to synchronize SCN neurons [334], the effect of mutations in core clock genes [335] or the role of post-translational processes on clock components [336] and have then been validated experimentally. An ongoing and future challenge to clock modelers is to address the interactions between the mammalian circadian clock and other systems, including the many emerging links between the clock and metabolism.

From a broader point of view, living cells are dynamical systems whose behavior is governed by nonlinear interactions among genes, proteins and metabolites in time and space. The huge complexity in the picture of molecular details makes it extremely difficult (if not impossible) for our intuitive minds to understand how such cellular systems work under normal and perturbed conditions, and even more to predict how the system will behave when exposed to novel conditions. But, fortunately, the theory of nonlinear dynamics can help. The tools of analysis and simulation of nonlinear differential equations provide a starting point in making accurate and reliable assessments of the system's behavior, and even in designing and constructing artificial biological networks with functional properties. But, if we want to understand biological systems in detail, biologists and modelers must speak a common language and must work in close collaboration to incorporate experimental results into models, such that models may be used to make testable predictions.

3.4 Results: A Robust Model for Circadian Redox Oscillations

As has been already described in previous sections, it is becoming clear that other mechanisms, apart from the TTFL, can contribute to the generation of circadian rhythms. Peroxiredoxins might be one of the candidates, since they exhibit 24 h rhythms in all kingdoms of life [37], often without a functional canonical TTFL [36, 37]. In

this project, we used mathematical modeling to investigate the principles for Prx/Srx oscillations in mitochondria from adrenal gland, heart and brown adipose tissue.

Our results show that the combination of a fast Prx hyperoxidation event followed by a slow and delayed negative feedback loop is the minimal backbone that is necessary and sufficient for the system to generate self-sustained limit cycle oscillations. We also found that this minimal motif produces relaxation-like oscillations with two temporal switch-like events, highlighting the importance of switches in the generation of oscillations. The results have been published in [232].

Nevertheless, the novel redox model only describes the generation of redox oscillations at a fraction of individual mitochondrial membranes. We hypothesized that mitochondria might behave as noisy oscillators that act as an ensemble to transduce information about the cellular redox state to the cell, and converted the redox model to a stochastic amplitude-phase model. Our results show that, similar to cells in culture, an ensemble of noisy redox oscillators can temporarily synchronize to a pulse-like perturbation, can entrain to Zeitgeber signals and can synchronize via mean-field coupling.

3.4.1 A novel kinetic deterministic model for circadian redox oscillations

ROS molecules are a double-edged sword. They play an important role as regulatory signals, but because of their potential to oxidize and damage cellular biomolecules when in excess, their levels must be under tight regulation. Prx3 is one of the major antioxidant molecules involved in H_2O_2 removal in mitochondria. The conserved peroxidatic cysteine (Cys) residue in its active site scavenges H_2O_2 molecules by getting oxidized to a sulfenic acid (Prx-SOH, reaction k_1 in Figure 3.2). This intermediate reacts with a second conserved Cys (the resolving Cys_R) from a second Prx3 subunit to produce an intermolecular disulfide bond (reaction k_2 in Figure 3.2), which can be reduced by the thioredoxin (Trx) system of the cell (reaction k_3). Prx3-SOH can further eliminate H_2O_2 molecules and undergo further oxidation, termed hyperoxidation, in an S-sulfinylation reaction, to form a sulfinic acid (Prx-SO_2H, reaction k_4) [304, 305]. Prx-SO_2H is catalytically inactive [304, 305] but, in adrenal gland, heart and brown adipose tissue, it can be reduced back and reactivated to Prx3-SOH by sulfiredoxin (Srx) (reaction k_5) [307]. In other cell types and other model organisms, Srx-mediated reduction of Prx-SO_2 is not required for rhythm generation [306].

As described in Section 3.1.3, in mitochondria from brown adipose tissue, adrenal glands and heart, Prx3-SO_2 and Srx levels oscillate with a circadian period [307]. H_2O_2 increase results in the oxidation and inactivation of Prx3 (reactions k_1 and k_4 from Figure 3.2). The consequence is the accumulation of H_2O_2 inside mitochondria and the overflow to the cytosol (k_6 in Figure 3.2). Cytosolic H_2O_2 activates pathways to control its own production, among which is the oxidation of Srx. Srx forms an intermolecular

disulfide bridge with Hsp90 (reaction k_7) and it translocates to mitochondria, ~8 h after the peak of Prx3-SO_2H, where it can reduce and reactivate hyperoxidized Prx3 (reaction k_5) with the use of ATP. The translocation of Srx to mitochondria thus constitutes the negative feedback loop necessary for oscillations that enables a new cycle of Prx3 inactivation and H_2O_2 accumulation to start.

To understand how fast biochemical redox reactions generate long 24 h period rhythms, we developed a deterministic model containing the biochemical species from the Prx3/Srx system shown in Figure 3.2. The diagram is shown in Figure 3.4A and the complete set of equations from this large model, which we refer to as "detailed model", are shown in Appendix B.1. Unfortunately, as discussed in Section 3.3.1, quantitative details of kinetic processes in large models are usually not known, and this is the case for the redox system presented here. Thus, estimating parameters in such a large model represented a challenge. For this reason, and in order to understand the design principles of redox rhythms in the Prx3/Srx oscillating system, we simplified the detailed model to its core motif (Figures 3.4B and C). Details of the model reduction are found in Appendix B.2 and are briefly discussed in the next section.

3.4.2 The core Prx3-SO_2H/Srx circadian oscillator: A 3-ODE model

To identify the core motif that is necessary and sufficient for generation of Prx3-SO_2 and mitochondrial Srx circadian oscillations, we systematically explored the parameter space and simulated constitutive expression of the different variables with a strategy that has been termed clamping [103]. In brief, the clamping approach aims to unravel which variables are needed for the system to oscillate, by setting the expression levels of a given variable to its mean value. Clamping to the mean values ensures that the system remains near the carefully tuned and physiologically reasonable default configuration. Thus, clamping of genes mimics constitutively expressed genes by non-rhythmic promoter constructs, rather than simulating overexpression or knockout studies [103]. If oscillations disappeared after clamping a variable, we concluded that the clamped variable was necessary for the generation of oscillations. If, on the other hand, the system kept oscillating after clamping, we concluded that the clamped variable was not required for the system to oscillate and we removed the variable (see Appendix B.2 for details on model simplification). The scheme and equations of the minimal core model are shown in Figures 3.4B and C. It only contains the variables, kinetic parameters and reactions that are necessary and sufficient for self-sustained rhythm generation.

The core oscillator model is represented by only five variables (out of the 11 from the detailed model) and one oxidation event (Figure 3.4B). A represents the *active* but partially oxidized Prx3 (Prx3-SOH) that gets further hyperoxidized by the *danger 1* (D_1, mitochondrial H_2O_2) to produce the *inactive* Prx3-SO_2H I. As the hyperoxidation reaction occurs to "clean" mitochondria from D_1, A levels decrease, and the result is

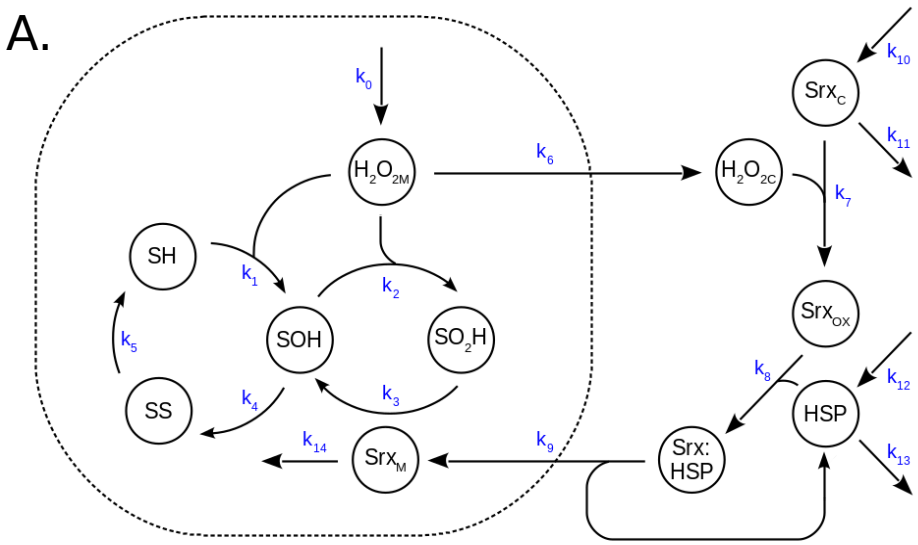

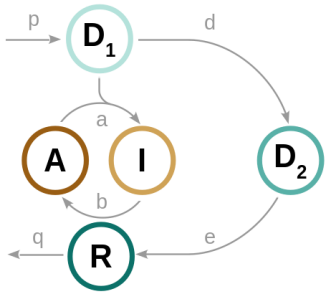

C.

$$
\begin{aligned}
\frac{dD_1}{dt} &= p - ab\frac{D_1 R}{bR + aD_1} - dD_1, \\
\frac{dD_2}{dt} &= dD_1 - eD_2, \\
\frac{dR}{dt} &= eD_2 - qR, \\
A &= \frac{bR}{bR + aD_1}, \\
I &= 1 - A = \frac{aD_1}{bR + aD_1}
\end{aligned}
\tag{3.3}
$$

Figure 3.4: Scheme and equations of the novel Prx3/Srx circadian redox model. Schemes of the detailed (**A**) and reduced core (**B**) redox oscillator model. (**C**) Equations of the core model. A represents active Prx3 (Prx3-SOH); I, inactive Prx3 (Prx3-SO_2H); D_1, mitochondrial H_2O_2; D_2, cytosolic H_2O_2; R, mitochondrial Srx. See main text and Appendix B.2 for details on the oscillating system and model simplification, respectively. Figure modified from [232].

a mitochondrion with a diminished ability of removing D_1. As mitochondria become unable of eliminating the oxidant, D_1 levels accumulate and overflow to the cytosol, where we refer to it as *danger 2* (D_2, cytosolic H_2O_2). D_2 activates the translocation of the *rescuer* R (mitochondrial Srx), that reduces ("rescues") I back to the active Prx A, closing the negative feedback loop. The oxidation of Prx3-SH to Prx-SOH and the D_2-induced oxidation of cytosolic Srx (reactions k_1 and k_7 in Figure 3.4A) were found to be dispensable for rhythm generation and thus were omitted from the minimal model.

We formulated ODEs to model the change of the system over time. Production and removal terms were modeled with mass action kinetics (Figure 3.4B). There is one nonlinear term that resulted from the quasi-steady state approximation [337, 338] on variable A, whose production and removal reactions were modeled as bilinear terms (details provided in Appendix B.2). We assumed constant D_1 production (parameter p in the model) and constant Prx pool $A + I$ over time. Moreover, we only considered the negative feedback of the R-induced reactivation of A, which is stimulated by the

cytosolic D_2 increase. However, other negative feedback loops have been shown to feed back and decrease D_1 production by activation of the stress-activated protein kinase p38 MAPK, among other pathways [339].

3.4.3 Design principles of the redox oscillator: fast A inactivation followed by a slow, delayed negative feedback loop

We have discussed in Section 3.3 how the dynamics of a system greatly depend on parameter values, and how most kinetic rates in biological systems are unfortunately not known in quantitative detail in the cellular context in which they occur. This was indeed the case of the Prx3/Srx oscillating system and, thus, finding reasonable parameters was a major challenge. Nevertheless, some constraints could be taken into account to narrow down the plausible range of parameter values. First of all, the system needed to oscillate with a circadian period. Second, the phase relationship between I and R had to be approximately 8 h, according to previously published data [307]. Moreover, other constraints came from *in vitro* enzymatic assays performed with Prx3 and Srx, as well as from studies that have focused on H_2O_2 signaling and transport [303, 307, 340–345]. These biochemical studies have estimated rates for Prx hyperoxidation, Srx-mediated Prx3-SO_2H reduction, Srx degradation and have allowed the derivation of a reasonable rate for H_2O_2 translocation across biological membranes (Table 3.1).

In order to obtain a reasonable set of parameters that satisfied the physiological constraints, we systematically varied all model parameters and performed bifurcation and control analyses. Bifurcation diagrams show under which parameter values the

Table 3.1: Physiological constraints that allowed finding plausible parameter ranges in the Prx3/Srx oscillating system. The rates of Prx3 hyperoxidation (I formation), Srx-mediated Prx3 reduction (rescue of A) and Srx degradation (R removal) have been determined by enzymatic assays in previous studies. The rate of mitochondrial H_2O_2 translocation* was estimated from experimental and theoretical studies that have focused on H_2O_2 transport and signaling. Table from [232].

Parameter	Biological Interpretation	Physiological Values	References
p	mitochondrial H_2O_2 production	-	-
a	Prx3-SOH hyperoxidation (and Prx3 inactivation)	$10^4\,M^{-1}\,s^{-1}$	[303]
b	Prx3-SO_2H reduction (and Prx3 reactivation)	$2\,M^{-1}\,s^{-1}$	[340]
d	H_2O_2 translocation to cytosol	$1\,s^{-1}$ *	[341–344]
e	Srx translocation to mitochondria	-	-
q	mitochondrial Srx degradation	$0.16\,h^{-1}$	[307, 345]

* H_2O_2 transport through biological membranes is thought to occur via aquaporins (Aqp) [341]. The typical diameter of an aquaporin is ~2 nm [342] and biological membranes typically contain 30 Aqp/µm^2 [343] (although this number might vary across cell and membrane types). Thus, the total Aqp area that can transport H_2O_2 out of the mitochondria is ~100 nm^2 per µm^2 of membrane. This means that ~0.01% of the membrane area contains Aqp. Very generally, the probability of an H_2O_2 molecule to diffuse can be assumed to be in the same order of magnitude of its probability to get reduced by Prxs [344]. With the limitation that only 0.01% of the membrane allows H_2O_2 translocation, the probability of H_2O_2 being transported out of the mitochondria is 0.01% of its probability of getting reduced, i.e. 10 000-fold lower than its reduction rate a.

system oscillated and control analyses address how the oscillation period (or amplitude) varied as a parameter was changed.

Bifurcation diagrams are presented for a selected choice of parameters in Figure 3.5A-C. The bifurcation plots show that the system oscillated for values of $d, e, q < 1$. The limit cycle emerged at $d = 0.02$ and disappeared at $d = 0.5$ (Figure 3.5A, bifurcation plots for parameters e and q are shown in Appendix B.4). We also found that, in contrast to small d, e, q parameter values, the system required a 1000 – 10,000-fold higher a oxidation rate to enter into the oscillatory regime. The Hopf bifurcation occurred at $a = 120$ (Figure 3.5B) and once this value was reached, oscillations persisted for a wide range of kinetic parameters, with little effects in oscillation amplitude or period, indicating robustness of the model. Control analysis revealed that the oscillation period strongly depended on the translocation rates d and e and on the R degradation parameter q, being most sensitive to changes in parameter d (Figure 3.5C and Appendix B.4).

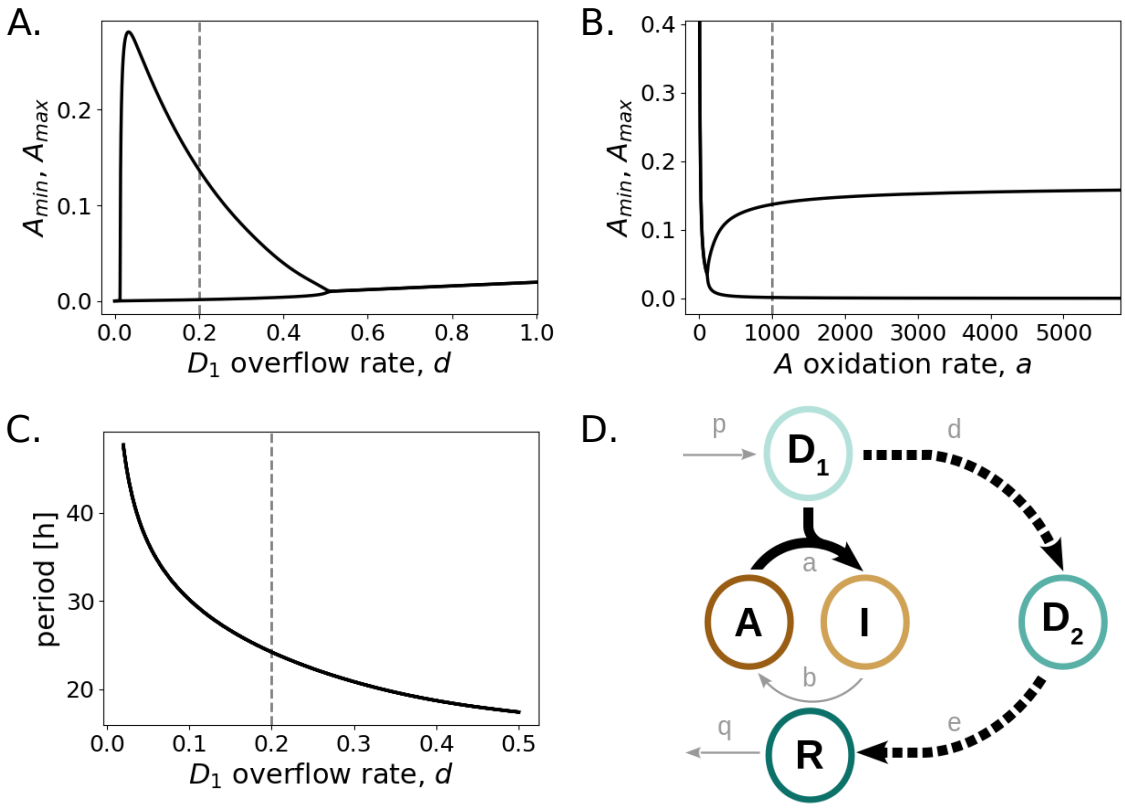

Figure 3.5: Fast A inactivation followed by a slow negative feedback loop is the design principle of the Prx3/Srx redox oscillator. Bifurcation diagrams as a function of the model parameters d (**A**) and a (**B**). At $d = 0.02$ and $a = 120$ self-sustained oscillations emerged. A_{min} and A_{max} represent the minimum and maximum values of A in the oscillatory regime. (**C**) Variation of period as a function of d. The curves shown in panels (A)-(C) were obtained for the default parameter set given in the caption of Figure 3.6. The dashed gray lines depict the default parameter values. (**D**) Sketch of the core backbone for I/R redox oscillations: fast D_1-induced A inactivation (continuous thick line) followed by a slow $D_1 - D_2 - R$ negative feedback loop (dashed line). Figure from [232].

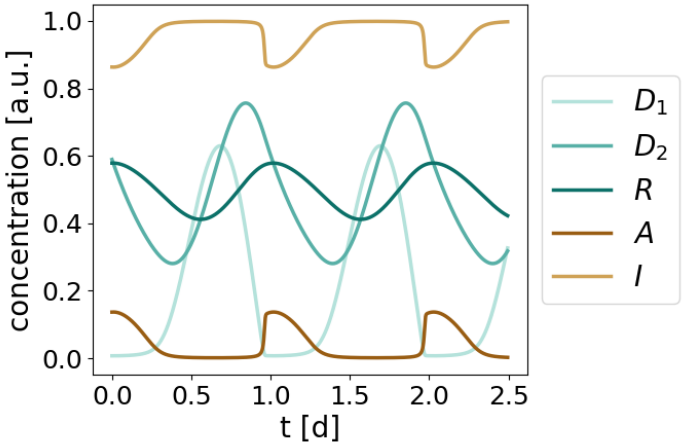

Figure 3.6: Self-sustained limit cycle oscillations of the redox model. Results were obtained by numerical integration of the equations shown in Figure 3.4C for the following parameter values (arbitrary units, a.u.): $p = 1, a = 1\,000, b = 2, d = 0.2, e = q = 0.1$. Consistent with experimental data [307] and with the model constraints (Table 3.1), the resulting period was 24.2 h and the phase shift between I and R was 8.7 h. Figure from [232].

These findings show that a fast A inactivation reaction (high a value) in combination with a slower negative feedback loop (1000–10 000-fold lower d, e, q rates) constitute the backbone of the redox oscillator model (Figure 3.5). We thus found a plausible set of model parameter values that produced robust circadian oscillations with the expected characteristics: a period of 24.2 h and a I/R phase difference of 8.7 h, as determined by maxima estimation of the R and I dynamics (Figure 3.6). Moreover, the parameter choice was in agreement with the high Prx3 oxidation rate measured experimentally [303] and with the ~10,000-fold slower physiological H_2O_2 translocation (Table 3.1).

According to our results, only a small fraction of active Prx3 A is needed to keep D_1 levels close to 0, as seen by the higher I levels compared to A during the whole simulated time (Figure 3.6). The results also predict that D_2 levels peak 3.9 h after D_1 (or 4.5 h after I), an observation that could be relevant in the context of the canonical TTFL and will be further addressed in the next section.

Interestingly, insights from the redox oscillator model can be applied as well to larger and more complex models. Firstly, negative feedback loops ($D_1 - D_2 - R$ in the minimal model) as well as nonlinear terms (given by the A equation, Figure 3.4C) are required to achieve self-sustained oscillations [111]. Secondly, overcritical delays about quarter to half of a period are necessary for oscillations to arise [111, 346, 347] (in the minimal model, slow d, e, q rates are required to yield the 8.7 h delay). Lastly, translocation and degradation rates have profound effects on the period [102, 115, 333, 348]. It should be noted, nevertheless, that the choice of parameters presented here was not tailored to specific kinetic data. Kinetic parameters might differ among tissues and might also depend on physiological conditions.

Two temporal switches in the I/R oscillator model

We have shown that, in order to oscillate, the mitochondrial Prx3-SO_2H/Srx (I/R) system required a fast D_1-induced inactivation of A followed by a lengthy and slower

negative feedback loop $D_1 - D_2 - R$ that reactivated A (Figure 3.5D). As seen by the equations from Figure 3.4C, the dynamics of A, I and D_1 depended on the fast a oxidation rate compared to the slower dynamics of D_2 or R. This is reflected in the relaxation- or triangular-like waveforms of A, I and D_1 (Figure 3.6). Such relaxation oscillations are generally characterized by two consecutive processes that occur on different timescales [57]. There are intervals of time, during which little happens ($A = 0$ or $I = 1$ in the system's dynamics), followed by time intervals with considerable changes. The result is the triangular-like dynamics observed for A, I and D_1 (Figure 3.6).

It is known that oscillations depend on negative feedbacks but, that in the absence of appropriate delays or nonlinear terms, negative feedback circuits often settle into a stable steady state termed homeostasis [111–113]. Several computational studies have demonstrated that sufficiently strong nonlinearities are required to destabilize the steady state and generate self-sustained oscillations [333, 349–351]. Such nonlinear terms often exhibit sigmoidal or "switch-like" characteristics. Moreover, the dynamics of "switching on" and "off", characteristic of relaxation oscillations, typically require some form of hysteresis [57]. Surprisingly, no switch-like nor hysteretic curve was evident from the single nonlinear term of the model $ab\frac{D_1 R}{bR+aD_1}$ (Figure 3.4C and Appendix B.2), nor from the response of any variable to upstream components (data not shown). Nonetheless, we found that this term was at the core of the oscillations, as its linearization resulted in the stabilization of the steady state. The large value of a allowed the generation of a fast and a slow timescale and destabilized the steady state. Thus, self-sustained rhythms were produced, even in the absence of an explicit kinetic switch.

In order to emphasize the importance of the nonlinear term in the context of oscillations, and given the switch-like dynamics of A, I and D_1, we still used the term *switch*. Instead of using it to describe how the steady state of a first component responds to a second component which is upstream of the former (often done in the literature [328–330, 351]), we focused here on temporal switches, characteristic of relaxation oscillations, that mark transitions between the fast and slow timescales. We found that the model dynamics could be split into three phases separated by two temporal switches (Figure 3.7).

The first phase was characterized by the inactivation of A as a result of D_1 removal. As long as there was active Prx3 (A) in the system, mitochondrial H_2O_2 (D_1) levels were kept in check and D_1 was removed. But the cost of the D_1 clearance was the inactivation of A to I, and thus A levels decreased as I increased (first box in Figure 3.7). When most of the active Prx3 pool A had been hyperoxidized and inactivated to I, the first switch occurred and the system progressed to the next phase. As a consequence of the A *inactivation*, its ability to remove D_1 molecules decreased. The dynamics of D_1 now entered the phase of important changes in the relaxation oscillation: it accumulated and *leaked* to the cytosol. In other words, the flux of D_1 changed from inactivating A to leaking, what gave this first temporal switch its name: *inactivation/leakage* (I/L) switch.

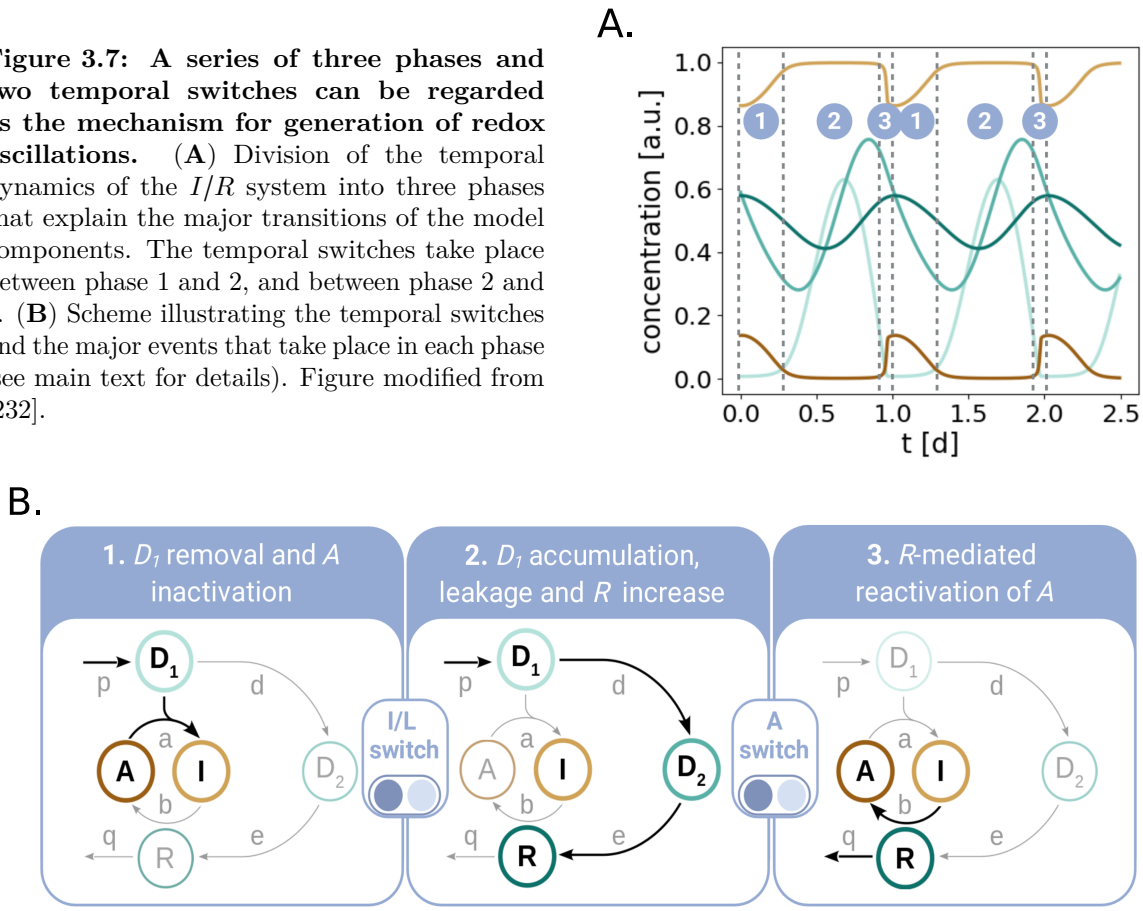

Figure 3.7: A series of three phases and two temporal switches can be regarded as the mechanism for generation of redox oscillations. (**A**) Division of the temporal dynamics of the I/R system into three phases that explain the major transitions of the model components. The temporal switches take place between phase 1 and 2, and between phase 2 and 3. (**B**) Scheme illustrating the temporal switches and the major events that take place in each phase (see main text for details). Figure modified from [232].

As a result of the I/L switch, D_1 accumulated, leaked and activated the $D_1 - D_2 - R$ negative feedback. Consequently, D_2 and R levels increased (phase 2, second box in Figure 3.7). At the end of the second phase, the increase in R was accompanied by a decrease in D_1. Once D_1 and R reached critical values in the nonlinear term, the negative feedback became effective and the dynamics of A, that are governed by the nonlinearity (Figure 3.4C), changed suddenly. This triggered the *activation* (A) switch and the sharp increase in A levels (phase 3, third box in Figure 3.7). The system was thus switched to its active state and a new round of D_1 removal could start. Furthermore, R became sensitive to degradation. The series of two temporal switches separate the two timescales in the relaxation oscillations. The I/L switch set the start of the slow timescale (the negative feedback loop), whereas the A switch marked the beginning of the fast clearance of D_1.

3.4.4 A stochastic amplitude-phase model for circadian redox oscillations

Modeling cell physiology with ODEs, as has been done so far, presumes a "deterministic" view of the molecular interactions and translocation processes within cells. Mitochondria are very small organelles (0.5-1.0 µm) and so stochastic fluctuations in abundance of molecules and movements are likely to be significant [321, 352]. Our novel deterministic

model describes circadian rhythms at the level of a fraction of mitochondrial membrane. But, if we take into account the stochasticity that might be present at the level of single mitochondria, it seems likely that these organelles behave as noisy (rather than deterministic) oscillators. Moreover, mitochondria vary in number depending on the cell type. For example, a human liver cell contains 1 000 – 2 000 mitochondria, whereas a cardiac myocyte can have up to 10 000 [352]. Although single mitochondria might be competent noisy redox oscillators, it seems plausible that they synchronize their redox circadian cycles to each other, as seen by the clear bands in published western blots of Prx3-SO_2H or Srx [307], in order to transmit a coherent output of the redox state as an ensemble to the cell and to the TTFL, or to respond to external Zeitgebers as a whole.

For this reason, we converted the deterministic model into a stochastic amplitude-phase model of N individual D_1-D_2 leaks, to account for fluctuations at the level of single mitochondria. The relevance of stochastic models is discussed in this paragraph, and the advantages of amplitude-phase models, in the next one. Building effective stochastic models requires, on one hand, a solid foundation based on a preliminary deterministic model, and on the other hand, substantial amounts of additional quantitative data about cell constituents (e.g., counts of protein or molecule numbers within cells) and cell behavior (e.g., statistical distributions of cell responses to a specific stimulus) [321]. Although quantitative data at the level of mitochondrial H_2O_2, Prx and Srx oscillations is still missing, converting our deterministic model into a stochastic amplitude-phase model allowed us to qualitatively analyze the emergent and ensemble properties that arise from networks of N stochastic oscillators in response to pulses, entrainment by Zeitgebers or mean-field synchronization. The roles of stochastic fluctuations in determining the variability of cell behavioral responses have been reviewed by Rao *et al.* [353], Paulsson [354] and Shahrezaie and Swain [355].

Amplitude phase oscillators are one of the most abstract yet intuitive class of models, with only two variables, namely amplitude and phase of oscillations, that can relate to any observed rhythm. Thus, they do not necessarily have to account for the concentration levels of a given protein or metabolite. The equations can describe phenomenologically the oscillatory dynamics of a system, independently of molecular details [281, 327]. Amplitude phase models have been used in clock research to study generic properties of phase-response curves [356], entrainment [357], the behavior of ensembles of coupled oscillators [281, 346, 358–361], or to interpret experimental results [362]. In the context of modeling redox oscillations, we decided to describe cytoplasmatic H_2O_2 (D_2) oscillations with an amplitude-phase model, as this variable will be the coupling link between the redox oscillator and the TTFL in the next chapter.

We numerically simulated an ensemble of noisy D_2 oscillations using a stochastic, self-sustained amplitude-phase model in Cartesian coordinates modeled with explicit

twist. The twist term describes the period dependence on amplitude. The stochastic differential equations used for numerical simulations are the following:

$$\begin{aligned} dx_i &= \lambda x_i(A - \sqrt{x_i^2 + y_i^2}) - y_i(\frac{2\pi}{\tau} + \epsilon(A - \sqrt{x_i^2 + y_i^2})) + \sigma_x dW_{1t}, \\ dy_i &= \lambda y_i(A - \sqrt{x_i^2 + y_i^2}) + x_i(\frac{2\pi}{\tau} + \epsilon(A - \sqrt{x_i^2 + y_i^2})) + \sigma_y dW_{2t}, \end{aligned} \tag{3.4}$$

where A represents the amplitude of the D_2 oscillator ($A = 1$ for convenience); λ, the amplitude relaxation rate (i.e., a measure of how fast a perturbation relaxes back to the limit cycle [273, 278, 281, 346, 363], $\lambda = 1\,\text{day}^{-1}$); τ the intrinsic period ($\tau = 24.23\,\text{h}$) and ϵ, the oscillator's explicit twist ($\epsilon = 0.1$). Given the limited availability of quantitative data in mitochondrial redox oscillations, noise was introduced heuristically, by adding a Wiener process dW_t with $\sigma_x = 0.1$ and $\sigma_y = 0.1$. Estimation of the amplitude-phase model parameters (amplitude relaxation rate λ, twist ϵ and period τ) is described in the Materials and Methods Section 6.5.

We simulated 10 stochastic D_2 amplitude oscillators using the Euler-Maruyama method to solve stochastic differential equations [364] (Figure 3.8). The time series illustrate how, despite all oscillators starting with the same initial conditions, they drifted apart in phase over time due to the white noise component. Power spectra revealed a peak at $\tau = 24.2\,\text{h}$, as expected from the period of D_2 oscillations (although the results shown in Figure 3.8 were normalized to the maximum power peak). Moreover, we found that the autocovariance function of an individual noisy oscillator (the covariance of one noisy amplitude-phase oscillator with itself, after a time delay) decayed exponentially over time due to the noise component (Figure 3.8D), as described previously [278].

3.4.5 Stochastic oscillators can entrain, respond to pulses and synchronize via mean-field coupling

We next wanted to investigate what ensemble properties emerge in a collection of noisy redox oscillators, and if they can collectively respond to pulse-like perturbations, Zeitgeber signals or synchronizing agents. For this reason, we analyzed how an ensemble of 100 stochastic amplitude-phase D_2 oscillators responded to a short pulse, to an external time-periodic forcing signal and to inter-mitochondrial coupling. As parameter values we took the parameters specified in the caption of Figure 3.8, calculated from D_2 deterministic oscillations as described in Section 6.5.

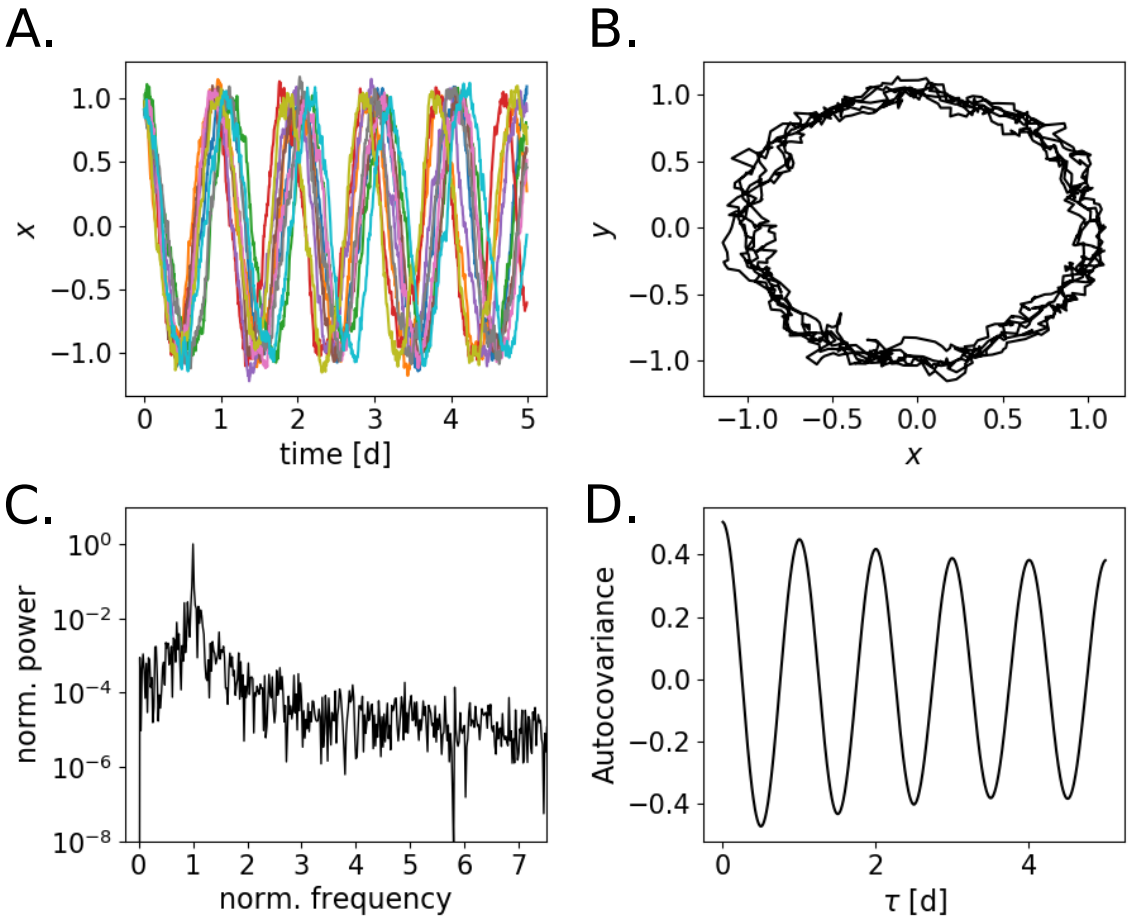

Figure 3.8: Stochastic amplitude-phase model of D_2 oscillations. (**A**) Time series of 10 individual oscillators. (**B**) Phase portrait of one single D_2 amplitude-phase oscillator. (**C**) Power spectral density. The period in the power spectra was normalized to the period with maximum power, 24.2 h. (**D**) Autocovariance function of one single oscillator. Results were obtained by solving the stochastic differential equations using the Euler-Maruyama method, for the following model parameters: $A = 1$, $\tau = 24.23$ h, $\lambda = 1\,\text{day}^{-1}$, $\epsilon = 0.1$, $\sigma_x = 0.1$, $\sigma_y = 0.1$. Numerical simulations were obtained for a total integration time of 24.23h x 100 at Δt=0.1 h. Details of the model derivation are found in Section 6.5.

Noisy D_2 amplitude-phase oscillators synchronize temporarily via a pulse-like perturbation

In cells in culture, stimuli such as fresh serum, forskolin, dexamethasone, or temperature pulses can temporarily synchronize rhythms [68, 365, 366]. When the stimuli disappear, synchrony is lost within a few cycles and the averaged signal dampens out. It should be noted, however, that there is an ongoing debate about whether single cells behave as heterogeneous self-sustained or rather weakly-damped oscillators [32, 278, 279]. Depending on the model considered, one can argue that the damping will be caused by single cell damping (if one considers an individual oscillator as weakly-damped) or by dephasing due to different oscillator periods and/or noise, or both.

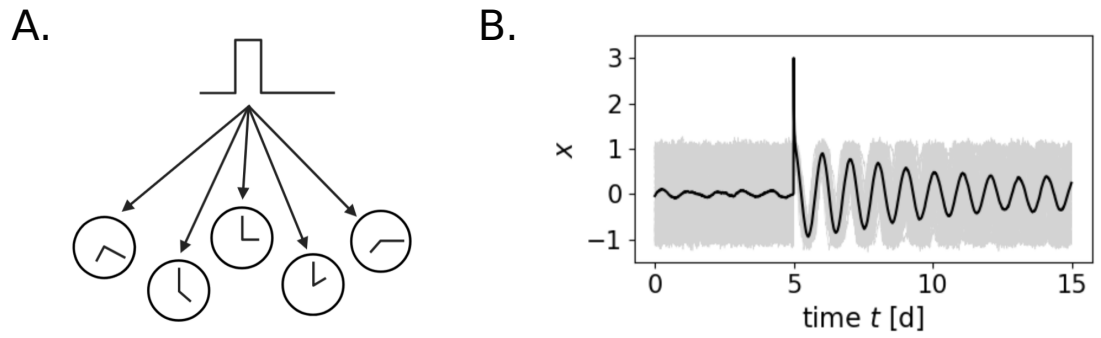

Figure 3.9: 100 noisy amplitude-phase oscillators synchronized temporarily via a pulse-like perturbation. (**A**) Cartoon visualizing a pulse acting on oscillators. Panel modified from [346]. (**B**) Ensemble of 100 noisy limit cycle oscillators. Results were obtained by solving the stochastic differential equations using the Euler-Maruyama method, for the following model parameters: $A = 1$, $\tau = 24.23\,\mathrm{h}$, $\lambda = 1\,\mathrm{day}^{-1}$, $\epsilon = 0.1$, $\sigma_x = 0.1$, $\sigma_y = 0.1$. The perturbation was introduced by shifting all x coordinates of the D_2 oscillators in a specific direction by 3 dimensional units. The thick black line represents the averaged signal.

Under the assumption that mitochondria behave as self-sustained oscillators (Equations 3.4), we hypothesized that D_2 leaking from single mitochondria might also be temporarily synchronized by a pulse-like perturbation such an H_2O_2 bolus in cell culture. In Figure 3.9 we analyze the response of 100 simulated noisy D_2 amplitude-phase oscillators to a short pulse. We observed damping in the averaged population rhythms which, in this case, is a result of the noisy component in the model (since we assumed the same period for all individual oscillators, $\tau = 24.23\,\mathrm{h}$). The average signal dampened faster (i.e., oscillators remained synchronized for less time) with decreasing amplitude relaxation rate (for a fixed $\sigma_x \neq 0$), as well as with increasing noise term σ_x (Appendix B.5). This means that pulse-like perturbations were able to temporarily synchronize a population of stochastic oscillators the more rigid and less noisy an oscillator was (high λ and low σ_x values, Figure B.6).

Noisy D_2 amplitude-phase oscillators synchronize to an external time-periodic Zeitgeber

We next analyzed whether stochastic D_2 amplitude-phase oscillators could also entrain to Zeitgeber cycles. We simulated the effect of a periodic force (a Zeitgeber) by adding the following sinusoidal term to the right hand side of the x stochastic differential equation (Equation 3.4):

$$Z(t) = F\cos(\frac{2\pi}{T}t + \phi), \tag{3.5}$$

where F, T and ϕ represent the amplitude, period and phase of the periodic forcing signal, respectively.

We found that relatively weak external signals (a Zeitgeber amplitude that is 5% of the intrinsic oscillator amplitude) can result in fairly precise rhythms of the average signal (black thick line in Figure 3.10), even though single cells remained quite noisy (grey lines in the same figure). It should be noted, however, that the Zeitgeber period T should be close the intrinsic oscillator period τ to for effective entrainment. The further apart τ and T are, the larger the Zeitgeber amplitude F should be for successful entrainment [46, 273, 363]. This dependence will be further addressed in the next chapter.

It is well known from the theory of coupled oscillators that if a periodic stimulus is of the same or nearly the same period as the natural vibrating period of a system, the amplitude of the system will increase; a phenomenon called resonance [367]. For a network of oscillators, like in this case, resonance can be interpreted as amplification of the amplitude of individual oscillators. In physics this relationship is described by the so called resonance curve, which predicts that resonance is maximized as the frequencies of a forcing and a forced oscillator approach each other [367]. This way, as a consequence of frequency locking, entrainment affects the amplitude of a network leading to amplitude expansion by resonance effects [281]. Amplitude relaxation rate of individual oscillators is inversely correlated with amplitude resonance: as the oscillator relaxation rate increases, amplitude expansions decrease [281, 363]. This means that the amplitude of rigid oscillators (high amplitude relaxation rate λ) displays little change upon coupling or entrainment, while less rigid oscillators display stronger amplitude expansions. This is indeed what we found in our system of stochastic D_2 oscillators. Since the amplitude relaxation rate of the redox system was large ($\lambda = 1\,\mathrm{day}^{-1}$), resonance effects were not

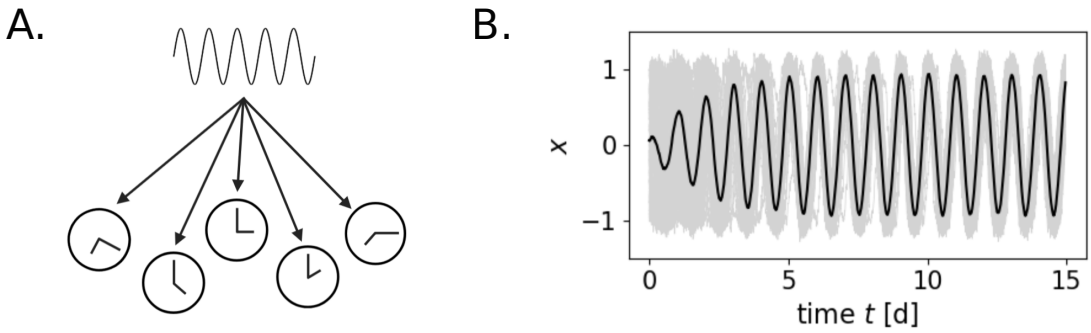

Figure 3.10: 100 noisy amplitude-phase oscillators synchronized to an external time-periodic Zeitgeber. (**A**) Cartoon visualizing a common periodic Zeitgeber acting on oscillators. Panel modified from [346]. (**B**) Ensemble of 100 noisy limit cycle oscillators. Results were obtained by solving the stochastic differential equations using the Euler-Maruyama method, for the following model parameters: $A = 1$, $\tau = 24.23\,\mathrm{h}$, $\lambda = 1\,\mathrm{day}^{-1}$, $\epsilon = 0.1$, $\sigma_x = 0.1$, $\sigma_y = 0.1$, $F = 0.05$, $T = 24\,\mathrm{h}$, $\phi = 0$. The thick black line represents the averaged signal, indicating that precise rhythms could be established in an ensemble of self-sustained oscillators.

evident. Decreasing λ led to stronger amplitude expansions, as illustrated in Appendix B.5.

Noisy D_2 amplitude-phase oscillators can couple through a common mean-field

So far we only simulated uncoupled D_2 oscillations synchronized via external signals. But it seems likely that a cell might sense collective D_2 molecules leaking from different mitochondria, in order to coordinate the import of Srx to the organelles as an ensemble. Thus, one can assume that coupling might be achieved by D_2 molecules released by each mitochondrion, and that spatial transmission is fast with respect to the timescale of the 24 h oscillations. Under these conditions, it is a reasonable hypothesis to consider global coupling, achieved through a mean-field M [279], defined as the average concentration of the synchronizer D_2 as follows:

$$M = \frac{K_{coup}}{N} \sum_{i=1}^{N} x_i, \tag{3.6}$$

where K_{coup} is a dimensionless parameter that denotes the coupling strength, N represents the total number of oscillators and x_i refers to the Cartesian x coordinate of the stochastic D_2 amplitude-phase oscillator. The mean-field term was again added to the right hand side of the x coordinate from Equations 3.4.

Figure 3.11 demonstrates that such mean-field coupling could easily synchronize an ensemble of 100 noisy oscillators. Although x_i acted as a periodic driving signal with

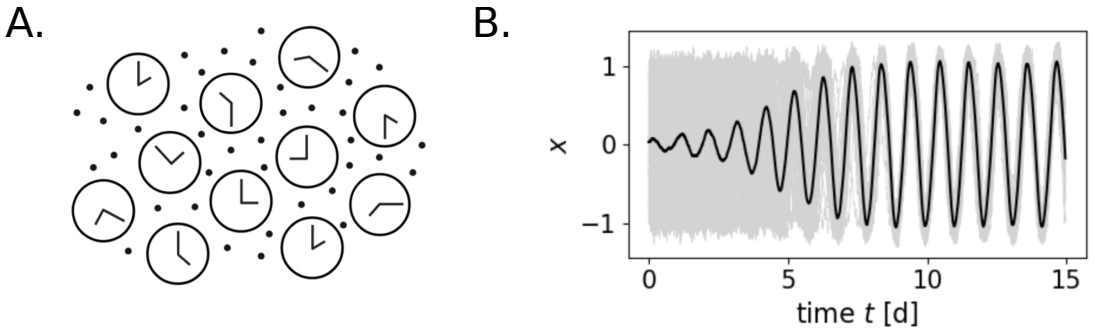

Figure 3.11: Synchronization of 100 noisy oscillators coupled through a common mean-field (**A**) Cartoon visualizing a synchronization by mean-field coupling (black dots in the backgroud). Panel modified from [346]. (**B**) Within a few cycles, coupling could induce synchrony in an ensemble of 100 noisy limit cycle oscillators. Results were obtained by solving the stochastic differential equations using the Euler-Maruyama method, for the following model parameters: A = 1, τ = 24.23 h, λ = 1 day^{-1}, ϵ = 0.1, σ_x = 0.1, σ_y = 0.1, K_{coup} = 0.1. The thick black line represents the averaged signal, indicating that precise rhythms could be established in an ensemble of coupled self-sustained oscillators.

the same frequency as the oscillator frequency, coupling via mean-field did not lead to pronounced amplitude expansions, due to the large amplitude relaxation rate from the D_2 oscillator. We did find, however, large resonance effects for lower amplitude relaxation rates (Appendix B.5). Amplitude expansions were even more pronounced in highly coupled systems (i.e., in systems with large K_{coup}, Appendix B.5), in agreement with previous theoretical results [281]. Moreover, we found that mean-field coupling among D_2 autonomous oscillators affected not only the amplitude of oscillators, but also their phase. Again supporting previous computational findings [281], we found that phase coherence was induced as a function of the inter-oscillator coupling strength K_{coup}, and observed that coupling led to phase synchronization, as seen by the narrower phase distributions in coupled compared to uncoupled networks (Figure B.8A in Appendix B.5).

3.5 Discussion

3.5.1 A novel model for circadian redox oscillations

In this project, we designed the first model for the complex biochemical system of Prx3-SO_2H/Srx redox oscillations and found that the loop Prx3-SOH – Prx3-SO_2H, together with the negative feedback mediated by Srx (Figure 3.2), is necessary and sufficient for the generation of oscillations. The design principles of this oscillator are (i) a fast Prx3-SOH inactivation followed by (ii) a slow and delayed negative feedback loop, where mitochondrial H_2O_2 leaks to the cytosol to promote mitochondrial import of cytosolic Srx, approximately 9 h after the inactivation of Prx3-SOH. This simple backbone reproduced the previously described circadian oscillations of mitochondrial Prx3-SO_2H and Srx as well as the delay in mitochondrial Srx import.

Although quantitative details of the kinetic parameters in the context of the Prx3/Srx system remain largely unknown, we found a reasonable set of parameters consistent with the biology they describe. Previous biochemical studies have estimated *in vitro* that Prxs are 1 000 – 10 000 times more reactive to H_2O_2 than other reduced cellular thiols [303], and that thus they can confine the diffusion of the oxidant [344]. Under the assumption that 0.01% of the membrane area contains transport proteins (Aqp) that can passively transport H_2O_2 out of the compartment [343], the translocation rate of H_2O_2 is 10 000-fold smaller than its reduction rate (Table 3.1). This is in agreement with the parameter values, $a = 1000$ and $d = 0.2$. Since the import of Srx to mitochondria also requires a protein transporter, we assumed this rate to be in the same order of magnitude as the translocation of H_2O_2 to the cytosol. Nonetheless, the estimation of translocation kinetics was only preliminary. The experimental determination of the rate at which a protein is transported through a membrane is challenging, because the transport depends on a number of factors including pH, membrane voltage, protein length, 3D conformation,

membrane fatty acid composition, and ATP levels (if the transport is active), among others. Furthermore, the choices for Srx degradation rate q and hyperoxidized Prx3 reduction rate by Srx b were consistent with previous experimental studies, which have estimated a half-life of sulfiredoxin of 4-5 h [307, 345], and a rate of reduction of hyperoxidized Prx by Srx of approximately $2\,M^{-1}s^{-1}$, 1 000 – 10 000 times smaller than its oxidation rate [340] (Table 3.1).

It is known that relaxation oscillations typically depend on positive feedback loops [57, 310, 312]. However, even in the absence of explicit positive feedback loops, the redox oscillator model still produced oscillations of Prx3-SOH, Prx3-SO_2H and mitochondrial H_2O_2 that were of relaxation type. Two temporal switches characterized their triangular-like waveform and divided the system's dynamics into three phases. A summary is shown in Figure 3.12. This scheme with three phases and two switches is reminiscent to that of the cell cycle. A series of biochemical switches controls transitions between the various phases of the cell cycle. They maintain its orderly progression and act as checkpoints to ensure that each phase has been properly completed before progression to the next phase. Such switches have been shown to generate decisive, robust (and potentially irreversible) transitions and trigger stable oscillations [113, 368, 369]. It should be noted, however, that the switches that regulate cell cycle transitions are the consequence of a complicated network of positive and negative feedback loops and result in bistability, as opposed to our simple model that (strikingly) contains only one negative feedback loop. The redox model highlights the importance of negative feedbacks and the diversity of switches in the context of oscillations. Our results might be of particular interest for biological systems with fast inactivation events followed by lengthy negative feedback loops, since we predict that relaxation oscillations might arise in such networks as well.

Also the detailed model (Appendix B.1) oscillated along the lines of the design principles identified for the reduced model. It showed the same characteristics: relaxation oscillations, temporal switches and the expected period and I/R phase delay, supporting the robustness of the minimal core model. According to biochemical assays, the rate constant for Prx3-SH oxidation to sulfenic acid Prx3-SOH is in the order of $10^7\,M^{-1}s^{-1}$ [303]. From the simulations of the detailed model we saw that when this rate (k_1 in the model) increased, the amplitude of Prx3-SO_2H and Srx oscillations also increased (Appendix B.1). This suggested that, although the loop Prx3-SH – Prx3-SOH – Prx3-SS – Prx3-SH is not required for oscillations, it probably fine-tunes the dynamics of the Prx3/Srx oscillatory system. Large Prx3-SO_2H and Srx amplitudes are in agreement with experimental data. Western blots show intense bands at the peak of Prx3-SO_2H or Srx oscillations and no bands at the trough [307].

The stochastic redox amplitude-phase model was developed to account for fluctuations that might occur at the level of single mitochondria. Although there is limited data on the variances of the noise terms in the context of H_2O_2 oscillations, we found that, qualitatively, an ensemble of stochastic redox amplitude-phase oscillators can temporarily

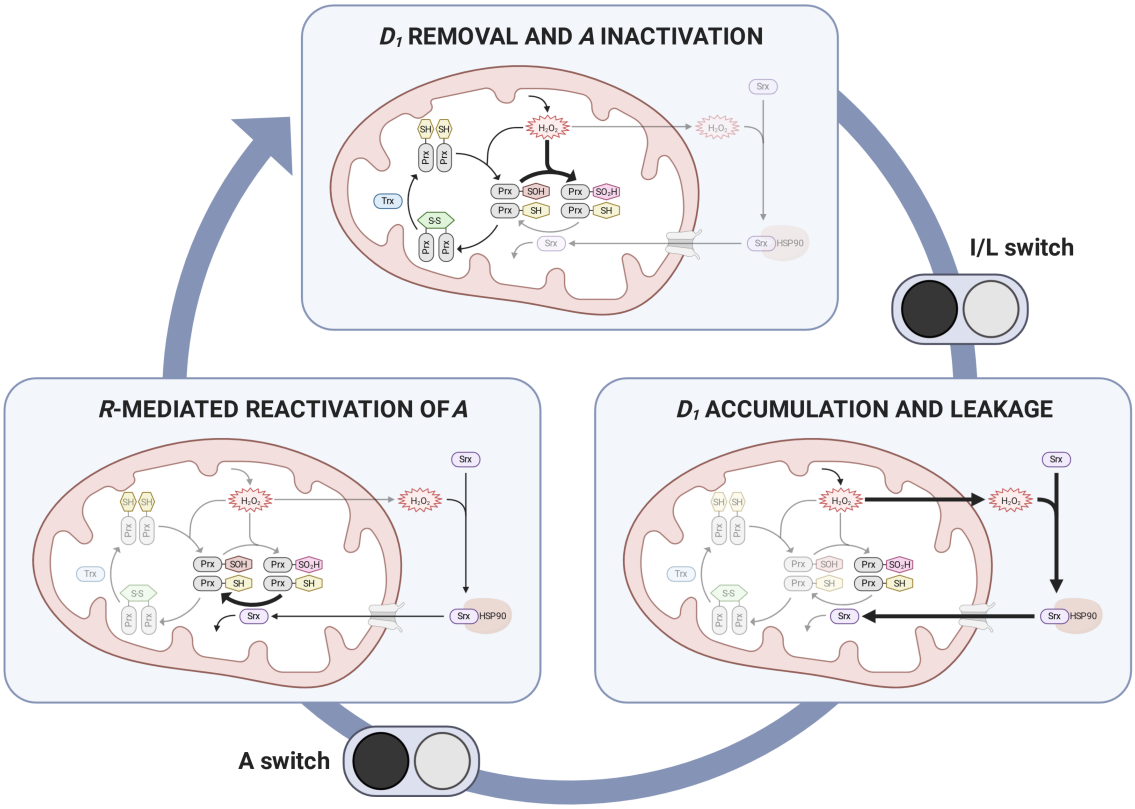

Figure 3.12: Model for the mechanism underlying circadian oscillations of Prx3-SO_2H and Srx in mitochondria of mammalian adrenal gland, heart and brown adipose tissue. Three phases and two temporal switches conceptually explain the generation of oscillations. The switches are represented by the black/gray icons. Figure modified from [232].

synchronize to a pulse-like stimulus, as well as to a periodic Zeitgeber signal and to mean-field coupling. These findings are relevant in the context of the Prx/Srx oscillating system: western blot data show clear bands of Prx3-SO_2H and/or Srx [36, 37, 307], what speaks for redox rhythms likely being synchronized in cells. Also more recent findings from Pei *et al.* show that H_2O_2 undergoes robust circadian rhythms in cultured cells and mouse liver [370]. Taken together, these findings support our hypothesis that single mitochondria might synchronize their redox circadian cycles to each other in order to transmit a coherent redox output to the cell or to receive and respond to external Zeitgeber inputs as a whole.

3.5.2 Alternative views on the nature of the negative feedback in the redox oscillator

The oscillator model presented here applies to Prx oscillations in mammalian adrenal gland, heart and brown adipose tissue. But Prx daily rhythms have been found not only in mammals, also in a variety of eukaryotes, cyanobacteria and archaea, making these oscillation an evolutionarily conserved circadian rhythm marker [37]. A key unanswered question is what determines Prx oscillations in other cell types and phyla. Srx indeed accounts for the oscillations in adrenal gland, brown adipose tissue and heart [307] but

other organisms that display oscillations in Prx do not express Srx homologs (e.g., *C. elegans* and *N. crassa*), suggesting that other mechanisms might be in place. The same is true for mouse red blood cells. Although they express Srx, Prx-SO_2H rhythms are largely unaltered in erythrocytes derived from Srx knockout mice and, by contrast, application of proteasome inhibitors eliminated the decay phase of the Prx-SO_2H rhythm in wild-type mouse erythrocytes [306]. Taken together, these findings suggest that proteasomal degradation might account for the decay phase and hence for the negative feedback of the Prx-SO_2H oscillations in other cell types and phyla.

3.5.3 Crosstalk between Prx and TTFL rhythms in eukaryotes

Given that Prx proteins and their oxidation rhythms are highly conserved among species, Prx rhythms seem to be evolutionarily ancient. It is also likely that they emerged before the circadian TTFL, which is believed to have evolved independently in separate species [37]. It is an important goal to now understand the relationship between the canonical TTFL and Prx oscillations, as it is becoming evident that there is a reciprocal interplay between the two. In one direction, the period length of Prx-SO_2H rhythms is extended in embryonic fibroblasts derived from *Cry1,2*$^{-/-}$ mice [36]. In behaviorally arrhythmic *Drosophila* mutants and *N. crassa* mutants displaying lengthened periods, Prx oscillations are perturbed in phase [37]. In the other direction, *Arabidopsis* mutants lacking *prx* genes display TTFL rhythms that are altered in phase or amplitude [37], and knockdown of specific PRX isoforms in human U-2 OS cells affects the period length and amplitude of clock gene rhythms [270].

The modeling approach described in this study assumes constant H_2O_2 production. Nevertheless, the sources of mitochondrial H_2O_2 in tissues where the redox clockwork is present have been shown to be, at least in part, under the control of the circadian TTFL. In adrenal gland, for example, the major source of H_2O_2 is steroidogenesis, a process which is under the regulation of the TTFL [371, 372]. In heart or brown adipose tissue, in which oxidative metabolism is very high, the respiratory component becomes an important source of H_2O_2, and respiration rate has also been shown to be rhythmically controlled by the canonical TTFL [373].

Moreover, the Prx3/Srx redox oscillator model contains only one negative feedback, namely the reduction of Prx3-SO_2H (I) by Srx (R), which is stimulated by the cytosolic H_2O_2 (D_2) increase. Cytosolic H_2O_2, however, can signal as a second messenger and activate the p38 MAPK pathway to decrease mitochondrial H_2O_2 production [307, 339]. The periodic H_2O_2 release to the cytosol is expected to act on other cytosolic or nuclear targets that have not been identified yet. Canonical clock proteins might be directly or indirectly affected by the cytosolic H_2O_2 increase. This idea is supported by a study from 2014, that showed that the interaction of the two mammalian core clock proteins PER2 and CRY1 is redox-sensitive [374], as well as by other studies that have shown that

the cellular redox poise can regulate the TTFL oscillator through NAD^+ levels or heme [136, 375]. Moreover, Pei *et al.* have recently reported that H_2O_2 oscillates robustly in cultured cells and mouse liver [370], and they have shown that CLOCK contains a redox-sensitive Cys that respond to changes in intracellular H_2O_2, providing compelling evidence for a role of this reactive oxygen species in regulating the TTFL. The H_2O_2 leakage might thus represent a potential coupling node between both redox and TTFL clocks. The reciprocal interplay between the Prx system and the local TTFL clock might allow synchronization between local metabolic activity and systemic circadian regulation, but this will be the subject of matter in the next chapter. The presence of Srx as part of the Prx clockwork in adrenal gland, brown adipose tissue or heart, but not in the liver, for instance, might indicate differences in how metabolic signals are integrated within the systemic clock network.

3.5.4 Model predictions

Mathematical models are most useful when they make predictions that can be tested (and hopefully validated) *in vivo*. Because the Prx3/Srx oscillator model is not quantitative in detail due to the limited knowledge of rate constants, it only allows to make some basic predictions. Interfering with the expression of Srx or specific aquoporin (Aqp) isoforms involved in the H_2O_2 translocation across mitochondrial membranes would, intuitively, disrupt Prx3/Srx oscillations. Moreover, the simulations show that H_2O_2 peaks in the cytoplasm ~4.5 h after the peak of Prx3-SO_2H (or ~ 4 h after mitochondrial H_2O_2), a finding that might represent an attractive target for the development redox sensors that could measure when H_2O_2 peaks in the cytosol in relation to its peak in mitochondria. It seems likely that single mitochondria synchronize their redox circadian cycles to each other, as seen by the clear bands in published western blots of Prx3-SO_2H or Srx [307]. Thus, the peak of cytoplasmatic H_2O_2, coming from the whole ensemble at a proper time might be of importance to transmit appropriately timed signals about the redox state of the cell to the canonical TTFL oscillator, or to receive timing information as an ensemble. It is likely that a stable phase relationship is required between both oscillators for their optimal function. Our model also predicts that the system should be able to oscillate even under conditions of constant mitochondrial H_2O_2 production. Such a self-sustained nature of the Prx3 cycle could be tested in isolated mitochondria led to respire in a constant environment.

3.5.5 Concluding remarks

We close with a short remark about the beauty of simple and generic models. Although a full representation of the biological systems is hard to reach due to modeling limitations, the presented model elaborates on the basic ingredients that constitute the Prx3/Srx redox oscillator in mammalian mitochondria from adrenal gland, heart and brown

adipose tissue. We have found the core motif that turned out to be necessary and sufficient to generate self-sustained rhythms, and that reproduced previously published experimental data. Our model has been implemented using plausible and simple, yet generic mathematical representations. This five-variable network might be relevant for other simplified oscillatory systems that follow the same logic of fast (in)activation followed by slow negative feedback, such as the mitotic oscillator involving cyclin and Cdc2 kinase interactions or the Ca^{2+} oscillations based on Ca^{2+}-induced Ca^{2+} release [376]. The fact that nature has converged on common mathematical structures underlines the links between similar dynamic phenomena occurring in widely different biological settings. It might even constitute a step forward in the synthetic design of reliable and robust biological clocks [311, 377].

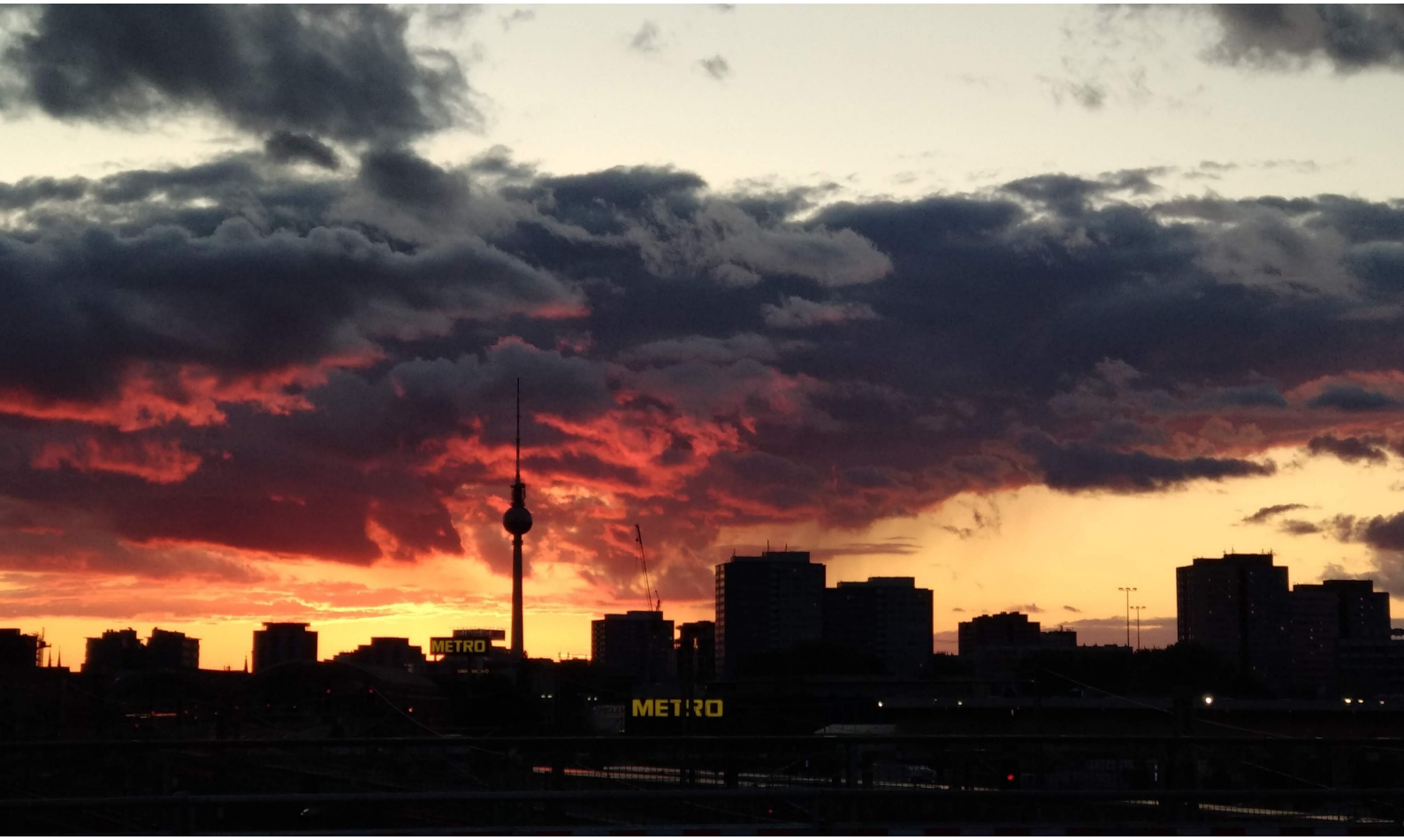

Warschauer Brücke

:

4

Coupling Redox and TTFL Rhythms

4.1 Crosstalk Between Redox and TTFL Timing Systems: A Brief Overview

We have already introduced in previous chapters that metabolic changes can directly impinge on the transcriptional oscillator. This raises the question of what are the mechanisms mediating this coupling. From all of the parameters that change as a function of cellular metabolism, redox balance represents a strong candidate. This is not solely due to its crucial role in regulating metabolism, but also because of the tight interplay that seems to exist between redox and circadian timing systems. Accumulating evidence in the last years has pointed to many potential nodes that might couple both systems. The following sections summarize some of the most important discoveries. We start by introducing some findings that have shown that certain metabolites involved in redox regulation oscillate in a circadian fashion. We then give an overview on how the redox state of the cell can affect TTFL circadian rhythmicity, and lastly how the TTFL also controls redox rhythms. For a detailed review, see [378].

4.1.1 Circadian redox rhythms

Evidence for circadian oscillations in redox pathways has been documented since the early days of chronobiological research. Before any of the clock genes were discovered, rhythms in $NADP^+$:NADPH ratio, as well as rhythms in the abundance of adenosine dinucleotides were demonstrated in plant seedlings kept in constant darkness [150]. In addition, profiling of energy and redox metabolites in rodent tissues across the circadian time has provided evidence for oscillations in NAD(P)H, ATP and numerous metabolic

intermediates [151, 379, 380]. Glutathione levels exhibit diurnal variations in mouse liver [151, 381], gut [382], pancreas [380] and lung [383] (Figure 4.1A). Although these oscillations might be partially driven by feeding schedules, glutathione levels in platelets kept *in vitro* [153, 154] and in blood serum [155] also display diurnal variation, implying that the blood redox balance somehow resonates with day-night cycles. Interestingly, also the pancreas exhibits robust glutathione rhythms which are unaffected by fasting, suggesting that the regulation of glutathione might be tissue-specific [380]. Moreover, it has been demonstrated that such redox fluctuations (even if they are partially driven by feeding/fasting regimes) play a role in modulating the cytoprotective capability of the liver. The liver displays increased sensitivity to toxicity by the analgesic paracetamol [384] and the chemotherapeutic drug cisplatin [382], during periods of low glutathione levels. One of the most striking examples of circadian redox oscillations described until now are the redox cycles in PRX proteins, which persist even in the absence of transcription [36, 140, 306] (Figure 4.1A). Moreover, the high phylogenetic conservation of these redox oscillations suggests that their evolution might have preceded that of the transcriptional clockwork, thus forcing the reassessment of the current paradigm of the TTFL for circadian timekeeping. PRX oscillations have been discussed in more detail in Chapter 3.

But redox oscillations are not limited to the periphery. The redox status of the central nervous system pacemaker in the SCN, as measured by the abundance of NAD(P)H, FAD^+ and protein glutathionylation, also oscillates in a circadian manner [385] (Figure 4.1A). These rhythms have been found to determine the rate of neuronal firing by regulating membrane excitability via redox-regulated potassium (K^+) channels [385].

4.1.2 Indications of redox regulation of TTFL rhythms

The first evidence for coupling of the redox and circadian TTFL systems came from biochemical studies that demonstrated that the DNA-binding affinity of CLOCK:BMAL1 is regulated by the redox state of the adenine dinucleotide coenzymes NAD(P)H *in vitro* [136] (Figure 4.1B). Nevertheless, these experiments were performed in a purified system using concentrations of NAD(P)H in the millimolar range, thus leaving unanswered the question about the physiological relevance of these findings *in vivo*. However, there are a number of examples that show direct interaction between the redox state and circadian gene regulation. The SIRT1 deacetylase is dependent on NAD^+, and has been shown to interact with CLOCK:BMAL1, leading to deacetylation of PER2 [135] and BMAL1 [134] (Figure 4.1B). SIRT1 also suppresses CLOCK:BMAL1-mediated transcription, resulting in decreased expression of *Per2* [134, 298] and *Dbp* [134] (Figure 4.1B). In zebrafish Z3 cells, it was demonstrated that light induces H_2O_2 release, which in turn drives the rhythmic transcription of clock genes [386]. In addition, this was recapitulated by application of a single H_2O_2 bolus, suggesting that H_2O_2 is the signal transducer in the light entrainment of zebrafish. Redox regulation of clock components has also been

demonstrated in the cyanobacterium *Synechococcus elongatus* [387]. The light-sensitive protein ldpA, which acts as redox sensor by means of two iron-sulfur clusters, was shown to interact with the core clock machinery in a redox-regulated manner, thereby adjusting the organism's period length. The authors suggested that this mechanism acts to fine-tune the core oscillation by relaying nutritional (i.e., redox) cues [387].

Genetic and biochemical studies have also provided compelling evidence towards the regulation of TTFL rhythms by the cellular redox state. For example, as discussed in previous sections, *Arabidopsis* mutants lacking *prx* genes display TTFL rhythms that are altered in phase or amplitude [37], and knockdown of specific PRX isoforms in human U-2 OS cells affects the period length and amplitude of clock gene rhythms [270] (also Figures 2.2 and 2.3). Moreover, acute treatment with high levels of extracellular oxidative stress has been shown to alter circadian rhythms in mammalian cells [54, 308, 309], and in these same lines, results from the Kramer laboratory have shown that reducing and oxidizing conditions disrupt the PER2:CRY1 interaction *in vitro* and result in disrupted circadian dynamics. Reducing conditions promote the dissociation of the complex, whereas oxidative conditions seem to stabilize the interaction (unpublished data), although these results lack *in vivo* validation still, as the reducing and oxidizing agents were used at high concentrations, out of the physiological range. ROS stress has also been shown to reset circadian clocks and to synergistically evoke protective responses for cell survival [388].

Another redox-sensitive mechanism implicated in the control of the circadian clockwork involves heme sensing by a number of clock-associated transcription factors. For instance, heme binding can control BMAL1 activity by inhibiting DNA binding

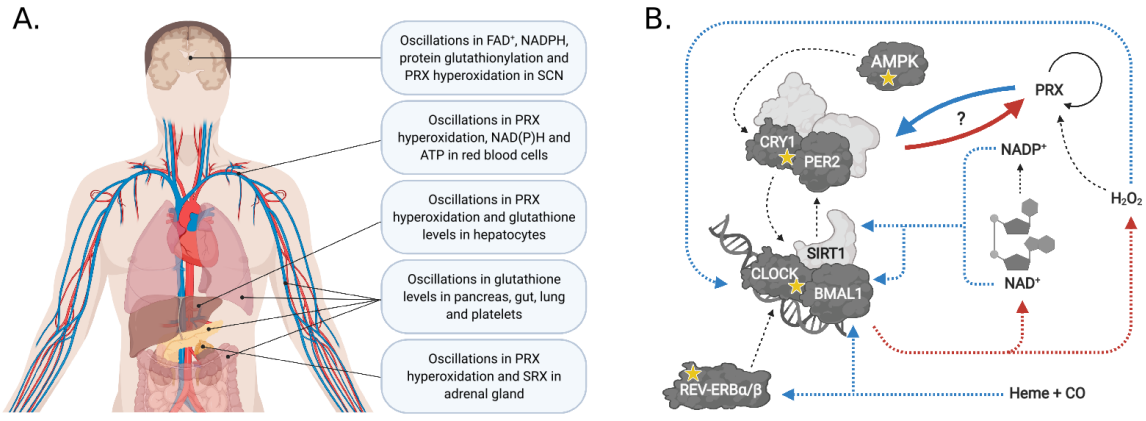

Figure 4.1: Circadian redox oscillations and their interaction with the transcriptional clockwork in mammals. (**A**) Circadian redox oscillations in mammalian physiology. Oscillations in the redox status of FAD^+, NAD(P)H, glutathione and PRX have been measured in different mammalian tissues. Figure modified from [378]. (**B**) Potential nodes of interaction between redox oscillations and the canonical TTFL. Dashed arrows indicate regulations (positive or negative regulations are not differentiated). In red we illustrate how the TTFL might regulate redox oscillations; in blue, how redox might regulate the transcriptional clockwork. Yellow stars represent redox-reactive cysteine residues in different clock-related proteins. See main text for details.

in response to carbon monoxide (CO) [389] (Figure 4.1B). Moreover, rhythmic heme degradation, which generates CO, is required for normal circadian rhythms as well as circadian metabolic outputs, as CO supresses circadian transcription by attenuating CLOCK:BMAL1 binding to target promoters [390]. Similarly, the activity of the nuclear hormone receptors RevErbα and RevErbβ is modulated by heme [375, 391, 392] (Figure 4.1B). And finally, heme also regulates the negative limb of the TTFL because it inhibits the complex formation between PERs and CRYs [393].

In addition to regulation by redox-active ligands, these metabolic systems also impinge on the molecular clockwork directly by means of reactive cysteine residues present in a number of clock proteins. For example, heme binding and, consequently, the activity of RevErbβ, is governed by the formation of a disulfide bridge at a redox-sensitive cysteine residue in the heme binding pocket [375]. Moreover, in a study from last year, Pei *et al.* showed that CLOCK contains a cysteine residue that can sense H_2O_2 levels and regulate its binding to DNA [370]. In fact, the same authors showed, for the first time, that H_2O_2 oscillates robustly with a near 24 h rhythmicity in cultured cells and mouse livers [370], providing solid evidence for the role of this reactive oxygen species in the consolidation of circadian clock gene expression, as the CLOCK binding affinity to DNA might be under circadian redox control. In 2014, two independent studies reported the structure of the PER2:CRY1 protein complex and demonstrated that, at its interface, coordination with a zinc ion is essential for complex stabilization and activity. Interestingly, the binding of the metal ion was governed by a regulatory disulfide switch and other stabilizing cysteine residues embedded in the structure of CRY1 [374, 394]. Mutation of cysteine residues involved in the coordination with the zinc ion disrupted the PER2:CRY1 interaction [374]. In the same lines, mice carrying mutations in one of the conserved Cys residues from the regulatory couple displayed a markedly prolonged period of locomotor activity [395].

Post-translational control of the stability and degradation of clock proteins is an integral part of the clockwork. Interestingly, a number of proteins involved in this mode of regulation have been shown to be under redox regulation. Degradation of CRY1, for example, is induced by phosphorylation by AMPK [267], which has been shown to be under redox control (again, a regulatory disulfide couple was found to be essential for AMPK activation) [396]. Taken together, these findings suggest that redox regulation by modification of reactive cysteine residues might be a common theme in clock signaling (Figure 4.1B).

4.1.3 Indications of TTFL regulation of redox rhythms

In the other direction, also some redox components have been shown to be regulated directly or indirectly by the TTFL. A well-established example is the NAD^+-producing enzyme nicotinamide phosphorybosyltransferase (NAMPT), involved in the NAD^+-

salvage pathway. The rhythmic transcription of this enzyme results in the rhythmic output of NAD^+ (Figure 4.1B), which subsequently has the potential to feed back to the TTFL either indirectly, by modulating the activity of key regulatory enzymes such as the deacetylase SIRT1, that regulates BMAL1 and PER2 activity [134, 135], or directly via control of the binding affinity to DNA of redox-sensitive transcription factors (although the latter lacks *in vivo* confirmation) [136, 298, 397]. In addition, rhythmic NAD^+ production has the potential to generate rhythmic NADPH (Figure 4.1B), since one of the major sources of NADPH is the enzymatic conversion of NADH to NADPH, catalyzed by mitochondrial nicotinamide nucleotide transhydrogenases (NNT) and cytosolic NAD kinases (NADK) [398]. Rhythmic NADPH production then impinges on cellular metabolism, as this molecule is an important electron carrier for anabolic reactions. Moreover, glutathione synthesis has been shown to be under direct TTFL control in flies [399]. Rhythmic synthesis of redox metabolites, however, does not necessarily imply rhythms in the ratio of their reduced and oxidized forms, which more likely depend on functional metabolic oscillations. This thus demonstrates an inherent difficulty in separating cause and effect in the interaction between the TTFL and redox oscillations, since the two processes are no doubt intertwined at the molecular and biochemical levels.

Furthermore, genetic studies have demonstrated that ablation of core clock components affects the antioxidant capacity of the cell as well as peroxiredoxin rhythms. *Drosophila per* mutants, for example, exhibit compromised antioxidant defense [400]. Similarly, behaviorally arrhythmic *Bmal1*$^{-/-}$ mice display increased accumulation of ROS and premature aging [401], neurodegenerative change [402] and marked decreased NAD^+ levels [298, 373]. But given that not all clock gene mutants exhibit such phenotypes, the effects could be due to non-circadian activities of BMAL1 as a transcription factor, beyond its role in the clockwork. Conversely, the absence of the negative regulators Per2 and Cry1 results in an increase of the NAD^+ levels [373]. Moreover, the period length of Prx-SO_2H rhythms is extended in embryonic fibroblasts derived from *Cry1,2*$^{-/-}$ mice [36]. And in behaviorally arrhythmic *Drosophila* mutants and *N. crassa* mutants displaying lengthened periods, Prx oscillations are perturbed in phase [37].

Two last links between the circadian and redox systems involve the circadian-regulated pineal hormone melatonin, and the circadian control of adrenocorticotropic hormone (ACTH) release from pituitary. Melatonin has been shown to possess antioxidant features (although its concentration in plasma is much lower than that of other known antioxidants) by stimulating the NFκB, AP-1 and Nrf2 pathways, resulting in up-regulation of the expression of antioxidant detoxification proteins [403, 404]. Moreover, Rhee and colleagues have shown that, in adrenal gland, mitochondrial H_2O_2 is produced as a by-product during corticosterone synthesis from cholesterol [339], which is stimulated by the circadian release of ACTH from the pituitary [372]. Interestingly, the H_2O_2 release to cytosol, when mitochondrial H_2O_2 levels accumulate, serves to regulate its own levels, and thus also corticosterone synthesis. Cytosolic H_2O_2 activates, on one hand,

import of Srx to mitochondria to control H_2O_2 levels and, on the other hand, the p38 MAPK pathway, which ultimately inhibits cholesterol transport to mitochondria [339]. In the absence of mitochondrial cholesterol, corticosterone synthesis halts. Thus, in addition to ACTH control [372], a negative feedback loop is generated and corticosterone synthesis is additionally regulated independently of the TTFL by means of the Prx/H_2O_2 oscillating system [339]. In other highly oxidative tissues, such as heart and brown adipose tissue, mitochondrial respiration (and thus inevitable ROS generation) has been shown to be under the control of the NAD^+-dependent mitochondrial SIRT3, which is in turn regulated by CLOCK:BMAL1 [373].

4.1.4 Physiological relevance of the TTFL-redox crosstalk

We have summarized the numerous nodes of interaction between the circadian and redox systems. Although Prx proteins are highly conserved through evolution, their functional relevance is yet to be deciphered. The presence of such autonomous oscillations suggests the existence of an underlying redox oscillator, but whether these rhythms are indeed an oscillator or rather the output of some other oscillating system remains to be elucidated. Regardless of the details, it is highly likely that in a nucleated cell, transcriptional and redox rhythms are tightly coupled in order to unambiguously coordinate cellular physiology, and that disturbance of one will affect the other. Consistent with this hypothesis, clock mutants display disturbed Prx rhythms, and conversely, ablation of Prx isoforms affects the TTFL [36, 270] (Figures 2.2 and 2.3).

The medical significance of the interaction between the circadian and redox systems is illustrated by numerous pathologies that manifest both redox and circadian disturbances, such as aging, neurodegenerative disorders, cancers and various metabolic conditions (for a detailed review, see [405]). The links between circadian timekeeping and aging have long been recognized and there appears to be a reciprocal interaction [406]. It has been shown that numerous circadian parameters are affected by aging, and that aging seems to affect the ability of the SCN to reset peripheral clocks. Interestingly, transplantation of neonatal SCN into an aged hamster reversed this effect and resulted in an increased lifespan [407]. Conversely, disruption of the circadian clockwork by systemic deletion of clock genes has been shown, in some cases, to significantly affect aging processes [406]. *Bmal1* knockout mice are perhaps the best example. These animals display shortened lifespan and develop many age-related pathologies such as cataracts or reduction in bone and muscle mass [401]. Whether these effects are due to the circadian functions of BMAL1, or a consequence of other non-circadian roles, remains to be answered. Aging is also accompanied by alterations in the cellular redox balance, resulting in increased ROS levels. It was proposed that one of the drivers of premature aging in *Bmal1* knockout animals could be the high levels of ROS. In agreement with this hypothesis, it has been demonstrated that supplementation with the antioxidant *N*-acetyl-L-cysteine increases the longevity of *Bmal1* knockout animals [408]. Interestingly, also feeding schedules have

been shown to affect lifespan, circadian rhythms and redox balance. For instance, caloric restriction can entrain peripheral and central clocks and increase longevity, partially through a decrease of oxidative stress [406]. SIRT1 has been shown to increase in response to caloric restriction and is proportional to lifespan [409]. Another interesting example of where circadian and redox systems converge is cancer. It has been shown that aberrant ROS signaling, as well as altered circadian rhythmicity, can contribute to cancer progression [410, 411]. SIRT1 function has also been linked to cancer, as its primary targets include the tumor suppressors p53 or FOXO1, both of which are misregulated in cancer.

Nevertheless, despite the numerous links supporting the interaction between redox metabolism and circadian rhythmicity, there is still a lack of direct experimental evidence revealing how both processes actually couple *in vivo*. This is mainly due to the intrinsic difficulty that comes from trying to separate two processes that seem, *a priori*, so fundamental for cellular physiology. Modeling can be useful in this regard, as we might uncover which coupling nodes are more likely to be relevant depending on the redox/TTFL oscillating properties.

4.2 Aim: Coupling Redox and TTFL Oscillations

The aim of this chapter was to analyze the synergistic crosstalk that exists between the circadian and redox timing systems from a computational perspective. From the multiple links that interconnect the circadian and redox systems, we chose to focus on the following nodes. First, we hypothesized that H_2O_2 rhythms are under TTFL control, based on experimental evidence that shows that this is the case in adrenal gland, where circadian control of ACTH stimulates the synthesis of corticosterone and the inevitable generation of H_2O_2 [339, 372]. Second, and now in the other direction, since the PER2:CRY1 interaction seems to be redox-sensitive [374, 394], we analyzed how cytosolic H_2O_2 oscillations might modulate this complex formation. Lastly, we analyzed the synergistic and simultaneous crosstalk of both oscillators.

In order to study the effect of redox on the TTFL we searched in the literature for models of the mammalian TTFL clockwork that contained Per2:Cry1 as an explicit variable. We found two models of different complexity that we present in this chapter, namely the Rélogio [102] and Almeida models [233].

Bioinformatic analyses have suggested that the most essential feedback loops which result in rhythm generation can differ among tissues [69]. In these same lines, we speculated that the redox oscillator properties might also vary across tissues. The results shown here are, however, the first steps of the project and come from relatively straightforward mathematical analyses. The most interesting questions still remain to be answered and will be discussed in Section 4.5. Are there differences in how redox

signals are relayed to the TTFL among tissues? Are there more coupling nodes between the TTFL and redox clockworks? What is the relevance of each node in each tissue? What are the conditions for redox/TTFL entrainment in the different tissues? Is there evidence for differences in redox oscillator properties among tissues? What are the advantages of having bidirectional coupling between the redox and TTFL clocks, if any? So far we still have more questions than answers but further research will give insights into some of the questions.

4.3 How to Achieve Clock Synchronization? Coupling from a Theoretical Perspective

Again, before jumping into the results section, I have chosen to give a brief overview on coupled oscillator history and theory. Scientists have long been baffled by the existence of spontaneous order (and thus synchronization) that exists in the universe. Until some decades ago, the study of synchrony was a rare affair, with biologists, physicians, mathematicians, sociologists, astronomers, etc. working in separate fields and pursuing seemingly different lines of inquiry. But, with time, the science of synchronization has emerged from insights coming from these and other disciplines. This "new science" centers on the study of coupled oscillators, which are widespread throughout the living and non-living worlds. Groups of fireflies, planets or pacemaker cells are collection of oscillators in which one can find some "underlying order". Understanding the basic rules of their theory can help us to gain understanding into how coupling of oscillators results in order or synchronization.

4.3.1 A brief introduction to coupled oscillator theory

Coupling between oscillators was first studied by the great Dutch physicist Huygens in 1673, who noticed that pendulum clocks in the same room became synchronized. Nevertheless, the field of nonlinear dynamics (a branch of mathematics devoted to study how systems evolve in time) did not properly evolve until the late 19^{th} century. It was Henri Poincaré who, in 1889, laid the foundations of the theory of dynamical systems with his studies on the stability of the solar system. He was also the first person to glimpse the possibility of chaos, in which a deterministic system exhibits aperiodic behavior that is highly sensitive to initial conditions [310]. The field of dynamics has since then been largely concerned with nonlinear oscillators and their applications in physics and engineering. Nonlinear oscillators played a vital role in the development of technologies such as radar, radio or lasers. But today we know that coupled oscillators are also prevalent in biological systems. Most organisms appear to be coupled to various periodicities present in our surroundings, such as the rotation of the Earth around the sun, alternation of night and day, or the tides.

Two or more oscillators are said to be coupled if some physical of chemical process allows them to influence one another. Fireflies communicate with light, planets attract themselves with gravity, heart cells exchange electrical currents back and forth... And the result of this mutual influence is often synchrony, or entrainment. When synchrony occurs, oscillators acquire a rational $\frac{m}{n}$ period locking, meaning that one oscillator will undergo m cycles in the time in which the second one undergoes n cycles. Some examples can be seen by the 1:4 frequency locking between respiratory and cardiac rhythms in some individuals (i.e., 1 inhalation and exhalation occur for every 4 heart beats) [412, 413], or by the 1:1 synchronization of circadian clocks to the day-night cycle. In very general terms, entrainment is the process in which oscillators synchronize to an external signal at a fixed m to n ratio, and it is common to all systems of coupled oscillators. The regions of $\frac{m}{n}$ synchronization can be plotted as Arnold tongues, named after the mathematician Vladimir I. Arnold, who described them in 1963. The dynamics are more or less simple at low coupling: tori (limit cycles of two frequencies that are not locked) and some zones of synchronization (and thus period- and phase-locking) dominate the parameter space. Higher coupling, although it increases the regions in which the tongues (and thus synchronization) exist, can also lead to more complex behavior, including chaos. Arnold tongues are generic to coupled oscillators and there is a vast amount of literature on their theory and the results of mathematical modeling [45–48, 273, 414].

Researchers working in the emerging field of coupled oscillator theory ask themselves questions such as the following. How exactly do coupled oscillators synchronize themselves, and under what conditions? When is synchronization possible? What other modes of organization are to be expected when synchronization breaks down? And what are the practical implications of all that we are trying to learn?

4.3.2 Coupled oscillators in the context of the circadian clock

Circadian clocks can be regarded as a system of coupled nonlinear oscillators. Firstly, because a number of feedback loops are intertwined (see Figure 1.4 for a graphical representation), and secondly, because they respond and adjust to external periodic Zeitgebers. As was described already in Chapter 1, in the absence of external Zeitgebers, clocks run with its characteristic period τ, which may deviate from 24 h. But if the strength of the Zeitgeber is capable to overcome the period mismatch between its period T and the clock's intrinsic period τ, the Zeitgeber will enforce its natural periodicity on the clock. This situation is called synchronization or entrainment [45, 273, 363, 414, 415]. The range of period mismatches $\tau - T$ for which entrainment occurs is called the range of entrainment. It is in fact the *difference* of both periods τ and T, rather than the single periods *per se*, what determines whether a clock can be entrained or not for a given Zeitgeber strength [45, 273, 414].

In the synchronized scenario, the intrinsic clock's phase ϕ adopts a stable relationship with the phase of the Zeitgeber Φ. The difference $\Phi - \phi$ is referred to as "phase of entrainment" Ψ and, in case of entrainment, it takes a well-defined value. A collection of experimental and theoretical studies have focused on understanding the phase of entrainment, since it is critical for the coordination of daily rhythms in physiology, metabolism and behavior [416]. Variations in the phase of entrainment have been extensively studied in the past decades [253, 416–419]. From an evolutionary perspective, the phase of entrainment is a parameter under selection [40] (probably even more than the intrinsic clock's period) and, hence, a tight regulation does not come as a surprise. Moreover, differences in this parameter is what determines the chronotype of an individual. The so called "early birds" have earlier phases of entrainment than those "night owls".

4.4 Results: Towards a Coupled Model of Redox-TTFL Circadian Oscillations

As has been previously introduced, there is accumulating evidence supporting that the mammalian canonical TTFL interacts with redox rhythms. We hypothesized, on one hand, that the TTFL can drive H_2O_2 production and, on the other hand, that H_2O_2 rhythms regulate PER2:CRY1 complex formation, in line with previous experimental findings [339, 372, 374, 394]. For this reason, we looked for mathematical ODE models of the mammalian clockwork where the PER2:CRY1 complex was explicitly included as a variable.

Our results show, firstly, that a TTFL model can entrain to the D_2 oscillations from our novel redox model and, secondly, that our redox oscillator model can also be driven by (and entrained to) a TTFL periodic input. Moreover, we showed that reducing the "rigidity" (measured with the relaxation rate λ) of the redox oscillator model resulted in a system that can entrain to a wider range of TTFL periods, in agreement with previous computational studies. In addition, upon coupling the TTFL clockwork with our redox oscillator model, we saw that applying the design principles of the redox oscillator in combination with the published parameter set of the TTFL model produced circadian oscillations with the expected features, thus supporting robustness of both oscillators. The biological relevance of our findings is discussed in the last Section 4.5 from this chapter.

4.4.1 Choice and reproduction of TTFL models

In order to analyze the crosstalk between our newly developed redox model and the TTFL, we searched in the literature for ODE-based models of the mammalian TTFL

clockwork that contained Per2:Cry1 as explicit variable. The Relógio and Almeida models are two ODE-based models of different complexity that were tailored for different purposes. The Relógio system is an extensive 19 variable model containing clock transcripts, cytoplasmatic and nuclear proteins, either alone or in complex with other clock proteins [102]. It was built from available data on phases and amplitudes of clock components to understand the mechanisms that govern circadian rhythm generation in mammalian cells [102]. It answered questions such as what are the roles of *Per2* degradation rates, or the role of the Ror-BMAL1-RevErb loop, and provided *in silico* evidence, for the first time, that the Ror-BMAL1-RevErb loop could act as an oscillator independent of the Per2:Cry1 loop [102]. The Almeida model, on the other hand, is a simpler model with only 8 variables. It was tailored to identify the essential interactions that are needed to generate phase opposition between the activating CLOCK:BMAL1 and the repressing Per2:Cry1 complexes [233].

The Per2:Cry1 complex appears as an explicit variable in both models (as well as other proteins such as RevErbα, Ror, BMAL1, Per2 or Cry1). Moreover, both models include regulation of clock gene expression at the level of E-boxes and RORE elements. The regulatory interactions of clock proteins on clock gene expression are modeled with Michaelis Menten-like and Hill-like kinetics, thus accounting for the degree of "nonlinearity" that models need to achieve self-sustained oscillations [111, 113]. The models assume first order degradation kinetics of the clock components, and degradation processes are thus modeled with mass action kinetics (Equations in Appendix C.1).

The first step in driving any of the TTFL models with an external redox Zeitgeber input was to reproduce their oscillatory dynamics. We successfully implemented both models and replicated the expected periods ($\tau_{\text{Relógio}} = 23.65\,\text{h}$ and $\tau_{\text{Almeida}} = 20\,\text{h}$), amplitudes and phase relationships (Figure 4.2, model equations in Appendix C.1).

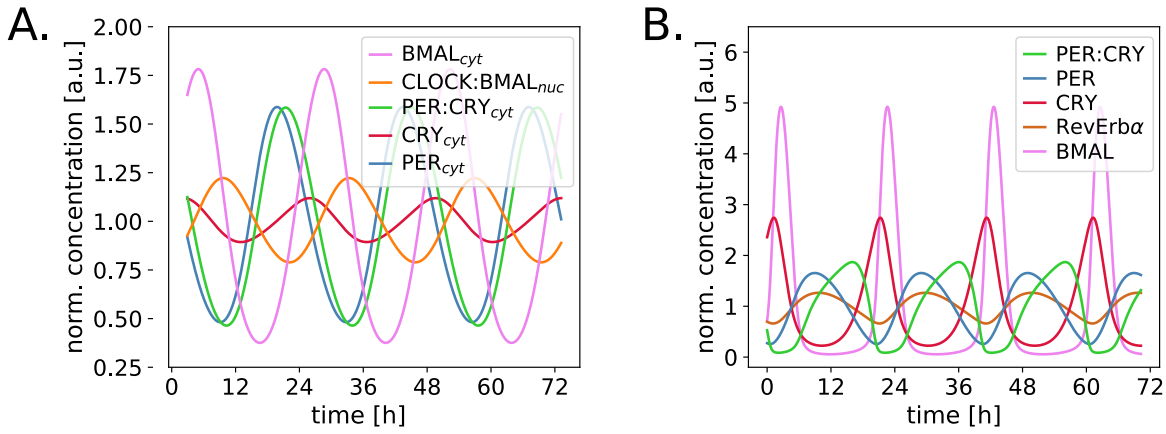

Figure 4.2: Reproduction of the oscillatory time series of the Relógio (A) and Almeida (B) models of the transcriptional-translational mammalian clockwork. Results were obtained by numerical integration of Equations C.1 (A) and C.3 (B) with the original model parameters (Tables C.1 and C.2). Time series were normalized to their means. Periods, amplitudes and phase relationships from the original models were reproduced ($\tau_{\text{Relógio}} = 23.65\,\text{h}$ and $\tau_{\text{Almeida}} = 20\,\text{h}$).

4.4.2 Entrainment of the TTFL by a periodic redox Zeitgeber input: Unidirectional redox→TTFL coupling

Based on published experimental evidence, we hypothesized that redox rhythms regulate the TTFL at the level of Per2:Cry1 complex formation such that high oxidant levels strengthen the interaction. We thus simulated H_2O_2-mediated control of Per2:Cry1 interaction by including a sinusoidal modulatory function within the complex formation term of Per2 and Cry1 (and phosphorylated Per2, $Per2^P$, to Cry1, as this reaction is explicitly modeled in the Relógio model as well). The periodical redox input used to force the Relógio model, similarly to Equation 3.5, took the following sinusoidal form:

$$\text{Redox}(t) = 1 + \frac{F}{2}\cos\left(\frac{2\pi}{T}t + \phi\right) \tag{4.1}$$

where F is the Zeitgeber strength (or amplitude) of the redox input defined as peak-to-trough distance ($F = 0.5$ a.u., as seen from the D_2 time series in Figure 3.6), T is the period ($T = 24.23$ h) and ϕ is the phase of the periodical input. The full system of ODEs, with the specific modulations in the terms describing the formation of Per2:Cry1 and $Per2^P$:Cry1 complexes is shown in Appendix C.1. The numerical simulations are depicted in Figure 4.3. They illustrate that the amplitude of TTFL variables and intrinsic period τ slightly changed to adjust to the 24.23 h period T of the redox Zeitgeber input (compare to the unforced system in Figure 4.2A). Moreover, we saw that the system adopted a stable phase relationship with the Zeitgeber. From the cytoplasmatic Per2 oscillations ($Per2_{cyt}$, Figure 4.3), we observed that the phase of entrainment $\Psi = \Phi_{\text{Zeitgeber}} - \phi_{\text{TTFL}}$ was roughly 12 h. We can thus say that the TTFL entrains to a redox oscillatory Zeitgeber input with $T = 24.23$ h and $F = 0.5$ a.u. in a 1:1 fashion (i.e., TTFL variables

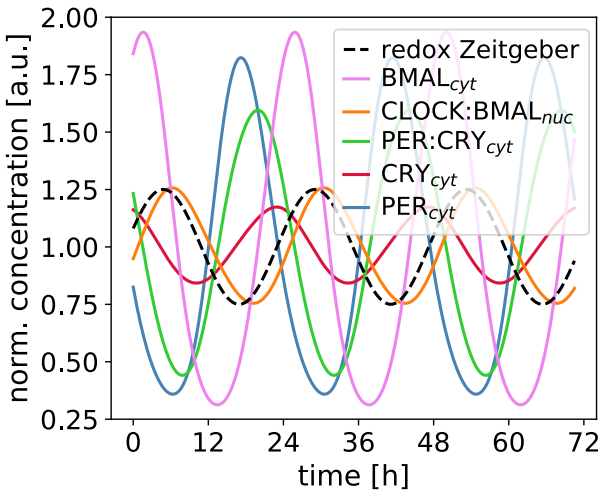

Figure 4.3: Time series of the Relógio model of the transcriptional-translational mammalian clockwork regulated by a periodic redox input at the level of the Per2:Cry1 interaction. Results were obtained by numerical integration of Equations C.2 with the original model parameters (Table C.1). As redox input parameters, we used the following values: peak-to-trough distance $F = 0.5$ a.u., $T = 24.23$ h, $\phi = 0$, determined from the D_2 oscillations (Figure 3.6). Time series were normalized to their means.

complete one period in the time that it takes for the Zeitgeber input to also complete one period).

From the theory of coupled oscillators we know that sufficiently strong Zeitgebers can entrain oscillators even if the period difference between the intrinsic oscillator and the Zeitgeber (i.e., the period mismatch $\tau - T$) is large [45–48, 129, 273, 310, 356, 363, 367, 414, 415]. In this case, the period mismatch $\tau - T$ was not too big (τ_{TTFL}=23.65 h, T_{redox}=24.23 h), and thus entrainment could be expected. Nevertheless, we explored the Zeitgeber strength F – period mismatch $\tau - T$ parameter space to see which combinations led to entrainment, and we plotted the results as an Arnold tongue (Figure 4.4). As seen by the inclination of the tongue towards the left in Figure 4.4A, for a given Zeitgeber strength, the TTFL system entrained more easily to longer periods of redox oscillations (values of $\tau - T < 0$) than to shorter periods ($\tau - T > 0$). Moreover, we saw that the phase of entrainment of $\mathrm{Per2_{cyt}}$ became smaller as the period mismatch $\tau - T$ increased (Figure 4.4B), and that entrainment led to amplitude expansions due to resonance effects for faster running TTFL clocks or slower running redox clocks (lower values of the period mismatch $\tau - T$, Figure 4.4C).

To check that entrainment to a sinusoidal redox Zeitgeber of F=0.5 and τ=24.23 h was a general feature of TTFL models and not simply specific to the Relógio model, we performed the same numerical simulations with the Almeida model [233]. The Almeida model was modified accordingly by adding a sinusoidal modulation to the association constant between Per2 and Cry1 (Equations in Appendix C.1). To our surprise, the original model (with the published parameter set) did not synchronize to the periodic redox D_2 Zeitgeber input, and chaotic oscillations emerged (Figure C.2 and Appendix C.2). A collection of modeling studies have shown that chaotic dynamics can occur in oscillators that are driven by external periodical signals [45, 129, 310, 415, 420, 421]. We nevertheless wondered whether the model was already "prone" to such complex oscillatory dynamics in the absence of external forcing.

To investigate whether chaotic oscillations and other complex nonlinear phenomena also occurred in the absence of external forcing in the Almeida model, together with a master student from the University of Utrecht, Inge van Soest, we performed detailed bifurcation analyses of the original model. We found that this, and other models of the mammalian circadian clockwork, even in the absence of external forcing, produced period doubling, toroidal or chaotic dynamics upon changes in degradation rates of clock proteins or transcripts. This work suggests that, apart from knockout of core clock components, also changes in degradation rates of clock proteins and transcripts might result in arrhythmicities. The results have been published in [286], but for the sake of length and scope of this dissertation they are not described here. Further analyses are needed to understand the conditions in which a periodical redox input entrains the Almeida model of the circadian clockwork when modulating the Per2:Cry1 interaction.

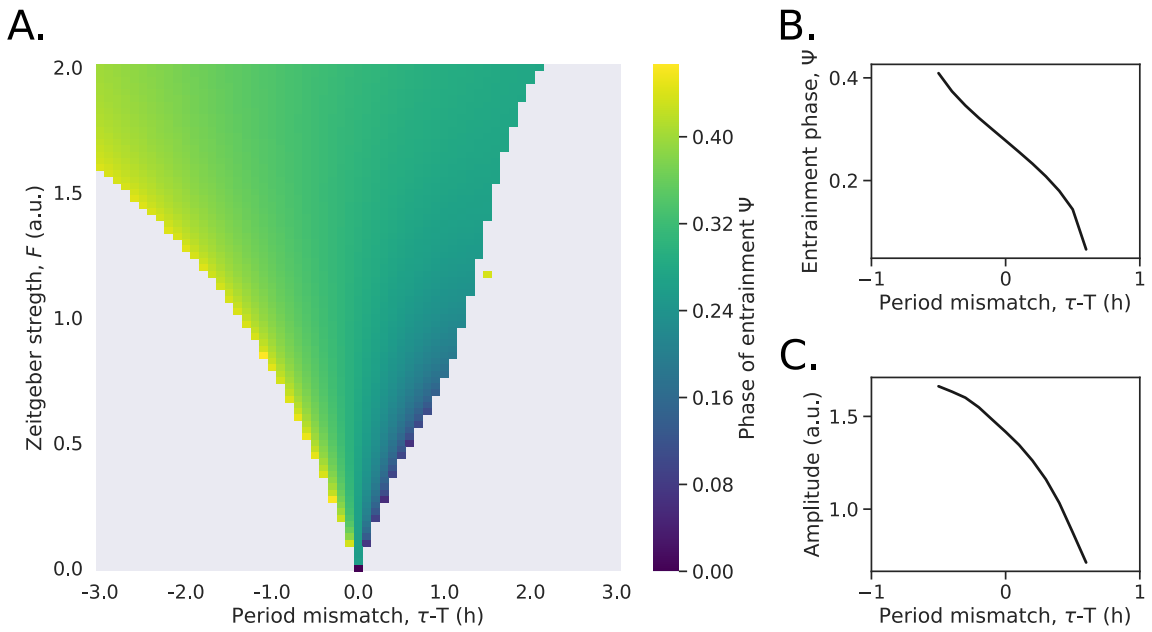

Figure 4.4: The Relógio TTFL oscillator can entrain in a 1:1 fashion to D_2 redox periodic signals. (**A**) Arnold tongue of the Relógio TTFL oscillator when driven by a periodic redox stimulus; phases of entrainment are color-coded within the 1:1 entrained region. Results were obtained by numerical integration of Equations C.2, for redox periods between $T = 20.65$ h and $T = 26.65$ h, and amplitudes (peak-to-trough distances) from $F = 0$ to $F = 2$. Phases of entrainment $\Psi = \Phi - \phi$ were normalized to the $\tau = T$ entrained period. Redox and TTFL phases, Φ and ϕ respectively, were calculated as acrophases (position of peak). (**B**) Dependence of entrainment phase Ψ on period mismatch between endogenous and Zeitgeber periods $\tau - T$ for redox Zeitgeber strength $F = 0.5$. The phase of entrainment, in agreement with [414], varies over a range of about 180° within the entrainment range. Note that the $\Psi(\tau - T)$ function appears decreasing, unlike the increasing functions published by Granada *et al.* [414] and Pittendrigh [416] due to our definition of phase: we defined phases as acrophases, whereas they define phase mathematically as ϕ in $\cos(\omega t + \phi)$. The two definitions give opposite signs for the phase, and thus opposite slopes. (**C**) Dependence of amplitude expansions on period mismatch between endogenous and Zeitgeber periods $\tau - T$ for redox Zeitgeber strength $F = 0.5$. TTFL amplitudes and phases were calculated from the cytoplasmatic unphosphorylated Per2 timeseries (variable $z2$ in the Relógio model in Equations C.2).

4.4.3 Entrainment of the redox oscillator by a periodic TTFL input: Unidirectional TTFL→redox coupling

Corticosterone synthesis in adrenal gland, and the inevitable generation of H_2O_2, has been shown to be under TTFL control [339, 372]. Thus, we next analyzed the effects of the D_2 oscillating system driven by a CLOCK:BMAL1 periodic signal. For simplicity, we numerically simulated a deterministic amplitude-phase redox oscillator. The equations, in Cartesian coordinates, read the following (see Section 6.5 for details on model derivation):

$$\begin{aligned}\frac{dx}{dt} &= \lambda x(A - \sqrt{x^2 + y^2}) - y(\frac{2\pi}{\tau} + \epsilon(A - \sqrt{x^2 + y^2})) + \text{TTFL}(t),\\ \frac{dy}{dt} &= \lambda y(A - \sqrt{x^2 + y^2}) + x(\frac{2\pi}{\tau} + \epsilon(A - \sqrt{x^2 + y^2})),\end{aligned} \tag{4.2}$$

where λ, A, τ and ϵ represent the redox oscillator amplitude relaxation rate ($\lambda = 1\,\text{day}^{-1}$), amplitude ($A = 1$), period ($\tau = 24.23\,\text{h}$) and explicit twist ($\epsilon = 0.1$), respectively (see Section 6.5 for details on parameter estimation). We assumed that the TTFL modulates the oscillatory dynamics of x and, as shown in Equation 4.2, we included the following additive TTFL regulatory term on the right hand side of the x ODE:

$$\text{TTFL}(t) = 1 + \frac{F}{2}\cos(\frac{2\pi}{T}t + \phi) \tag{4.3}$$

where F, T and ϕ represent the Zeitgeber strength (TTFL amplitude, defined as peak-to-trough distance), period and phase, respectively. As parameters of the Zeitgeber input, we took the oscillation parameters from the nuclear CLOCK:BMAL1 oscillations in the Relógio model, $F = 0.45$ (peak-to-trough distance) and $T = 23.65\,\text{h}$ (as determined from the simulations of the Relógio model, Figure 4.2A).

The numerical simulations of the redox deterministic amplitude-phase model in the absence and presence of external CLOCK:BMAL1 forcing are shown in Figure 4.5. Similarly to the results presented in Figure 3.10 in the previous chapter, we observed that a nuclear CLOCK:BMAL1 Zeitgeber input that modulates D_2 levels entrained the redox oscillator in a 1:1 manner. We did not observe large amplitude expansions upon coupling the redox oscillator with the TTFL input, which is probably due to the high relaxation rate of the redox clock ($\lambda = 1\,\text{day}^{-1}$), what makes it a strong oscillator (for a relationship on amplitude expansion with relaxation rate, see Figure B.7).

Since the parameters from the redox amplitude-phase model were derived from the kinetic core redox oscillator (Equations 3.3), we checked the robustness of the results from our driven amplitude-phase redox D_2 oscillator and performed the same analyses now adding a periodic input to the kinetic core redox model (Equations 3.3). We replaced the mitochondrial H_2O_2 production parameter p from the redox model (Equations 3.3), assumed to be constant until now, by the sinusoidal term from Equation 4.3 (full equations shown in Appendix C.3). This way, we simulated periodical production of mitochondrial H_2O_2 D_1. The results are presented in Appendix C.3 and Figure C.3. Similar to the periodically driven redox amplitude-phase oscillator, as expected, we observed 1:1 entrainment of the kinetic oscillator model to the TTFL Zeitgeber and an amplitude expansion of D_2 oscillations comparable to that of the driven amplitude-phase oscillator (Figure C.3).

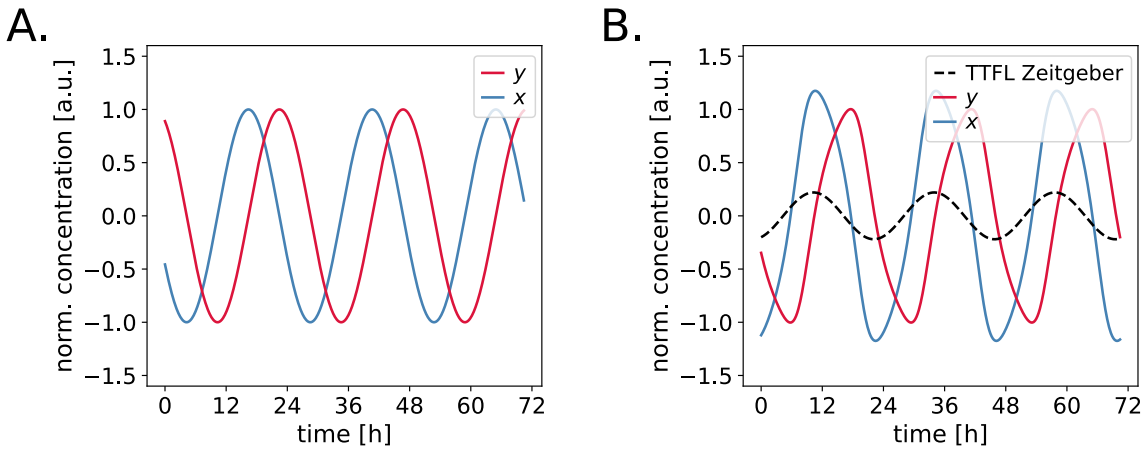

Figure 4.5: Time series of the amplitude-phase D_2 redox oscillator model in the absence (A) or presence (B) of TTFL-regulated control of D_2 production. Results were obtained by numerical integration of Equations 4.2 with $\lambda = 1\,\text{day}^{-1}$, $A = 1$, $\tau = 24.23\,\text{h}$ and $\epsilon = 0.1\,\text{h}$. The TTFL input parameters used in (B) were the following: peak-to-trough distance $F = 0.45\,\text{a.u.}$, $T = 23.65\,\text{h}$, $\phi = 0$, determined from the nuclear CLOCK:BMAL1 oscillations from the Relógio model. Time series were normalized to their means.

The amplitude-phase model that we derived in the previous chapter applies to redox oscillations from heart, brown adipose tissue and adrenal gland. It seems plausible that redox oscillation parameters (relaxation rates, periods, amplitudes or phases) vary across tissues, and even within these three tissues, as seen by the higher amplitude rhythms from Prx3-SO_2H in adrenal gland cells and cardiomyocytes compared to brown adipocytes in western blot data from Kil *et al.* [307]. We discussed in the previous chapter how amplitude expansions depend on oscillator properties such as the relaxation rate λ. But computational studies have shown that resonance effects are not the only phenomena that are modulated by λ. In 2010 and 2015, research from our groups showed that oscillators with large amplitude A and large relaxation rate λ exhibit narrower entrainment ranges than those clocks with lower values of A and λ [273, 363, 414]. The former have been termed "strong oscillators" and the latter, "weak". We thus hypothesized that the redox oscillator might be stronger in some oxidative tissues (e.g., adrenal gland or heart), but weaker in others (e.g., white adipose), and sought to confirm the theoretical predictions in the TTFL-driven amplitude-phase redox oscillator. To do this, we compared the redox amplitude-phase model (with an inherently high $\lambda = 1\,\text{day}^{-1}$) to a modified weaker redox oscillator (with lower $\lambda = 0.05\,\text{day}^{-1}$). To find which TTFL periods and strengths could entrain the strong redox oscillator and a modified weaker oscillator, we again systematically explored the Zeitgeber strength F – period mismatch $\tau - T$ parameter space. The results are plotted as Arnold tongues in Figure 4.6.

In agreement with theoretical expectations, we found that the range of entrainment was wider for the weaker oscillator (Figures 4.6A and B). Figure 4.6C shows the phase of entrainment Ψ as a function of the mismatch $\tau - T$ for strong and weak oscillators. Our simulation results show that the entrainment phase decreased with mismatch $\tau - T$.

This implies that redox rhythms with shorter intrinsic periods have earlier phases, an observation that matches the findings from human chronotypes, where "early larks" are known to display faster endogenous periods and earlier circadian phases than "late owls" [422]. An obvious difference was the steepness of the decreasing function $\Psi(\tau - T)$. The strong redox oscillator (black in Figure 4.6C) exhibited a higher sensitivity on the phase of entrainment towards changes on the period mismatch, compared to the weaker oscillator. In addition, Figure 4.6D illustrates that the weaker oscillator displayed higher amplitude expansions due to resonance effects, especially for redox oscillators with shorter intrinsic periods (or for large TTFL periods that are able to entrain the redox oscillator), as seen by the peak of the weak redox oscillator curve (red in Figure 4.6D) at $\tau - T < 0$. In short, for a given Zeitgeber strength, the rigidity of the oscillatory system (i.e., the relaxation rate upon perturbations) determined the entrainment properties: stronger oscillators showed narrower entrainment ranges, exhibited more flexible entrainment phases and displayed less amplitude expansions, compared to weaker oscillators.

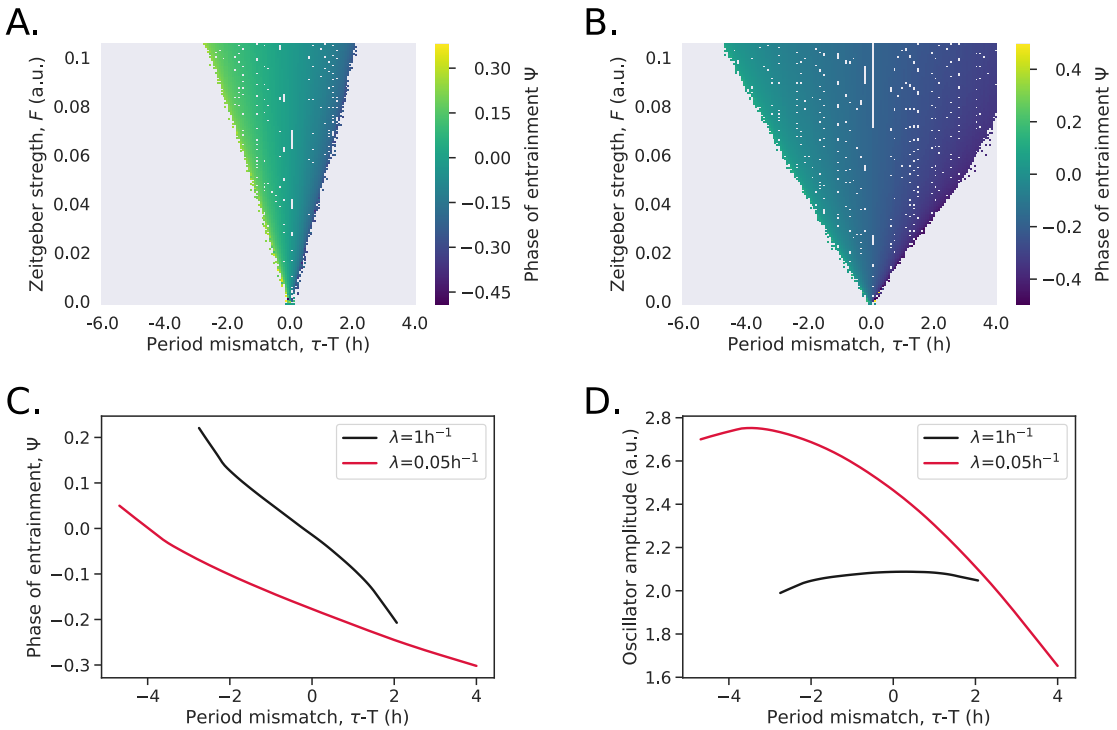

Figure 4.6: Strong redox oscillators (e.g., adrenal gland, heart, brown adipose tissue) display narrow entrainment ranges, flexible entrainment phases and less amplitude expansions than weaker redox oscillators. Arnold tongues of the strong ($\lambda = 1\,\text{day}^{-1}$) (**A**) and weak ($\lambda = 0.05\,\text{day}^{-1}$) (**B**) amplitude-phase redox-oscillators; phases of entrainment are color-coded within the 1:1 entrained region. Results were obtained by numerical integration of Equations 4.2, for TTFL periods between $T = 18.23$ h and $T = 28.23$ h, and amplitudes (peak-to-trough distances) from $F = 0$ to $F = 0.1$. Phases of entrainment $\Psi = \Phi - \phi$ were normalized to the $\tau = T$ entrained period. TTFL and redox phases, Φ and ϕ respectively, were calculated as acrophases (position of peak). (**C**) Dependence of entrainment phase Ψ on period mismatch between endogenous and Zeitgeber periods $\tau - T$ for TTFL Zeitgeber strength $F = 0.1$ in strong ($\lambda = 1\,\text{day}^{-1}$) and weak ($\lambda = 0.05\,\text{day}^{-1}$) oscillators. (**D**) Dependence of amplitude expansions on period mismatch between endogenous and Zeitgeber periods $\tau - T$ for TTFL Zeitgeber strength $F = 0.1$ in strong ($\lambda = 1\,\text{day}^{-1}$) and weak ($\lambda = 0.05\,\text{day}^{-1}$) oscillators. See caption of Figure 4.4 for further details.

4.4.4 Mutual coupling of TTFL and redox oscillators: Bidirectional TTFL⇆redox coupling

So far we described the results from unidirectional coupling, this is, either a redox input modulating the TTFL oscillator or vice versa. We next checked how bidirectional coupling affected both oscillators and simulated a system where we combined the two previous assumptions, namely that mitochondrial D_1 production is under CLOCK:BMAL1 control *and* that Per2:Cry1 interaction is under H_2O_2 regulation. We used the kinetic redox model for this purpose. The full coupled model equations are shown in Appendix C.4.

We found that applying the design principles of the redox oscillator (fast A inactivation and slow $D_1 - D_2 - R$ negative feedback loop) in a coupled TTFL/redox system with the parameter set published by Relógio *et al.* [102] resulted in a network that underwent self-sustained oscillations with a 23.87 h period (Figure 4.7), a value which appeared close to the average period from the Relógio model ($\tau_{\text{Relógio}} = 23.65$ h) and the novel redox oscillator model ($\tau_{\text{redox}} = 24.2$ h). The amplitude of nuclear CLOCK:BMAL1 rhythms, surprisingly, decreased significantly, but was still enough to modulate redox rhythmicity. Despite the low value, close to 0, this complex was still required for the coupled network to display self-sustained oscillations, since clamping of the nuclear CLOCK:BMAL1 variable resulted in the vanishing of rhythmicity. Moreover, the relaxation-like features of the redox variables and the phase-relationship between the inactive Prx3-SO_2H I and mitochondrial Srx R (in this case 8.6 h) were conserved, supporting robustness of our novel kinetic redox model. Interestingly, none of the parameters from the original Relógio model had to be tuned to achieve circadian oscillations, what indicates robustness of this TTFL model as well.

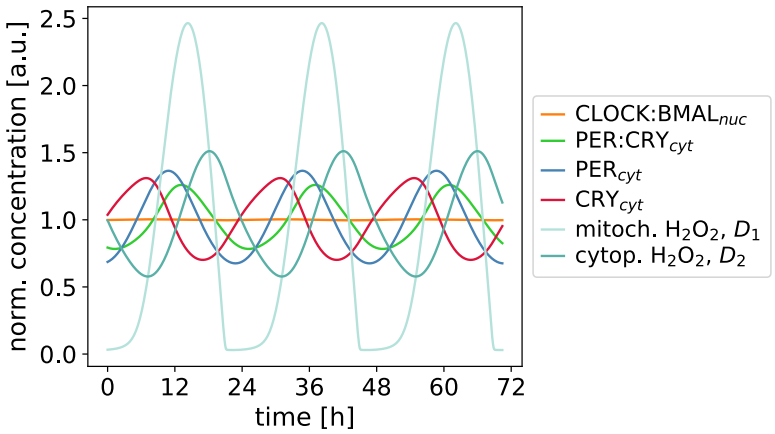

Figure 4.7: Self-sustained limit cycle oscillations of the coupled TTFL/redox model. Results were obtained by numerical integration of the equations shown in Appendix C.4 for the parameter values of the minimal redox and Relógio models. We assumed CLOCK:BMAL1 control of mitochondrial D_1 production (instead of constant production, like in the minimal kinetic model) and D_2 regulation of the Per2:Cry1 interaction. Consistent with previously published data [102, 307] and with the redox model constraints (Table 3.1), the resulting period was 23.87 h and the phase shift between I and R was 8.6 h, supporting robustness of the minimal kinetic redox model.

As mentioned before, the results presented in this chapter are the first steps of the analysis of the mutually coupled network. Further research will be performed to elucidate which other coupling nodes are relevant, whether other types of entrainment ratios (different to 1:1) are possible, and which parameters prove to be most relevant when coupling both oscillators in a 1:1 or any other m to n manner.

4.5 Discussion

In this chapter we examined the dynamics of the coupled redox and mammalian cellular TTFL oscillators under two different forms of unidirectional coupling, namely from the TTFL to redox rhythms by sinusoidal modulation of H_2O_2 production and from the redox oscillator to the TTFL by sinusoidal control of the Per2:Cry1 interaction. Secondly, we analyzed the dynamics of the system under conditions of bidirectional coupling, where we combined both unidirectional coupling assumptions. Our results show that the 1:1 synchronized state dominated the parameter space, in agreement with empirical observations that show that both systems cycle with similar periods, roughly once every day. Moreover, the 1:1 period-locked ratio was obtained without any model parameters variations, what supports robustness of the Relógio and redox models.

4.5.1 Control of the redox:TTFL synchronization ratios

We have shown here that a 1:1 entrainment between the Relógio model of the TTFL and our newly developed redox oscillator model is possible for both modes of unidirectional coupling (namely redox→TTFL and TTFL→redox), as well as for the case of bidirectional coupling (TTFL⇆redox). Nevertheless, other $\frac{m}{n}$ synchronization ratios might be possible as well. There is little knowledge of what mechanisms could result in dynamical redox/TTFL synchronization ratios. Modeling studies can help to verify their existence in reduced models and can give insights into the design principles that result in synchronized redox/TTFL clocks. It was not guaranteed that TTFL models would phase-lock in a rational value under the application of the specific redox input that we derived from the kinetic redox oscillator. With the original TTFL model parameter sets, 1:1 entrainment indeed happened in the Relógio model but not in the Almeida model. The chaotic dynamics observed when coupling the amplitude-phase redox oscillator to the Almeida TTFL model (Figure C.1) proved to be of interest in this regard. Further analyses are needed to explore if different Zeitgeber strengths F, periods T or any other control parameter from the original Almeida model can result in 1:1 or any other $\frac{m}{n}$ synchronization ratios. Extensive bifurcation analyses of the coupled system can give insights into some of the answers, and we might observe that different synchronization ratios exist depending on control parameters.

Understanding the redox/TTFL dynamical coupling is one of the main motivations and points of interest in this work. Thus, our future work in this direction aims to study which conditions result in synchronized redox and TTFL oscillators. Nevertheless, from the many nodes that exist in the regulation of the TTFL by the redox state, we only considered so far the redox→TTFL crosstalk at the level of Per2:Cry1 interaction. But other coupling nodes exist and are worth investigating too. For example, the $NAD(P)^+$:NAD(P)H ratio has been shown, on one hand, to modulate the binding affinity of CLOCK:BMAL1 to DNA [136] and, on the other hand, to regulate PER2 activity through SIRT1 [135]. Moreover, rhythmic redox control of CLOCK directly by endogenous H_2O_2 oscillations has been shown to be required for proper intracellular clock function [370]. In this regard, it is interesting to analyze these additional coupling nodes and see which ratios of synchronization dominate, and what are the control parameters that influence the entrainment ratio.

There are a manifold questions that remain to be answered. Are there additional nodes that might entrain more easily the coupled oscillator system? If so, what is their biological relevance? Are they tissue-dependent? What are the biological implications of having a $\frac{m}{n}$ synchronized ratio different to 1:1, if it at all exists? Is there experimental evidence? Why would have this been optimized in a cellular system? In case of aberrant redox signaling, are there particular TTFL strategies that might allow slowing down the disturbed signaling as a means to protect the TTFL oscillator? Is it possible to control the period of one oscillator by adding an external Zeitgeber (e.g., dexamethasone, temperature cycles, glucocorticoids, etc.) affecting the other? Modeling work can help in finding answers to some of these questions, and might give insights into what are the parameters that predominantly control period-locking in different coupled systems. The physiological relevance of period-locking and synchronization control lies in the relation that the two oscillators have with a variety of cellular states of health and disease such as cancer or metabolic disorders, which are characterized by aberrant ROS signaling. Finding the appropriate control parameters that determine the synchronized 1:1 state might be of relevance for the cellular system and could help in the development of chronotherapies that control the coupled oscillator's synchronized state.

4.5.2 Tissue-specificity of redox oscillators and coupling nodes

In this chapter we investigated two plausible molecular mechanisms for coupling between the redox and circadian systems. A general assumption done throughout this chapter was that, in the unidirectional redox→TTFL coupling, cytoplasmatic H_2O_2 levels strengthen the Per2:Cry1 interaction. Nevertheless, bioinformatic analyses have shown that there seems to be a tissue-specific use of the network of feedback loops that generate circadian rhythmicity across tissues [69]. This means that the most essential loops in the core clock network vary across tissues. It has been suggested that the primary rhythm-generating loop in adrenal gland and heart is the BMAL1-RevErb loop [69]. Although

not incompatible with our coupling assumption, this finding questions the relevance of the redox modulation occurring at the level of the Per2:Cry1 complex formation. If Per and Cry proteins are not essential for rhythm generation in these tissues, it might be that other more relevant coupling TTFL/redox nodes exist. On the other hand, however, the self-inhibiting Per2 and Cry1 loops, together with the repressilator motif, which contains Per2, Cry1 and RevErbα in a chain of three inhibiting reactions, have been shown to occur with comparable frequencies in mouse liver. Thus, it is plausible that the Per2:Cry1 coupling node between redox and TTFL oscillators is more relevant in this tissue. More research has to be done in these lines, in order to find whether tissue-specific redox/TTFL coupling nodes exist and what is the specific relevance of each node across tissues.

In the other direction, namely unidirectional TTFL→redox coupling, we assumed that mitochondrial D_1 production (and consequently leakage to the cytosol, where we refer to the oxidant as D_2) is under TTFL control. Experimental evidence supporting this assumption comes from studies performed in adrenal gland cells, where it has been suggested that mitochondrial corticosterone production (and the inevitable generation of H_2O_2 as by-product) is under ACTH control, which in turn is regulated by the TTFL clockwork [339, 372]. Thus, it is likely that cytosolic H_2O_2 peaks at a specific phase in this tissue. Nevertheless, the peak time of H_2O_2 might be different in other cell types such as red blood cells, where the oxidant is generated as a result of hemoglobin auto-oxidation [306]. Moreover, mitochondria vary in number depending on the cell type [352]. Cells with more mitochondria are therefore more likely to have higher amplitude redox rhythms than tissues with fewer mitochondria. In fact, adrenal gland cells and cardiomyocytes seem to have higher amplitude rhythms of Prx3-SO_2H compared to brown adipose tissue, as seen by western blot data from Kil *et al.* [307]. Also the rhythms in p38 MAPK phosphorylation, which occur as a result of H_2O_2 leakage from mitochondria to the cytosol to ultimately control mitochondrial H_2O_2 production, seem to have different amplitudes in adrenal gland, heart or brown adipose tissue [307]. Differences in amplitudes might make some tissues "stronger redox oscillators" than others. This difference in rigidity will inevitably have consequences in how the oscillators respond to external signals, and weaker redox clocks are predicted to show bigger responses to local or systemic Zeitgebers compared to stronger redox clocks, in line with previous computational findings [414]. Taken together, these hypotheses suggest that tissue-specific redox oscillators (with various amplitudes, rigidity or phases) might display different dynamics and differentially entrain to TTFL signals.

4.5.3 Concluding remarks and outlook

Major differences between tissues have been reported regarding amplitude and phases of clock-controlled genes [31, 80–82], which are presumably induced by tissue-specific transcription factors [423–425]. Moreover, organs differ in the metabolic and

neuroendocrine inputs that they receive, leading to quite various rhythmic transcriptomes. These systemic tissue divergences can modify the core clock dynamics and it would not appear as a surprise if tissues show also specificities in redox oscillator properties. Depending on which feedback loops dominate in a tissue, the nodes of the coupled redox/TTFL system as well as entrainment properties might differ across cell types. Nevertheless, experimental work will have to confirm these hypotheses. This, however, represents a limitation due to, firstly, the inherent difficulty that comes from measuring small and highly reactive molecules like H_2O_2 or other ROS, and secondly, the low physiological concentrations at which they are present in cellular systems. Moreover, it is very difficult to separate the redox oscillating system from the TTFL, since both processes seem, *a priori*, so fundamental for cellular physiology. Typically, any experiment performed under laboratory conditions uses unphysiological concentrations of oxidants or reducing agents, and thus the *in vivo* validation can be under debate. It would be interesting to see whether disruption of metabolic pathways important for maintenance of cellular redox balance leads to perturbations in transcriptional rhythms. Conversely, more gentle methods (rather than genetic ablation) could be applied to study the effect of the TTFL on redox rhythms. As pointed our earlier, genetic ablation of clock genes might result in pleiotropic effects and these results would thus be hard to interpret. It will be interesting to reproduce experimental data with numerical simulations, and to check whether *in silico* knockout of one of the variables in the mutually coupled model reproduces the disturbances at the level of Prx or canonical clock protein oscillations.

It is known that synergies of feedback mechanisms improve oscillator quality [102, 129, 312]. In this regard, the coupled redox/TTFL system can be seen as a network with additional synergistic feedback loops (Figure 4.1B). Coupled oscillator systems might help to maintain a more accurate circadian timing in the face of molecular noise and might confer more robust timekeeping properties over a wide range of disturbances of clock components. Moreover, the different biochemistry of redox and TTFL systems within the coupled network might be particularly advantageous when one oscillator fails. This has been shown to be the case for coupling between the mammalian cell cycle and the circadian clock, which serves to prevent the inevitable transcriptional pause that is associated with mitosis from disrupting TTFL timing [426].

Whether TTFL and redox oscillators have ever existed separately during evolution remains to be elucidated, but mathematical and empirical evidence suggest that there is an adaptive advantage of strongly coupled systems that can be found in any network of coupled oscillators [102, 129, 312, 427, 428]. Insights into what are the mechanistic basis of Prx oscillations, how organisms (or individual cells) combine outputs from biochemically diverse oscillators into unambiguous cellular time, or what are the physiological roles of redox oscillators are eagerly anticipated and hopefully the next years of research will unravel details in the coupling of redox oscillations to TTFL clocks.

Teufelsberg

5

General Discussion and Outlook

5.1 Redox and TTFL Clocks: State of the Art

Biological timing is a necessity in all organisms which is driven by the need to adapt to cyclic changes in the environment. The circadian clockwork in mammals is a highly complex system composed of oscillators at the molecular, tissue and organismic levels. Multiple transcription-translation feedback loops are coupled to generate cell-autonomous and self-sustained circadian rhythms in gene expression, that further coordinate circadian physiology and behavior. Nevertheless, accumulating evidence in the last years has hinted at the possibility that TTFLs might not be the only means by which cells track time, and that there might be additional systems capable of telling cellular time, responding to external time and maintaining the timekeeping system buffered against internal and external perturbations. The discovery of the self-autonomous redox rhythms exhibited by peroxiredoxin proteins provided the first convincing example of such transcription-independent oscillations in eukaryotes [36, 140]. These highly conserved oscillations, found in organisms from Archaea to humans [37], suggest a strong link between circadian rhythmicity and redox metabolism. Whether or not redox oscillations that run in the absence of TTFL-based circadian oscillators exist in nucleated mammalian cells, is still a matter of debate. But these provocative findings bring us to the question of the interdependence of circadian and metabolic (redox) systems. How do the two processes communicate reciprocally? The cofactor signaling molecules that link the two systems are of important interest, especially given the role of circadian disruption in metabolic disorders.

5.1.1 Metabolic clocks: Temporal separation of cellular metabolism

Circadian clocks only confer advantages when they beat in harmony with the external environment. Separating metabolic processes in time might have been a cellular adaptation to prevent the simultaneous occurrence of mutually antagonistic reactions that would otherwise result in futile cycles wasting energy. Consistent with this, numerous metabolic pathways and metabolites have been shown to be under circadian control, and both genetic (i.e., clock gene mutants) and physiological (i.e., shift work) disturbances of the clockwork can increase susceptibility to metabolic stress [153, 221].

But metabolic regulation is not a mere output of the circadian system. Nutrient, energy and redox levels can signal back to cellular clocks to reinforce circadian rhythmicity and to adapt physiology to temporal tissue-specific needs. There is good evidence showing that disruption of either metabolism or the circadian clock affects the other at physiological and molecular levels (reviewed in detail in [249]). High fat diet, for example, lengthens the behavioral period of rhythms in mice and changes the expression pattern of canonical clock-controlled genes [199]. Moreover, restricted feeding schedules in mice can entrain the liver clock in SCN-lesioned animals [429]; can phase-shift locomotor activity rhythms as well as circadian gene transcription in peripheral organs (but not in the SCN) [75]; and can restore oxygen and CO_2 rhythms in mouse models, which have been shown to be clock-controlled, the former following activity rhythms and the latter aligned to food intake [430]. In addition, healthy patients subjected to three weeks of circadian disruption showed a marked decrease in the resting metabolic rate and increased plasma glucose concentration after a meal, two symptoms which are normally associated with the onset of diabetes mellitus [431]. These findings suggest that transcriptional oscillators must be tightly coupled to metabolic cycles. And this hypothesis is indeed strongly supported by the numerous examples of accessory loops, including NAD cofactors [135], AMPK [267], PPAR proteins [268] or HIF1α [432], among others, that embed the circadian transcriptional clock within cellular metabolism (for a detailed review, see [74, 221, 249]).

As described in Chapter 2, most of the recent metabolism/clock research has been dedicated to study how clocks regulate metabolism and the impact of metabolic feedback into the clock. However, the profound compensation that these timekeepers show in the face of metabolic (and other internal) changes has not been studied in detail. The response of clocks to large changes in ATP/ADP ratio, glucose concentration, transcription, or redox disturbances [51–54] reminds to the response to temperature steps. Thus, there might be an underlying homeostatic mechanism that conserves the period within a narrow range upon perturbation of the oscillator's intracellular (metabolic changes) or extracellular (temperature changes) milieu. If this is the case, and a circadian compensatory phenomenon exists, then we might find that the molecular mechanisms underlying temperature compensation are shared with other ways by which the cell buffers metabolic changes.

5.1.2 Redox balance as the mediator between cellular metabolism and canonical circadian timekeeping?

The fact that changes in metabolism can impinge on the molecular clockwork raises the question of what are the mechanisms mediating this interaction. From all the parameters that change as a function of cellular metabolism, redox balance represents one of the strongest candidates. Reduction and oxidation reactions are at the core of cell metabolism. An exquisite balance between the amount of oxidants that are generated through metabolic processes, and the amount of available reducing agents is needed in the cell for it to respond to the specific time-of-day metabolic demands and to coordinate cellular physiology.

But, besides its critical role in cellular metabolism, redox balance has also been shown to be tightly connected to the circadian timing system. The idea that redox flux *per se* might couple circadian and metabolic cycles was first suggested by McKnight and colleagues, who showed that varying the $NAD(P)^+$:NAD(P)H ratio affected the binding affinity of CLOCK:BMAL1 to DNA [136]. These hypotheses gained further support from a vast collection of subsequent research, that over the last years has pointed to the many potential nodes of interaction between the circadian and redox systems (discussed in detail in Section 4.1). The NAD^+:NADH ratio is likely to play an important role in connecting cellular redox state to transcriptional clock components such as PER2 [135] and CLOCK:BMAL1 [134, 136]. Other redox-sensitive mechanisms have been identified in the mammalian clockwork and, in particular, redox regulation by modification of reactive cysteine residues might be a common theme in clock signaling. The activity of AMPK, which ultimately regulates CRY1 stability, and the activity of CLOCK have been shown to be under redox control at the level of Cys residues [267, 370]. Moreover, the stability of the PER2:CRY1 repressive complex is governed by stabilizing cysteine residues embedded in the structure of CRY1 that coordinate with a zinc ion at the interface with PER2 [374, 394]. Also in cyanobacteria, redox balance might be a means by which cells sense changes in fluctuations of the external or internal milieu and transfer it to the clock. The cyanobacterial clock does not absorb light, but rather it appears to sense the redox state of the intracellular quinone pool [387]. Light drives large changes in the redox potential via photosynthesis, and this seems to be a phase-resetting and entraining cue for cyanobacteria [433].

But, why might redox regulation be tightly linked with circadian biology? Some chronobiologists think that the origin of this coupling may have been laid down around the time of the Great Oxidation Event, some 3 billion years ago. Atmospheric oxygen levels increased as a consequence of the newly acquired ability of photosynthetic bacteria to use water as the main electron donor [36, 145]. Rhythmic photosynthesis (and thus oxygen production as a function of the day-night cycles) as well as the generation of reactive oxygen species by metabolic reactions, or directly by UV radiation, could have forced the co-evolution of the circadian and redox systems. This way, ROS production

and those processes which are more sensitive to oxidation might have been temporally segregated, preventing harmful oxidative stress at times of day that would have otherwise led to cell dysfunction and death. Nevertheless, whether redox oscillators in fact exist as such, and whether they are the "primordial" metabolic clock that appeared in evolution is still under debate. The question of how the TTFL evolved, and if it was independent to these redox timing systems, is still unknown.

5.1.3 Reciprocal TTFL-redox crosstalk, in both directions

As has been discussed throughout previous chapters, redox state and TTFL rhythms seem to be intimately connected (see Section 4.1). The reciprocal relationship is supported by findings that have shown that compromising the TTFL clockwork or the redox oscillating system results in a perturbation of the other [37]. But despite the multiple coupling links that exist between metabolic and TTFL cycles, the plethora of redox and metabolic pathways have yet to point to more coherent and specific mechanisms by which reduction and oxidation may govern circadian rhythms. Unfortunately, we know from nature as a whole that answers to these questions are rarely simple and clear cut. Nevertheless, the common narrative that emerges from these studies is that cellular metabolism, and consequently the redox balance, does interact with an organisms's clock. The reciprocal relationship between redox and circadian systems indicates that they both probably play a crucial role in maintaining the function of the organism as it proceeds through time.

5.2 Key Findings Discussed

This doctoral project aimed at gaining some insights into how metabolic, redox and canonical circadian timing systems might be interconnected. More specifically, we sought to (i) gather additional experimental evidence for coupling between metabolic and circadian timing systems, and how disturbance of metabolism can interfere with circadian compensation mechanisms. Next, we hypothesized very generally that clocks might be equipped with metabolic sensors involving redox pathways where Prx proteins (among other enzymatic families) could be involved in adjusting circadian rates against external and internal perturbations. Thus, our next big goal was to understand (at least partially) how cellular redox state might be conveying timing information to the canonical TTFL system, but this time from a computational perspective. Since no model accounting for redox circadian oscillations was available at the start of this project, we sought to (ii) develop a novel minimal mathematical model that reproduced the previously reported circadian oscillations in Prx and Srx in adrenal gland, heart and brown adipose tissue. This novel model shed some light on the "basic ingredients" that the Prx/Srx system must fulfill in order to oscillate in a circadian and self-sustained

manner. Lastly, (iii) we coupled our redox model to previously published models of the mammalian TTFL to understand which coupling nodes might be relevant and under which conditions do the two oscillating systems remain synchronized.

5.2.1 Metabolism and the clock: A means for circadian resilience?

In this study we identified various metabolic genes that affect the core clock oscillator through a small-scale RNAi screen (Figures 2.2, 2.3 and 2.4). Already Zhang *et al.* published a genome-wide RNAi screen for modifiers of the circadian clock in human cells [270] and identified many of the genes which we also found to regulate canonical circadian rhythmicity, supporting our results and demonstrating the deep integration of metabolism/redox and circadian clock control.

Nevertheless, besides regulating properties of circadian rhythmicity, we found that some of the identified genes also play a key role in maintaining the period relatively robust to temperature changes. Based on experimental evidence [51–54], we hypothesized that clocks might not only be compensated against temperature changes, but also to metabolic fluctuations, and that both compensatory phenomena might actually be part of a larger compensation phenomenon, thus re-considering Pittendrigh's old proposition [245]. Intuitively, clocks that speed up or slow down with changes in temperature, nutrients, or any other external or internal cue would not be useful, in the sense that they would not be capable of accurately adjusting its internal cellular time to the external time. If our hypothesis were true, we speculated that interfering with cellular metabolism would yield cellular systems more sensitive to temperature steps. Indeed we found evidence for this: genetic knockdown of PRX isoforms, AMPK subunits as well as members of the family of sirtuins (Figure 2.5) led to disturbances in temperature compensation. In the other direction, preliminary results from the Johnson laboratory have shown that mutant cyanobacteria with suppressed temperature compensation are also more sensitive to metabolic perturbations. Taken together, these results support the "almost-forgotten" 40-year old proposition that a universal property of circadian clocks – temperature compensation – may actually be a subset of a larger phenomenon which creates a general homeostasis of the period of circadian oscillators [245].

Our results, although they lack validation by further pharmacological or genetic analyses, highlight the link between energy sensing, redox state and the circadian clock, which is nowadays a hot topic in chronobiology. These candidate genes might hint towards mechanisms (e.g., Prx rhythms) by which the mammalian circadian clockwork senses and compensates for environmental and metabolic fluctuations. Our results add a level of complexity to the metabolism/redox/TTFL clockwork picture, in that PRX rhythms might not only regulate the clock, but also represent a sensor by which cellular clocks adjust and compensate their period to changes in intracellular metabolic rates and maybe even extracellular fluctuations such as temperature.

5.2.2 Modeling Prx/Srx circadian redox oscillations

A major goal towards understanding a biological system is to successfully model it mathematically. Mathematical models help simplifying the huge complexity of molecular details that there is in a biological system to understand the basic "building blocks" in which the systems are built upon. Models can give insights into how such cellular systems work under normal and perturbed conditions, and can even predict how the system will behave when exposed to novel conditions.

Our contribution to the field of modeling circadian clocks has been a novel model that describes Prx/Srx oscillations in mitochondria from adrenal gland, heart and brown adipose tissue. Although the quantitative details of the kinetic processes in the Prx/Srx oscillating system are unknown, we investigated the basic principles that generate mitochondrial rhythms using computational modeling and bifurcation analyses. We found that the delay in mitochondrial Srx import, in combination with an appropriate separation of fast and slow reactions (Figure 3.5), is necessary and sufficient to generate robust self-sustained relaxation-like oscillations (Figure 3.6), [232]. We found that our conceptual model can be regarded as a series of three consecutive phases and two temporal switches (Figure 3.7), highlighting the importance of delayed negative feedbacks and switches in the generation of self-sustained oscillations.

Developing mathematical models goes in hand with making assumptions that can always be questioned from a physiological or biochemical perspective. In this regard, we assumed the production of mitochondrial H_2O_2 to be constant over time. Under this assumption, the rhythmicity in Prx-SO_2H, Srx and mitochondrial and cytosolic H_2O_2 that we observed, appeared totally independent of transcriptional clocks. Such a self-sustained nature of the Prx/Srx cycle could be tested in isolated mitochondria respiring in a constant environment.

Yet, one can argue about our modeling assumption. The sources of mitochondrial H_2O_2 differ among tissues in which the redox clockwork is present. As previously shown by Rhee and colleagues, in adrenal gland, mitochondrial H_2O_2 is produced as a by-product of CYP11B1 catalytic activity during corticosterone synthesis [339], which is stimulated by the circadian pituitary release of ACTH [372]. In this case, the "leak" of mitochondrial H_2O_2 to the cytosol serves to establish a negative feedback loop of corticosterone synthesis by inhibiting mitochondrial import of cholesterol (the substrate of CYP11B1) through activation of the p38 MAPK pathway. Thus, even though ACTH dictates the rhythm of corticosterone release, it is the Prx/Srx system the one that is essential as the negative limb of the loop. In fact, mice lacking Srx in adrenal gland displayed supressed circadian rythms of adrenal corticosterone production [339], an important systemic cue that normally prepares animal physiology for its active phase. Predictably, the Prx/Srx system will be necessary for rhythm recovery also if the adrenal gland undergoes any kind of unscheduled stress perturbation. Indeed there is

evidence supporting that Prx/Srx oscillations are required to protect cells from increased mitochondrial ROS generation due to steroidogenesis during the sleep phase [339].

In heart and brown adipose tissue, in which oxidative metabolism is very high, the respiratory source becomes important. It is thus important in these tissues to consider respiration rate rhythmicity, which is under SIRT3 control, a deacetylase that senses NAD^+ levels and that is in turn under CLOCK:BMAL1 regulation [373]. In these tissues, the Prx/Srx system must be able to adapt to the predicted oscillatory respiratory production of H_2O_2 and, as in adrenal gland, might become important when dealing with oxidative stress. For example, cardiotonic exercise will make the heart respire at a higher rate and ambient temperature drop will make the brown adipose tissue generate more heat (to maintain body temperature) by also increasing the respiration rate. In these cases, it is likely that the Prx/Srx system deals with the extra H_2O_2 generation and buffers the excess release of the oxidant.

Many other questions that might be addressed with our novel model are nevertheless left unanswered. What are the roles of acetylation and phosphorylation processes in the Prx/Srx clockwork, which are known to change Prx sensitivity to hyperoxidation [434]? What is the purpose of the daily mitochondrial H_2O_2 release? Even without a detailed understanding of the molecular underpinnings to circadian regulation of the cellular redox state, it is interesting to speculate on the functional consequences that redox oscillations might have on normal cell signaling. Just as the clock affects cellular function by regulating the abundance of many key proteins involved in signal transduction and metabolic pathways [435, 436], so might circadian rhythms in redox balance impact upon redox-sensitive signaling and metabolism. Given the known signaling role of this oxidant, such a cyclic release should alter in a timed fashion transcriptional clock regulators, many of which are thiol-redox sensitive (such as RevErbs or the PER2:CRY1 complex [374, 375, 394]), but also a manifold of additional thiol-redox regulatory factors such as nuclear receptors, kinases, phosphatases and transcription factors that might (or might not) be involved in circadian regulation. In this regard, Kil *et al.* have shown that activation of the p38 MAPK in adrenal gland and brown adipose tissue oscillates with a phase and period equal to that of Prx3-SO_2H, which also reflects the oscillatory release of H_2O_2 into the cytosol. Lastly, given the promiscuous nature of H_2O_2 reactivity and its ubiquitous signaling effects, this oxidant might operate as a signal that acts in combination with other more specific signals to consolidate cellular activities by recruiting, timing and tuning signaling pathways in accordance with the metabolic state and demands of the cell [292]. The temporal segregation of H_2O_2 release to the cytosol, which our model predicts to be 4.5 h after the Prx-SO_2H peak, now provides strong support for this concept.

5.2.3 Coupling between redox and TTFL clocks

We have discussed in Section 4.1 the numerous links that exist and support the interaction between redox metabolism and circadian rhythmicity. With our simulations, we have shown that cytosolic H_2O_2 oscillations can entrain in a 1:1 manner the canonical TTFL (Figure 4.4), and that rhythmic TTFL-driven production of mitochondrial H_2O_2 also results in a 1:1 synchronization between the redox and Relógio TTFL systems (Figure 4.6). Additional coupling nodes, however, remain to be studied, and it remains to be understood whether the nodes that link circadian and redox timing systems differ across tissues. Depending on the number of mitochondria or on the oxidative capacity of the cell, the properties redox oscillators (amplitude, amplitude relaxation rate, phase...) might also be tissue-dependent. But, as discussed in previous sections, unraveling tissue-specific redox properties is difficult in circadian biology due to the inherent high reactivity of reactive oxygen species and the low concentrations at which they are present in cellular systems. Thus, quantification of redox circadian biology across tissues, as of today, represents a major challenge.

But, what are the advantages of having a coupled TTFL-redox system? Firstly, synergies of feedback loops have been shown to confer robustness to the system [102, 129, 312, 427]. Robustness can be defined as the ability of a system to maintain functionality under perturbations (such as molecular or cellular noise), and thus is an important parameter in any biomolecular regulatory network. Molecular noise may obliterate single redox oscillators, as we speculated in Section 3.4.5 (Figure 3.8), but inter-oscillator coupling can make the system more robust. Modeling has been shown to be helpful in this regard, because even unintuitive questions such as the robustness of oscillator systems to molecular noise (and their link to oscillator design), or the coupling mechanisms necessary to ensure synchrony, etc., can be explored with the help of theoretical modeling. These fundamental issues would otherwise be hard to address experimentally. Van Ooijen and Miller review in [437] an interesting term in the field of clock modeling: the concept of flexibility. They argue that "the flexibility of a clock system refers to the theoretical number of distinct, independent ways that waveforms can change for a given amount of parameter changes" [437]. Rand *et al.* showed that simple, one-loop clock models were typically inflexible, whereas flexibility could grow as the number of feedback loops increased, independently of the biochemical mechanisms involved [438]. It has been hypothesized that flexibility might allow clocks to tune multiple rhythmic phases and amplitudes in response to evolutionary pressures [439], and to show plastic changes within an individual in different environments [440], and maybe even in different tissues. These concepts still lack experimental verification, but they would provide general mechanisms for coupled TTFL-redox oscillators to gain adaptive dynamics. The analysis of flexibility assumes that both oscillators continually operate, but the different biochemistry of redox and TTFL systems might be particularly advantageous when one oscillator fails.

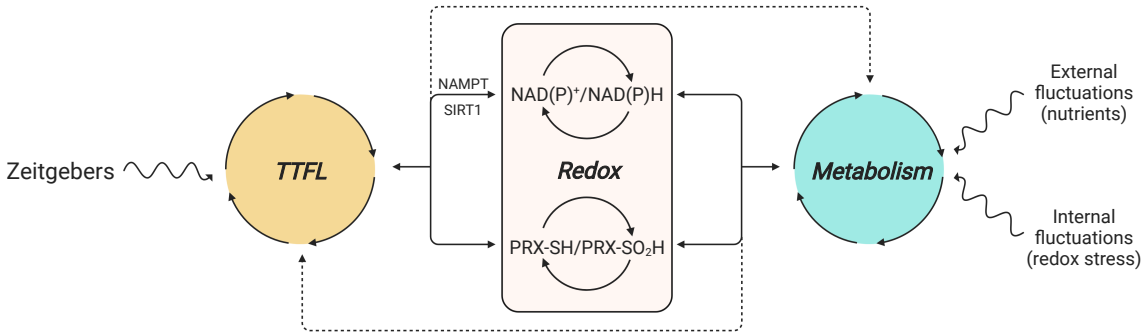

Figure 5.1: Crosstalk of metabolic, redox and transcriptional circadian timing systems in mammals. The results from our work show that metabolism and transcriptional timekeeping are intimately related, and suggest that redox oscillators might be involved in mediating this crosstalk. Redox PRX rhythms or oscillations in $NAD(P)^+/NAD(P)H$ represent potential coupling nodes. The mechanistic details of the coupling nodes between the different layers (i.e., metabolism, redox, TTFL) remain to be further investigated. Figure modified from [441].

Understanding how redox and circadian cycles are coupled together will be of great importance to gain insights into how basic timekeeping mechanisms are integrated into cellular physiology. The presented examples of crosstalk between circadian and redox pathways highlight their numerous connections, even if the relative importance of most of these links remains to be mechanistically investigated. It is plausible that the architecture of the circadian system is based on several interlocked layers, including transcriptional and redox oscillations (Figure 5.1). Given that misalignment of an individual's internal clock with geophysical time is associated with long-term health deficits, defining the metabolic origins of circadian timekeeping is likely to have a great impact in understanding endemic metabolic diseases, cancer progression or aging.

5.3 Limitations and Perspectives

5.3.1 Can we speak about redox "clocks"?

There is an ongoing debate on what were the "primordial" clocks that appeared in evolution, and how timekeeping systems evolved with time. Some scientists believe that the high conservation of PRX rhythms suggests that they might predate the evolution of the transcriptional oscillators, and could thus be part of a primordial circadian redox/metabolic oscillator. Transcriptional timekeeping mechanisms might have evolved after, as outputs of this metabolic proto-clock. Nevertheless, whether redox oscillations that run in the absence of TTFL-based circadian oscillators exist in nucleated mammalian cells is still a matter of debate. O'Neill's group has reported that cellular redox homeostasis reinforces high amplitude oscillations [54]. Nevertheless, pharmacological and genetic perturbations that affect the cellular redox state did not affect period length of the TTFL. And, if TTFLs were outputs of redox cycles, period changes would have been expected. However, absence of evidence is not evidence for

absence. The recent study by Pei *et al.* [370] may help in resolving the question of whether TTFL-independent redox oscillators exist in mammalian cells other than red blood cells. The authors reported that redox control of CLOCK directly by endogenous H_2O_2 oscillations is required for proper intracellular clock function, and identified Cys195 as the residue which is involved in the H_2O_2-mediated oxidative regulation of CLOCK. With these findings taken into account, we can speculate that if TTFL-independent redox oscillators indeed exist in mammalian cells, CLOCK:BMAL1, but not $CLOCK^{C195S}$:BMAL1 (CLOCK with a substitution at the redox-sensitive residue C195 by serine) should rhythmically activate its target genes even in the absence of PER and CRY proteins.

Nevertheless, it has not been strictly established that redox balance needs to oscillate for the cellular clock to function. Although we have used the terms "redox oscillators" or "redox clock" throughout this dissertation, strictly speaking, it might be inadvisable to use such term until these issues have been resolved, since these phrases imply self-sufficiency. Until the underlying mechanisms and modes of coupling with the TTFL are firmly established, it cannot be excluded that circadian cycles of redox balance are just reporters, or an output, of some other underlying clock.

5.3.2 Future perspectives

We have shown that genetic perturbations in systems that regulate the cellular redox balance have an effect on circadian parameters (Figures 2.2, 2.3, 2.4 and 2.5), in agreement with previous experimental findings [36, 37, 270]. Moreover, redox has been shown to act as a Zeitgeber that can reset cellular clocks [54], and according to our results, redox oscillators can entrain TTFL clocks (Figure 4.4). It remains to be understood how exactly do redox Zeitgebers impinge on the molecular clockwork, and whether these mechanisms differ depending on the tissue. In this regard, we want to understand how redox Zeitgebers act to switch the circadian oscillator to a new state (i.e., to phase-shift). The input nodes, the order and in particular the kinetics of switching the different state variables of the circadian oscillator are poorly understood, and essentially unknown at the single cell level. We plan to study the impact of redox (and other mechanistically different) Zeitgebers on the kinetics of network switching, by measuring the response kinetics of different clock proteins at the single cell-level. The Kramer laboratory has generated novel knock-in reporter cells expressing clock proteins fused to fluorescent tags from endogenous promoters. This new data set will allow the development of new mathematical models that will uncover the principles of network switching, i.e., on which nodes does a Zeitgeber act and how are the kinetics of phase-shifting conveyed to the rest of the clock network.

As pointed out earlier, there is still a lack of direct experimental evidence showing how redox and TTFL timing processes are coupled in cells *in vivo*, since separating

these two processes that are so essential for cellular physiology poses a major challenge. Moreover, in order to approach the biological significance of the redox control of the canonical TTFL clock, we also need to understand the molecular underpinnings of PRX-SO_2H oscillations. What is the timing mechanism that drives them? Robust post-translational or genetically-encoded reporters for redox balance and ROS levels, rather than indirect markers such as PRX-SO_2H detection, might help in answering this question. In addition, it would be interesting to see whether disruption of metabolic pathways that are important for maintenance of cellular redox balance, in a tissue-specific manner, leads to perturbations in transcriptional rhythms. Conversely, more sophisticated and gentle genetic tools are required (apart from genetic ablation) to study the effect of the TTFL on redox rhythms. Inducible expression and repression models would be of great utility here.

In conclusion, there is great potential in the research between redox signaling and circadian rhythms. From a basic research perspective, it is of prime importance to establish explicitly how does the crosstalk occur and what are the detailed mechanisms. This will undoubtedly constitute a step forward in understanding how cells interpret redox signals differently, depending on the tissue and on the biological time of the day.

5.3.3 Interlocked vs. dissociated feedback loops: Circadian physiology vs. pathophysiology?

A large amount of evidence has shown that regulation of the mammalian timekeeping system involves multiple and interlocked feedback loops (Figures 1.4 and 4.1). As has been already introduced in previous sections, negative feedback loops are required to generate self-sustained oscillations [111–113], but it is often said that single-negative feedback loops are not robust to molecular noise [428]. An advantage of modeling is that one can study alternative network architectures, and we can thus compare models with and without additional feedback loops. Theoretical approaches have shown that adding interlocked positive or negative feedback loops in a network provides robustness to the system, can amplify oscillation amplitude and can make oscillators more flexible and tunable to perturbations [102, 129, 312, 427, 437–440].

The collection of feedback loops within the mammalian circadian clock constitute multiple potential sources for oscillations [102, 103, 315]. As a consequence, if a gene involved in one of the loops is mutated or removed, sustained oscillations in other components can subsist [103, 129]. This redundancy of feedback loops thus provides robustness to mutations and partial disruption of the circadian clock. But these observations raise an important question: can the interlocked feedback loops "decouple" or dissociate, such that they might lose the 1:1 synchrony that they have between them? And what are the physiological implications of this dissociation (or splitting) of loops? Rhythm splitting has been shown at the organismic level, for example in the

old experiments performed by Wever and Aschoff in humans under constant conditions [12, 442]. They found circadian rhythms in body temperature and activity rhythms in most of the subjects but, interestingly, some individuals displayed 24 h rhythms of body temperature and 30 h activity and sleep-wake cycles. Also in rodents, two periods in behavioral activity recordings have been shown to co-exist [443]. The presence of two rhythms of different frequencies within a system has been termed "dissociation" or "splitting" in the literature [12, 421, 442, 443]. At the molecular level, however, rhythm splitting has only been suggested. In the experimental part of this thesis, we found that U-2 OS cells harboring either a *Per2-luc* or a *Bmal1-luc* reporter displayed different periods. Supporting our results are previous observations from Myung *et al.* and Ono *et al.*, who also found distinct periods in different reporter constructs in SCN slices [274, 275]. Although the different periods of our reporter cells are likely explained by different clonal lines, our results might also hint to feedback loops dissociating at the molecular level.

In the same lines, in a parallel project to this thesis, and together with Inge van Soest, a master student from the University of Utrecht, we studied models of the mammalian circadian clockwork of different complexity and mathematical structure, and found that feedback loops can dissociate and give rise to complex nonlinear cyclic phenomena such as toroidal or chaotic oscillations upon variations in degradation rates of clock components [286]. Toroidal dynamics are generated by two limit cycles of different frequencies that are not locked (i.e., $\frac{\tau_1}{\tau_2} \neq \frac{m}{n}$); chaotic oscillations, on the other hand, are aperiodic [310]. Broad power spectra, mimicking background noise, are a characteristic signature of chaos. This is the reason why chaotic dynamics are frequently termed "arrhythmic" among biologists, as they appear to lack a dominant frequency. If we combine our findings, namely the conditions under which tori or chaos occur, together with previously published results, that suggest that different synergistic feedback loops co-exist and generate tissue specific rhythms [69], we might contribute to the further understanding of organismic and tissue circadian desynchronization.

If we now conceptually couple the redox oscillator with the transcriptional clockwork, one easily sees that the number of feedback loops in the system increases (at least) by one. Thus, increased robustness and flexibility is expected. A question that arises now, related to the one asked in the previous paragraphs, is whether a perturbation in the redox loop might affect the network of interlocked loops within the TTFL, or vice versa. We might find that, in case of aberrant redox signaling, different TTFL strategies allow slowing down the disturbed signaling, and controlling the period of the altered oscillator. Modeling studies, again, can be helpful in this regard. Finding appropriate control parameters within the coupled system might be of medical relevance, and could even help in the development of chronotherapies that control the coupled oscillator's synchronized state.

5.3.4 Modeling limitations

The ongoing development of models of the mammalian circadian clock has been particularly helpful recently, as they take into account the "combinatorial complexity" of clock component interactions as well as stochastic properties [444]. Model-based predictions regarding the role of the Ror-BMAL1-RevErb loop [102], effects of mutations in core clock genes [335], the role of post-translational processes on clock components [336], and the electrical properties of the SCN [445], have been validated empirically. The necessity for both molecular noise and intercellular coupling to induce rhythms in a population of SCN neurons has also been predicted via modeling and subsequently confirmed with experiments [334]. A future challenge to clock modelers is now to address the complex connections and interactions between the mammalian circadian clock and other systems, including the many emerging links between the clock, redox and metabolism.

However, toy models, like the ones presented in this dissertation, give hints, ideas and speculative explanations, but they are subjected to several caveats. The most common criticism towards models is that the type of equations and the values of parameters are (mostly) arbitrary. Whereas molecular models are based on well-established genetic regulations, the quantitative details of the molecular mechanisms are usually unknown. For instance, we, as modelers, often choose Michaelis Menten- and Hill-like functions to describe cellular systems. This is because, on one hand, such terms are realistic representations of enzymatic processes and, on the other hand, because they account for the necessary degree of nonlinearity that models need to oscillate. The hypotheses underlying these approximations, however, are not always shown to be satisfied. Thus, theoretical models, although qualified as molecular, should many times be regarded as phenomenological models. Simple models, like the ones developed and analyzed in this dissertation, do not allow to investigate quantitative details of physiological processes, but they allow to study qualitatively the dynamical properties of circadian clocks. Since quantitative data (parameter values, number of molecules, etc.) are rarely available, it is almost impossible to accurately develop quantitative models of circadian clocks.

Second, most models for circadian clocks are based on ordinary differential equations. These models, as well as their stochastic versions, only account for the regulation of physiological responses *in time*, and neglect the aspects *in space*. They assume that the underlying molecular mechanisms occur in "well-stirred" reaction vessels and that the variables (typically mRNA and protein molecules) move freely around the cell. But eukaryotic cells are far from being well-stirred reaction vessels. Cells are very crowded spaces and cellular processes are organized in space. They are divided into compartments, which might need to be modeled individually to take into account space and diffusion, two variables are likely to play critical roles in the dynamics of cellular systems. Nevertheless, regardless of the assumptions, the credibility of the model and its

dynamic properties should ultimately be supported by a good fit between the predicted behavior and the measured data.

It is important to be aware that none of the models, as detailed as they might be, bring really definitive answers. Rather, they provide elements for reflection. For example, the role of positive feedback loops in the molecular mechanism of circadian clocks is not fully elucidated yet. But modeling has provided us with clues to possible functions of these additional loops: increasing robustness to parameter variations, allowing period tunability, etc. But the beauty of simple models lies in that they provide us with additional perspectives of the system and they allow the constant self-formulation of new questions. In the words of the great Albert Einstein, and invoking Occam's razor, "everything should be made as simple as possible, but not simpler".

5.4 Final Conclusions and Open Questions

Metabolism, redox balance and circadian rhythmicity are essential in a myriad of physiological processes to maintain homeostasis, from blood pressure and sleep/wake cycles down to cellular signaling pathways that play critical roles in health and disease. However, the detailed mechanisms by which redox and circadian cycles are coupled together are not known, and will be of great importance to understand the basic mechanisms of timekeeping, and their integration into cellular physiology. Although we have presented a number of examples in the crosstalk between circadian, metabolism and redox pathways, highlighting their intimate interaction, the relative importance of these links remains to be mechanistically investigated. Many systemic physiological functions are not carried out by a single organ but are rather the result of different inputs and outputs from various tissues. Hence, dissecting the contributions of the circadian clocks in all organs is essential for understanding the global control of metabolic/redox pathways by the circadian system. Does the relative contribution of the two oscillators vary between different model systems, in different tissues and organs, and during the life span of a cell? Can the interaction between circadian and redox systems be exploited in order to treat disorders that manifest disturbances in either or both systems? We believe that unraveling links between redox, metabolic and transcriptional circadian timekeeping will likely constitute a step forward towards understanding and developing treatments for metabolic diseases, cancer progression or aging.

There is a collection of greatly interesting questions left unanswered. What drives the rhythmic oxidation of peroxiredoxins and what is the functional significance of these redox oscillations for cellular timekeeping? How essential are TTFL components for circadian timekeeping? Are there different models for circadian rhythm generation that evolved differently? How many clocks are there, and can they have potential conflicting sources of information to sense a single time of day? How do clocks distinguish circadian-relevant signaling cues from irrelevant ones? And, why do we need clocks that beat in

sync with the external environment? We hope that future research will give insights into some of these questions.

Because of the multiple roles of circadian rhythms in physiology, and the large amount of information regarding the molecular mechanisms of circadian clocks, circadian biology has become a fascinating topic and a very active field of research in the last decades. There is an increasing number of publications related to circadian research every year, each adding a small piece to the huge puzzle. We thus need a synthetic way to summarize these observations, to provide possible explanations (which are sometimes counter-intuitive) for surprising experimental observations, and to suggest new experiments. To this end, theoretical modeling is of considerable help, as it provides different approaches to studying the dynamics of complex systems and can successfully complement experimental approaches. One of the reasons that make the field of circadian clocks so interesting is their dynamic character, in which enormous numbers of components keep changing their state from moment to moment, looping back on one another in ways that are difficult to study if one examines any individual part in isolation. In such cases, the whole is surely not equal to the sum of the parts. These phenomena, like many others in the universe, are fundamentally nonlinear. And that's why nonlinear dynamics and theoretical modeling is important for the future of circadian biology.

I finish with a quote from the father of nonlinear dynamics, Henri Poincaré, that illustrates his view on science and the world in general: "the scientist does not study nature because it is useful; (s)he studies it because (s)he delights in it, and (s)he delights in it because it is beautiful. If nature were not beautiful, it would not be worth knowing, and if nature were not worth knowing, life would not be worth living".

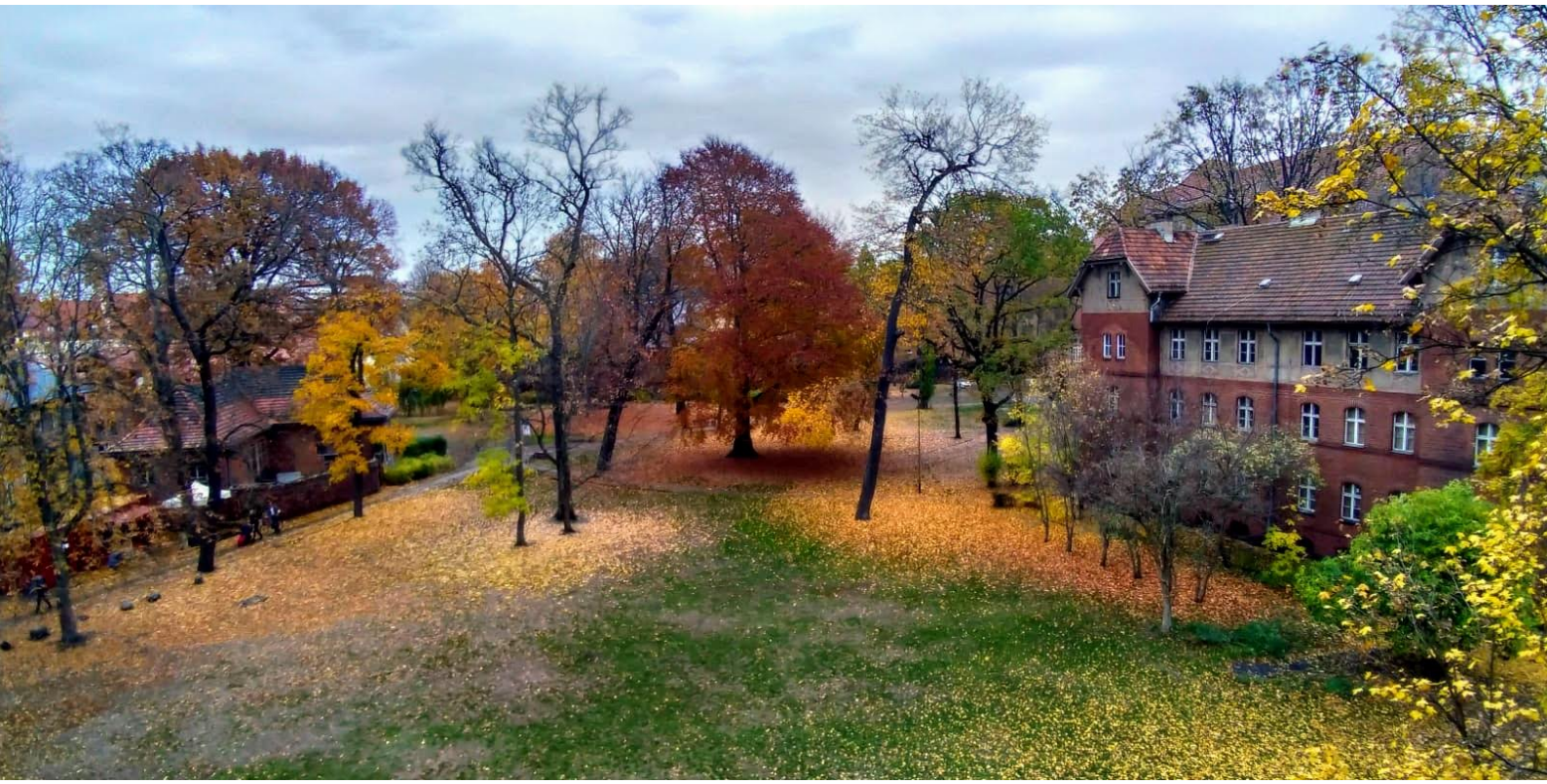

Autumn from the Institute for Theoretical Biology

:

6

Materials and Methods

6.1 Cell culture

Cultivation, passaging and counting of human cells

Cells (HEK293T or U-2 OS) were cultured in complete medium and passaged two or three times a week at a confluency of ~80%. For splitting, cells were washed once with pre-warmed 1x phosphate buffered saline (PBS) prior to enzymatic detachment using trypsine for 5 min at 37°C. The detached cells were dispersed in culture medium at an appropriate ratio and kept in an incubator at a constant temperature of 37°C, 5% CO_2 and 95% relative humidity.

When necessary, cells were counted using trypan blue and a Neubauer chamber. For cell counting, the cells were detached using trypsin and diluted 1:1 in trypan blue. The cell:trypan blue mix was placed in the Neubauer chamber and all cells in the four big squares (each composed of 4x small squares) were counted. The cell concentration was calculated as described in Equation 6.1.

$$\text{conc (cells/mL)} = \frac{\text{counted cells} \times \text{dilution factor} \times 10\,000}{\text{number of counted squares}} = \frac{\text{counted cells} \times 2 \times 10\,000}{4} \tag{6.1}$$

Reporter cells

U-2 OS cells (provided as kind gift of AG Hagemeier, Charité Universitätsmedizin Berlin, Germany, originally purchased from the American Type Culture Collection ATCC #HTB-96) harboring the firefly luciferase driven by a fragment of the mouse *Bmal1* (cloned by B. Maier in the Kramer lab, Charité Universitätsmedizin Berlin, Germany) or *Per2* (kind gift from A. Liu, University of Memphis, USA) promoter were used to monitor bioluminescence in a TopCount luminometer in order to assess the persistence and character of the rhythms following a genetic knockdown. The reporter cells are referred to as *Bmal1-luc* or *Per2-luc* cells.

6.2 RNAi screen

RNA interference (RNAi) refers to dsRNA-induced gene silencing, a cellular process that degrades RNA homologous to one strand of the dsRNA [446]. The intermediates of long dsRNA-initiated RNAi are double-stranded small interfering RNAs (siRNAs), typically 21 to 23 nucleotides long. siRNAs, when introduced into cells, can be used to silence genes in mammalian cells, where the long dsRNAs result in non-specific RNA degradation and shutdown of protein synthesis. siRNAs can be generated inside the cell by introducing vectors that express short-hairpin (shRNA) precursors of siRNAs [447]. The cellular RNAi machinery that naturally processes genome-encoded miRNAs that regulate gene expression is involved in the processing of shRNAs into functional siRNAs [447].

We used shRNA for knockdown of gene expression in order to study if temperature and metabolic compensation are manifestations of the same underlying principle, and whether metabolic perturbation rendered the timekeeping system more sensitive to temperature changes. 78 genes were individually knocked down (see Table 6.1 and Suppl. table S1) via RNAi. The resulting oscillations were compared at two different temperatures, 32°C and 39°C. Non-silencing shRNAs served as negative controls. No positive controls were included although one could argue that, for a proof of concept, we should have tested whether silencing known clock components (*CRY1, CRY2, BMAL1, CLOCK*) phenocopied, for instance, the effects observed in mouse knockout studies.

Two prerequisites for the success of an RNAi screen are, on one hand, robustness of circadian oscillation in the cell culture model and, on the other hand, efficient RNAi-mediated knockdown. U-2 OS cells were chosen because this model has been extensively characterized by functional studies examining knockdown effects of all known clock components that have cellular and behavioral phenotypes in knockout mice [128]. Also, circadian rhythms of these cells can be robustly monitored in 96-well plates via live-cell imaging of luciferase activity using a *Bmal1*- or a *Per2*-promoter fragment driving the

Table 6.1: Alphabetical list of RNAi-targeted transcripts. The genes and number of different shRNA constructs that were tested are indicated in the columns.

Gene	# Constructs	Gene	# Constructs	Gene	# Constructs	Gene	# Constructs
ACO1	3	*GYS1*	3	*PDHB*	3	*SDHA*	3
ACO2	3	*HIF1A*	3	*PFKL*	2	*SDHB*	1
ADIPOQ	3	*HK2*	3	*PKLR*	1	*SDHC*	2
COX4I2	3	*HSP90AA1*	3	*PPARA*	14	*SDHD*	3
COX5A	2	*HSP90AB1*	3	*PPARD*	2	*SIRT1*	5
COX5B	2	*IDH1*	1	*PPARG*	11	*SIRT3*	2
COX6A1	3	*IDH2*	3	*PRDX1*	3	*SIRT4*	1
COX6B1	2	*LDHB*	3	*PRDX2*	3	*SIRT6*	1
COX6C	3	*LDHC*	3	*PRDX3*	3	*SIRT7*	5
COX7A1	3	*LONP1*	3	*PRKAA1*	7	*SREBF1*	2
COX7B	3	*LPL*	3	*PRKAA2*	8	*SRXN1*	3
COX8A	3	*MDH1*	3	*PRKAB1*	7	*SUCLA2*	2
CS	3	*MDH2*	3	*PRKAB2*	5	*SUCLG1*	3
CYBB	2	*NAMPT*	3	*PRKAG1*	6	*SUCLG2*	3
FH	3	*NMNAT1*	3	*PRKAG2*	8	*TXN*	2
G6PD	2	*NMNAT2*	3	*PRKAG3*	8	*TXNRD1*	3
GCK	3	*NMNAT3*	3	*RRM1*	3	*TXNRD2*	4
GLS	3	*OGDH*	1	*RRM2*	3	*TXNRD3*	4
GRS	2	*PDHA1*	3	*RRM2B*	3		
GSS	5	*PDHA2*	3	*RXRA*	3		

expression of luciferase [270, 448] for up to ~7 days. Moreover, the RNAi library used in this study was extensively studied and optimized in U-2 OS cells [449, 450].

Isolation of bacterial plasmids containing the shRNAs of interest

A second generation library from the Hannon-Elledge laboratories with the shRNAs of interest was available in the Kramer laboratory. The RNAi constructs targeting the genes of interest had been designed previously [448] using the rules given in the RNAi codex database [451]. Oligos had been cloned into pGIPZ lentiviral shRNAmir empty vectors and *E. coli* had been transformed with the cloned pGIPZ plasmids. Plasmidic DNA containing the shRNAs was purified after growing bacterial cultures with ampicillin and zeocin overnight using a PureLink® DNA extraction kit in a 96-well format.

Three different 96-well plate setups were used to produce virus of all 288 shRNA constructs, correspondent to 78 genes and also including the negative non-silencing controls. Six plates were processed in one experimental run, as two reporter cells were used. Two experimental runs were performed in a TopCount luminometer to measure the bioluminescence of the reporter cells with a constant temperature of 32 or 39°C.

Transfection of HEK293T cells and lentivirus production

Lentiviruses were produced in HEK293T cells in a 96-well plate format, using a Liquidator™96 pipetting system for this purpose. As described in Figure 6.1, HEK293T cells were seeded one day prior to transfection and grown to a confluency of ~80%. Transfection was performed using Lipofectamine2000® as described in the manufacturer's protocol. After one day, the medium was exchanged and virus particles were collected

the two following days by decanting the supernatants into filter plates. Supernatants containing the viral particles were filtered to remove floating cells and the filtered lentiviral supernatant was ready to use (or could alternatively be stored at -80°C).

Transduction and synchronization of U-2 OS reporter cells

U-2 OS reporter cells (*Bmal1-luc, Per2-luc*) were seeded in 96-well plates and transduced with 100 µL of virus filtrate plus 8 ng/µL protamine sulfate (Figure 6.1). After 1 day, medium was exchanged to puromycin-containing (10 µL/mL) medium to select for the transduced cells. 3 days later, cells were synchronized with dexamethasone (1 µM) for 30 min (Figure 6.1).

The decrease in gene expression after each knockdown was not determined, but the GFP fluorescence, prior to the bioluminescence recordings, was measured with a TECAN Infinite F200Pro® microplate reader. This served as a proxy for transduction efficiency, as the pGIPZ vectors used for the RNAi knockdown contained an open reading frame for GFP, leading to co-expression of the shRNA construct and GFP.

Bioluminescence recordings

After synchronization, cells were washed with PBS and incubated in medium without phenol red supplemented with 0.1 mM luciferin (reporter medium, Figure 6.1). Bioluminescence was recorded in a TopCount luminometer with a stacker unit (sampling rate: ~15 min) for 5-7 days as described in Maier *et al.* (2009) [448].

Twelve 96-well plates were assayed in the TopCount luminometer in two experimental runs. Three different 96-well plate setups harbored the transduced U-2 OS reporter cells containing viruses of all 288 shRNAs (including eight non-silencing controls per plate). Since two reporter cells were used (*Bmal1-luc* and *Per2-luc* cells), six plates (3 plate setups × 2 reporter cells) were processed in each experimental run. The first run was performed at a constant temperature of 32°C and the second one, at 39°C. Bioluminescence was recorded for ~7 days with a sampling rate of ~15 min.

6.3 Processing of bioluminescent data

Time series were processed using the ChronoStar V3.0 software as described in [452]. The first 24 and last 12 h were excluded from the analysis. Raw data was detrended by dividing by the 24 h-running average. Periods, amplitudes, phases and damping coefficients were estimated by fitting the following exponentially decaying sinusoidal curve to the detrended data:

$$f(t) = Ae^{-bt}\cos(\frac{24}{\tau}2\pi t + \phi) \tag{6.2}$$

Here, A represents amplitude; b, damping rate; τ, period and ϕ, phase of the oscillation. By fitting Equation 6.2 to the oscillatory time series, circadian parameters were extracted.

Quality control of the raw data

Extreme values of amplitudes, phases or damping rates (more than four standard deviations away from the mean of the respective plate) were excluded. Regarding the period, since deviations of ~2 h have been reported in the literature [448], we thus did not exclude "extreme" period values in order not to remove potential hits.

The ChronoStar software also provided an error parameter that served as a proxy for the quality of the fit (error = 1 – correlation coefficient). Time series from *Per2-luc* cells with an error greater than 0.20, as well as time series from *Bmal1-luc* cells with an error greater than 0.08, were excluded from further analysis. The oscillations of *Per2-luc* cells were less robust (Suppl. Figures A.1, A.2) and thus a less stringent error cutoff was set.

Trend analysis of 96-well plates: removal of well effects

We found a systematic trend in the edges of some 96-well plates. Such effects can be a combination of (i) border artifacts known to appear in plates due to evaporation of the chemicals, presumably within the days before the recording started (see [453] for more information) and (ii) effects of the multichannel pipettes used to seed cells, which could have systematic trend effects too.

The quality control based on the error of fit accounted for the removal of some obvious trends (see yellow squares in Suppl. Figure A.1). But in order to remove other possible effects that were not so visually evident, we compared all parameter values from same wells to parameter values of the 24 non-silencing controls for each reporter cell line via t-tests (this is, period values of *Bmal1-luc*-A01 wells vs. non-silencing controls wells, amplitude values of *Bmal1-luc*-A02 wells vs. non-silencing controls wells, etc.). If the parameter values were significantly different to the non-silencing controls (p-value<0.05) in all six *Bmal1-luc* and *Per2-luc* plates, the corresponding well was excluded from further analysis, since the observation of that effect is likely to be a trend or an artifact.

Whenever the results from different plates were compared (like in the previous case where wells in different plates are compared), the raw data was normalized based on quantiles.

Standard Operating Procedure

RNAi Screen Liquidator

Day 0

Seed HEK293T cells.

HEK293T cells (culture time < 9 weeks) should have grown in log phase, trypsinized with Trypsin/EDTA (BIOCHROM AG #L2143) for ~5 min at 37 °C. One 175 cm^2 flask will give ~ 60 * 10^6 cells - about seven 96 well plates.
Seed 30*10^3 cells in 100 µl per well in culture media on clear 96 well plate (BD Falcon™, #35 3072), flat well tissue culture treated. Use one set of 200 µl liquidatortips for the entire procedure and the Z-spacer.

Day 1

Transfection of HEK293T cells with packaging plasmid and pGIPZ

Prepare a prediluted pGIPZ sublibrary in 96 format with ~ 0.14 µg/µl in HPLC H_2O. Prepare two solutions with 2.75 ml OptiMEM per plate (GIBCO, #31985) each. Add 11 µg psPAX and 6.6 µg pMD2G plasmid per plate to solution A. Add 55 µl Lipofectamin2000© per plate to solution B, incubate for 5 min at RT. For a more convenient method of calculating the required volumes and amounts use the Excel-calculator (see SOP folder on Tauschplatte, "Screen transfectionmix calculator.xls").
Use one set of 200 µl liquidatortips for the entire procedure without a spacer to pipette 25 µl of solution A from the reservoir onto 96 PCR V-bottom microtiter plate (Costar, #3363). Use 30 µl liquidatortips without a spacer to transfer 1 µl of prediluted pGIPZ sublibrary in the same 96 well PCR microtiter plate take new tips for each plate. Use the 300 µl multichannel pipette to pipette 25 µl of solution B onto 96 well PCR microtiter plate. Spin down with ~1000 x g. Incubate for 20 – 40 min at RT. Transfer transfection mix to 96 well microtiter plate with HEK293T cells (from day 0). Therefore use 200 µl liquidatortips and the Z-spacer, take new tips for each plate.

Day 2

Replace Culture Media

Take off supernatant from HEK293T cells (from day 1) therefore use a 200 µl liquidatortips and the D-spacer, and replace with 150 µl fresh culture media, using the same set of tips and the Z-spacer. Handle with care because cells stick only loosely to the plastic.

Day 3

Reporter cell preparation

Prepare reporter cell line U-2 OS BLH TD1 2K5 (culture time < 9 weeks) grown in log phase (one 175 cm^2 flask gives cells for 3-4 plates). Trypsinize with trypsin/EDTA for ~ 5 min at 37 °C. Seed reporter cells (20 * 10^3/well) in 50 µl culture media plus 32 µg/ml protamine sulfate (final concentration 8µg/ml) in white 96 well culture plate

(NUNC, #136101). Use one set of 200 µl liquidatortips for the seeding procedure and the Z-spacer.

Transfer supernatant

Use a new set of 200 µl liquidatortips and the D-spacer to transfer supernatant from HEK293T cells (from day 2) to MultiScreen® HTS filter plates (Milipore, #MSFBN6B50) which are placed on top of V-bottom plates (COSTAR, #3363). Use the same set of liquidatortips for all plates. Filter supernatant onto plates by spinning at 3000 x g for 1 min. Transfer 100µl filtrate with another set of 200µl tips to the U2OSBLH TD1 2K5 cells, taking the Z-spacer. Measure the GFP expression of the HEK293T cells with the Infinite F200Pro™ Device (TECAN™).

Day 4

Replace culture media

Take of supernatant from reporter cell plate (from day 3) using one set of 200µl liquidatortips and the W-spacer and replace with 150 µl fresh culture media plus puromycin (10 µg/ml) with the same set of tips and the Z-spacer.

Day 7

Start long term monitoring

For all steps on day 7 use the same set of 200 µl liquidatortips. Use the W-spacer to remove media or PBS and use the Z-spacer to add PBS or new media. Prepare 50 µl/well of culture media with 4 µM dexamethason (Sigma-Aldrich™, #D4902, solubilized in EtOH). Synchronize cells by adding 50 µl of dexamethason solution to reporter cell plate (from day 4). Incubate for 15-30 min at at 37 °C, 5 % CO_2. Wash reporter cell plate twice with 150 µl prewarmed PBS/well. During the second wash with PBS on plate, measure the GFP expression of the U-2 OS cells with the Infinite F200Pro™ Device (TECAN™). Finally ad 150µl reporter media per well to the plate and seal with Diamont Seal™ (Abgene™, #AB-0812) and the ALPS 50™ device (Abgene™) (2 times with 165 °C, 2 s each, rotating the plate for 180° in the horizontal plane). Start luminescence recording in TopCount™/LumiStar™/OrionII™.

Restart procedure with next pGIPZ sublibrary

Go to day 0 of this protocoll to screen the next pGIPZ sublibrary.

Media

Culture Media

500 ml	High Glucose DMEM	(PAA™, #E15810)
50 ml	FBS	(GIBCO™, #10270-106)
12.5 ml	HEPES 1M, pH 7.3	
5 ml	Penicillin/Streptomycin, 100x	(PAA™, #P11-010)

Reporter Media

500 ml	High Glucose DMEM, Phenolred free	(GIBCO™, #21063-029)
50 ml	FBS	(GIBCO™, #10270-106)
5 ml	Penicillin/Streptomycin, 100x	(PAA™, #P11-010)
5 ml	D-Luciferin 25 mM	(PJK, #102111)
500 µl	Puromycin 10mg/ml	(Sigma-Aldrich™, #P9620)

Laboratory of Chronobiology – Achim-Kramer Lab Version: 07.03.2011

Figure 6.1: Standard operating procedure for RNA interference screens with a Liquidator™96 pipetting system. Available at the Kramer laboratory.

6.4 Simulations of Ordinary Differential Equations

All temporal simulations and model analyses from ODE models have been performed with Python, using the `odeint` integrator from the `scipy` module. Results were stored and plotted with the `matplotlib` module from Python.

6.5 Simulations of Stochastic Differential Equations

The dynamical properties of single D_2 oscillators were conveniently parameterized by means of generic amplitude-phase models, which can be used to describe any oscillator:

$$\begin{aligned} \frac{dr}{dt} &= \lambda r(A - r), \\ \frac{d\phi}{dt} &= \frac{2\pi}{\tau} + \epsilon(A - r), \end{aligned} \tag{6.3}$$

This model is considered a simple description of a stable limit cycle in a 2-dimensional plane and is commonly termed as well Poincaré oscillator [45]. Equations 6.3 determine the dynamical evolution of the radial coordinate $r(t)$ (i.e., the time-dependent distance from the origin), and that of the angular coordinate $\phi(t)$. The parameters τ, A and λ denote the free-running period, amplitude and amplitude relaxation rate of the D_2 oscillator, respectively. The difference to the ordinary Poincaré oscillator is the twist ϵ, which explicitly adds a radius dependency on the phase dynamics, resulting in a system where the period depends on the oscillator amplitude. In contrast to contextual (i.e., organism or even cell-type specific) models, such conceptual or phenomenological oscillator models allow for a straightforward analysis and interpretation of how specific entrainment or synchronization behaviors rely on fundamental clock properties, such as amplitudes relaxation rates or free-running periods [281, 327].

For a more intuitive interpretation of the oscillator, the polar coordinates r and ϕ can be transformed into the Cartesian coordinates x and y as follows:

$$\begin{aligned} x &= r\cos\phi \\ y &= r\sin\phi \end{aligned} \tag{6.4}$$

and by substituting Equations 6.4 in Equations 6.3, the system can be rewritten in Cartesian coordinates:

$$\begin{aligned}\frac{dx}{dt} &= \lambda x(A - \sqrt{x^2+y^2}) - y(\frac{2\pi}{\tau} + \epsilon(A - \sqrt{x^2+y^2})),\\ \frac{dy}{dt} &= \lambda y(A - \sqrt{x^2+y^2}) + x(\frac{2\pi}{\tau} + \epsilon(A - \sqrt{x^2+y^2}))\end{aligned} \tag{6.5}$$

To model stochastic D_2 oscillations, noise was introduced by adding a Wiener process dW_t to the right-hand side of the x and y equations from Equation 6.5:

$$\begin{aligned}dx &= \lambda x(A - \sqrt{x^2+y^2}) - y(\frac{2\pi}{\tau} + \epsilon(A - \sqrt{x^2+y^2})) + \sigma_x dW_{1t},\\ dy &= \lambda y(A - \sqrt{x^2+y^2}) + x(\frac{2\pi}{\tau} + \epsilon(A - \sqrt{x^2+y^2})) + \sigma_y dW_{2t},\end{aligned} \tag{6.6}$$

Estimation of model parameters

The model parameters $\tau, A, \lambda, \epsilon, \sigma_x$ and σ_y from Equation 6.6 were determined as follows. The free running period of D_2 oscillations was 24.23 h (Figure 3.6). The amplitude A was set to 1 for convenience, following previous theoretical studies [281, 346, 363]. The amplitude relaxation rate was determined from exponential fits after simulating a perturbation on D_2 deterministic oscillations. More specifically, we introduced a pulse-like perturbation at a certain moment in time and let the oscillator relax back to the limit cycle. We then determined the decay rate of the relaxation by fitting an exponential curve to the maxima of the relaxing oscillation. We defined amplitude relaxation rate as this decay rate after a perturbation, and estimated a value of λ=1.45 day^{-1}. Such high λ values are a feature of rigid oscillators. Thus, the D_2 oscillator seems to be a stiff oscillator that very quickly "neutralizes" any kind of perturbation, returning back fast to the limit cycle. For convenience, we rounded the amplitude relaxation rate to λ=1 day^{-1}. The explicit twist parameter was determined from simulations where we evaluated the period-amplitude dependency as a response to a perturbation on the D_2 ODE (Equation 3.3) out of the limit cycle. We plotted peak-to-peak amplitudes against peak-to-peak periods following 100 random perturbations and calculated the slopes of the lines. Twist was defined as the average of all slopes, $\epsilon = 0.1$. The variances of the noise terms could not be estimated due to the lack of experimental data, and thus were heuristically set to different values (in most simulations $\sigma_x = \sigma_y = 0.1$).

Results were obtained by solving the stochastic differential equations using the Euler-Maruyama method [364] for the following model parameters: $A = 1$, $\tau = 24.23\,\mathrm{h}$, $\lambda = 1\,\mathrm{day}^{-1}$, $\epsilon = 0.1$. Numerical simulations were obtained for a total integration time of $24.23\,\mathrm{h} \times 100$ at $\Delta\mathrm{t}{=}0.1\,\mathrm{h}$. At each time step, we introduced the white noise component by adding a random number in the x and y coordinates with standard deviations $\sigma_x = 0.1$ and $\sigma_y = 0.1$.

Three simulation protocols were realized:

- Synchronization by a pulse-like perturbation: at a certain moment in time, we simultaneously shifted each x coordinate of the D_2 oscillator in a specific direction by 3 dimensionless units (see Figure 3.9).
- External periodic forcing: for the results presented in Figure 3.10, we subjected the redox oscillators to an external periodic force with a 24 h period T and amplitude F of 0.05 dimensionless units. The driving force was much smaller than the typical oscillator amplitude ($A = 1$). The Zeitgeber signal (Equation 3.5) was added solely on the x coordinate from Equations 6.6.
- Synchronization via mean-field: in the third protocol (Figure 3.11), the oscillators were subjected to a mean-field M (Equation 3.6), which resulted from averaging all x_i across the ensemble. The M term was additively coupled only to the x coordinate from Equations 6.6.

Single oscillator amplitude and phases were estimated by fitting the following cosine curve to the oscillator traces from the numerical simulations, after removing transients:

$$x(t) = A\cos(\frac{2\pi}{\tau}24t + \phi), \tag{6.7}$$

where A, τ and ϕ represent amplitude, period and phase of the trace, respectively.

In order to determine the damping rate of the ensemble after a perturbation, we calculated the mean oscillatory signal and fitted the following exponentially decaying cosine curve:

$$x(t) = Ae^{-\mathrm{bt}}\cos(\frac{2\pi}{\tau}24t + \phi), \tag{6.8}$$

where A, b, τ and ϕ represent the amplitude, damping rate, period and phase of the bulk (mean) signal, respectively.

Volkspark Friedrichshain

:

References

[1] C. Linneaus. *Philosophia Botanica*. Stockholm and Amsterdam, 1751.

[2] N. Kleitman. *Sleep and Wakefullness as Alternating Phases in the Cycle of Existence*. The University of Chicago Press, 1939.

[3] C. P. McCord and F. P. Allen. "Evidences associating pineal gland function with alterations in pigmentation". In: *J Exptl Zool* 23 (1917), pp. 207–24.

[4] A. B. Lerner et al. "Isolation of melatonin, the pineal fland factor that lightens melanocytes". In: *J Am Chem Soc* 80 (1958), p. 2587.

[5] F. Halberg et al. "Glossary of chronobiology". In: *Chronobiologia* 4 (1977), pp. 1–189.

[6] C. S. Pittendrigh and S. Daan. "A functional analysis of circadian pacemakers in nocturnal rodents". In: *J Comp Physiol* 106 (1976), pp. 333–55.

[7] F. Halberg. "Physiologic 24-hour periodicity; general and procedural considerations with reference to the adrenal cycle". In: *Internationale Zeitschrift für Vitaminforschung. Beiheft* (1959).

[8] C. F. Ehret. "The sense of time: evidence for its molecular basis in the eukaryotic gene-action system". In: *Adv Biol Med Phys* 15 (1974), pp. 47–77.

[9] A. Chovnick. *1960 Cold Spring Harbor Symposium: Biological Clocks, Vol. XXV*.

[10] E. Bünning. *Zur Kenntnis der erblichen Tagesperiodizität bei den Primärblättern von Phaseolus multiflorus*. Vol. 81. Jahrb Wiss Bot, 1935, pp. 411–8.

[11] E. Bünning. *Die endonome Tagesrhythmik als Grundlage der photoperiodischen Reaktion*. Vol. 54. Ber Dtsch Bot Ges, 1936, pp. 590–607.

[12] J. Aschoff. "Circadian rhythms in man: a self-sustained oscillator with an inherent frequency underlies human 24-hour periodicity". In: *Science* 148 (1965), pp. 1427–32.

[13] A. B. Lerner, J. D. Case, and R. V. Heinzelman. "Structure of melatonin". In: *J Am Chem Soc* 81 (1959), pp. 6084–5.

[14] S. H. Snyder and J. Axelrod. "Circadian rhythms in pineal serotonin: Effect of monoamine oxidase inhibition and reserpine". In: *Science* 149 (1965), pp. 542–4.

[15] R. J. Reiter. "The melatonin rhythm: both a clock and a calendar". In: *Experientia* 49 (1993), pp. 654–64.

[16] R. J. Konopka and S. Benzer. "Clock mutants of *Drosophila melanogaster*". In: *Proc Natl Acad Sci U S A* 68 (1971), pp. 2112–6.

[17] M. R. Ralph and M. Menaker. "A mutation of the circadian system in golden hamsters". In: *Science* 241 (1988), pp. 1225–7.

[18] W. A. Zehring et al. "P-element transformation with period locus DNA restores rhythmicity to mutant, arrhythmic *Drosophila melanogaster*". In: *Cell* 39 (1984), pp. 369–76.

[19] M. H. Vitaterna et al. "Mutagenesis and mapping of a mouse gene, *Clock*, essential for circadian behavior". In: *Science* 264 (1994), pp. 719–25.

[20] P. E. Hardin, J. C. Hall, and M. Rosbash. "Feedback of the *Drosophila period* gene product on circadian cycling of its messenger RNA levels". In: *Nature* 343 (1990), pp. 536–40.

[21] S. Daan. "The Colin S. Pittendrigh lecture. Colin Pittendrigh, Jürgen Aschoff, and the natural entrainment of circadian systems". In: *J Biol Rhythms* 15 (2000), pp. 195–207.

[22] S. Daan and J. Aschoff. "The entrainment of circadian systems". In: *Circadian Clocks*. Ed. by J. S. Takahashi, F. W. Turek, and R. Y. Moore. Springer, Boston, MA, 2001, pp. 7–43.

[23] R. Y. Moore and N. J. Lenn. "A retinohypothalamic projection in the rat". In: *J Comp Neurol* 146 (1972), pp. 1–14.

[24] C. P. Richter. "Sleep and activity: their relation to the 24-hour clock". In: *Res Publ Assoc Res Nerv Ment Dis* 45 (1967), pp. 8–29.

[25] M. R. Ralph et al. "Transplanted suprachiasmatic nucleus determines circadian period". In: *Science* 247 (1990), pp. 975–8.

[26] R. A. Akhtar et al. "Circadian cycling of the mouse liver transcriptome, as revealed by cDNA microarray, is driven by the suprachiasmatic nucleus". In: *Curr Biol* 12 (2002), pp. 540–50.

[27] G. E. Duffield et al. "Circadian programs of transcriptional activation, signaling, and protein turnover revealed by microarray analysis of mammalian cells". In: *Curr Biol* 12 (2002), pp. 551–7.

[28] B. H. Miller et al. "Circadian and CLOCK-controlled regulation of the mouse transcriptome and cell proliferation". In: *Proc Natl Acad Sci U S A* 104 (2007), pp. 3342–7.

[29] S. Panda et al. "Coordinated transcription of key pathways in the mouse by the circadian clock". In: *Cell* 109 (2002), pp. 307–20.

[30] M. Keller et al. "A circadian clock in macrophages controls inflammatory immune responses". In: *Proc Natl Acad Sci U S A* 106 (2009), pp. 21407–12.

[31] K. Storch et al. "Extensive and divergent circadian gene expression in liver and heart". In: *Nature* 417 (2002), pp. 78–83.

[32] E. Nagoshi et al. "Circadian gene expression in individual fibroblasts: Cell-autonomous and self-sustained oscillators pass time to daughter cells". In: *Cell* 119 (2004), pp. 693–705.

[33] D. K. Welsh et al. “Bioluminescence imaging of individual fibroblasts reveals persistent, independently phased circadian rhythms of clock gene expression”. In: *Curr Biol* 14 (2004), pp. 2289–95.

[34] M. Ishiura et al. “Expression of a gene cluster *kaiABC* as a circadian feedback process in cyanobacteria”. In: *Science* 281 (1998), pp. 1519–23.

[35] M. Nakajima et al. “Reconstitution of circadian oscillation of cyanobacterial KaiC phosphorylation in vitro”. In: *Science* 308 (2005), pp. 414–5.

[36] J. S. O’Neill and A. B. Reddy. “Circadian clocks in human red blood cells”. In: *Nature* 469 (2011), pp. 498–503.

[37] R. S. Edgar et al. “Peroxiredoxins are conserved markers of circadian rhythms”. In: *Nature* 485 (2012), pp. 459–64.

[38] J. Aschoff. “Free running and entrained circadian rhythms”. In: *Handbook of Behavioral Neurobiology*. Ed. by J. Aschoff. Plenum Press, New York, 1981. Chap. 4.

[39] C. S. Pittendrigh. “Circadian rhythms and the circadian organization of living systems”. In: *Cold Spring Harbor Symposia on Quantitative Biology: Volume XXV. Biological Clocks*. New York: Cold Spring Harbor Press, 1960, pp. 159–84.

[40] J. Aschoff. “Exogenous and endogenous components in circadian rhythms”. In: *Cold Spring Harbor Symposia on Quantitative Biology: Volume XXV. Biological Clocks*. New York: Cold Spring Harbor Press, 1960, pp. 11–28.

[41] A. Granada et al. “Phase response curves: elucidating the dynamics of coupled oscillators”. In: *Methods in Enzymology*. Ed. by M. L. Johnson and L. Brand. Academic Press, 2009. Chap. 1.

[42] D. B. Forger. *Biological Clocks, Rhythms, and Oscillations: The Theory of Biological Timekeeping*. Cambridge MA: University Press, 2017.

[43] A. T. Winfree. *The Geometry of Biological Time*. Springer, New York, NY, 2001. Chap. 19.

[44] H. Ukai et al. “Melanopsin-dependent photo-perturbation reveals desynchronization underlying the singularity of mammalian circadian clocks”. In: *Nat Cell Biol* 9 (2007), pp. 1327–34.

[45] L. Glass and M. C. Mackey. *From Clocks to Chaos*. Princeton University Press, 1988.

[46] C. Schmal et al. “A theoretical study on seasonality”. In: *Front Neurol* 6 (2015), p. 94.

[47] V. Arnold. *Geometrical Methods in the Theory of Ordinary Differential Equations*. Springer, New York, NY, 1988.

[48] L. Glass and J. Bélair. “Continuation of Arnold tongues in mathematical models of periodically forced biological oscillators”. In: *Nonlinear Oscillations in Biology and Chemistry*. Ed. by H. G. Othmer. New York: Springer Verlag Berlin Heidelberg, 1986.

[49] C.H. Johnson et al. “Fundamental properties of circadian rhythms”. In: *Chronobiology: Biological Timekeeping*. Ed. by JC. Dunlap, JJ. Loros, and PJ. Decoursey. Sunderland: Sinauer Associates Inc, 2004. Chap. 3, pp. 67–106.

[50] R. Narasimamurthy and D. M. Virshup. "Molecular mechanisms regulating temperature compensation of the circadian clock". In: *Front Neurol* 8 (2017), p. 161.

[51] M. J. Rust, S. S. Golden, and E. K. O'Shea. "Light-driven changes in energy metabolism directly entrain the cyanobacterial circadian oscillator". In: *Science* 331 (2011), pp. 220–3.

[52] G. Sancar, C. Sancar, and M. Brunner. "Metabolic compensation of the *Neurospora* clock by a glucose-dependent feedback of the circadian repressor CSP1 on the core oscillator". In: *Genes Dev* 26 (2012), pp. 2435–42.

[53] C. Dibner et al. "Circadian gene expression is resilient to large fluctuations in overall transcription rates". In: *EMBO J* 28 (2009), pp. 123–34.

[54] M. Putker et al. "Mammalian circadian period, but not phase and amplitude, is robust against redox and metabolic perturbations". In: *Antioxid Redox Signal* 28 (2017), pp. 507–20.

[55] C. J. Johnson and M. Egli. "Metabolic compensation and circadian resilience in prokaryotic cyanobacteria". In: *Annu Rev Biochem* 83 (2014), pp. 221–47.

[56] C. H. Johnson. *An Atlas of Phase Responses Curves for Circadian and Circatidal Rhythms*. Nashville, TN, Vanderbilt University, 1990.

[57] E. Jackson. *Perspectives of Nonlinear Dynamics 1*. Cambridge University Press, 1989.

[58] C. Dibner, U. Schibler, and U. Albrecht. "The mammalian circadian timing system: organization and coordination of central and peripheral clocks". In: *Annu Rev Physiol* 72 (2010), pp. 517–49.

[59] D. Klein, R. Y. Moore, and S. M. Reppert. *Suprachiasmatic Nucleus: The Mind's Clock*. Oxford University Press, New York, 1991.

[60] D. K. Welsh, J. S. Takahashi, and S. A. Kay. "Suprachiasmatic nucleus: cell autonomy and network properties". In: *Annu Rev Physiol* 72 (2010), pp. 551–77.

[61] D. K. Welsh et al. "Individual neurons dissociated from rat suprachiasmatic nucleus express independently phased circadian firing rhythms". In: *Neuron* 14 (1995), pp. 697–706.

[62] R. G. Foster et al. "Circadian photoreception in the retinally degenerate mouse (Rd/Rd)". In: *J Comp Physiol A.* 169 (1991), pp. 39–50.

[63] B. G. Soni et al. "Novel retinal photoreceptors". In: *Nature* 394 (1998), pp. 27–8.

[64] F. H. Zaidi et al. "Short-wavelength light sensitivity of circadian, pupillary, and visual awareness in humans lacking an outer retina". In: *Curr Biol* 17 (2007), pp. 2122–8.

[65] S. Hattar et al. "Melanopsin-containing retinal ganglion cells: architecture, projections, and intrinsic photosensitivity". In: *Science* 295 (2002), pp. 1065–70.

[66] S. Hattar et al. "Central projections of melanopsin-expressing retinal ganglion cells in the mouse". In: *J Comp Neurol* 497 (2006), pp. 326–49.

[67] S. Yamazaki et al. "Resetting central and peripheral circadian oscillators in transgenic rats". In: *Science* 288 (1995), pp. 682–5.

[68] A. Balsalobre, F. Damiola, and U. Schibler. "A serum shock induces circadian gene expression in mammalian tissue culture cells". In: *Cell* 93 (1998), pp. 929–37.

[69] J. P. Pett et al. "Co-existing feedback loops generate tissue-specific circadian rhythms". In: *Life Sci Alliance* 1 (2018), e201800078.

[70] S. A. Brown et al. "Rhythms of mammalian body temperature can sustain peripheral circadian clocks". In: *Curr Biol* 12 (2002), pp. 1574–83.

[71] H. Guo et al. "Differential control of peripheral circadian rhythms by suprachiasmatic-dependent neural signals". In: *Proc Natl Acad Sci U S A* 102 (2005), pp. 3111–6.

[72] A. Ishida et al. "Light activates the adrenal gland: Timing of gene expression and glucocorticoid release". In: *Cell Metab* 2 (2005), pp. 297–307.

[73] U. Albrecht. "Timing to perfection: the biology of central and peripheral circadian clocks". In: *Neuron* 74 (2012), pp. 246–60.

[74] H. Reinke and G. Asher. "Crosstalk between metabolism and circadian clocks". In: *Nat Rev Mol Cell Biol* 20 (2019), pp. 227–41.

[75] F. Damiola et al. "Restricted feeding uncouples circadian oscillators in peripheral tissues from the central pacemaker in the suprachiasmatic nucleus". In: *Genes Dev* 14 (2000), pp. 2950–61.

[76] K. A. Stokkan et al. "Entrainment of the circadian clock in the liver by feeding". In: *Science* 291 (2001), pp. 490–3.

[77] C. Vollmers et al. "Time of feeding and the intrinsic circadian clock drive rhythms in hepatic gene expression". In: *Proc Natl Acad Sci U S A* 106 (2009), pp. 21453–8.

[78] F. Sinturel et al. "Circadian hepatocyte clocks keep synchrony in the absence of a master pacemaker in the suprachiasmatic nucleus or other extrahepatic clocks". In: *Genes Dev* 25 (2021), pp. 1–6.

[79] S Yoo et al. "PERIOD2::LUCIFERASE real-time reporting of circadian dynamics reveals persistent circadian oscillations in mouse peripheral tissues". In: *Proc Natl Acad Sci U S A* 101 (2004), pp. 5339–46.

[80] R. Zhang et al. "A circadian gene expression atlas in mammals: Implications for biology and medicine". In: *Proc Natl Acad Sci U S A* 111 (2014), pp. 16219–24.

[81] L. S. Mure et al. "Diurnal transcriptome atlas of a primate across major neural and peripheral tissues". In: *Science* 359 (2018), eaao0318.

[82] A. Korenčič et al. "Timing of circadian genes in mammalian tissues". In: *Sci Rep* 4 (2014), p. 5782.

[83] R. E. Mistlberger. "Circadian food-anticipatory activity: formal models and physiological mechanisms". In: *Neurosci Biobehav Rev* 18 (1994), pp. 171–95.

[84] F. K. Stephan. "The "other" circadian system: food as a Zeitgeber". In: *J Biol Rhythms* 17 (2002), pp. 284–92.

[85] A. Natsubori, K. Honma, and S. Honma. "Dual regulation of clock gene *Per2* expression in discrete brain areas by the circadian pacemaker and methamphetamine-induced oscillator in rats". In: *Eur J Neurosci* 39 (2014), pp. 229–40.

[86] K. Honma and S. Honma. "The SCN-independent clocks, methamphetamine and food restriction". In: *Eur J Neurosci* 30 (2009), pp. 1707–17.

[87] P. Pezuk et al. "Circadian organization is governed by extra-SCN pacemakers". In: *J Biol Rhythms* 25 (2010), pp. 432–41.

[88] N. Gekakis et al. "Role of the CLOCK protein in the mammalian circadian mechanism". In: *Science* 280 (1998), pp. 1564–9.

[89] H. Tei et al. "Circadian oscillation of a mammalian homologue of the *Drosophila period* gene". In: *Nature* 389 (1997), pp. 512–6.

[90] M. Ikeda and M. Nomura. "cDNA cloning and tissue-specific expression of a novel basic helix-loop-helix/PAS protein (BMAL1) and identification of alternatively spliced variants With alternative translation initiation site usage". In: *Biochem Biophys Res Commun* 233 (1997), pp. 258–64.

[91] P. L. Lowrey and J. S. Takahashi. "Genetics of circadian rhythms in mammalian model organisms". In: *Adv Genet* 74 (2011), pp. 175–230.

[92] R. P. Aryal et al. "Macromolecular assemblies of the mammalian circadian clock". In: *Mol Cell* 67 (2017), pp. 770–82.

[93] J. B. Hogenesch et al. "The basic-helix–loop–helix-PAS orphan MOP3 forms transcriptionally active complexes with circadian and hypoxia factors". In: *Proc Natl Acad Sci U S A* 95 (1998), pp. 5474–9.

[94] K. Kume et al. "mCRY1 and mCRY2 are essential components of the negative limb of the circadian clock feedback loop". In: *Cell* 98 (1999), pp. 193–205.

[95] S. Honma et al. "Dec1 and Dec2 are regulators of the mammalian molecular clock". In: *Nature* 419 (2002), pp. 841–4.

[96] B. A. Hodge et al. "Dec1 and Dec2 are regulators of the mammalian molecular clock". In: *eLife* 8 (2019), e43017.

[97] Y. Wu et al. "Reciprocal regulation between the circadian clock and hypoxia signaling at the genome level in mammals". In: *Cell Metab* 25 (2017), pp. 73–85.

[98] N. Preitner et al. "The orphan nuclear receptor REV-ERBalpha controls circadian transcription within the positive limb of the mammalian circadian oscillator". In: *Cell* 110 (2002), pp. 251–60.

[99] F. Guillaumond et al. "Differential control of Bmal1 circadian transcription by REV-ERB and ROR nuclear receptors". In: *J Biol Rhythms* 20 (2005), pp. 391–403.

[100] T. K. Sato et al. "A functional genomics strategy reveals Rora as a component of the mammalian circadian clock". In: *Neuron* 43 (2004), pp. 527–37.

[101] H. Cho et al. "Regulation of circadian behaviour and metabolism by REV-ERB-α and REV-ERB-β". In: *Nature* 485 (2012), pp. 123–7.

[102] A. Relógio et al. "Tuning the mammalian circadian clock: robust synergy of two loops". In: *PLoS Comput Biol* 7 (2011), e1002309.

[103] J. P. Pett et al. "Feedback loops of the mammalian circadian clock constitute repressilator". In: *PLoS Comput Biol* 12 (2016), e1005266.

[104] E. Falvey, F. Fleury-Olela, and U. Schibler. "The rat Hepatic Leukemia Factor (HLF) gene encodes two transcriptional activators with distinct circadian rhythms, tissue distributions and target preferences". In: *EMBO J* 14 (1995), pp. 4307–17.

[105] L. Lopez-Molina et al. "The DBP gene is expressed according to a circadian rhythm in the suprachiasmatic nucleus and influences circadian behavior". In: *EMBO J* 16 (1997), pp. 6762–71.

[106] S. Mitsui et al. "Antagonistic role of E4BP4 and PAR proteins in the circadian oscillatory mechanism". In: *Genes Dev* 15 (2001), pp. 995–1006.

[107] M. Ukai-Tadenuma et al. "Delay in feedback repression by Cryptochrome 1 is required for circadian clock function". In: *Cell* 144 (2011), pp. 268–81.

[108] J. S. Takahashi. "Transcriptional architecture of the mammalian circadian clock". In: *Nat Rev Genet* 18 (2016), pp. 164–79.

[109] J. S. O'Neill et al. "cAMP-dependent signaling as a core component of the mammalian circadian pacemaker". In: *Science* 320 (2008), pp. 949–53.

[110] K. Obrietan et al. "Circadian regulation of cAMP response element-mediated gene expression in the suprachiasmatic nuclei". In: *J Biol Chem* 274 (1999), pp. 17748–56.

[111] B. Novák and J. J. Tyson. "Design principles of biochemical oscillators". In: *Nat Rev Mol Cell Biol* 9 (2008), pp. 981–91.

[112] J. J. Tyson, K. C. Chen, and B. Novak. "Sniffers, buzzers, toggles and blinkers: dynamics of regulatory and signaling pathways in the cell". In: *Curr Opin Cell Biol* 15 (2003), pp. 221–31.

[113] J. E. Jr. Ferrell, T. Y. Tsai, and Q. Yang. "Modeling the cell cycle: why do certain circuits oscillate?" In: *Cell* 144 (2011), pp. 874–85.

[114] P. L. Lowrey et al. "Positional syntenic cloning and functional characterization of the mammalian circadian mutation Tau". In: *Science* 288 (2000), pp. 483–92.

[115] K. Vanselow et al. "Differential effects of PER2 phosphorylation: molecular basis for the human Familial Advanced Sleep Phase Syndrome (FASPS)". In: *Genes Dev* 20 (2006), pp. 2660–72.

[116] J Shirogane T. Jin, X. L. Ang, and J. W. Harper. "SCF β-TRCP controls clock-dependent transcription via casein kinase 1-dependent degradation of the mammalian Period-1 (Per1) protein". In: *J Biol Chem* 280 (2005), pp. 26863–72.

[117] E. J. Eide et al. "Control of mammalian circadian rhythm by CKIϵ-regulated proteasome-mediated PER2 degradation". In: *Mol Cell Biol* 25 (2005), pp. 2795–2807.

[118] F. Camacho et al. "Human casein kinase Iδ phosphorylation of human circadian clock proteins period 1 and 2". In: *FEBS Lett* 489 (2001), pp. 159–65.

[119] L. Busino et al. "SCF Fbxl3 controls the oscillation of the circadian clock by directing the degradation of cryptochrome proteins". In: *Science* 316 (2007), pp. 900–4.

[120] J. A. Ripperger and U. Schibler. "Rhythmic CLOCK-BMAL1 binding to multiple E-box motifs drives circadian Dbp transcription and chromatin transitions". In: *Nat Genet* 38 (2006), pp. 369–74.

[121] B. Zheng et al. “Nonredundant roles of the mPer1 and mPer2 genes in the mammalian circadian clock”. In: *Cell* 105 (2001), pp. 683–94.

[122] N. Cermakian et al. “Altered behavioral rhythms and clock gene expression in mice with a targeted mutation in the Period1 gene”. In: *EMBO J* 20 (2001), pp. 3967–74.

[123] K. Bae et al. “Differential functions of mPer1, mPer2, and mPer3 in the SCN circadian clock”. In: *Neuron* 30 (2001), pp. 525–36.

[124] B. Zheng et al. “The mPer2 gene encodes a functional component of the mammalian circadian clock”. In: *Nature* 400 (1999), pp. 169–73.

[125] R. J. Thresher et al. “Role of mouse cryptochrome blue-light photoreceptor in circadian photoresponses”. In: *Science* 282 (1998), pp. 1490–4.

[126] M. H. Vitaterna et al. “Differential regulation of mammalian Period genes and circadian rhythmicity by cryptochromes 1 and 2”. In: *Proc Natl Acad Sci U S A* 96 (1999), pp. 12114–9.

[127] G. T. Van der Horst et al. “Mammalian Cry1 and Cry2 are essential for maintenance of circadian rhythms”. In: *Nature* 398 (1999), pp. 627–30.

[128] J. E. Baggs et al. “Network features of the mammalian circadian clock”. In: *PLoS Biol* 7 (2009), e1000052.

[129] A. Erzberger et al. “Genetic redundancy strengthens the circadian clock leading to a narrow entrainment range”. In: *J R Soc Interface* 10 (2013), p. 20130221.

[130] D. Ono, S. Honma, and K. Honma. “Cryptochromes are critical for the development of coherent circadian rhythms in the mouse suprachiasmatic nucleus”. In: *Nat Commun* 4 (2013), p. 1666.

[131] M. Putker et al. “CRYPTOCHROMES confer robustness, not rhythmicity, to circadian timekeeping”. In: *BioRxiv* (2020).

[132] J. Etchegaray et al. “Rhythmic histone acetylation underlies transcription in the mammalian circadian clock”. In: *Nature* 421 (2003), pp. 177–82.

[133] M. Doi, J. Hirayama, and P. Sassone-Corsi. “Circadian regulator CLOCK is a histone acetyltransferase”. In: *Cell* 125 (2006), pp. 497–508.

[134] Y. Nakahata et al. “The NAD^+-dependent deacetylase SIRT1 modulates CLOCK-mediated chromatin remodeling and circadian control”. In: *Cell* 134 (2008), pp. 329–40.

[135] G. Asher et al. “SIRT1 regulates circadian clock gene expression through PER2 deacetylation”. In: *Cell* 134 (2008), pp. 317–28.

[136] J. Rutter et al. “Regulation of Clock and NPAS2 DNA binding by the redox state of NAD cofactors”. In: *Science* 293 (2001), pp. 510–4.

[137] H. Iwasaki et al. “KaiA-stimulated KaiC phosphorylation in circadian timing loops in cyanobacteria”. In: *Proc Natl Acad Sci U S A* 99 (2002), pp. 15788–93.

[138] T. Nishiwaki et al. “Nucleotide binding and autophosphorylation of the clock protein KaiC as a circadian timing process of cyanobacteria”. In: *Proc Natl Acad Sci U S A* 97 (2000), pp. 495–9.

[139] Y. Kitayama et al. “KaiB functions as an attenuator of KaiC phosphorylation in the cyanobacterial circadian clock system”. In: *EMBO J* 22 (2003), pp. 2127–34.

[140] J. S. O’Neill et al. “Circadian rhythms persist without transcription in a eukaryote”. In: *Nature* 469 (2011), pp. 554–8.

[141] Y. Fan et al. “Cycling of cryptochrome proteins is not necessary for circadian-clock function in mammalian fibroblasts”. In: *Curr Biol* 17 (2007), pp. 1091–100.

[142] A. C. Liu et al. “Redundant function of REV-ERBalpha and beta and non-essential role for Bmal1 cycling in transcriptional regulation of intracellular circadian rhythms”. In: *PLoS Genet* 4 (2008), e1000023.

[143] A. B. Reddy et al. “Circadian orchestration of the hepatic proteome”. In: *Curr Biol* 16 (2006), pp. 1107–15.

[144] T. Dobzhansky. “Nothing in biology makes sense except in the light of evolution”. In: *Am Biol Teach* 35 (1973), pp. 125–9.

[145] S. A. Crowe et al. “Atmospheric oxygenation three billion years ago”. In: *Nature* 501 (2013), pp. 535–8.

[146] K. O. Konhauser et al. “Aerobic bacterial pyrite oxidation and acid rock drainage during the great oxidation event”. In: *Nature* 478 (2011), pp. 369–73.

[147] B. E. Schirrmeister et al. “Evolution of multicellularity coincided with increased diversification of cyanobacteria and the great oxidation event”. In: *Proc Natl Acad Sci U S A* 110 (2013), pp. 1791–6.

[148] N. B. Milev et al. “Analysis of the redox oscillations in the circadian clockwork”. In: *Enzymol* 552 (2014), pp. 185–210.

[149] R. Machne. “Temporal Organization of Cellular Growth in *Saccharomyces cerevisiae*”. PhD thesis. Universität Wien, 2017.

[150] E. Wagner and S. Frosch. “Endogenous rhythmicity and energy transduction VI. Rhythmicity in reduced and oxidized pyridine nucleotide levels in seedlings of *Chenopodium rubrum*”. In: *J Interdiscipl Cycle Res* 5 (1974), pp. 231–9.

[151] L. S. Kaminsky et al. “Human hepatic cytochrome P-450 composition as probed by in vitro microsomal metabolism of warfarin”. In: *Drug Metab Dispos* 12 (1984), pp. 470–7.

[152] A. E. Ahmed and M. Y. H. Farooqui. “Metabolism and toxicity of N, N’-dimethyl aminopropionitrile in rats”. In: *Pharmacologist* 26 (1984), p. 198.

[153] F. A. J. L. Scheer et al. “The human endogenous circadian system causes greatest platelet activation during the biological morning independent of behaviors”. In: *PLoS One* 6 (2011), e24549.

[154] E. Radha et al. “Glutathione levels in human platelets display a circadian rhythm in vitro”. In: *Thromb Res* 40 (1985), pp. 823–31.

[155] R. A. Blanco et al. “Diurnal variation in glutathione and cysteine redox states in human plasma”. In: *Am J Clin Nutr* 86 (2007), pp. 1016–23.

[156] A. Sancar. “Structure and function of DNA photolyase and cryptochrome blue-light photoreceptors”. In: *Chem Rev* 103 (2003), pp. 2203–37.

[157] C. S. Pittendrigh. “Temporal organization: Reflections of a Darwinian clock-watcher”. In: *Annu Rev Physiol* 55 (1993), pp. 17–54.

[158] W. Gehring and M. Rosbash. “The coevolution of blue-light photoreception and circadian rhythms”. In: *J Mol Evol* 57 (2003), S286–9.

[159] P. Emery et al. “*Drosophila* CRY is a deep brain circadian photoreceptor”. In: *Neuron* 26 (2000), pp. 493–504.

[160] A. Czarna et al. “Structures of *Drosophila* cryptochrome and mouse cryptochrome 1 provide insight into circadian function”. In: *Cell* 153 (2013), pp. 1394–405.

[161] C. Lin and D. Shalitin. “Cryptochrome structure and signal transduction”. In: *Annu Rev Plant Biol* 54 (2003), pp. 469–96.

[162] I. Chaves et al. “Functional evolution of the photolyase/cryptochrome protein family: importance of the C terminus of mammalian CRY1 for circadian core oscillator performance”. In: *Mol Cell Biol* 26 (2006), pp. 1743–53.

[163] K. M. Vaze, K. L. Nikhil, and V. K. Sharma. “Circadian rhythms. 4. Why do living organisms have them?” In: *Resonance* 19 (2014), pp. 175–89.

[164] C. H. Johnson. “Endogenous timekeepers in photosynthetic organisms”. In: *Annu Rev Physiol* 63 (2001), pp. 695–728.

[165] A. Mitsui et al. “Strategy by which nitrogen-fixing unicellular cyanobacteria grow photoautotrophically”. In: *Nature* 323 (1986), pp. 720–2.

[166] T. Huang et al. “Circadian rhythm of the prokaryote Synechococcus sp. RF-1”. In: *Plant Physiol* 92 (1990), pp. 531–3.

[167] M. J. P. Simons. “The evolution of the cyanobacterial posttranslational clock from a primitive “Phoscillator””. In: *J Biol Rhythms* 24 (2009), pp. 175–82.

[168] Y. Ouyang et al. “Resonating circadian clocks enhance fitness in cyanobacteria”. In: *Proc Natl Acad Sci U S A* 95 (1998), pp. 8660–4.

[169] M. A. Woelfle et al. “The adaptive value of circadian clocks: an experimental assessment in cyanobacteria”. In: *Curr Biol* 14 (2004), pp. 1481–6.

[170] B. Tu and S. L. McKnight. “Metabolic cycles as an underlying basis of biological oscillations”. In: *Nat Rev Mol Cell Biol* 7 (2006), pp. 696–701.

[171] M. J. McDonald and M. Rosbash. “Microarray analysis and organization of circadian gene expression in *Drosophila*”. In: *Cell* 107 (2001), pp. 567–78.

[172] C. S. Pittendrigh and D. H. Minis. “Circadian systems: longevity as a function of circadian resonance in *Drosophila melanogaster*”. In: *Proc Natl Acad Sci U S A* 69 (1972), pp. 1537–9.

[173] J. Aschoff, U. Saint Paul, and R. Wever. “Die Lebensdauer von Fliegen unter dem Einfluß von Zeit-Verschiebungen”. In: *Naturwissenschaften* 58 (1971), p. 574.

[174] U. Saint Paul and J. Aschoff. “Longevity among blowflies *Phormia terraenovae* R.D. kept in non-24-hour light-dark cycles”. In: *J Comp Physiol* 127 (1978), pp. 191–5.

[175] D. S. Saunders. “Circadian Control of Larval Growth Rate in *Sarcophaga argyrostoma*”. In: *Proc Natl Acad Sci U S A* 69 (1972), pp. 2738–40.

[176] A. P. Withrow and R. B. Withrow. “Photoperiodic chlorosis in tomato”. In: *Plant Physiol* 24 (1949), pp. 657–63.

[177] H. R. Highkin and J. B. Hanson. “Possible interaction between light-dark cycles and endogenous daily rhythms on the growth of tomato plants”. In: *Plant Physiol* 29 (1954), pp. 301–2.

[178] F. W. Went. “Photo- and thermoperiodic effects in plant growth”. In: *Cold Spring Harbor Symposia on Quantitative Biology: Volume XXV. Biological Clocks*. New York: Cold Spring Harbor Press, 1960, pp. 221–30.

[179] P. J. DeCoursey et al. “Circadian performance of duprachiasmatic nuclei (SCN)-lesioned antelope ground squirrels in a desert enclosure”. In: *Physiol Behav* 62 (1997), pp. 1099–108.

[180] P. J. DeCoursey, J. K. Walker, and S. A. Smith. “A circadian pacemaker in free-living chipmunks: essential for survival?” In: *J Comp Physiol A* 186 (2000), pp. 169–80.

[181] K. J. Emerson, W. E. Bradshaw, and C. M. Holzapfel. “Concordance of the circadian clock with the environment is necessary to maximize fitness in natural populations”. In: *Evolution* 62 (2009), pp. 979–83.

[182] L. M. Beaver et al. “Loss of circadian clock function decreases reproductive fitness in males of *Drosophila melanogaster*”. In: *Proc Natl Acad Sci U S A* 99 (2002), pp. 2134–9.

[183] L. M. Beaver et al. “Noncircadian regulation and function of clock genes period and timeless in oogenesis of *Drosophila melanogaster*”. In: *J Biol Rhythms* 18 (2003), pp. 463–72.

[184] T. A. Martino et al. “Circadian rhythm disorganization produces profound cardiovascular and renal disease in hamsters”. In: *Am J Physiol Regul Integr Comp Physiol* 294 (2008), R1675–83.

[185] K. Spoelstra et al. “Natural selection against a circadian clock gene mutation in mice”. In: *Proc Natl Acad Sci U S A* 113 (2016), pp. 686–91.

[186] S. R. Lone et al. “Circadian resonance in the development of two sympatric species of *Camponotus* ants”. In: *J Insect Physiol* 56 (2010), pp. 1611–6.

[187] Z. Gerhart-Hines and M. A. Lazar. “Circadian metabolism in the light of evolution”. In: *Endocr Rev* 36 (2015), pp. 289–304.

[188] S. Sahar and P. Sassone-Corsi. “Metabolism and cancer: The circadian clock connection”. In: *Nat Rev Cancer* 9 (2009), pp. 886–96.

[189] W. Huang et al. “Circadian rhythms, sleep, and metabolism”. In: *J Clin Invest* 121 (2011), pp. 2133–41.

[190] F. Gachon et al. “The mammalian circadian timing system: from gene expression to physiology”. In: *Chromosoma* 113 (2004), pp. 103–12.

[191] X. S. Wang et al. “Shift work and chronic disease: the epidemiological evidence”. In: *Occup Med (Lond)* 61 (2011), pp. 78–89.

[192] R. L. Sack et al. “Circadian rhythm sleep disorders: Part II, advanced sleep phase disorder, delayed sleep phase disorder, free-running disorder, and irregular sleep-wake rhythm. An American academy of sleep medicine review”. In: *Sleep* 30 (2007), pp. 1484–501.

[193] R. L. Sack et al. “Circadian rhythm sleep disorders: Part I, basic principles, shift work and jet lag disorders. An American academy of sleep medicine review”. In: *Sleep* 30 (2007), pp. 1460–83.

[194] A. Pan et al. “Rotating night shift work and risk of Type 2 Diabetes: Two prospective cohort studies in women”. In: *PLoS Med* 8 (2011), e1001141.

[195] T. Roenneberg et al. “Social jetlag and obesity”. In: *Curr Biol* 22 (2012), pp. 939–43.

[196] D. A. Beihl, A. D. Liese, and S. M. Haffner. “Sleep duration as a risk factor for incident Type 2 Diabetes in a multiethnic cohort”. In: *Ann Epidemiol* 19 (2009), pp. 351–7.

[197] C. Meisinger, M. Heier, and H. Loewel. “Sleep disturbance as a predictor of Type 2 Diabetes Mellitus in men and women from the general population”. In: *Diabetologia* 48 (2005), pp. 235–41.

[198] K. Spiegel, R. Leproult, and E. Van Cauter. “Impact of sleep debt on metabolic and endocrine function”. In: *Lancet* 354 (1999), pp. 1435–9.

[199] A. Kohsaka et al. “High-fat diet disrupts behavioral and molecular circadian rhythms in mice”. In: *Cell Metab* 6 (2007), pp. 414–21.

[200] D. M. Arble et al. “Circadian timing of food intake contributes to weight gain”. In: *Obesity (Silver Spring)* 17 (2009), pp. 2100–2.

[201] M. Hatori et al. “Time-restricted feeding without reducing caloric intake prevents metabolic diseases in mice fed a high-fat diet”. In: *Cell Metab* 15 (2012), pp. 848–60.

[202] E. S. Schernhammer et al. “Rotating night shifts and risk of breast cancer in women participating in the Nurses’ Health Study”. In: *J Natl Cancer Inst* 93 (2001), pp. 1563–8.

[203] A. Chang et al. “Evening use of light-emitting eReaders negatively affects sleep, circadian timing, and next-morning alertness”. In: *Proc Natl Acad Sci U S A* 112 (2001), pp. 1232–7.

[204] M. Wittmann et al. “Social jetlag: misalignment of biological and social time”. In: *Chronobiol Int* 23 (2006), pp. 497–509.

[205] J. A. Horne and O. Ostberg. “A self-assessment questionnaire to determine morningness-eveningness in human circadian rhythms”. In: *Int J Chronobiol* 4 (1976), pp. 97–110.

[206] T. Roenneberg et al. “Epidemiology of the human circadian clock”. In: *Sleep Med Rev* 11 (2007), pp. 429–38.

[207] T. Roenneberg, A. Wirz-Justice, and M. Merrow. “Life between clocks: daily temporal patterns of human chronotypes”. In: *J Biol Rhythms* 18 (2003), pp. 80–90.

[208] C. Vetter. “Circadian disruption: What do we actually mean?” In: *Eur J Neurosci* 51 (2020), pp. 531–50.

[209] C. A. Vadnie and C. A. McClung. "Circadian rhythm disturbances in mood disorders: insights into the role of the suprachiasmatic nucleus". In: *Neural Plast* 2017 (2017), p. 1504507.

[210] F. Rutters et al. "Is social jetlag associated with an adverse endocrine, behavioral, and cardiovascular risk profile?" In: *J Biol Rhythms* 29 (2014), pp. 377–83.

[211] D. M. McMahon et al. "Persistence of social jetlag and sleep disruption in healthy young adults". In: *Chronobiol Int* 35 (2018), pp. 312–28.

[212] M. Merrow and T. Roenneberg. "Circadian clocks: how rhythms structure life". In: *Coursera, Ludwigs Maximilians Universität München.*

[213] K. J. Reid and P. C. Zee. "Circadian rhythm disorders". In: *Semin Neurol* 29 (2009), pp. 393–405.

[214] K. L. Toh et al. "An *hPer2* phosphorylation site mutation in Familial Advanced Sleep Phase Syndrome". In: *Science* 291 (2001), pp. 1040–3.

[215] Y. Xu et al. "Functional consequences of a *CKIδ* mutation causing familial advanced sleep phase syndrome". In: *Nature* 434 (2005), pp. 640–4.

[216] Y. Xu et al. "Modeling of a human circadian mutation yields novel insights into clock regulation by PER2". In: *Cell* 128 (2007), pp. 59–70.

[217] T. Iwase et al. "Mutation screening of the human *Clock* gene in circadian rhythm sleep disorders". In: *Psychiatry Res* 109 (2002), pp. 121–8.

[218] C. B. Green, J. S. Takahashi, and J. Bass. "The meter of metabolism". In: *Cell* 134 (2008), pp. 728–42.

[219] B. Marcheva et al. "Disruption of the clock components CLOCK and BMAL1 leads to hypoinsulinaemia and diabetes". In: *Nature* 466 (2010), pp. 627–31.

[220] F. W. Turek et al. "Obesity and metabolic syndrome in circadian clock mutant mice". In: *Science* 308 (2005), pp. 1043–5.

[221] J. Bass and J. S. Takahashi. "Circadian integration of metabolism and energetics". In: *Science* 330 (2010), pp. 1349–54.

[222] D. Feng and M. A. Lazar. "Clocks, metabolism and epigenome". In: *Mol Cell* 47 (2012), pp. 158–67.

[223] J. E. Muller et al. "Circadian variation in the frequency of onset of acute myocardial infarction". In: *N Engl J Med* 313 (1985), pp. 1315–22.

[224] R. Stephenson. "Circadian rhythms and sleep-related breathing disorders". In: *Sleep Med* 8 (2007), pp. 681–7.

[225] S. Gaddameedhi et al. "Control of skin cancer by the circadian rhythm". In: *Proc Natl Acad Sci U S A* 108 (2011), pp. 18790–5.

[226] V. Y. Gorbacheva et al. "Circadian sensitivity to the chemotherapeutic agent cyclophosphamide depends on the functional status of the CLOCK/BMAL1 transactivation complex". In: *Proc Natl Acad Sci U S A* 102 (2005), pp. 3407–12.

[227] G. Kaur et al. “Timing is important in medication administration: a timely review of chronotherapy research”. In: *Int J Clin Pharmacol* 35 (2013), pp. 344–58.

[228] R. Pick et al. “Time-of-day-dependent trafficking and function of leukocyte subsets”. In: *Trends Immunol* 40 (2019), pp. 524–37.

[229] C. C. Nobis et al. “The circadian clock of CD8 T cells modulates their early response to vaccination and the rhythmicity of related signaling pathways”. In: *Proc Natl Acad Sci U S A* 116 (2019), pp. 20077–86.

[230] F. Lévi et al. “Circadian timing in cancer treatments”. In: *Annu Rev Pharmacol Toxicol* 50 (2010), pp. 377–421.

[231] T. C. Erren. “A chronology of chronobiology”. In: *Physiology News Magazine* 113 (2018), pp. 32–5.

[232] M. Del Olmo, A. Kramer, and H. Herzel. “A robust model for circadian redox oscillations”. In: *Int J Mol Sci* 20 (2019), p. 2368.

[233] S. Almeida, M. Chaves, and F. Delaunay. “Transcription-based circadian mechanism controls the duration of molecular clock states in response to signaling inputs”. In: *J Theor Biol* 484 (2020), p. 110015.

[234] Y. Tsuchiya, M. Akashi, and E. Nishida. “Temperature compensation and temperature resetting of circadian rhythms in mammalian cultured fibroblasts”. In: *Genes Cells* 8 (2003), pp. 713–20.

[235] C. S. Pittendrigh. “On temperature independence in the clock system controlling emergence time in *Drosophila*”. In: *Proc Natl Acad Sci USA* 40 (1954), pp. 1018–29.

[236] L. N. Jr. Edmunds. *Cellular and Molecular Bases of Biological Clocks*. Springer, New York, NY, 1988.

[237] N. F. Ruby, D. E. Burns, and H. C. Heller. “Circadian rhythms in the suprachiasmatic nucleus are temperature-compensated and phase-shifted by heat pulses in vitro”. In: *J Neurosci* 19 (1999), pp. 8630–6.

[238] K. Terauchi et al. “ATPase activity of KaiC determines the basic timing for circadian clock of cyanobacteria”. In: *Proc Natl Acad Sci USA* 104 (2007), pp. 16377–81.

[239] Y. Isojima et al. “CKIepsilon/delta-dependent phosphorylation is a temperature-insensitive, period-determining process in the mammalian circadian clock”. In: *Proc Natl Acad Sci USA* 106 (2009), pp. 15744–9.

[240] Y. Shinohara et al. “Temperature-sensitive substrate binding and product binding underlie temperature-compensated phosphorylation in the clock”. In: *Mol Cell* 67 (2017), pp. 783–98.

[241] J.W. Hastings and B.M. Sweeney. “On the mechanisms of temperature independence in a biological clock”. In: *Proc Natl Acad Sci USA* 43 (1957), pp. 804–11.

[242] P. Ruoff. “Introducing temperature-compensation in any reaction kinetic oscillator model”. In: *J Interdiscipl Cycle Res* 23 (1992), pp. 92–9.

[243] P.L. Lakin-Thomas, S. Brody, and G.G. Coté. "Amplitude model for the effects of mutations and temperature on period phase resetting of the *Neurospora* circadian oscillator". In: *J Biol Rhythms* 6 (1991), pp. 281–97.

[244] G. Kurosawa et al. "Temperature-amplitude coupling for stable biological rhythms at different temperatures". In: *PLoS Comput Biol* 13 (2017), e1005501.

[245] C.S. Pittendrigh and P.C. Caldarola. "General homeostasis of the frequency of circadian oscillations". In: *Proc Natl Acad Sci USA* 70 (1973), pp. 2697–701.

[246] I. Mihalcescu, W. Hsing, and S. Leibler. "Resilient circadian oscillator revealed in individual cyanobacteria". In: *Nature* 430 (2004), pp. 81–5.

[247] C.J. Johnson. "Circadian clocks and cell division: what's the pacemaker?" In: *Cell Cycle* 9 (2010), pp. 3864–73.

[248] K. Eckel-Mahan and P. Sassone-Corsi. "Metabolism and the circadian clock converge". In: *Physiol Rev* 93 (2013), pp. 107–35.

[249] J. Bass. "Circadian topology of metabolism". In: *Nature* 491 (2012), pp. 348–56.

[250] T. Nishiwaki et al. "Role of KaiC phosphorylation in the circadian clock system of *Synechococcus elongatus* PCC 7942". In: *Proc Natl Acad Sci USA* 101 (2004), pp. 13927–32.

[251] Y. Xu, T. Mori, and C.H. Johnson. "Circadian clock-protein expression in cyanobacteria: rhythms and phase setting". In: *EMBO J.* 19 (2000), pp. 3349–57.

[252] J. Tomita et al. "Circadian autodephosphorylation of cyanobacterial clock protein KaiC occurs via formation of ATP as intermediate". In: *Science* 307 (2005), pp. 251–4.

[253] C. H. Johnson, J. A. Elliott, and R. Foster. "Entrainment of circadian programs". In: *Chronobiol Int* 20 (2003), pp. 741–74.

[254] L. Schneper, K. Duvel, and J. R. Broach. "Sense and sensibility: nutritional response and signal integration in yeast". In: *Curr Opin Microbiol* 7 (2004), pp. 624–30.

[255] T. Ferenci. "Sensing nutrient levels in bacteria". In: *Nat Chem Biol* 3 (2007), pp. 607–8.

[256] V. M. Boer et al. "Growth-limiting intracellular metabolites in yeast growing under diverse nutrient limitations". In: *Mol Biol Cell* 21 (2010), pp. 198–211.

[257] A.A. Dovzhenok et al. "Mathematical modeling and validation of glucose compensation of the *Neurospora* circadian clock". In: *Biophys J* 108 (2015), pp. 1830–9.

[258] A. Upadhyay, M. Brunner, and H. Herzel. "An inactivation switch enables rhythms in a *Neurospora* clock model". In: *Int J Mol Sci* 20 (2019), p. 2985.

[259] D.L. Denault, J.J. Loros, and J.C Dunlap. "WC-2 mediates WC-1-FRQ interaction within the PAS protein-linked circadian feedback loop of *Neurospora*". In: *EMBO J* 20 (2001), pp. 109–17.

[260] S.K. Crosthwaite, J.C Dunlap, and J.J. Loros. "*Neurospora wc-1* and *wc-2*: transcription, photoresponses and the origins of circadian rhythmicity". In: *Science* 276 (1997), pp. 763–9.

[261] C.L. Baker, A.N. Kettenbach, and J.C. Dunlap. "Quantitative proteomics reveals a dynamic interactome and phase-specific phosphorylation in the *Neurospora* circadian clock". In: *Mol Cell* 34 (2009), pp. 354–63.

[262] T. Schafmeier, A. Diernfellner, and M. Brunner. "Quantitative proteomics reveals a dynamic interactome and phase-specific phosphorylation in the *Neurospora* circadian clock". In: *Genes Dev* 22 (2008), pp. 3397–402.

[263] C.I. Hong, P. Ruoff, and J.C. Dunlap. "Closing the circadian negative feedback loop: FRQ-dependent clearance of WC-1 from the nucleus". In: *Genes Dev* 22 (2008), pp. 3196–204.

[264] G. Sancar et al. "A global circadian repressor controls antiphasic expression of metabolic genes in *Neurospora*". In: *Mol Cell* 44 (2011), pp. 687–97.

[265] M. Putker et al. "CRYPTOCHROMES confer robustness, not rhythmicity, to circadian timekeeping". In: *BioRxiv* (2020).

[266] B.M. Sweeney and F.T. Haxo. "Persistence of a photosynthetic rhythm in enucleated *Acetabularia*". In: *Science* 134 (1961), pp. 1361–3.

[267] K .A. Lamia et al. "AMPK regulates the circadian clock by cryptochrome phosphorylation and degradation". In: *Science* 326 (2009), pp. 437–40.

[268] X. Yang et al. "Nuclear receptor expression links the circadian clock to metabolism". In: *Cell* 126 (2006), pp. 801–10.

[269] Y. Benjamini and Y. Hochberg. "Controlling the false discovery rate: A practical and powerful approach to multiple testing". In: *Journal of the Royal Statistical Society. Series B (Methodological)* 57 (1995), pp. 289–300.

[270] E.E. Zhang et al. "A genome-wide RNAi screen for modifiers of the circadian clock in human cells". In: *Cell* 139 (2009), pp. 199–210.

[271] J. Myung et al. "The choroid plexus is an important circadian clock component". In: *Nat Commun* 9 (2018), p. 1062.

[272] A. Pizarro et al. "CircaDB: a database of mammalian circadian gene expression profiles". In: *Nucleic Acids Res* 41 (2013), pp. D1009–13.

[273] G. Bordyugov et al. "Tuning the phase of circadian entrainment". In: *J R Soc Interface* 12 (2015), p. 20150282.

[274] D. Ono et al. "Dissociation of Per1 and Bmal1 circadian rhythms in the suprachiasmatic nucleus in parallel with behavioral outputs". In: *Proc Natl Acad Sci USA* 114 (2017), e3699–708.

[275] J. Myung et al. "Period coding of Bmal1 oscillators in the suprachiasmatic nucleus". In: *J Neurosci* 32 (2012), pp. 8900–18.

[276] S.D. Jordan and K.A. Lamia. "AMPK at the crossroads of circadian clocks and metabolism". In: *Mol Cell Endocrinol* 366 (2012), pp. 163–9.

[277] A. Woller et al. "A mathematical model of the liver circadian clock linking feeding and fasting cycles to clock function". In: *Cell Rep* 17 (2016), pp. 1087–97.

[278] P. O. Westermark et al. “Quantification of circadian rhythms in single cells”. In: *PLoS Comput Biol* 5 (2009), e1000580.

[279] D. Gonze et al. “Spontaneous synchronization of coupled circadian oscillations”. In: *Biophys J* 89 (2005), pp. 120–9.

[280] S. Bernard et al. “Synchronization-induced rhythmicity of circadian oscillators in the suprachiasmatic nucleus”. In: *PLoS Comput Biol* 3 (2007), e68.

[281] C. Schmal, E. D. Herzog, and H. Herzel. “Measuring relative coupling strength in circadian systems”. In: *J Biol Rhythms* 33 (2018), pp. 84–98.

[282] A. M. Finger. “Molecular Mechanisms of Intercellular Coupling among Peripheral Circadian Oscillators”. PhD thesis. Humboldt-Universität zu Berlin, 2020.

[283] K. L. Nikhil, S. Korge, and A. Kramer. “Heritable gene expression variability and stochasticity govern clonal heterogeneity in circadian period”. In: *PLoS Biol* 18 (2020), e3000792.

[284] Y. Li et al. “Noise-driven cellular heterogeneity in circadian periodicity”. In: *Proc Natl Acad Sci U S A* 117 (2020), pp. 10350–6.

[285] C. Schmal et al. “Weak coupling between intracellular feedback loops explains dissociation of clock gene dynamics”. In: *PLoS Comput Biol* 15 (2019), e1007330.

[286] I. Van Soest et al. “Nonlinear phenomena in models of the circadian clock”. In: *J R Soc Interface* 17 (2020), p. 20200556.

[287] H. Sies, C. Berndt, and D. P. Jones. “Oxidative stress”. In: *Anu Rev Biochem* 86 (2017), pp. 715–48.

[288] C. C. Winterbourn. “Reconciling the chemistry and biology of reactive oxygen species”. In: *Nat Chem Biol* 4 (2008), pp. 278–86.

[289] M. A. Aon et al. “Synchronized whole cell oscillations in mitochondrial metabolism triggered by a local release of Reactive Oxygen Species in cardiac myocytes”. In: *J Biol Chem* 278 (2003), pp. 44735–44.

[290] H. J. Forman, M. Maiorino, and F. Ursini. “Signaling functions of Reactive Oxygen Species”. In: *Biochemistry* 49 (2010), pp. 835–42.

[291] M. Giorgio et al. “Hydrogen peroxide: a metabolic by-product or a common mediator of ageing signals?” In: *Nat Rev Mol Cell Biol* 8 (2007), pp. 722–8.

[292] B. D’Autreaux and M. B. Toledano. “ROS as signalling molecules: mechanisms that generate specificity in ROS homeostasis”. In: *Nat Rev Mol Cell Biol* 8 (2007), pp. 813–24.

[293] R. Karisch et al. “Global proteomic assessment of the classical protein-tyrosine phosphatome and “redoxome””. In: *Cell* 146 (2011), pp. 826–40.

[294] N. M. Gruning, H. Lehrach, and Ralser M. “Regulatory crosstalk of the metabolic network”. In: *Trends Biochem Sci* 35 (2010), pp. 220–7.

[295] M. Ralser et al. “Dynamic rerouting of the carbohydrate flux is key to counteracting oxidative stress”. In: *J Biol* 6 (2007), p. 10.

[296] T. B. Dansen et al. "Redox-sensitive cysteines bridge p300/CBP-mediated acetylation and FoxO4 activity". In: *Nat Chem Biol* 5 (2009), pp. 664–72.

[297] D. L. Nelson, A. L. Lehninger, and M. M. Cox. *Lehninger Principles of Biochemistry*. W. H. Freeman, 2008.

[298] K. M. Ramsey et al. "Circadian clock feedback cycle through NAMPT-mediated NAD^+ biosynthesis". In: *Science* 324 (2009), pp. 651–4.

[299] J. S. O'Neill and K. A. Feeney. "Circadian redox and metabolic oscillations in mammalian systems". In: *Antioxid Redox Signal* 20 (2014), pp. 2966–81.

[300] P. D. Ray, B. W. Huang, and Y. Tsuji. "Reactive oxygen species (ROS) homeostasis and redox regulation in cellular signaling". In: *Cell Signal* 24 (2012), pp. 981–90.

[301] G. H. Kim, J. J. Ryan, and Archer S. L. "The role of redox signaling in epigenetics and cardiovascular disease". In: *Antioxid Redox Signal* 18 (2013), pp. 1920–36.

[302] A. Hall, P. A. Karplus, and L. B. Poole. "Typical 2-Cys peroxiredoxins—structures, mechanisms and functions". In: *FEBS J* 276 (2009), pp. 2469–77.

[303] A. V. Peskin et al. "Hyperoxidation of peroxiredoxins 2 and 3". In: *J Biol Chem* 288 (2013), pp. 14170–7.

[304] S. G. Rhee et al. "Sulfiredoxin, the cysteine sulfinic acid reductase specific to 2-Cys peroxiredoxin: its discovery, mechanism of action, and biological significance". In: *Kidney Int Suppl* (2007), S3–8.

[305] Z. A. Wood et al. "Structure, mechanism and regulation of peroxiredoxins". In: *Trends Biochem Sci* 28 (2003), pp. 32–40.

[306] C. Cho et al. "Circadian rhythm of hyperoxidized peroxiredoxin II Is determined by Hemoglobin autoxidation and the 20S proteasome in red blood cells". In: *Proc Natl Acad Sci U S A* 111 (2014), pp. 12043–8.

[307] I. S. Kil et al. "Circadian oscillation of sulfiredoxin in the mitochondria". In: *Mol Cell* 59 (2015), pp. 651–63.

[308] R. S. Wible et al. "NRF2 regulates core and stabilizing circadian clock loops, coupling redox and timekeeping in *Mus musculus*". In: *eLife* 7 (2018), e31656.

[309] Y. Tahara et al. "*In vitro* and *in vivo* phase changes of the mouse circadian clock by oxidative stress". In: *J Circadian Rhythms* 14 (2016), p. 4.

[310] S. H. Strogatz. *Nonlinear Dynamics and Chaos: with Applications to Physics, Biology, Chemistry and Engineering*. Cambridge MA: Westview Press, 2000.

[311] M. B. Elowitz and S. Leibler. "A synthetic oscillatory network of transcriptional regulators". In: *Nature* 403 (2000), pp. 335–8.

[312] B. Ananthasubramaniam and H. Herzel. "Positive feedback promotes oscillations in negative feedback loops". In: *PLoS One* 9 (2014), e104761.

[313] S. Becker-Weimann et al. "Modeling feedback loops of the mammalian circadian oscillator". In: *Biophys J* 87 (2004), pp. 3023–34.

[314] D. B. Forger and C. S. Peskin. "A detailed predictive model of the mammalian circadian clock". In: *Proc Natl Acad Sci USA* 100 (2003), pp. 14806–11.

[315] J. C. Leloup and A. Goldbeter. "Towards a detailed computational model for the mammalian circadian clock". In: *Proc Natl Acad Sci USA* 100 (2003), pp. 7051–6.

[316] P. Francois. "A model for the *Neurospora* circadian clock". In: *Biophys J* 88 (2005), pp. 2369–83.

[317] C. I. Hong et al. "Simulating dark expressions and interactions of frq and wc-1 in the *Neurospora* circadian clock". In: *Biophys J* 94 (2008), pp. 1221–32.

[318] H. M. Fathallah-Shaykh, J. L. Bona, and S. Kadener. "Mathematical model of the *Drosophila* circadian clock: loop regulation and transcriptional integration". In: *Biophys J* 97 (2009), pp. 2399–408.

[319] J. C. Leloup and A. Goldbeter. "A model for circadian rhythms in *Drosophila* incorporating the formation of a complex between the PER and TIM proteins". In: *J Biol Rhythms* 13 (1998), pp. 70–87.

[320] H. R. Ueda, M. Hagiwara, and H. Kitano. "Robust oscillations within the interlocked feedback model of *Drosophila* circadian rhythm". In: *J Theor Biol* 210 (2001), pp. 401–6.

[321] J. J Tyson and B. Novak. "A dynamical paradigm for molecular cell biology". In: *Trends Cell Biol* 30 (2020), pp. 504–15.

[322] B. C. Goodwin. "Oscillatory behavior in enzymatic control processes". In: *Adv Enzyme Regul* 3 (1965), pp. 425–38.

[323] P. Ruoff et al. "The Goodwin model: simulating the effect of light pulses on the circadian sporulation rhythm of *Neurospora crassa*". In: *J Theor Biol* 209 (2001), pp. 29–42.

[324] P. Ruoff, J. J. Loros, and J. C. Dunlap. "The relationship between FRQ-protein stability and temperature compensation in the *Neurospora* circadian clock". In: *Proc Natl Acad Sci USA* 102 (2005), pp. 17681–6.

[325] J. C. Locke et al. "Global parameter search reveals design principles of the mammalian circadian clock". In: *BMC Syst Biol* 2 (2008), p. 22.

[326] N. Komin et al. "Synchronization and entrainment of coupled circadian oscillators". In: *Interface Focus* 1 (2011), pp. 167–76.

[327] D. Gonze. "Modeling circadian clocks: from equations to oscillations". In: *Centr Eur J Biol* 6 (2011), pp. 699–711.

[328] J. E. Jr. Ferrell and SH. Ha. "Ultrasensitivity part I: Michaelian responses and zero-order ultrasensitivity". In: *Trends Biochem Sci* 39 (2014), pp. 496–503.

[329] J. E. Jr. Ferrell and SH. Ha. "Ultrasensitivity part II: multisite phosphorylation, stoichiometric inhibitors, and positive feedback". In: *Trends Biochem Sci* 39 (2014), pp. 556–69.

[330] J. E. Jr. Ferrell and SH. Ha. "Ultrasensitivity part III: cascades, bistable switches, and oscillators". In: *Trends Biochem Sci* 39 (2014), pp. 612–8.

[331] A. Cornish-Bowden. *Fundamentals of Enzyme Kinetics*. Portland Press, London, 1995.

[332] U. Alon. *An Introduction to Systems Biology - Design Principles of Biological Circuits*. CRC press, 2007.

[333] Griffith J.S. "Mathematics of cellular control processes. I. Negative feedback to one gene". In: *J Theor Biol* 20 (1968), pp. 202–8.

[334] C. H. Ko et al. "Emergence of noise-induced oscillations in the central circadian pacemaker". In: *PLoS Biol* 8 (2010), e1000513.

[335] A. C. Liu et al. "Intercellular coupling confers robustness against mutations in the SCN circadian clock network". In: *Cell* 129 (2007), pp. 605–16.

[336] M. Gallego et al. "An opposite role for *tau* in circadian rhythms revealed by mathematical modeling". In: *Proc Natl Acad Sci USA* 103 (2006), pp. 10618–23.

[337] E. H. Flach and S. Schnell. "Use and abuse of the quasi-steady-state approximation". In: *Syst Biol (Stevenage)* 153 (2006), pp. 187–91.

[338] J. K. Kim, K. Josić, and M. R. Bennett. "The relationship between stochastic and deterministic quasi-steady state approximations". In: *BMC Syst Biol* 9 (2015), p. 87.

[339] I. S. Kil et al. "Feedback control of adrenal steroidogenesis via H_2O_2-dependent, reversible inactivation of peroxiredoxin III in mitochondria". In: *Mol Cell* 46 (2012), pp. 584–94.

[340] X. Roussel et al. "Evidence for the formation of a covalent thiosulfinate intermediate with peroxiredoxin in the catalytic mechanism of sulfiredoxin". In: *J Biol Chem* 283 (2008), pp. 22371–82.

[341] G. P. Bienert, J. K. Schjoerring, and T. P. Jahn. "Membrane transport of hydrogen peroxide". In: *Biochim Biophys Acta* 1758 (2006), pp. 994–1003.

[342] A. S. Verkman. "Aquaporins at a glance". In: *J Cell Sci* 124 (2011), pp. 2107–12.

[343] X. Li et al. "Single-molecule analysis of PIP2;1 dynamics and partitioning reveals multiple modes of *Arabidopsis* plasma membrane aquaporin regulation". In: *Plant Cell* 23 (2011), pp. 3780–97.

[344] L. Packer and E. Cadenas. *Methods in Enzymology: Hydrogen Peroxide and Cell Signaling, Part B*. Academic Press, 2013.

[345] H. Kim et al. "Redox regulation of lipopolysaccharide-mediated sulfiredoxin induction, which depends on both AP-1 and Nrf2". In: *J Biol Chem* 285 (2010), pp. 34419–28.

[346] G. Bordyugov et al. "Mathematical modeling in chronobiology". In: *Circadian Clocks*. Ed. by A. Kramer and M. Merrow. Springr, 2013, pp. 45–66.

[347] N. MacDonald. *Biological Delay Systems: Linear Stability Theory*. Cambridge: University Press, 1989.

[348] C. Gérard, D. Gonze, and A. Goldbeter. "Dependence of the period on the rate of protein degradation in minimal models for circadian oscillations". In: *Philos Trans A Math Phys Eng Sci* 3674 (2009), pp. 4665–83.

[349] N. Blüthgen et al. "Mechanisms generating ultrasensitivity, bistability, and oscillations in signal transduction". In: *Introduction to systems biology*. Ed. by S. Choi. Humana Press, 2007. Chap. 15, pp. 282–99.

[350] D. Gonze and W. Abou-Jaoudé. “The Goodwin model: behind the Hill function”. In: *PLoS One* 8 (2013), e69573.

[351] J. K. Kim. “Protein sequestration versus Hill-type repression in circadian clock models”. In: *IET Syst Biol* 10 (2016), pp. 125–35.

[352] M. Nivala et al. “Linking flickering to waves and whole-cell oscillations in a mitochondrial network model”. In: *Biophys J* 101 (2011), pp. 2102–11.

[353] C. V. Rao, D. M. Wolf, and A. P. Arkin. “Control, exploitation and tolerance of intracellular noise”. In: *Nature* 420 (2002), pp. 231–7.

[354] J. Paulsson. “Summing up the noise in gene networks”. In: *Nature* 427 (2004), pp. 415–8.

[355] V. Shahrezaie and P. S. Swain. “The stochastic nature of biochemical networks”. In: *Curr Opin Biotechnol* 19 (2008), pp. 369–74.

[356] A. E. Granada and H. Herzel. “How to achieve fast entrainment? The timescale to synchronization”. In: *PLoS One* 4 (2009), e7057.

[357] T. Roenneberg, Z. Dragovic, and M. Merrow. “Demasking biological oscillators: Properties and principles of entrainment exemplified by the *Neurospora* circadian clock”. In: *Proc Natl Acad Sci U S A* 102 (2005), pp. 7742–7.

[358] M. Amdaoud et al. “Cyanobacterial clock, a stable phase oscillator with negligible intercellular coupling”. In: *Proc Natl Acad Sci U S A* 104 (2007), pp. 7051–6.

[359] J. Rougemont and F. Naef. “Collective synchronization in populations of globally coupled phase oscillators with drifting frequencies”. In: *Phys Rev E Stat Nonlin Soft Matter Phys* 73 (2006), p. 011104.

[360] J. Rougemont and F. Naef. “Stochastic phase oscillator models for circadian clocks”. In: *Adv Exp Med Biol* 641 (2008), pp. 141–9.

[361] A. T. Winfree. “Biological rhythms and the behavior of populations of coupled oscillators”. In: *J Theor Biol* 16 (1967), pp. 15–42.

[362] Q. Yang et al. “Circadian gating of the cell cycle revealed in single cyanobacterial cells”. In: *Science* 327 (2010), pp. 1522–6.

[363] U. Abraham et al. “Coupling governs entrainment range of circadian clocks”. In: *Mol Syst Biol* 6 (2010), p. 438.

[364] K. Itô. *Memoirs of the American Mathematical Society, Number 4: On Stochastic Differential Equations*. American Mathematical Society, 1951.

[365] K. Yagita and H Okamura. “Forskolin induces circadian gene expression of rPer1, rPer2 and dbp in mammalian rat-1 fibroblasts”. In: *FEBS Letters* 465 (2000), pp. 79–82.

[366] U. Abraham et al. “Quantitative analysis of circadian single cell oscillations in response to temperature”. In: *PLoS One* 13 (2018), e0190004.

[367] A. Pikovsky, M. Rosenblum, and J. Kurths. *Synchronization: A Universal Concept in Nonlinear Sciences*. Cambridge University Press, 2001.

[368] S. D. M. Santos and J. E. Jr. Ferrell. “On the cell cycle and its switches”. In: *Nature* 454 (2008), pp. 288–9.

[369] J. E. Jr. Ferrell et al. “Simple, realistic models of complex biological processes: positive feedback and bistability in a cell fate switch and a cell cycle oscillator”. In: *FEBS Lett* 583 (2009), pp. 3999–4005.

[370] J. Pei et al. “Diurnal oscillations of endogenous H_2O_2 sustained by $p66^{Shc}$ regulate circadian clocks”. In: *Nat Cell Biol* 21 (2019), pp. 1553–64.

[371] R. M. Buijs and A. Kalsbeek. “Hypothalamic integration of central and peripheral clocks”. In: *Nat Rev Neurosci* 2 (2001), pp. 521–6.

[372] H. Oster et al. “The circadian rhythm of glucocorticoids is regulated by a gating mechanism residing in the adrenal cortical clock”. In: *Cell Metab* 4 (2006), pp. 163–73.

[373] C. B. Peek et al. “Circadian clock NAD+ cycle drives mitochondrial oxidative metabolism in mice”. In: *Science* 342 (2013), p. 1243417.

[374] R. Schmalen et al. “Interaction of circadian clock proteins CRY1 and PER2 is modulated by zinc binding and disulfide bond formation”. In: *Cell* 157 (2014), pp. 1203–15.

[375] N. Gupta and S. W. Ragsdale. “Thiol-disulfide redox dependence of heme binding and heme ligand switching in nuclear hormone receptor Rev-erbβ”. In: *J Biol Chem* 286 (2011), pp. 4392–403.

[376] A. Goldbeter. *Biochemical Oscillations and Cellular Rhythms. The Molecular Bases of Periodic and Chaotic Behavior*. Cambridge: University Press, 1996.

[377] M. R. Atkinson et al. “Development of genetic circuitry exhibiting toggle switch or oscillatory behavior in *Escherichia coli*”. In: *Cell* 113 (2003), pp. 597–607.

[378] N. B. Milev and A. B. Reddy. “Circadian redox oscillations and metabolism”. In: *Trends Endocrinol Metab* 26 (2015), pp. 430–7.

[379] J. L. Robinson et al. “Circadian variation of liver metabolites and amino acids in rats adapted to a high protein, carbohydrate-free diet”. In: *J Nutr* 111 (1981), pp. 1711–20.

[380] B. A. Neuschwander-Tetri and T. Rozin. “Diurnal variability of cysteine and glutathione content in the pancreas and liver of the mouse”. In: *Comp Biochem Physiol B Biochem Mol Biol* 114 (1996), pp. 91–5.

[381] M. Y. Farooqui and A. E. Ahmed. “Circadian periodicity of tissue glutathione and its relationship with lipid peroxidation in rats”. In: *Life Sci* 34 (1984), pp. 2413–8.

[382] X. M. Li et al. “Pharmacologic modulation of reduced glutathione circadian rhythms with buthionine sulfoximine: relationship with cisplatin toxicity in mice”. In: *Toxicol Appl Pharmacol* 143 (1997), pp. 281–90.

[383] V. Pekovic-Vaughan et al. “The circadian clock regulates rhythmic activation of the NRF2/glutathione-mediated antioxidant defense pathway to modulate pulmonary fibrosis”. In: *Genes Dev* 28 (2014), pp. 548–60.

[384] K. Mori et al. “Evaluation of hepatic damage by reactive metabolites–with consideration of circadian variation of murine hepatic glutathione levels”. In: *J Toxicol Sci* 39 (2014), pp. 537–44.

[385] T. A. Wang et al. “Circadian rhythm of redox state regulates excitability in suprachiasmatic nucleus neurons”. In: *Science* 337 (2012), pp. 839–42.

[386] J. Hirayama, S. Cho, and P. Sassone-Corsi. "Circadian control by the reduction/oxidation pathway: catalase represses light-dependent clock gene expression in the zebrafish". In: *Proc Natl Acad Sci U S A* 104 (2007), pp. 15747–52.

[387] N. B. Ivleva et al. "LdpA: a component of the circadian clock senses redox state of the cell". In: *EMBO J* 24 (2005), pp. 1202–10.

[388] T. Tamaru et al. "ROS stress resets circadian clocks to coordinate pro-survival signals". In: *PLoS One* 8 (2013), e82006.

[389] K. Kaasik and C. C. Lee. "Reciprocal regulation of haem biosynthesis and the circadian clock in mammals". In: *Nature* 430 (2004), pp. 467–71.

[390] R. Klemz et al. "Reciprocal regulation of carbon monoxide metabolism and the circadian clock". In: *Nat Struct Mol Biol* 24 (2017), pp. 15–22.

[391] L. Yin et al. "Rev-erbα, a heme sensor that coordinates metabolic and circadian pathways". In: *Science* 318 (2007), pp. 1786–9.

[392] S. Raghuram et al. "Identification of heme as the ligand for the orphan nuclear receptors REV-ERBα and REV-ERBβ". In: *Nat Struct Mol Biol* 14 (2007), pp. 1207–13.

[393] J. Yang et al. "A novel heme-regulatory motif mediates heme-dependent degradation of the circadian factor period 2". In: *Mol Cell Biol* 28 (2008), pp. 4697–711.

[394] S. N. Nangle et al. "Molecular assembly of the period-cryptochrome circadian transcriptional repressor complex". In: *eLife* 3 (2014), e03674.

[395] S. Okano et al. "Unusual circadian locomotor activity and pathophysiology in mutant CRY1 transgenic mice". In: *Neurosci Lett* 451 (2009), pp. 246–51.

[396] D. Shao et al. "A redox-dependent mechanism for regulation of AMPK activation by Thioredoxin-1 during energy starvation". In: *Cell Metab* 19 (2014), pp. 232–45.

[397] Y. Nakahata et al. "Circadian control of the NAD^+ salvage pathway by CLOCK-SIRT1". In: *Science* 324 (2009), pp. 654–7.

[398] M. L. Circu and T. Y. Aw. "Reactive oxygen species, cellular redox systems, and apoptosis". In: *Free Radic Biol Med* 48 (2010), pp. 749–62.

[399] L. M. Beaver et al. "Circadian regulation of glutathione levels and biosynthesis in *Drosophila melanogaster*". In: *PLoS One* 7 (2012), e50454.

[400] N. Krishnan, A. J. Davis, and J. M. Giebultowicz. "Circadian regulation of response to oxidative stress in *Drosophila melanogaster*". In: *Biochem Biophys Res Commun* 374 (2008), pp. 299–303.

[401] R. V. Kondratov et al. "Early aging and age-related pathologies in mice deficient in BMAL1, the core componentof the circadian clock". In: *Genes Dev* 20 (2006), pp. 1868–73.

[402] E. S. Musiek et al. "Circadian clock proteins regulate neuronal redox homeostasis and neurodegeneration". In: *J Clin Invest* 123 (2013), pp. 5389–400.

[403] F. Luchetti et al. "Melatonin signaling and cell protection function". In: *FASEB J* 24 (2010), pp. 3603–24.

[404] R. Hardeland, A. Coto-Montes, and B. Poeggeler. "Circadian rhythms, oxidative stress, and antioxidative defense mechanisms". In: *Chronobiol Int* 20 (2003), pp. 921–62.

[405] M. Wilking et al. "Circadian rhythm connections to oxidative stress: implications for human health". In: *Antioxid Redox Signal* 19 (2013), pp. 192–208.

[406] O. Froy. "Circadian rhythms, aging, and life span in mammals". In: *Physiology (Bethesda)* 26 (2011), pp. 225–35.

[407] M. W. Hurd and M. R. Ralph. "The significance of circadian organization for longevity in the golden hamster". In: *J Biol Rhythms* 13 (1998), pp. 430–6.

[408] R. V. Kondratov et al. "Antioxidant N-acetyl-L-cysteine ameliorates symptoms of premature aging associated with the deficiency of the circadian protein BMAL1". In: *Aging (Albany NY)* 1 (2009), pp. 979–87.

[409] C. Cantó and J. Auwerx. "Caloric restriction, SIRT1 and longevity". In: *Trends Endocrinol Metab* 20 (2009), pp. 325–31.

[410] F. C. Kelleher, A. Rao, and A. Maguire. "Circadian molecular clocks and cancer". In: *Cancer Lett* 342 (2014), pp. 9–18.

[411] A. Acharya et al. "Redox regulation in cancer: a double-edged sword with therapeutic potential". In: *Oxid Med Cell Longev* 3 (2010), pp. 23–34.

[412] S. Ahn, J. Solfest, and L. L. Rubchinsky. "Fine temporal structure of cardiorespiratory synchronization". In: *Am J Physiol Heart Circ Physiol* 306 (2014), H755–63.

[413] H. Seidel and H. Herzel. "Analyzing entrainment of heartbeat and respiration with surrogates". In: *IEEE Eng Med Biol Mag* 17 (1998), pp. 54–7.

[414] A. E. Granada et al. "Human chronotypes from a theoretical perspective". In: *PLoS One* 8 (2013), e59464.

[415] A. E. Granada et al. "Circadian desynchronization". In: *Interface Focus* 1 (2011), pp. 153–66.

[416] C. Pittendrigh. "Circadian systems: entrainment". In: *Biological Rhythms*. Ed. by J. Aschoff. Springer-Verlag US, 1981, pp. 95–124.

[417] S. Daan and J. Aschoff. "Circadian rhythms of locomotor activity in captive birds and mammals: their variations with season and latitude". In: *Oecologia* 18 (1975), pp. 269–316.

[418] J. Duffy and Jr. K. Wright. "Entrainment of the human circadian system by light". In: *J Biol Rhythms* 20 (2005), pp. 326–38.

[419] J. Rémi, M. Merrow, and T. Roenneberg. "A circadian surface of entrainment: varying t, , and photoperiod in *Neurospora crassa*". In: *J Biol Rhythms* 25 (2010), pp. 318–28.

[420] G. Kurosawa and A. Goldbeter. "Amplitude of circadian oscillations entrained by 24h light-dark cycles". In: *J Theor Biol* 242 (2006), pp. 479–88.

[421] S. Daan and C. Berde. "Two coupled oscillators: Simulations of the circadian pacemaker in mammalian activity rhythms". In: *J Theor Biol* 70 (1978), pp. 297–313.

[422] S. A. Brown et al. “Molecular insights into human daily behavior”. In: *Proc Natl Acad Sci U S A* 105 (2008), pp. 1602–7.

[423] A. Trott and J. S. Menet. “Regulation of circadian clock transcriptional output by CLOCK:BMAL1”. In: *PLoS Genet* 14 (2018), e1007156.

[424] J. Yan et al. “Analysis of gene regulatory networks in the mammalian circadian rhythm”. In: *PLoS Comput Biol* 4 (2008), e1000193.

[425] K. Bozek et al. “Regulation of clock-controlled genes in mammals”. In: *PLoS One* 4 (2009), e4882.

[426] B. Kang et al. “Modeling the effects of cell cycle M-phase transcriptional inhibition on circadian oscillation”. In: *PLoS Comput Biol* 4 (2008), e1000019.

[427] M. H. Hastings. “Circadian clockwork: two loops are better than one”. In: *Neurosci* 1 (2000), pp. 143–6.

[428] D. Gonze, J. Halloy, and A. Goldbeter. “Robustness of circadian rhythms with respect to molecular noise”. In: *Proc Natl Acad Sci U S A* 99 (2002), pp. 673–8.

[429] R. Hara et al. “Restricted feeding entrains liver clock without participation of the suprachiasmatic nucleus”. In: *Genes Cells* 6 (2001), pp. 269–78.

[430] Y. Adamovich et al. “Oxygen and carbon dioxide rhythms are circadian clock controlled and differentially directed by behavioral signals”. In: *Cell Metab* 29 (2019), pp. 1092–103.

[431] O. M. Buxton et al. “Adverse metabolic consequences in humans of prolonged sleep restriction combined with circadian disruption”. In: *Sci Transl Med* 4 (2012), 129ra43.

[432] Y. Adamovich et al. “Rhythmic oxygen levels reset circadian clocks through HIFα”. In: *Cell Metab* 25 (2017), pp. 93–101.

[433] Y. I. Kim et al. “Oxidized quinones signal onset of darkness directly to the cyanobacterial circadian oscillator”. In: *Proc Natl Acad Sci U S A* 109 (2012), pp. 17765–9.

[434] S. G. Rhee and H. A. Woo. “Multiple functions of 2-Cys peroxiredoxins, I and II, and their regulations via post-translational modifications”. In: *Free Radic Biol Med* 326 (2020), pp. 107–15.

[435] D. Mauvoisin et al. “Circadian clock-dependent and -independent rhythmic proteomes implement distinct diurnal functions in mouse liver”. In: *Proc Natl Acad Sci U S A* 111 (2014), pp. 167–72.

[436] M. S. Robles, J. Cox, and M. Mann. “In-vivo quantitative proteomics reveals a key contribution of post-transcriptional mechanisms to the circadian regulation of liver metabolism”. In: *PLoS Genet* 10 (2014), e1004047.

[437] G. van Ooijen and A. J. Millar. “Non-transcriptional oscillators in circadian timekeeping”. In: *Trends Biochem Sci* 37 (2012), pp. 484–92.

[438] D. A. Rand et al. “Design principles underlying circadian clocks”. In: *J R Soc Interface* 1 (2004), pp. 119–30.

[439] D. A. Rand et al. “Uncovering the design principles of circadian clocks: mathematical analysis of flexibility and evolutionary goals”. In: *J Theor Biol* 238 (2006), pp. 616–35.

[440] O. E. Akman et al. "Robustness from flexibility in the fungal circadian clock". In: *BMC Syst Biol* 4 (2010), p. 88.

[441] A. B. Reddy and G. Rey. "Metabolic and nontranscriptional circadian clocks: eukaryotes". In: *Annu Rev Biochem* 83 (2015), pp. 165–89.

[442] R. A. Wever. *The Circadian System of Man: Results of Experiments Under Temporal Isolation*. Springer Verlag, New York, Heidelberg, Berlin (West), 1979.

[443] P. Indic, W. J. Schwartz, and D. Paydarfar. "Design principles for phase-splitting behaviour of coupled cellular oscillators: Clues from hamsters with "split" circadian rhythms". In: *J R Soc Interface* 5 (2008), pp. 873–83.

[444] Y. Yamada and D. Forger. "Multiscale complexity in the mammalian circadian clock". In: *Curr Opin Genet Dev* 20 (2010), pp. 626–33.

[445] M. D. C. Belle et al. "Daily electrical silencing in the mammalian circadian clock". In: *Science* 326 (2009), pp. 281–4.

[446] G.J. Hannon. "RNA interference". In: *Nature* 418 (2002), pp. 244–51.

[447] M.T. McManus and P.A. Sharp. "Gene silencing in mammals by small interfering RNAs". In: *Nat Rev Genet* 3 (2002), pp. 737–47.

[448] B. Maier et al. "A large-scale functional RNAi screen reveals a role for CK2 in the mammalian circadian clock". In: *Genes Dev* 23 (2009), pp. 708–18.

[449] J.M. Silva et al. "Second-generation shRNA libraries covering the mouse and human genomes". In: *Nat Genet* 37 (2005), pp. 1281–8.

[450] F. Stegmeier et al. "A lentiviral microRNA-based system for single-copy polymerase II-regulated RNA interference in mammalian cells". In: *Proc Natl Acad Sci USA* 102 (2005), pp. 12312–7.

[451] URL: `http://codex.cshl.edu/scripts/newmain.pl`.

[452] B. Maier et al. "Searching novel clock genes using RNAi based screening". In: *Springer Methods in Molecular Biology: Circadian Clocks, Methods and Protocols*. Ed. by S. A. Brown. Springer US, 2020, p. 346.

[453] J.D Gordon et al. *Microplate edge effects in range finding studies using the Lumi-cellER bioassay: increasing assay throughput*. URL: `http://www.dioxins.com/pdf/lumi/lumi11.pdf`.

[454] O. Olesen. "Properties and units in the clinical laboratory sciences. I. Syntax and semantic rules (recommendation 1995). International Union of Pure and Applied Chemistry (IUPAC) and International Federation of Clinical Chemistry (IFCC)". In: *Eur J Clin Chem Clin Biochem* 33 (1995), pp. 627–36.

U Möckernbrücke

A

Appendix A

To analyze whether the effect of metabolic disruption in temperature compensation is a general circadian feature and not just specific to our *Bmal1-luc* U-2 OS reporter cell system, all experiments and analyses explained in Section 2.3 were repeated in U-2 OS cells harboring a second circadian reporter. Here, the luciferase gene was now under regulation of a *Per2* promoter and the cells are referred to as *Per2-luc* U-2 OS cells. It should be remarked that, after transduction, the *Per2-luc* cells that were assayed at 32°C showed fluorescence values (a proxy for transduction efficiency, see Section 6.2) that were in the lower limit of what would be considered efficient transduction (data not shown). The fluorescence in the rest of the plates was high enough to consider that the transduction had been qualitatively efficient in cells from most of the wells. Fluorescence values from *Bmal1-luc* cells were slightly higher than those from *Per2-luc*, indicating that the transduction might have been, to some extent, less efficient in the latter.

The time series were processed as described in Section 6.3 using the ChronoStar V3.0 software [452]. Raw data was detrended and fitted to an exponentially decaying cosine curve. Suppl. Figure A.1 shows the time series from all wells (*Bmal1-luc* and *Per2-luc* cells) after each individual knockdown. The quality of the oscillations was notably better in the *Bmal1-luc* cells compared to the *Per2-luc* (Suppl. Figure A.2).

Periods, amplitudes, phases and damping coefficients of the oscillations were estimated from the fits and a quality control was done over the raw data to remove oscillations with high error fits, outliers and plate/well trends (see Section 6.3). A summary of all time series parameters is found in Suppl. Tables S2 and S3 (provided as additional files), and the distributions are plotted in Suppl. Figure A.3. For each plate, mean values and standard deviations of all parameters (period, amplitude, phase and damping coefficient) are shown in Suppl. Table A.1. Plate-to-plate variation (within plates assayed at one of

the temperatures with the same reporter cells) in period length, amplitude and damping coefficient was modest in non-silencing control wells, as seen by Table A.1B.

In order to evaluate whether the temperature compensation property was lost or maintained after specific knockdown, we calculated the slope of a period (or amplitude) vs. temperature plot as described in Equation 2.2 and compared the slopes after knockdown with the slopes of the negative controls. Suppl. Figure A.4 shows the detrended oscillations of the hits at both temperatures and Suppl. Figures A.5 and A.6, the individual slopes of the period and amplitude change, respectively.

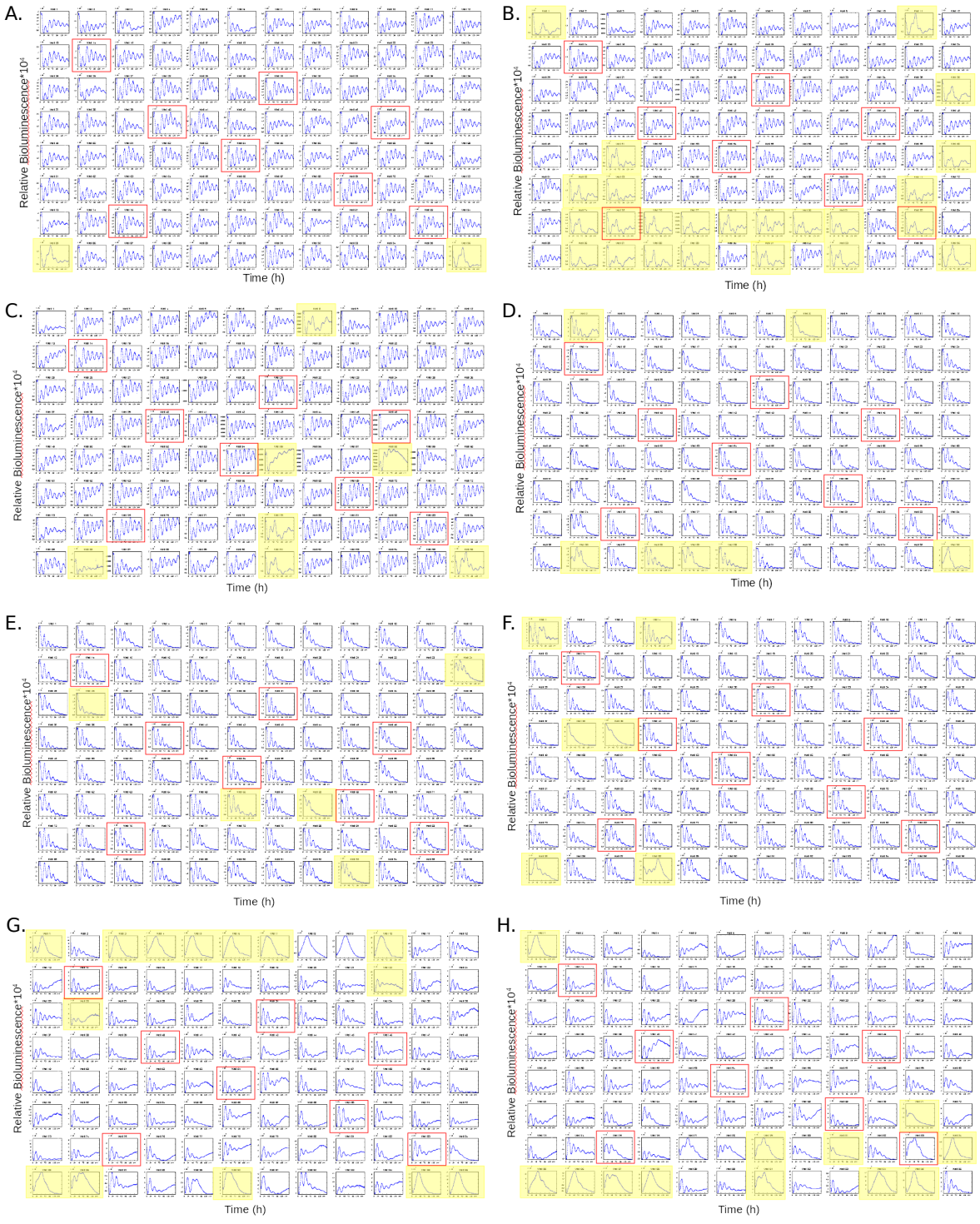

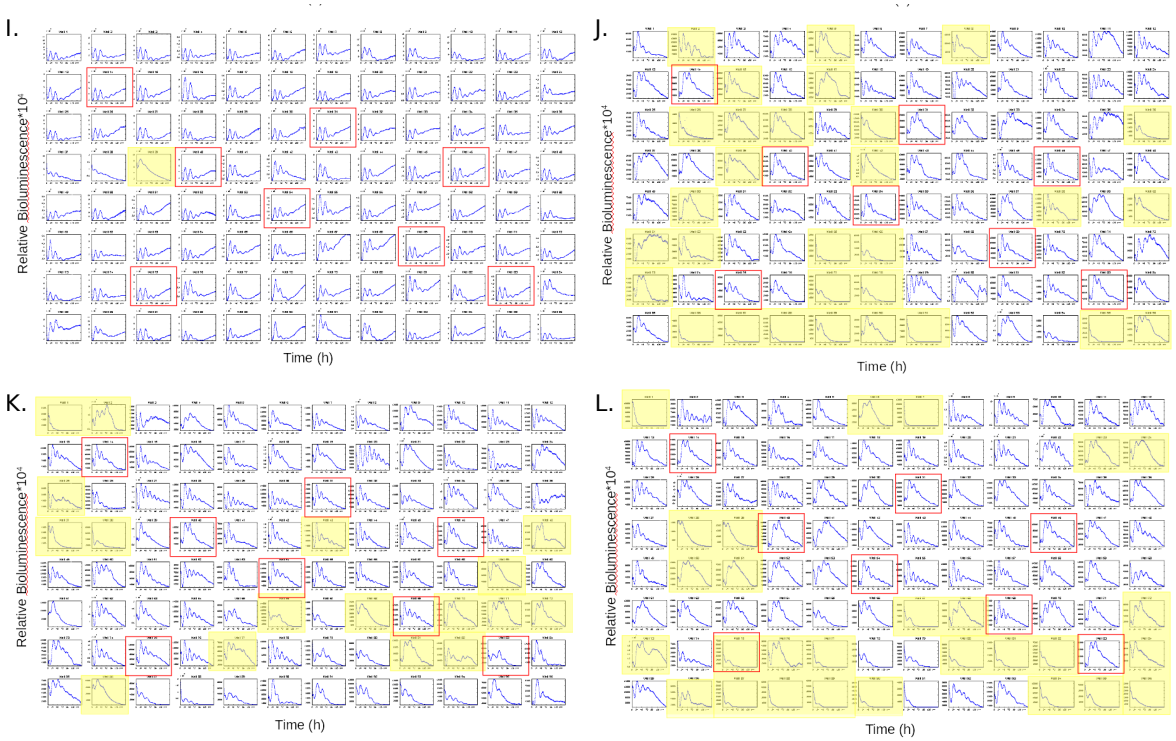

Figure A.1: Raw oscillations of the twelve plates processed in this study. *Bmal1-luc* cells assayed in the TopCount at 32°C (**A**), (**B**), (**C**) or 39°C (**D**), (**E**), (**F**). *Per2-luc* cells assayed in the TopCount at 32°C (**G**), (**H**), (**I**) or 39°C (**J**), (**K**), (**L**). Yellow squares represent oscillations that were excluded from analysis because of high error of fit (error>0.08 or >0.20 in *Bmal1-luc* or *Per2-luc* cells, respectively), outliers or well effects (see section 6.3). Red boxes represent the location of the negative non-silencing controls in the plates.

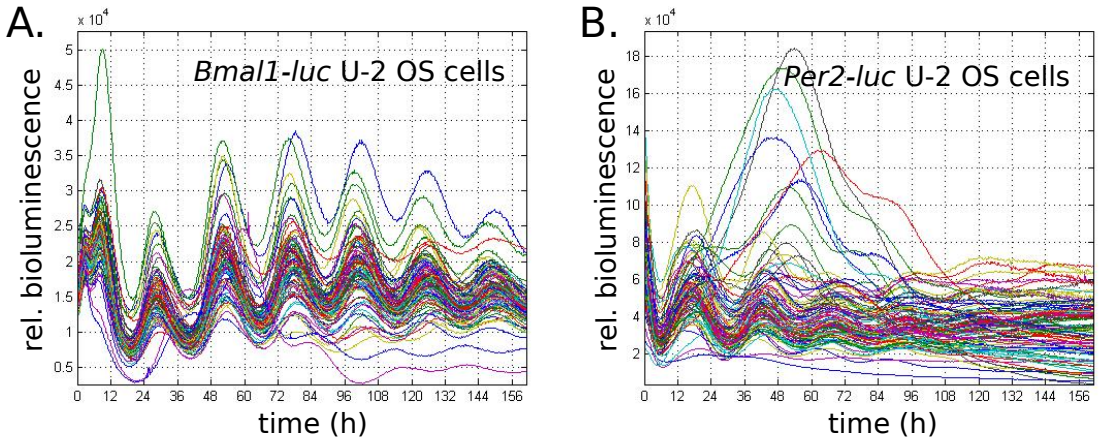

Figure A.2: Raw oscillations of two representative plates plotted in the same graph. A representative plate with *Bmal1-luc* cells (**A**) or *Per2-luc* cells (**B**) assayed in the TopCount luminometer at 32°C.

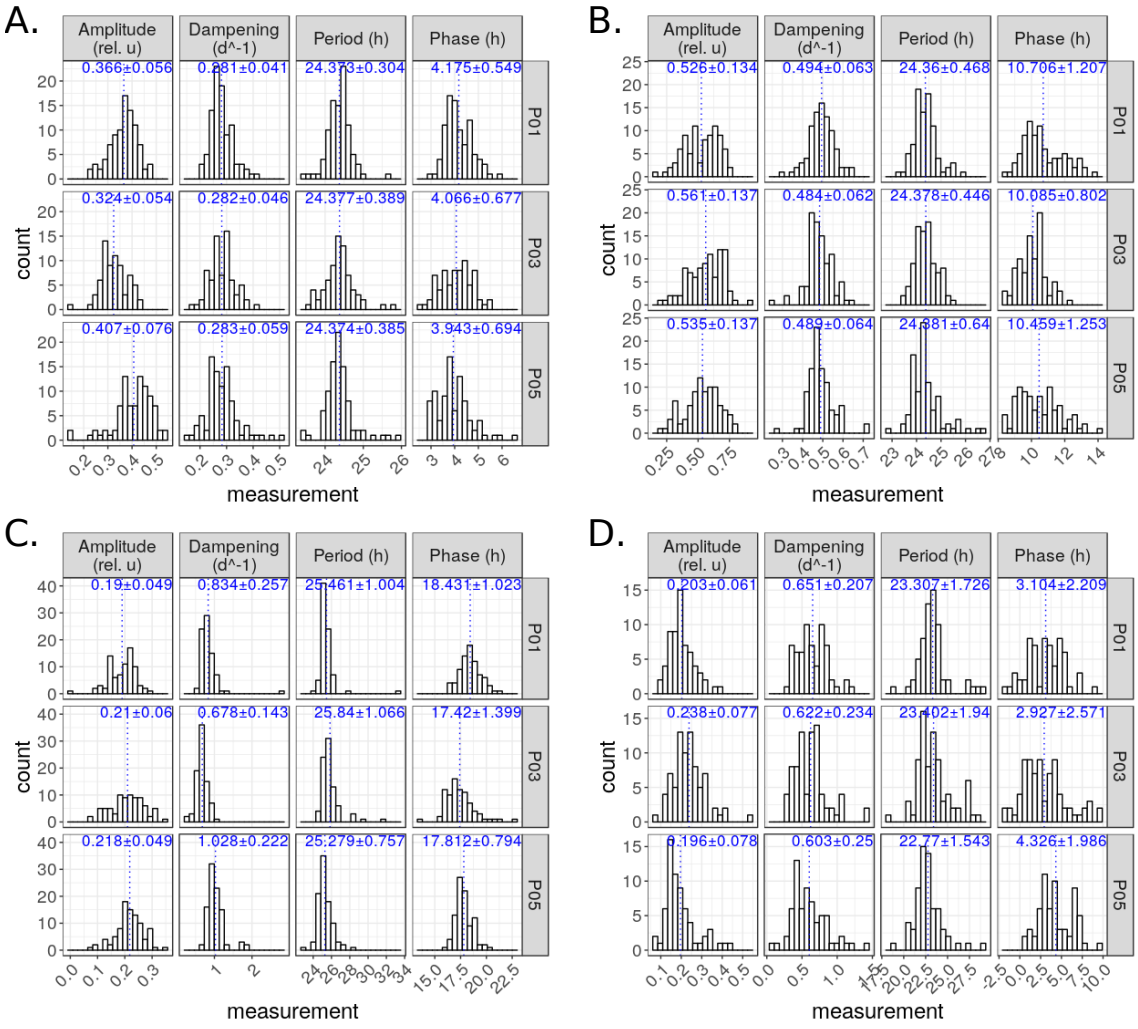

Figure A.3: Distributions of oscillations parameters (period, amplitude, damping coefficient and phase) extracted from the ChronoStar fits in all plates. The raw time series were detrended with a 24 h-running average and fitted to a cosine curve (Equation 6.2), after quality control (see section 6.3). The fitted parameters were extracted and their histograms are shown here. (**A**) *Bmal1-luc* cells assayed at 32°C, (**B**) *Bmal1-luc* cells assayed at 39°C, (**C**) *Per2-luc* cells assayed at 32°C, (**D**) *Per2-luc* cells assayed at 39°C. The mean parameter value ±SD is shown in blue (non quantile-normalized values).

Table A.1: Summary of the oscillation parameters estimated with ChronoStar V3.0. Means and standard deviations of all oscillations parameters (period, phase, amplitude and damping coefficient) are shown for all plates at 32°C (blue) and 39°C (red), after performing the quality control and trend removal on the raw data. (**A**) Oscillation parameters values from all wells in the plate. (**B**) Oscillation parameters values from the non-silencing controls in the plate ($n = 8$ non-silencing controls per plate). The data shown here is not normalized based on quantiles. A Student's t-test was performed in the data from *Bmal1-luc* cells; the results are depicted in the table (*: p<0.05, **: p<0.01, ***: p<0.001, ****: p<0.0001).

A.

		Temperature = 32°C				Temperature = 39°C			
		Period (h)	Phase (h)	Amplitude (rel. u.)	Damp. coeff. (day^{-1})	Period (h)	Phase (h)	Amplitude (rel. u.)	Damp. coeff. (day^{-1})
Bmal1-luc	Plate 1	24.37±0.30	4.17±0.55	0.37±0.06 ****	0.28±0.04	24.36±0.47	10.71±1.21 ****	0.53±0.13	0.49±0.06
	Plate 2	24.38±0.39	4.07±0.68 *	0.32±0.05 ****	0.28±0.05	24.38±0.45	10.08±0.80 *	0.56±0.14	0.48±0.06
	Plate 3	24.37±0.39	3.94±0.69	0.41±0.08 ****	0.28±0.06	24.38±0.64	10.46±1.25	0.53±0.14	0.49±0.06
Per2-luc	Plate 1	25.46±1.00	18.43±1.02	0.19±0.05	0.83±0.26	23.32±1.73	3.10±2.21	0.20±0.06	0.65±0.21
	Plate 2	25.84±1.07	17.42±1.40	0.21±0.06	0.68±0.14	23.40±1.94	2.93±2.57	0.24±0.08	0.62±0.23
	Plate 3	25.28±0.76	17.81±0.79	0.22±0.05	1.03±0.22	22.77±1.54	4.33±1.99	0.20±0.08	0.60±0.25

B.

		Temperature = 32°C				Temperature = 39°C			
		Period (h)	Phase (h)	Amplitude (rel. u.)	Damp. coeff. (day^{-1})	Period (h)	Phase (h)	Amplitude (rel. u.)	Damp. coeff. (day^{-1})
Bmal1-luc	Plate 1	24.31±0.15 *	4.12±0.47 **	0.40±0.05	0.27±0.02 *	24.50±0.31	10.05±0.76	0.62±0.10	0.47±0.07
	Plate 2	24.49±0.10 *	3.29±0.21	0.36±0.07	0.27±0.02	24.23±0.23	10.23±0.68	0.62±0.17	0.48±0.04
	Plate 3	24.21±0.23	3.77±0.59	0.42±0.12	0.23±0.04	24.25±0.19	10.55±0.98	0.59±0.09	0.46±0.01
Per2-luc	Plate 1	25.37±0.12	17.61±0.68	0.23±0.03	0.77±0.08	24.05±1.73	1.72±1.91	0.22±0.07	0.73±0.34
	Plate 2	26.43±1.39	17.94±0.67	0.18±0.08	0.61±0.20	23.97±1.41	1.16±1.78	0.22±0.03	0.57±0.16
	Plate 3	25.41±0.39	17.10±0.37	0.26±0.02	1.00±0.15	22.63±1.10	4.64±1.55	0.19±0.09	0.61±0.27

A. (1)

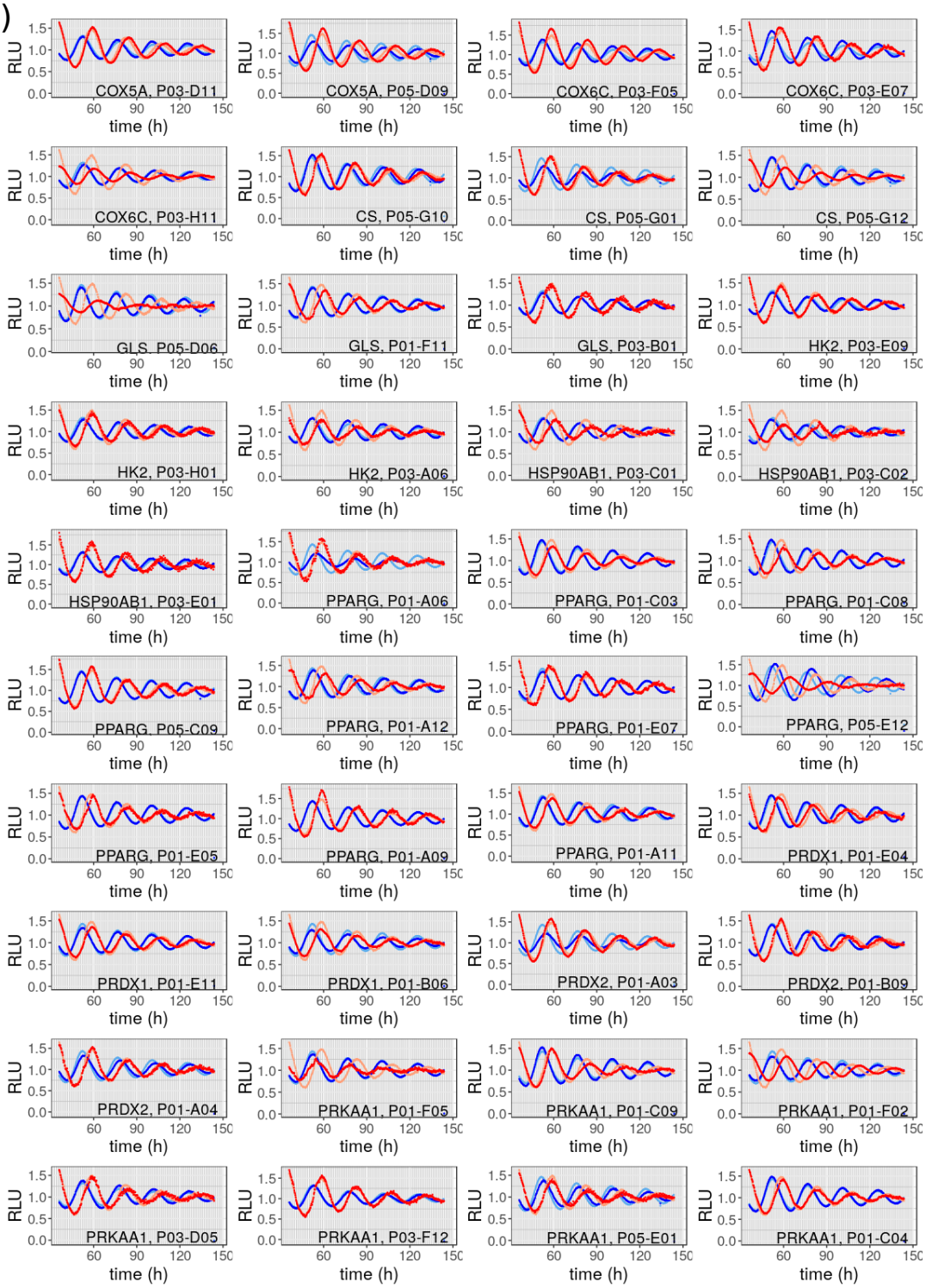
RLU
time (h)
COX5A, P03-D11
COX5A, P05-D09
COX6C, P03-F05
COX6C, P03-E07
COX6C, P03-H11
CS, P05-G10
CS, P05-G01
CS, P05-G12
GLS, P05-D06
GLS, P01-F11
GLS, P03-B01
HK2, P03-E09
HK2, P03-H01
HK2, P03-A06
HSP90AB1, P03-C01
HSP90AB1, P03-C02
HSP90AB1, P03-E01
PPARG, P01-A06
PPARG, P01-C03
PPARG, P01-C08
PPARG, P05-C09
PPARG, P01-A12
PPARG, P01-E07
PPARG, P05-E12
PPARG, P01-E05
PPARG, P01-A09
PPARG, P01-A11
PRDX1, P01-E04
PRDX1, P01-E11
PRDX1, P01-B06
PRDX2, P01-A03
PRDX2, P01-B09
PRDX2, P01-A04
PRKAA1, P01-F05
PRKAA1, P01-C09
PRKAA1, P01-F02
PRKAA1, P03-D05
PRKAA1, P03-F12
PRKAA1, P05-E01
PRKAA1, P01-C04

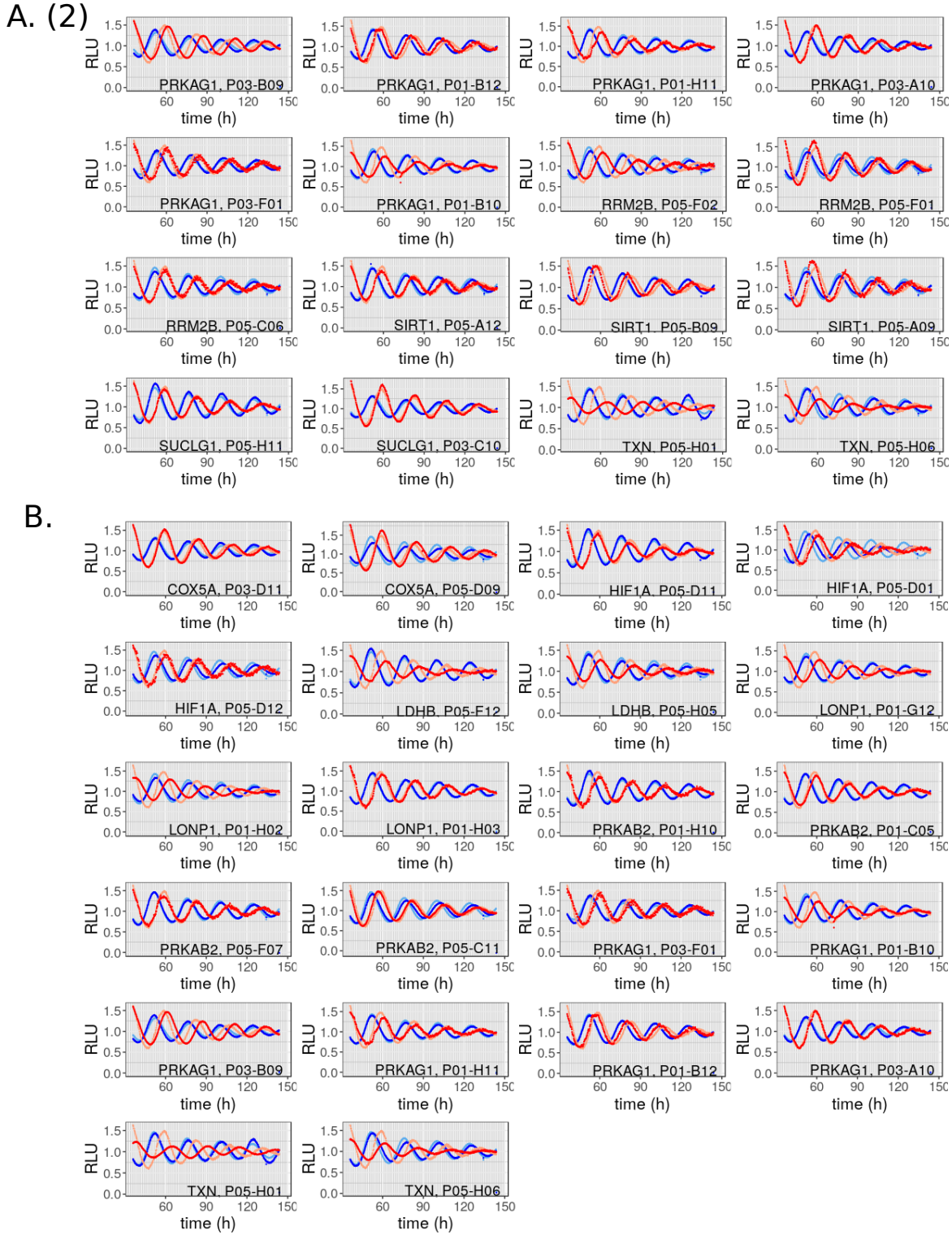

Figure A.4: Oscillations of *Bmal1-luc* cells after knocking down metabolic genes that modulate the response to temperature steps. Depicted here are the oscillations after detrending with the ChronoStar software. The oscillations at 32°C are shown in blue. The oscillations at 39°C, in red. The light colors (light red and light blue) stand for the oscillations of cells that were transduced with the negative non-silencing controls. Darker colors represent oscillations of cells where a gene was silenced via RNAi knockdown. (**A**) Oscillations after knocking down genes that modulate the period compensation against temperature changes (they correspond to the blue, red, green and yellow points in Figure 2.5). (**B**) Oscillations after knocking down genes that modulate the amplitude in response to temperature changes (they correspond to the blue points in Figure 2.6).

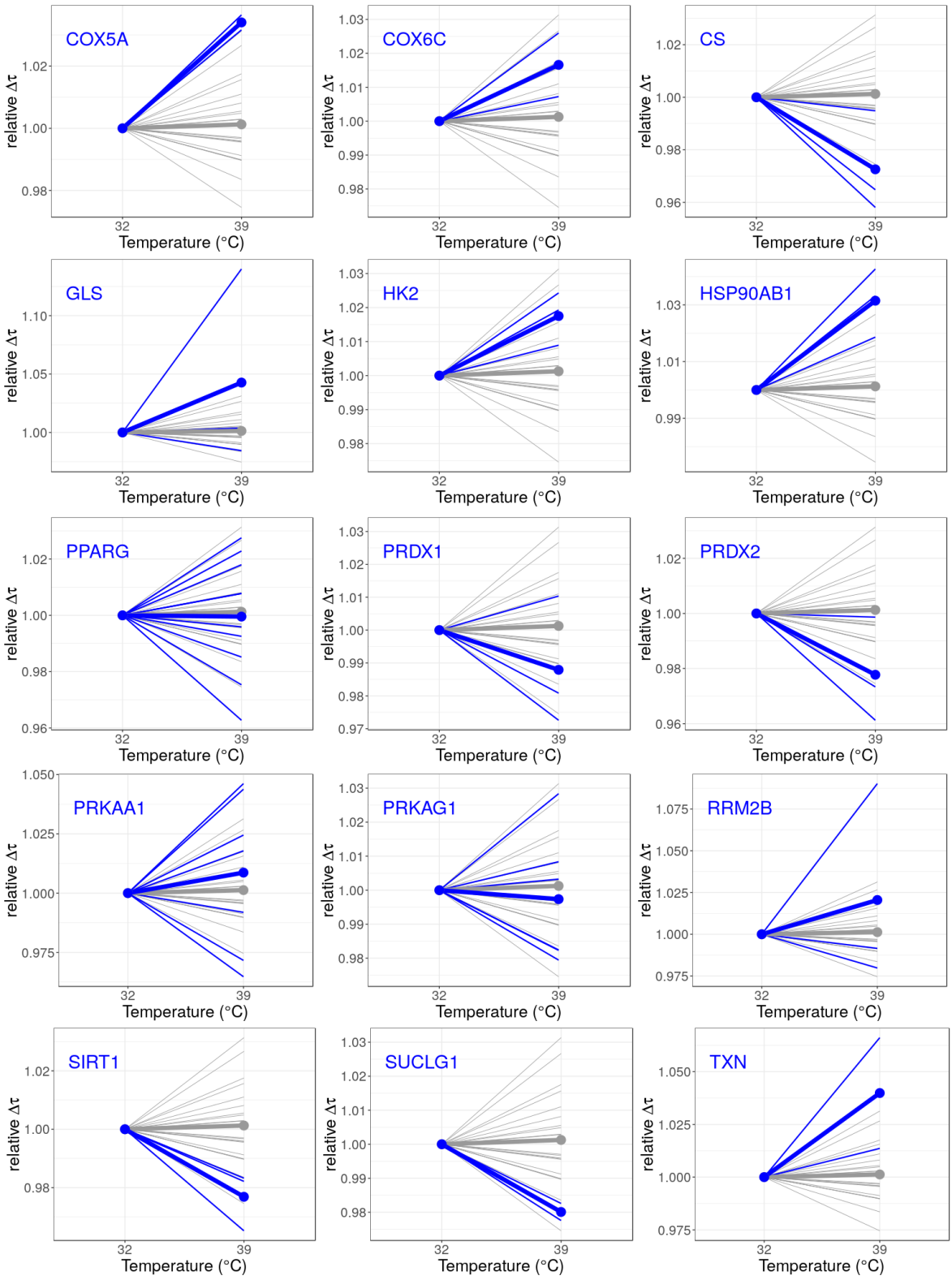

Figure A.5: Metabolic genes that modulate period compensation to temperature changes in *Bmal1-luc* cells. The relative $\Delta\tau$ for each construct, as defined in Equation 2.2, is plotted against temperature (32°C and 39°C). The slope of the line that connects both points informs about the period compensation of the system. Genes whose knockdown makes *Bmal1-luc* cells more sensitive to temperature steps are shown in blue (correspondent to the blue, red, green and yellow points in Figure 2.5). Period slopes of *Bmal1-luc* cells transduced with non-silencing constructs are depicted in gray. Thick lines represent the mean of the silencing (blue) or non silencing (gray) constructs. Thin lines, on the other hand, represent the individual slopes of each construct. The gene that is knocked down is shown in blue in the top left corner of each plot.

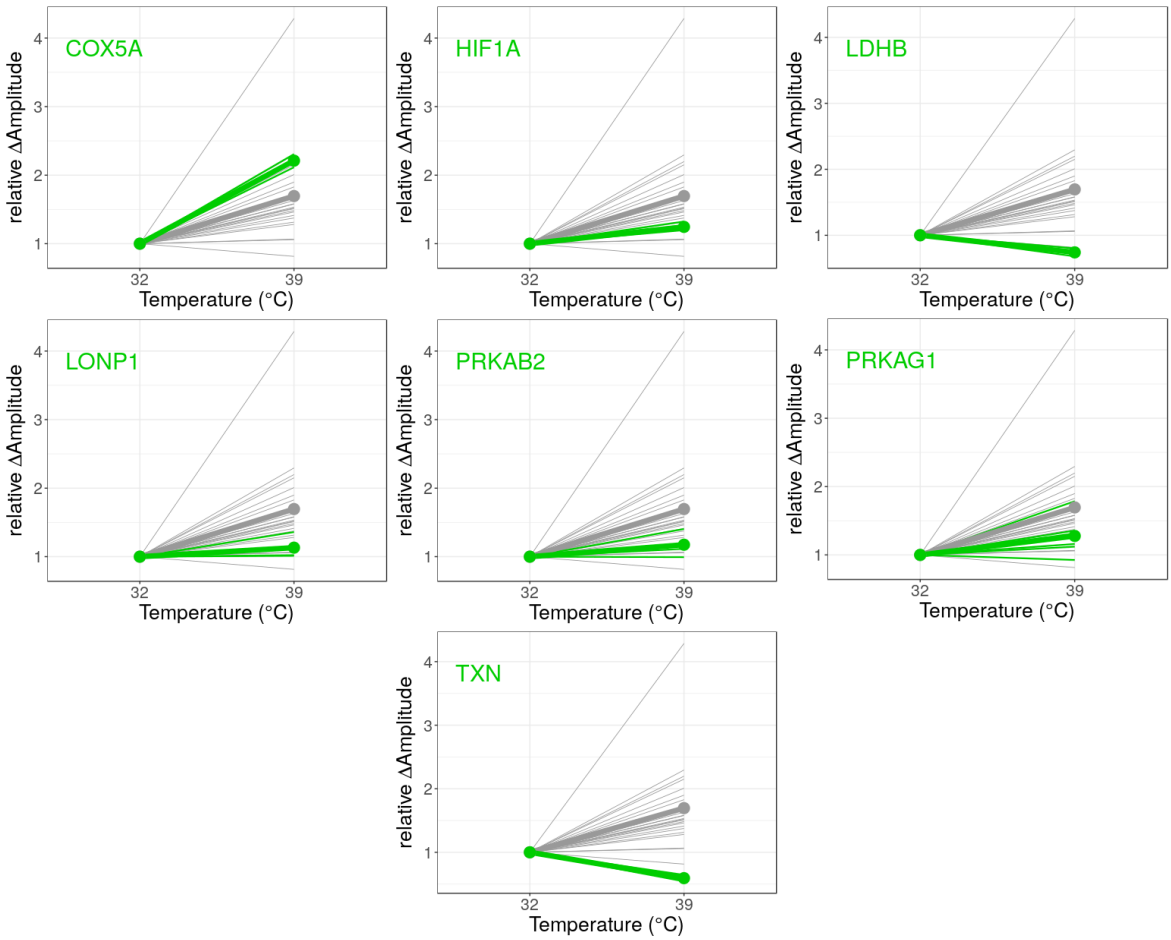

Figure A.6: Metabolic genes that modulate the amplitude's response to temperature compensation in *Bmal1-luc* cells. The relative ΔA for each construct, as defined in Equation 2.2 (but taking amplitude values instead of periods), is plotted against temperature (32°C and 39°C). The slope of the line that connects both points informs about the amplitude response to period compensation of the system. Genes whose knockdown makes amplitude in *Bmal1-luc* cells different to the amplitude of non-silencing controls are shown in green (correspondent to the blue points in Figure 2.6). Amplitude slopes of *Bmal1-luc* cells transduced with non-silencing constructs are depicted in gray. Thick lines represent the mean of the silencing (green) or non-silencing (gray) constructs. Thin lines, on the other hand, represent the individual slopes of each construct. The gene that is knocked down is shown in green in the top left corner of each plot.

A.1 Knockdown of metabolic genes affects rhythm parameters in *Per2-luc* U-2 OS cells

In the same lines as the analysis done on *Bmal1-luc* cells (Section 2.3.1), we firstly analyzed whether knockdown of metabolic genes affected oscillations parameters in *Per2-luc* cells. The results are shown in Suppl. Figure A.7. There were some interesting overlaps between the effect of the metabolic knockdown on oscillation parameters in *Bmal1-luc* and *Per2-luc* cells. For example, knockdown of *LDHC* and *TXN* has the same effect on period length at 39°C; knockdown of *MDH2* affects in a similar way the amplitude and period of the oscillation at 39°C in both reporter cells; and lastly interference with *COX5A* expression resulted in a faster damping in both reporter cells at 39°C as well. However, to our surprise, we found that knockdown of some genes such as *COX5A* or *HSP90AB1* produced opposite period phenotypes in *Bmal1-luc* and *Per2-luc* cells. As has been mentioned, we would have expected more overlap between both reporters since both reporter cells, although different clones, come from the same cell line. Nevertheless, it is not the first time that different circadian reporters result in differences in circadian parameters in experimental observations [274, 275].

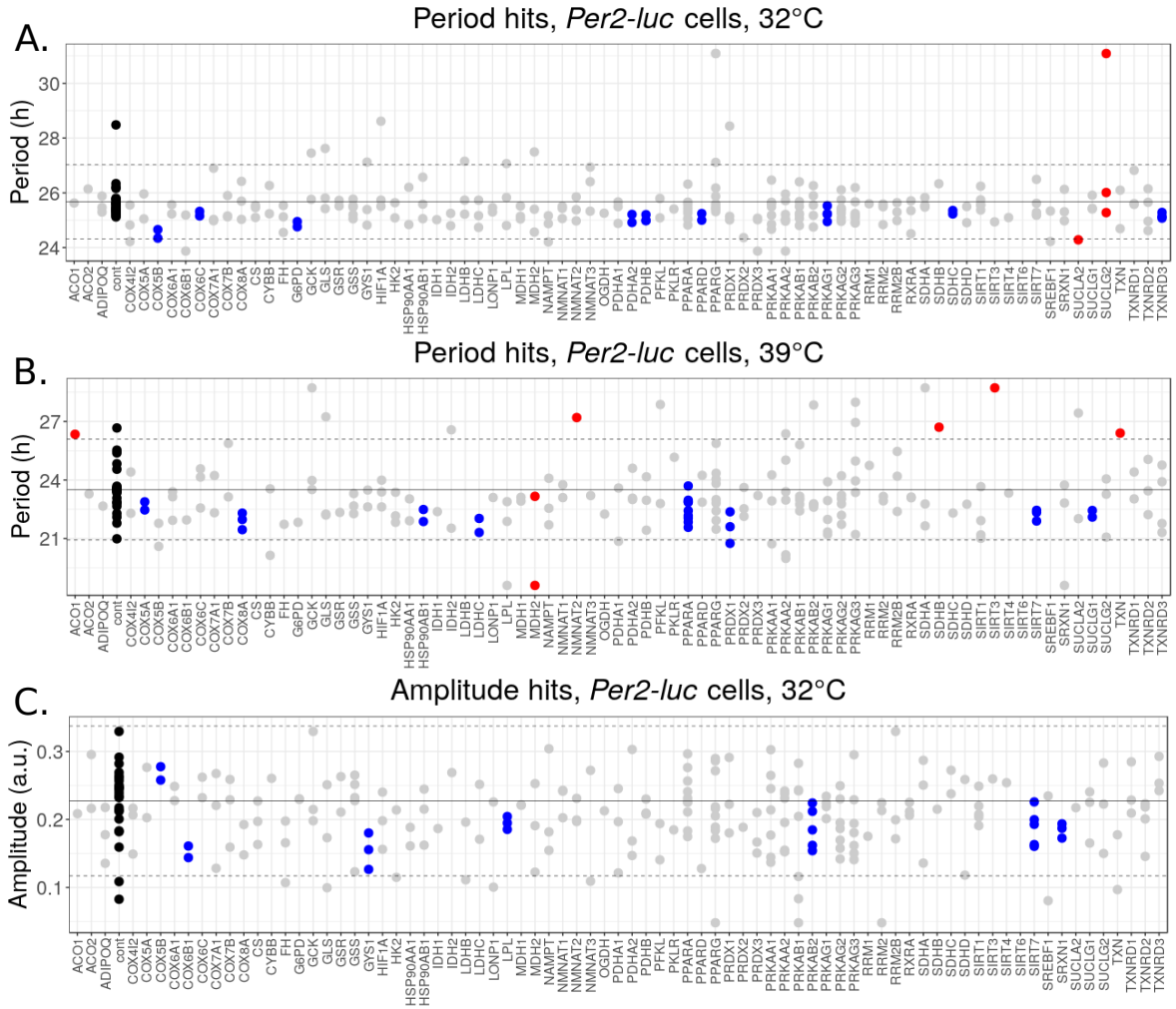

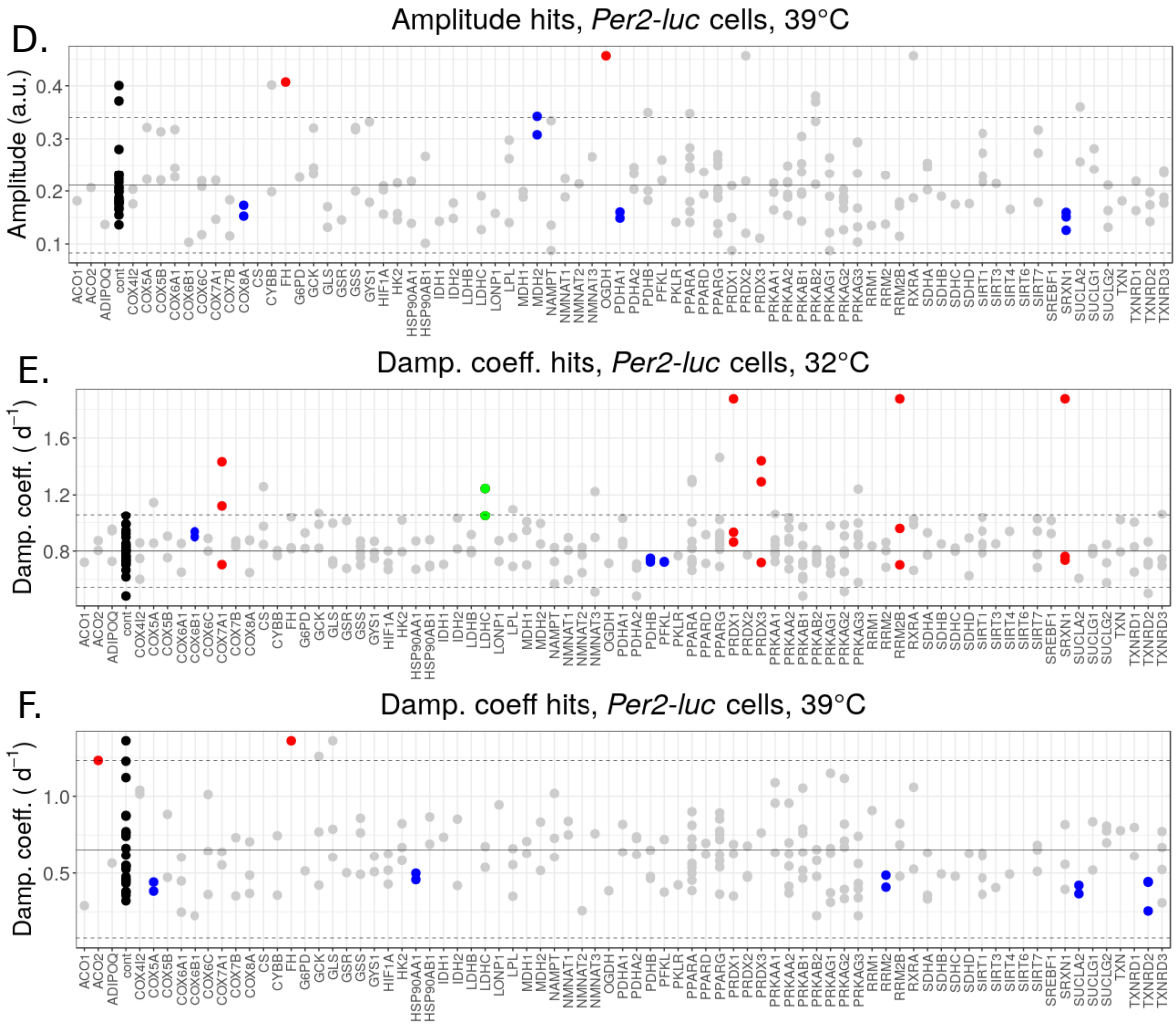

Figure A.7: Metabolic genes that modulate oscillation parameters in *Per2-luc* cells at 32°C and 39°C. Quantile-normalized data is represented here, since all plates were analyzed together to find putative hits. Depicted in black are the parameter values of the negative controls; in blue are those genes whose knockdown resulted in a mean period that was significantly different to the value of the non-silencing controls (p<0.05, t-test); in red, genes whose knockdown resulted in a mean period that was at least 2 SD away from that of the non-silencing controls ($|z|$>2); in green, genes for which the blue and red conditions were held true. The black horizontal lines depict the mean parameter value (continuous line) of the oscillations of cells transduced with non-silencing constructs ± 2 SD (dashed). n=1 single biological experiment with 2–14 shRNA constructs for each genetic knockdown.

A.2 Knockdown of metabolic genes affects period compensation against temperature steps in *Per2-luc* U-2 OS cells

To answer our main question, we next checked how temperature affected the change of period. If our initial hypothesis were true, we would expect that the genetic knockdown yields the system's period more sensitive to temperature steps. The results for *Per2-luc* cells are shown in Suppl. Figure A.8. We observed interesting overlaps with *Bmal1-luc* U-2 OS cells such as *PRDX1* and *SUCLG1*.

It should be remarked that *Per2-luc* cells were less temperature-compensated than *Bmal1-luc* reporter cells. Q_{10} temperature coefficients were calculated for both cell lines with the parameters shown in Suppl. Table A.1. We observed that *Per2-luc* cells ran faster at 39°C (Q_{10}=1.15), whereas there was almost no change in period length between the two temperatures in *Bmal1-luc* reporter cells (Q_{10}=0.996). The decrease in period length at 39°C in *Per2-luc* cells was a general effect, meaning that even negative control cells ran faster at the high temperature (Suppl. Figure A.11, Suppl. Table A.1B).

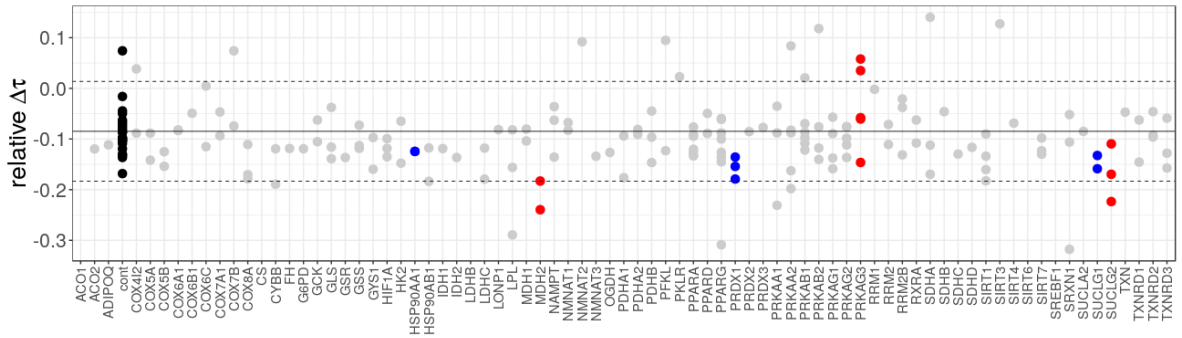

Figure A.8: Knockdown of some metabolic genes results in the loss of the temperature compensation property in *Per2-luc* cells. Quantile-normalized data is represented. Period sensitivity to temperature steps was calculated as shown in Equation 2.2. Color-coding is described in the caption of Figure A.7. n=1 single biological experiment with 2–14 shRNA constructs for each genetic knockdown.

A.3 Period lengths are stable across oscillations

We wanted to check the robustness of the time series, and thus analyzed if there was any kind of period trend throughout the cycles of each individual time series, in order to exclude artifacts. (A putative artifact could be, for instance, if the period values of cycles increased with the number of cycles in one oscillation). To make an estimate of the duration of each of the cycles, we looked for peaks in the detrended data and defined the period of a cycle as the time between two consecutive peaks ("peak picking" procedure). In order to find the peaks of the oscillation we (i) smoothed the detrended time series with a 24 h-running average, (ii) looked for the "reference peaks" (highest values around 30 neighboring points – 15 to each side, depicted in red in Suppl. Figure

A.9) and lastly (iii) fitted quadratic parabolae in the range of 25 points around the reference peak (depicted in green in Figure A.9). The extrema of the parabola (blue crosses) were defined as real peaks. The time between two consecutive real peaks defined the period of each cycle.

We calculated the length of consecutive cycles within individual oscillations and observed that cycle lengths did not change significantly. Moreover, the period value estimated by ChronoStar was in the range of the three or four peak-to-peak values determined via peak picking (Suppl. Figure A.10). We concluded, firstly, that the period was stable and did not change over time (i.e., there was no systematic period trend along oscillations) and, secondly, that the ChronoStar software gave an accurate estimate of the overall oscillation period.

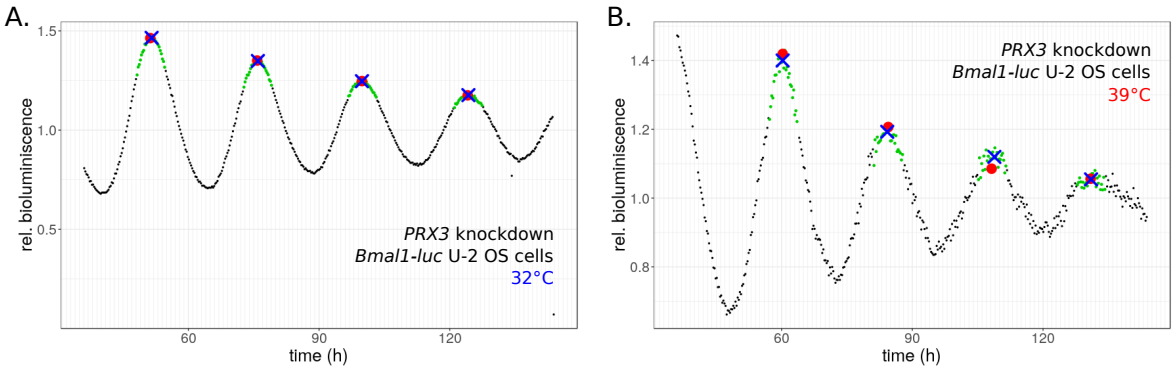

Figure A.9: Peak picking analysis to estimate cycle lengths. Depicted in panels (**A**) and (**B**) are representative smoothed time series of the effect of a metabolic knockdown (*PRDX3* in this case) at 32°C and 39°C, respectively, in *Bmal1-luc* U-2 OS cells. The detrended time series was smoothed with a 24 h-running average and "reference peaks" were found (highest value in 30 neighboring points, depicted in red). Quadratic parabolae were fit in the 25 points surrounding the reference peak (green), and the extrema of the parabola were defined as the real peaks (blue crosses). The length of a cycle was defined as the time between two consecutive real peaks.

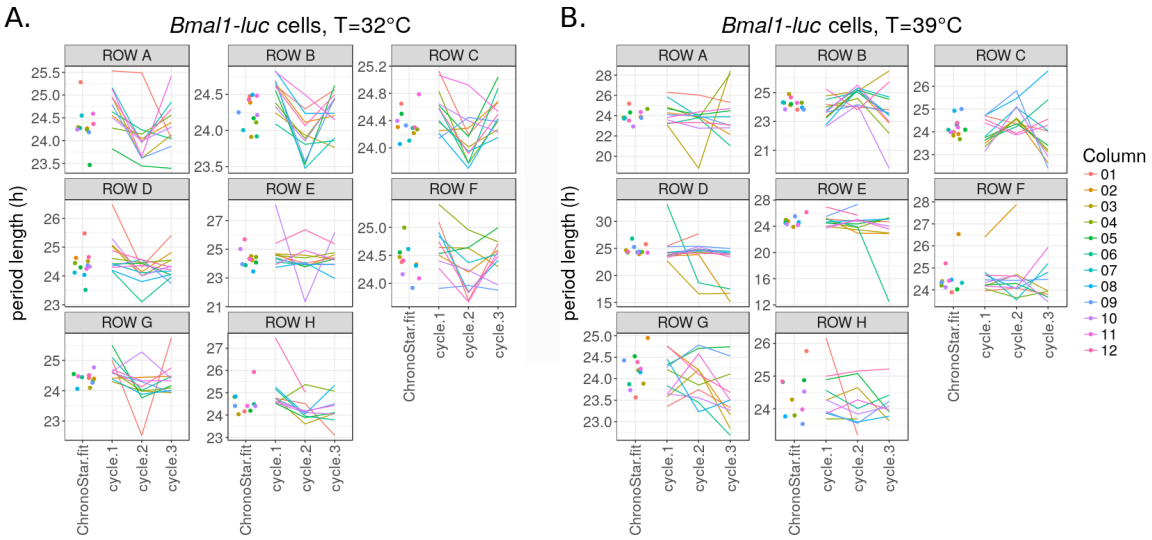

Figure A.10: Period lengths are relatively stable across oscillations and the ChronoStar software gives an accurate estimate of the overall oscillation period. Peak-to-peak values from three cycles (cycle.1, cycle.2 and cycle.3) obtained by peak-picking from oscillations of two representative plates. Data from a representative plate with *Bmal1-luc* cells assayed at 32°C (**A**) or 39°C (**B**). The period estimated by the ChronoStar software is also shown in the plots (ChronoStar.fit). Each panel represents one of the rows in the plate. The twelve columns are depicted in different colors in each panel. (Note that only oscillations that passed the quality control (Section 6.3) were peak-picked, and thus some panels have less than twelve different colors.)

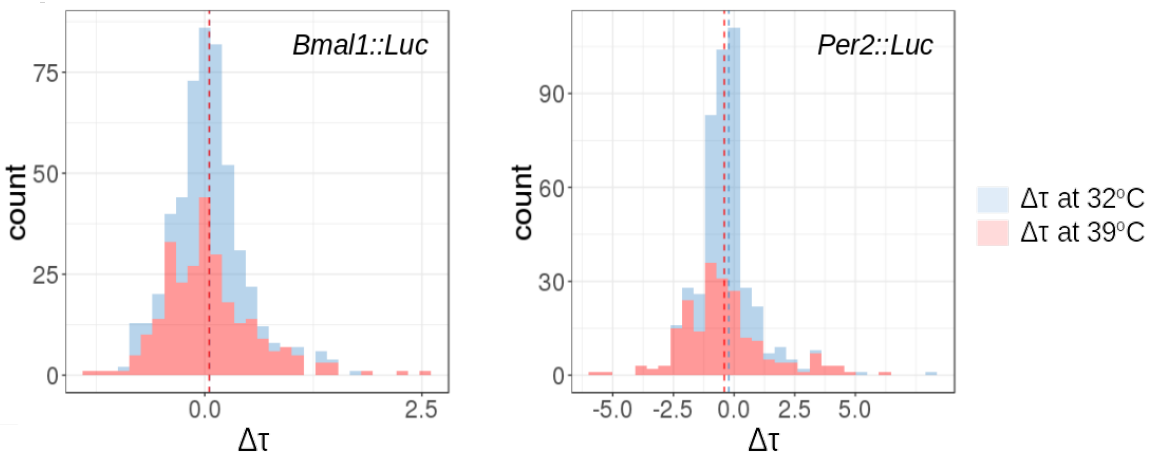

Figure A.11: Histograms of the difference in period between the silencing constructs and the average of the non silencing controls ($\Delta\tau$) from *Bmal1-luc* (A) or *Per2-luc* cells (B) at 32°C (blue) or 39°C (red). Raw oscillations were detrended, fitted to Equation 6.2 and the period of each oscillation was extracted. For each plate, we calculated $\Delta\tau$ by subtracting the mean period of the non-silencing controls to the period of each construct. (Data was not quantile-normalized here as we performed the $\Delta\tau$ calculations plate by plate). A $\Delta\tau$=0 means that the period of a silencing construct is exactly the same as the mean period of the negative controls. The means of the four distributions are centered in $\Delta\tau \simeq 0$, thus indicating that the period of *Bmal1-luc* and *Per2-luc* cells where a metabolic gene was knocked down was, overall, very similar to the negative control cells.

Blankensteinpark

:

B

Appendix B

B.1 Detailed Model of Redox Oscillations

We developed a deterministic model that contained all biochemical species from the Prx3/Srx oscillating system shown in Figure 3.2 [307]. A scheme of the model and its equations are shown in Figure B.1A and B. Production and degradation terms were modeled assuming mass action kinetics. The total Prx3 pool ($SH + SOH + SO_2H + SS$ in the model) and the production of H_2O_2 (k_0 in the model) were assumed to be constant over time.

Applying the two ingredients that we identified as design principles of the oscillator, namely fast SOH inactivation followed by slow H_2O_{2M}-H_2O_{2C}-Srx_{OX}-SrxHsp-Srx_M feedback, we obtained oscillations in all 11 variables. The time series of the 5 core variables that comprise the minimal oscillator are shown in Figure B.1C. The resulting period was 23.5 h and the phase difference between Prx3-S_2H and mitochondrial Srx was 7.3 h. These simulations support the robustness of the minimal model, since applying its design principles into a larger model also generated oscillations with similar characteristics.

Parameters were chosen according to the constraints that we used to infer the parameter values from the minimal model (Table 3.1). Degradation and translocation rates were kept in the order of magnitude of their corresponding parameters in the minimal model (d, e, q). We set k_7 (the rate of oxidation of cytosolic Srx that results in an intermolecular bridge with Hsp) to 2, following previous results, which have estimated that Prxs react 1 000 – 10 000 times faster with H_2O_2 than other reduced cellular thiols [303]. Biochemical assays have determined the rate constants for Prx3-SH

oxidation to sulfenic acid Prx3-SOH (k_1 in the detailed model) and hyperoxidation to Prx3-SO_2H (k_4 in the detailed model) to be in the order of $10^7\,M^{-1}s^{-1}$ and $10^4\,M^{-1}s^{-1}$, respectively [303]. We observed that the amplitude of Prx3-SO_2H and mitochondrial Srx oscillations increased as k_1 was increased, a result that reproduced the details from published western blot data. Kil and colleagues showed in [307] intense bands for both Prx3-SO_2H and mitochondrial Srx at their peak times and no bands at their troughs, implying that the oscillation amplitude is large.

A.

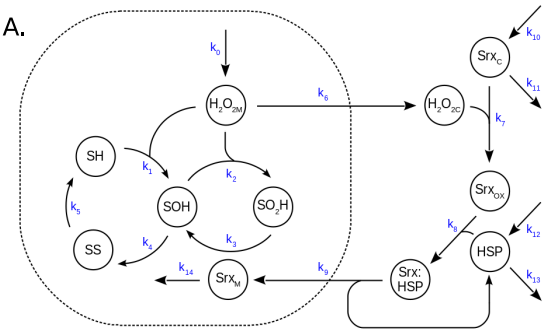

C.

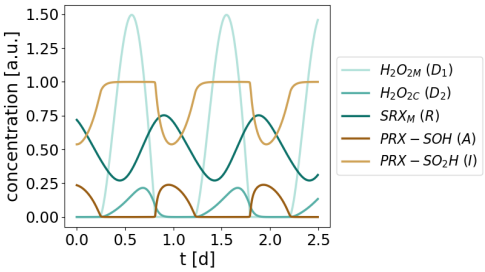

B.

$$
\begin{aligned}
\frac{dH_2O_{2M}}{dt} &= k_0 - k_1 \cdot SH \cdot H_2O_{2M} - k_4 \cdot H_2O_{2M} \cdot SOH - k_6 \cdot H_2O_{2M},\\
\frac{dH_2O_{2C}}{dt} &= k_6 \cdot H_2O_{2M} - k_7 \cdot Srx_C \cdot H_2O_{2C},\\
\frac{dSrx_C}{dt} &= k_{11} - k_7 \cdot Srx_C \cdot H_2O_{2C} - k_{12} \cdot Srx_C,\\
\frac{dSrx_{OX}}{dt} &= k_7 \cdot Srx_C \cdot H_2O_{2C} - k_8 \cdot Srx_{OX} \cdot HSP,\\
\frac{dHSP}{dt} &= k_{13} + k_9 \cdot SrxHSP - k_{14} \cdot HSP - k_8 \cdot Srx_{OX} \cdot HSP,\\
\frac{dSrxHSP}{dt} &= k_8 \cdot Srx_{OX} \cdot HSP - k_9 \cdot SrxHSP,\\
\frac{dSrx_M}{dt} &= k_9 \cdot SrxHSP - k_{10} \cdot Srx_M,\\
\frac{dSH}{dt} &= k_3 \cdot SS - k_1 \cdot SH \cdot H_2O_{2M},\\
\frac{dSOH}{dt} &= k_1 \cdot SH \cdot H_2O_{2M} + k_5 \cdot SO_2H \cdot Srx_M - k_2 \cdot SOH - k_4 \cdot H_2O_{2M} \cdot SOH,\\
\frac{dSO_2H}{dt} &= k_4 \cdot H_2O_{2M} \cdot SOH - k_5 \cdot SO_2H \cdot Srx_M,\\
SS &= 1 - SH - SOH - SO_2H.
\end{aligned}
\tag{B.1}
$$

Figure B.1: Detailed 10-ODE model for circadian redox oscillations. (**A**) Scheme of the biochemical species identified in the mitochondrial Prx3-SO_2H/Srx circadian oscillating system. (**B**) Equations of the model. (**C**) Limit cycle oscillations obtained by numerical integration of the equations shown in (B) for the following parameter values (a.u.): $k_0 = 1, k_1 = 10^7, k_2 = 1, k_3 = 1, k_4 = 10^4, k_5 = 2, k_6 = 0.2, k_7 = 2, k_8 = 0.5, k_9 = 0.2, k_{10} = 0.2, k_{11} = 0.2, k_{12} = 0.1, k_{13} = 0.2, k_{14} = 0.1$. The period of oscillation was 23.5 h; the phase shift between Prx3-SO_2H and mitochondrial Srx was 7.3 h.

B.2 Model Simplification

The minimal redox oscillator model used in this paper (Figure 3.4) is a condensed representation of the complex biochemistry of the Prx3/Srx oscillating system in

mitochondria from adrenal gland, heart and brown adipose tissue (Figure 3.2). Whereas the detailed model contains all 11 variables from Figure 3.2 (Appendix B.1), the minimal model is a relatively small network with only 5 variables. Because the detailed model contains 15 parameters, most of which are unknown, obtaining oscillations was challenging. For this reason, the 10-ODE detailed model was simplified to the 6-ODE model shown in Figure B.2. Apart from the 5 variables from the minimal model, S represents cytosolic Srx, A_1 represents the Prx3 in its reduced thiol form (Prx3-SH), and A_2 represents the sulfenic acid Prx3-SOH. Again, mass action kinetics was used to model production and degradation terms and we assumed constant mitochondrial H_2O_2 production p as well as constant Prx3 pool ($A_1 + A_2 + I$) over time. We found oscillations for the parameter set shown in the caption of Figure B.2.

To gain insights into the design principles of the Prx3/Srx oscillator and in line with previous theoretical studies [103], we systematically clamped all seven variables. To clamp a variable or a process means to set it to its mean (constant) value, trying to resemble conditions of constitutive expression from the wet lab. This strategy, instead of simply removing a variable, allows to compare the effect of rhythmic versus basal regulation. Thus, if a state variable is fixed at its mean level (i.e., clamped) and the network remains rhythmic, this means that the clamped variable is not required for the generation of oscillations. It might play a role in regulating the oscillation period, phase or amplitude, but it is not necessary to obtain self-sustained oscillations. By systematically clamping all 7 variables we found that neither A_1 nor S were necessary for the generation of self-sustained oscillations and thus the 6-ODE model from Figure B.2 was simplified to the model shown in Figure B.3A. This model version contains the 5 core variables from the minimal model described by 4 ODEs, 6 parameters and 2 bilinear reactions (equations are shown in Figure B.3B). It oscillated with a 24.5 h period and the phase difference between Prx3-SO_2H and mitochondrial Srx was 8.8 h (Figure B.3C), as expected.

Interestingly, and as shown in Figure B.2D, we observed that the production of A (defined by the bilinear term bIR, Figure B.3B) was very similar to its removal (defined by the second bilinear term aAD_1) during the whole simulated time. Therefore, and in order to further simplify the model, we assumed $aAD_1 = bIR$ over time (quasi-steady state assumption [337, 338]). This allowed the replacement of the A-ODE by the following algebraic equation:

$$A = \frac{bR}{bR + aD_1} \tag{B.2}$$

This is the equation in the minimal model described in the main text and shown in Figure 3.4C. The two bilinear terms, due to the quasi-steady state approximation, are thus coupled and transformed into the single nonlinear term in the minimal model (Figure

3.4C). The dynamics of the system did not change significantly (compare oscillations from Figures 3.6 and B.3C).

The fact that we could introduce the quasi-steady state approximation on A tells much about the system. In general, the quasi steady state assumption is used when one part of the system reacts much more quickly than another [337, 338]. The module that reacts faster is often said to have a shorter characteristic timescale or to equilibrate faster than the slower one. And in chemical terms, when something equilibrates fast, it can be said that it is in steady state with respect to the slower moving system. The time dependence of the faster reacting module can be simplified, thus reducing the number of variables that the system has to be solved for. In the context of the Prx3/Srx oscillating system, the quasi-steady state approximation performed on A meant that A and I reacted faster than the rest of the variables, and this can indeed be seen in their sharp changes of the relaxation-like oscillations and in the two switches that occur over time (Figure 3.7B).

A.

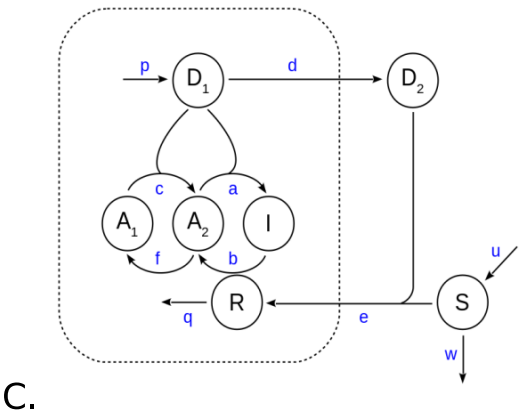

B.

$$
\begin{aligned}
\frac{dD_1}{dt} &= p - cA_1D_1 - aA_2D_1 - dD_1,\\
\frac{dD_2}{dt} &= dD_1 - eSD_2,\\
\frac{dS}{dt} &= u - eSD_2 - wS,\\
\frac{dR}{dt} &= eSD_2 - qR,\\
\frac{dA_2}{dt} &= cA_1D_1 + bIR - aA_2D_1 - fA_2,\\
\frac{dI}{dt} &= aA_2D_1 - bIR,\\
A_1 &= 1 - A_2 - I.
\end{aligned}
\tag{B.3}
$$

C.

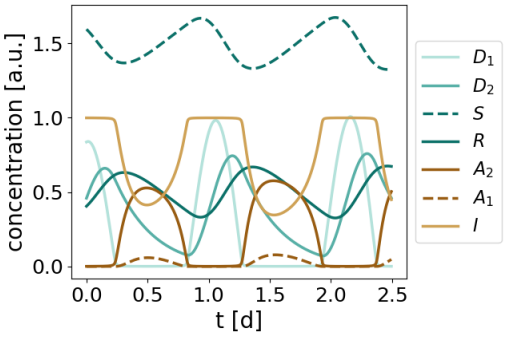

Figure B.2: 6-ODE model for circadian redox oscillations. (**A**) The 10-ODE detailed model was simplified to the 7-variable model shown in this figure. A_1 represents Prx3-SH; A_2, Prx3-SOH; I, Prx3-SO_2H; D_1, mitochondrial H_2O_2; D_2, cytosolic H_2O_2; S, cytosolic Srx and R, mitochondrial Srx. (**B**) Equations of the 7-variable model. We assumed constant $A_1 + A_2 + I$ over time and thus the number of ODEs was reduced to 6. The dynamics of A_1 were described by a mass conservation law. (**C**) Limit cycle oscillations obtained by numerical integration of the equations shown in (B) for the following parameter values (a.u.): $a = 1000, b = 2, c = 10000, d = u = 0.2, e = q = w = 0.1, f = p = 1$. The period of oscillation was 25.3 h; the phase shift between I and R was 8.3 h.

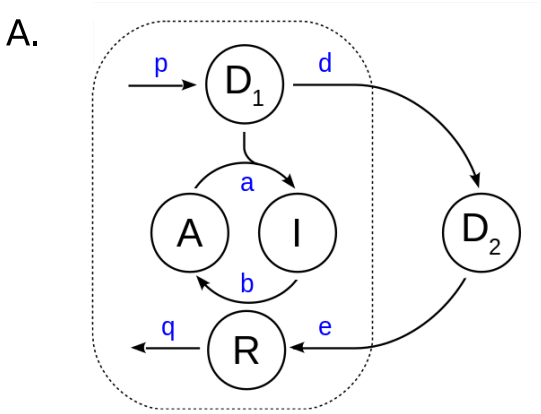

B.

$$\begin{aligned}
\frac{dD_1}{dt} &= p - aAD_1 - dD_1, \\
\frac{dD_2}{dt} &= dD_1 - eD_2, \\
\frac{dR}{dt} &= eD_2 - qR, \\
\frac{dA}{dt} &= bIR - aAD_1, \\
I &= 1 - A.
\end{aligned} \tag{B.4}$$

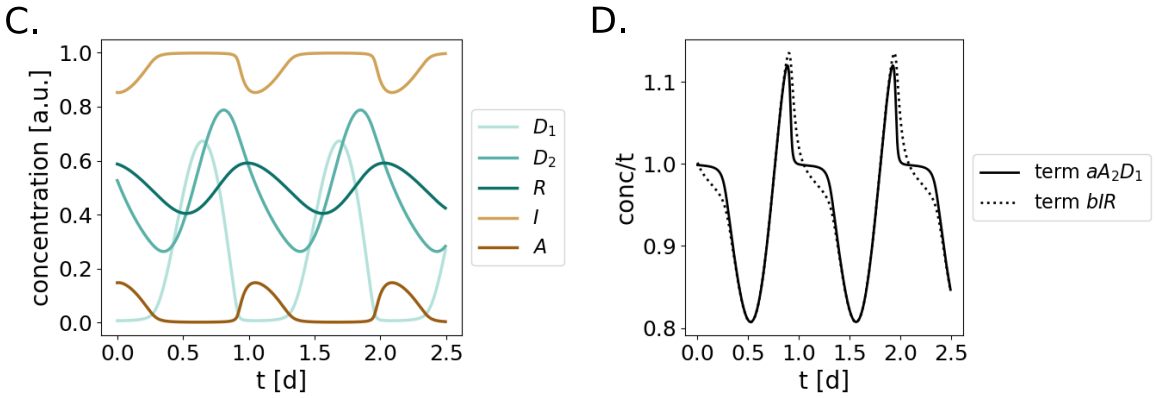

Figure B.3: Reduced 4-ODE model for circadian redox oscillations. (**A**) The 6-ODE model was simplified to the 5-variable model shown in this figure. A represents Prx3-SOH; I, Prx3-SO_2H; D_1, mitochondrial H_2O_2; D_2, cytosolic H_2O_2 and R, mitochondrial Srx. (**B**) Equations of the 5-variable model. We assumed constant $A + I$ over time and thus the number of ODEs was reduced to 4, with the dynamics of I being described by a mass conservation law. (**C**) Limit cycle oscillations obtained by numerical integration of the equations shown in (B) for the following parameter values (a.u.): $a = 1000, b = 2, c = 10000, d = 0.2, e = q = 0.1, p = 1$. The period of oscillation was 24.5 h; the phase shift between I and R was 8.8 h. (**D**) Similar evolution of the bilinear terms bIR and aAD_1 over time for the parameter values in (C), allowing the quasi-steady state state approximation that led to the simplified model shown in Figure 3.4C.

B.3 Bifurcation Analyses of the Core 3-ODE Redox Oscillator Model

We varied all model parameters and performed bifurcation analyses to obtain a plausible set of parameters that satisfied the physiological constraints (Table 3.1). Bifurcation diagrams for the Srx translocation rate (parameter e), mitochondrial Srx degradation rate (q), Prx3-SO_2H reduction rate by Srx (b) and mitochondrial H_2O_2 production (p) are shown in Figure B.4. A note on units: the first order translocation and degradation rates e and q have units of h^{-1}; the second order reduction rate b needs inverse units of time (h^{-1}) and inverse units of concentration (arbitrary) and D_1 production rate p has units of concentration (arbitrary) divided by time (h).

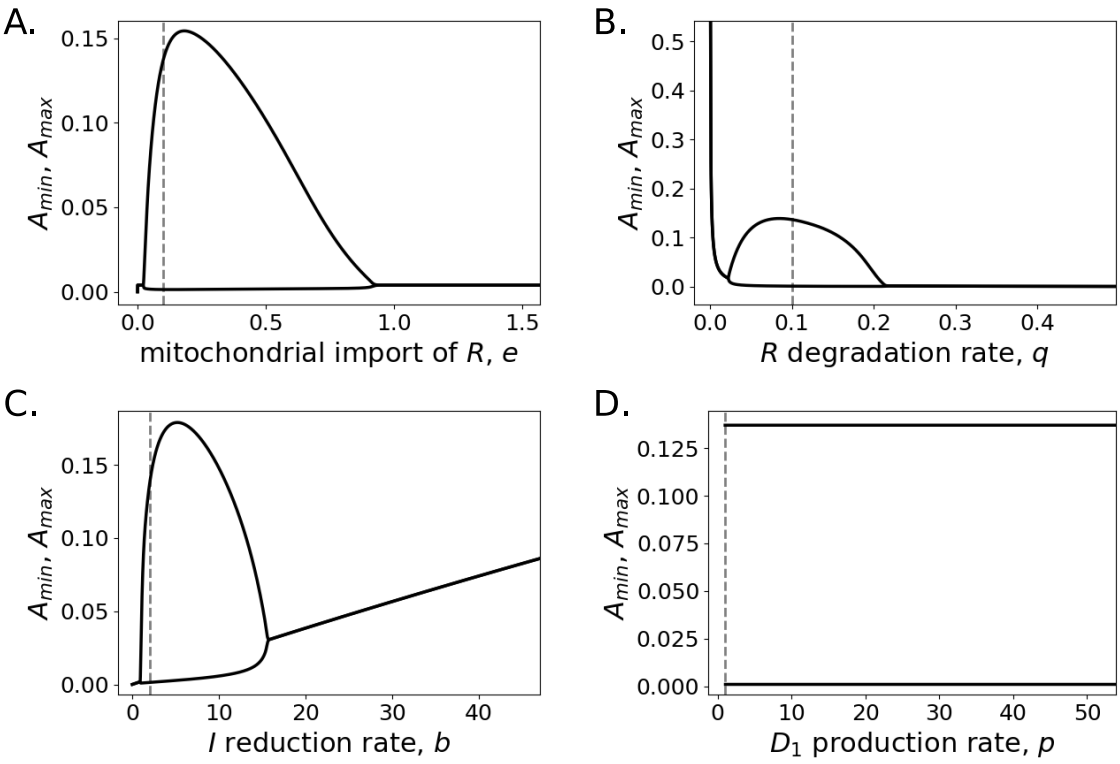

Figure B.4: Bifurcation diagrams as a function of the reduced core model parameters e (A), q (B), b (C) and p (D). At $e = 0.03, q = 0.025$ and $b = 1$ self-sustained oscillations emerged. The system oscillated for any positive value of p. A_{min} and A_{max} represent the minimum and maximum values of A in the oscillatory regime. The curves were obtained for the default parameter set shown in the caption of Figure 3.6, by numerical integration of the model equations given in Figure 3.4C. The dashed gray lines refer to the default parameter values.

B.4 Control Analysis of the Core 3-ODE Redox Oscillator Model

It is commonly admitted that circadian clocks produce robust oscillations in the sense that their period and amplitude are not affected by reasonable parameter changes

[327]. To quantify the impact of parameter changes in the redox oscillator model, we increased and decreased all model parameters by 10% and measured the effect of such change on the oscillation period (Figure B.5). As expected [333, 348], translocation and degradation rates d, e and q controlled the period most strongly, but interestingly also the reactivation kinetics represented by b had some effects on the period.

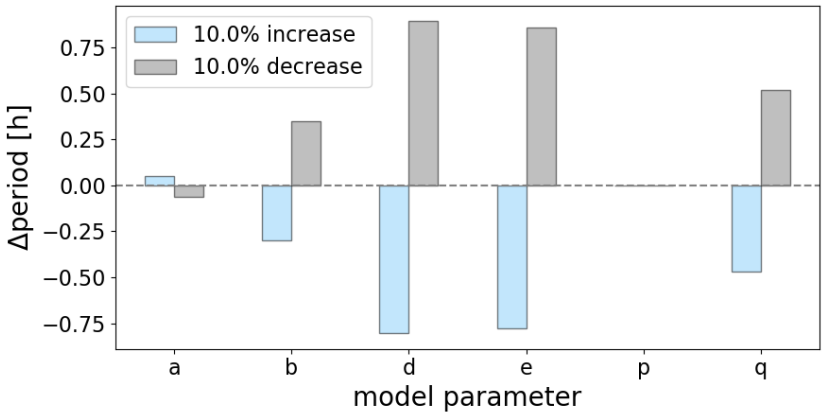

Figure B.5: Period sensitivity analysis as a function of a 10% increase (blue) or decrease (gray) of the default parameters from the core redox oscillator model. Δperiod represents the difference between the period calculated from the new parameter set compared to the default parameter set. Results are obtained for each parameter set by numerical integration of the model equations given in Figure 3.4C, with the parameters given in Figure 3.6.

B.5 Responses of an Ensemble of Noisy Oscillators to External Signals

In Section 3.4.5 we analyzed how pulse-like perturbations, periodic Zeitgeber signals or mean-field coupling synchronized an ensemble of stochastic D_2 amplitude-phase oscillators. The results shown in Section 3.4.5 come from simulations performed with fixed oscillator properties, namely fixed λ and fixed σ_x. Nonetheless, we found differential responses depending on the amplitude relaxation rate λ or the standard deviations of the additive x noise term σ_x.

Regarding pulse-like perturbations, we found that the average signal of an ensemble of 100 oscillators dampened faster (i.e., large damping rates) with decreasing amplitude relaxation rates of individual oscillators (for a fixed value of $\sigma_x \neq 0$) and with increasing σ_x (Figure B.6). This means that very rigid oscillators (high λ and low σ_x) are easier to transiently synchronize via Zeitgeber pulses than "sloppier" and noisier oscillators.

As for entrainment to Zeitgeber periodic stimuli, we found that a periodic forcing signal could synchronize an ensemble of 100 noisy self-sustained oscillators, as seen by the narrower phase distribution (Figure B.7A). It is known from the theory of coupled oscillators that if a periodic stimulus (the external Zeitgeber) is of the same or nearly the

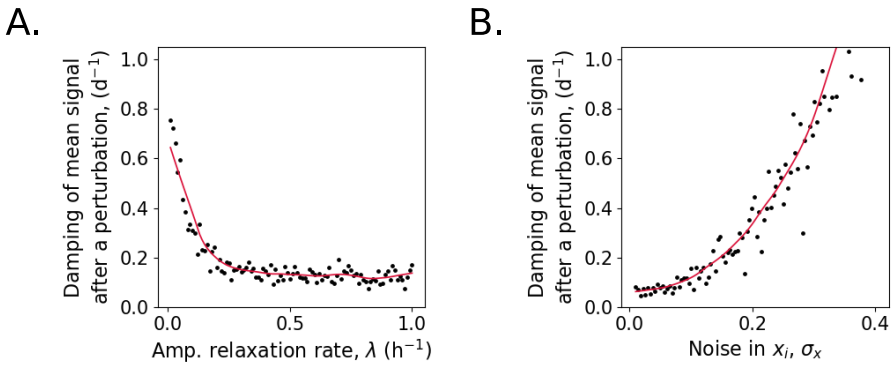

Figure B.6: Oscillator properties influence the response of an ensemble of 100 D_2 stochastic amplitude-phase oscillators to a pulse-like perturbation. (**A**) Effect of amplitude relaxation rate λ in the damping rate of the average signal after a pulse-like perturbation. The mean signal of "sloppy" (low λ) oscillators dampens faster in response to a perturbation than more rigid oscillators, for a given value of $\sigma_x \neq 0$. (**B**) Effect of σ_x in the damping rate of the average signal after a pulse-like perturbation. Again, the average signal from noisy oscillators (high σ_x) dampens out faster in response to a perturbation. Red lines show Lowess fits performed on the simulated data.

same period as the natural vibrating period of the oscillator, the amplitude of the system increases by a phenomenon termed resonance [367]. Nevertheless this phenomenon is dependent on oscillator properties. We observed that amplitude relaxation rate was inversely correlated with amplitude resonance (Figure B.7B). In other words, the mean amplitude of an ensemble of rigid oscillators (high λ) displayed almost no change upon Zeitgeber entrainment, compared to "sloppy" oscillators. These findings are consistent with previous computational studies that have focused on entrainment [273, 356, 363]. Interestingly, also noisier oscillators (higher σ_x) displayed less resonance effects than more deterministic oscillators (lower σ_x), as seen in Figure B.7C.

Since experimental data has shown clear western blot bands of Prx3-SO_2H and Srx, as well as robust H_2O_2 oscillations [36, 37, 307, 370], we hypothesized that D_2 oscillators might act in concert to coordinate import of Srx to mitochondria as a coupled ensemble. We thus introduced a mean-field coupling term in the stochastic differential equations as described in Section 3.4.5. We found that increasing coupling strength led to phase-pulling of the individual oscillators, supporting previous findings [281]. Uncoupled systems displayed a large phase dispersion, but phase coherence could be induced with increasing inter-oscillator coupling strength K_{coup} (Figure B.8A). In this case, the mean-field signal acted as periodic stimulus with the same frequency as the natural vibrating frequency of the oscillator. As described before, resonance in such systems is expected [367]. We again found that amplitude relaxation rate was inversely correlated with amplitude resonance (Figure B.8B). Thus, the mean amplitude of an ensemble of rigid oscillators (high λ) displayed almost no change upon coupling, compared to "sloppy" oscillators, in agreement with previous computational studies [281]. Interestingly, also noisier oscillators (higher σ_x) displayed less resonance effects than more deterministic oscillators (lower σ_x), as shown in Figure B.8C.

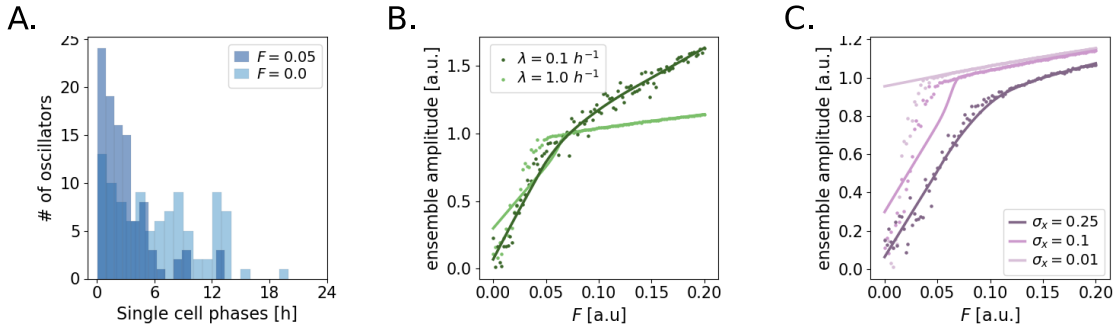

Figure B.7: Oscillator properties influence the response of an ensemble of 100 D_2 stochastic amplitude-phase oscillators to entrainment to an external periodic T = 24 h Zeitgeber signal (**A**) Distributions of single oscillator phases plotted as histograms as a function of the presence or absence of a periodic Zeitgeber signal with period T = 24 h and amplitude F = 0.05 a.u. Entrainment resulted in phase coherence of the ensemble, as seen by the narrower distribution of phase dispersion the entrained system (F = 0.05). (**B**) and (**C**) Entrainment to a T = 24 h periodic rhythm led to higher ensemble amplitudes due to resonance. The amplitude expansions, however, were inversely correlated with the oscillator amplitude relaxation rate (B) and to the noise in the system (C). Thus, more rigid (higher λ) and noisier oscillators (high σ_x) display less resonance effects. The colored lines in panels (B) and (C) indicate Lowess fits performed on the simulated data. Results were obtained by solving the stochastic differential equations from Equation 3.4 using the Euler-Maruyama method, for the following default parameters: A = 1, τ = 24.23 h, λ = 1 day^{-1}, ϵ = 0.1, σ_x = 0.1, σ_y = 0.1. Changes in these default parameter values (if any) are indicated in the panels.

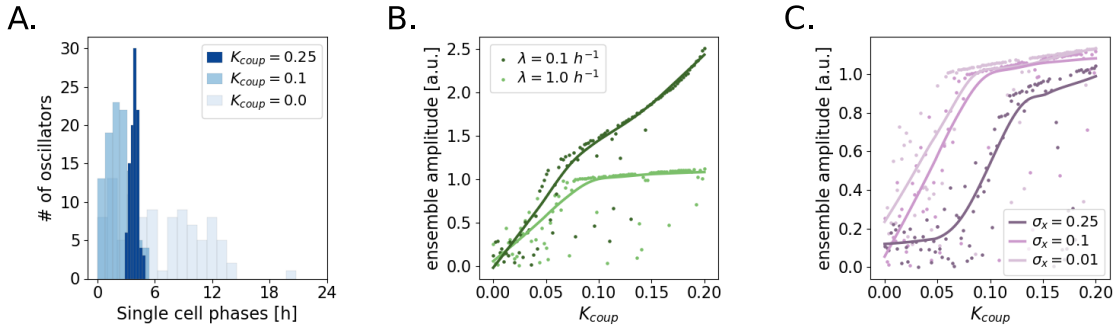

Figure B.8: Oscillator properties influence the response of an ensemble of 100 D_2 stochastic amplitude-phase oscillators to a mean-field coupling. (**A**) Distributions of single oscillator phases plotted as histograms for different coupling strengths. Coupling resulted in phase coherence of the ensemble, as seen by the narrower distribution of single oscillator phases for higher K_{coup}. (**B**) and (**C**) Coupling led to higher ensemble amplitudes due to resonance. The amplitude expansions, however, were inversely correlated with the oscillator amplitude relaxation rate (B) and to the noise in the system (C). Thus, more rigid (higher λ) and noisier oscillators (high σ_x) displayed less resonance effects. The colored lines in panels (B) and (C) indicate Lowess fits performed on the simulated data. The default parameter set used to obtain the results is shown in the caption of Figure B.7. Changes in default parameter values (if any) are indicated in the panels.

Reflection of Brandenburger Tor in the Tiergarten

:

Appendix C

C.1 Models of the Mammalian Circadian TTFL Clockwork

In order to analyze the crosstalk between our newly developed redox model and the mammalian canonical TTFL clockwork, we chose two ODE-based models of different complexity which both contained as explicit variable the Per2:Cry1 complex. The Relógio and Almeida models are two ODE-based models that were tailored for different purposes. The Relógio system is an extensive 19 variable model containing clock transcripts, cytoplasmatic and nuclear proteins, either alone or in complex with other clock proteins [102]. It was built from available data on phases and amplitudes of clock components to understand the mechanisms that govern circadian rhythm generation in mammalian cells [102]. It answered questions such as what are the roles of *Per2* degradation rates, or of the Ror-BMAL1-RevErb loop, and provided *in silico* evidence, for the first time, that the Ror-BMAL1-RevErb loop could act as an oscillator independent of the Per2:Cry1 loop [102]. The Almeida model, on the other hand, is a simpler model with only 8 variables. It was tailored to identify the essential interactions that are needed to generate phase opposition between the CLOCK:BMAL1 and Per2:Cry1 complexes [233].

The Per2:Cry1 complex appears as an explicit variable in both models (as well as other proteins such as RevErbα, Ror, BMAL1, Per2 or Cry1). Moreover, both models include regulation of clock gene expression at the level of E-boxes and RORE elements. The regulatory interactions of clock proteins on clock gene expression are modeled with Michaelis Menten-like and Hill-like kinetics, thus accounting for the degree of "nonlinearity" that models need to achieve self-sustained oscillations [111, 113]. Degradation kinetics of the clock components in both models was assumed to be of first order, and thus modeled with mass action kinetics.

C.1.1 Relógio model of the canonical TTFL

This model for the circadian clockwork was designed by Relógio *et al.* [102]. The ordinary differential equations for the clock elements are the following:

$$
\begin{aligned}
\frac{dx1}{dt} &= sf(kf_{x1}x7 - kd_{x1}x1 - d_{x1}x1),\\
\frac{dy3}{dt} &= sf(V_{3max}\frac{1+g(\frac{x1}{k_{t3}})^{v}}{1+(\frac{PC}{k_{i3}})^{w}(\frac{x1}{k_{t3}})^{v}+(\frac{x1}{k_{t3}})^{v}} - d_{y3}y3),\\
\frac{dy4}{dt} &= sf(V_{4max}\frac{1+h(\frac{x1}{k_{t4}})^{p}}{1+(\frac{PC}{k_{i4}})^{q}(\frac{x1}{k_{t4}})^{p}+(\frac{x1}{k_{t4}})^{p}} - d_{y4}y4),\\
\frac{dz6}{dt} &= sf(k_{p3}(y3+\mathrm{Rev}_0) - ki_{z6}z6 - d_{z6}z6),\\
\frac{dz7}{dt} &= sf(k_{p4}(y4+\mathrm{Ror}_0) - ki_{z7}z7 - d_{z7}z7),\\
\frac{dx5}{dt} &= sf(ki_{z6}(z6 - d_{x5}x5)),\\
\frac{dx6}{dt} &= sf(ki_{z7}(z7 - d_{x6}x6)),\\
\frac{dy5}{dt} &= sf(V_{5max}\frac{1+i(\frac{x6}{k_{t5}})^{n}}{1+(\frac{x5}{k_{i5}})^{m}+(\frac{x6}{k_{t5}})^{n}} - d_{y5}y5),\\
\frac{dz8}{dt} &= sf(k_{p5}(y5+\mathrm{Bmal}_0) - ki_{z8}z8 - d_{z8}z8),\\
\frac{dx7}{dt} &= sf(ki_{z8}z8 + kd_{x1}x1 - kf_{x1}x7 - d_{x7}x7),\\
\frac{dy1}{dt} &= sf(V_{1max}\frac{1+a(\frac{x1}{k_{t1}})^{b}}{1+(\frac{PC}{k_{i1}})^{c}(\frac{x1}{k_{t1}})^{b}+(\frac{x1}{k_{t1}})^{b}} - d_{y1}y1),\\
\frac{dy2}{dt} &= sf(V_{2max}\frac{(1+d(\frac{x1}{k_{t2}})^{e})}{1+(\frac{PC}{k_{i2}})^{f}(\frac{x1}{k_{t2}})^{e}+(\frac{x1}{k_{t2}})^{e}}\frac{1}{1+(\frac{x5}{k_{i21}})^{f1}} - d_{y2}y2),\\
\frac{dz1}{dt} &= sf(k_{p2}(y2+\mathrm{Cry}_0) + kd_{z4}z4 + kd_{z5}z5 - kf_{z5}z1z2 - kf_{z4}z1z3 - d_{z1}z1),\\
\frac{dz2}{dt} &= sf(k_{p1}(y1+\mathrm{Per}_0) + kd_{z5}z5 + kdf_{z3}z3 - kf_{z5}z1z2 - kf_{z2}z2 - d_{z2}z2),\\
\frac{dz3}{dt} &= sf(kf_{z2}z2 + kd_{z4}z4 - kdf_{z3}z3 - kf_{z4}z1z3 - d_{z3}z3),\\
\frac{dz4}{dt} &= sf(kf_{z4}z1z3 + ke_{x2}x2 - ki_{z4}z4 - kd_{z4}z4 - d_{z4}z4),\\
\frac{dz5}{dt} &= sf(kf_{z5}z1z2 + ke_{x3}x3 - ki_{z5}z5 - kd_{z5}z5 - d_{z5}z5),\\
\frac{dx2}{dt} &= sf(ki_{z4}z4 - ke_{x2}x2 - d_{x2}x2),\\
\frac{dx3}{dt} &= sf(ki_{z5}z5 - ke_{x3}x3 - d_{x3}x3),\\
PC &= x2 + x3
\end{aligned}
\tag{C.1}
$$

where $x1, x2, x3, x5, x6, x7$ represent the nuclear proteins or complexes CLOCK:BMAL1, Per2$^{\mathrm{P}}$:Cry1 (phosphorylated Per2 in complex with Cry1), Per2:Cry1, RevErbα, Ror

and BMAL1, respectively; $y1, y2, y3, y4, y5$ represent the clock transcripts *Per2, Cry1, RevErbα, Ror* and *Bmal1*, respectively; $z1, z2, z3, z4, z5, z6, z7, z8$ indicate the cytosolic clock proteins Cry1, Per2, $Per2^P$, $Per2^P$:Cry1, Per2:Cry1, RevErbα, Ror and BMAL1, respectively, and PC represents the inhibitory nuclear Per2:Cry1 pool. The published parameter set that produces 23.65 h limit cycle oscillations is shown in Table C.1, with time units given in hours and concentration units given as arbitrary units (arbitrary units cannot be compared across different publications according to IUPAC rules [454]).

Table C.1: List of parameters of the Relógio model. Time units are given in hours and concentration units as arbitrary units. Table from [102].

Parameter	Biological Interpretation	Value
d_{x1}	nuclear CLOCK:BMAL1 degradation rate [h^{-1}]	0.08
d_{x2}	nuclear $Per2^P$:Cry1 degradation rate [h^{-1}]	0.06
d_{x3}	nuclear Per2:Cry1 degradation rate [h^{-1}]	0.09
d_{x5}	nuclear RevErbα degradation rate [h^{-1}]	0.17
d_{x6}	nuclear Ror degradation rate [h^{-1}]	0.12
d_{x7}	nuclear BMAL1 degradation rate [h^{-1}]	0.15
d_{x2}	nuclear $Per2^P$:Cry1 degradation rate [h^{-1}]	0.06
d_{y1}	*Per2* mRNA degradation rate [h^{-1}]	0.3
d_{y2}	*Cry1* mRNA degradation rate [h^{-1}]	0.2
d_{y3}	*RevErbα* mRNA degradation rate [h^{-1}]	2
d_{y4}	*Ror* mRNA degradation rate [h^{-1}]	0.2
d_{y5}	*Bmal1* mRNA degradation rate [h^{-1}]	1.6
d_{z1}	cytoplasmatic Cry1 degradation rate [h^{-1}]	0.23
d_{z2}	cytoplasmatic Per2 degradation rate [h^{-1}]	0.25
d_{z3}	cytoplasmatic $Per2^P$ degradation rate [h^{-1}]	0.6
d_{z4}	cytoplasmatic $Per2^P$:Cry1 degradation rate [h^{-1}]	0.2
d_{z5}	cytoplasmatic Per2:Cry1 degradation rate [h^{-1}]	0.2
d_{z6}	cytoplasmatic RevErbα degradation rate [h^{-1}]	0.31
d_{z7}	cytoplasmatic Ror degradation rate [h^{-1}]	0.3
d_{z8}	cytoplasmatic BMAL1 degradation rate [h^{-1}]	0.73
kf_{x1}	CLOCK:BMAL1 complex formation [a.u. h^{-1}]	2.3
kd_{x1}	CLOCK:BMAL1 complex dissociation [h^{-1}]	0.01
kf_{z4}	cytoplasmatic $Per2^P$:Cry1 complex formation [a.u. h^{-1}]	1
kd_{z4}	cytoplasmatic $Per2^P$:Cry1 complex dissociation [h^{-1}]	1
kf_{z5}	cytoplasmatic Per2:Cry1 complex formation [a.u. h^{-1}]	1
kd_{z5}	cytoplasmatic Per2:Cry1 complex dissociation [h^{-1}]	1
kph_{z2}	cytoplasmatic Per2 phosphorylation rate [h^{-1}]	2
kd_{phz3}	cytoplasmatic $Per2^P$ dephosphorylation rate [h^{-1}]	0.05
V_{1max}	*Per2* transcription rate [a.u. h^{-1}]	1
V_{2max}	*Cry1* transcription rate [a.u. h^{-1}]	2.92
V_{3max}	*RevErbα* transcription rate [a.u. h^{-1}]	1.9
V_{4max}	*Ror* transcription rate [a.u. h^{-1}]	10.9
V_{5max}	*Bmal1* transcription rate [a.u. h^{-1}]	1
k_{t1}	*Per2* activation rate [a.u.]	3
k_{i1}	*Per2* inhibition rate [a.u.]	0.9
k_{t2}	*Cry1* activation rate [a.u.]	2.4
k_{i2}	*Cry1* inhibition rate [a.u.]	0.7
k_{i21}	*Cry1* inhibition rate [a.u.]	5.2

Parameter	Biological Interpretation	Value
k_{t3}	*RevErbα* activation rate [a.u.]	2.07
k_{i3}	*RevErbα* inhibition rate [a.u.]	3.3
k_{t4}	*Ror* activation rate [a.u.]	0.9
k_{i4}	*Ror* inhibition rate [a.u.]	0.4
k_{t5}	*Bmal1* activation rate [a.u.]	8.35
k_{i5}	*Bmal1* inhibition rate [a.u.]	1.94
a	*Per2* transcription fold activation [dimensionless]	12
d	*Cry1* transcription fold activation [dimensionless]	12
g	*RevErbα* transcription fold activation [dimensionless]	5
h	*Ror* transcription fold activation [dimensionless]	5
i	*Bmal1* transcription fold activation [dimensionless]	12
k_{p1}	cytoplasmatic Per2 translation rate [h^{-1}]	0.4
k_{p2}	cytoplasmatic Cry1 translation rate [h^{-1}]	0.26
k_{p3}	cytoplasmatic RevErbα translation rate [h^{-1}]	0.37
k_{p4}	cytoplasmatic Ror translation rate [h^{-1}]	0.76
k_{p5}	cytoplasmatic BMAL1 rate [h^{-1}]	1.21
ki_{z4}	cytoplasmatic $Per2^{P}$:Cry1 import rate [h^{-1}]	0.2
ki_{z5}	cytoplasmatic Per2:Cry1 import rate [h^{-1}]	0.1
ki_{z6}	cytoplasmatic RevErbα import rate [h^{-1}]	0.5
ki_{z7}	cytoplasmatic Ror import rate [h^{-1}]	0.1
ki_{z8}	cytoplasmatic BMAL1 import rate [h^{-1}]	0.1
ke_{x2}	nuclear $Per2^{P}$:Cry1 export rate [h^{-1}]	0.02
ke_{x3}	nuclear Per2:Cry1 export rate [h^{-1}]	0.02
b	*Per2* activation [dimensionless]	5
c	*Per2* inhibition [dimensionless]	7
e	*Cry1* activation rate [dimensionless]	6
f	*Cry1* activation [dimensionless]	4
$f1$	*Cry1* inhibition [dimensionless]	1
v	*RevErbα* activation [dimensionless]	6
w	*RevErbα* inhibition [dimensionless]	2
p	*Ror* activation [dimensionless]	6
q	*Ror* inhibition [dimensionless]	3
n	*Bmal1* activation [dimensionless]	2
m	*Bmal1* inhibition [dimensionless]	5
$y1_0$	exogenous *Per2* mRNA [a.u.]	0
$y2_0$	exogenous *Cry1* mRNA [a.u.]	0
$y3_0$	exogenous *RevErbα* mRNA [a.u.]	0
$y4_0$	exogenous *Ror* mRNA [a.u.]	0
$y5_0$	exogenous *Bmal1* mRNA [a.u.]	0

C.1.2 Redox regulation of the Relógio model of the canonical TTFL

We hypothesized that redox modulation of the TTFL occurs at the level of PER2:CRY1 complex formation, in agreement with published experimental studies that have demonstrated that the interaction of these two clock proteins is modulated by redox and disulfide bond formation [374, 394]. For this reason, we included the sinusoidal term from Equation 4.3 (i.e., $\text{Redox}(t) = 1 + \frac{F}{2}\cos(\frac{2\pi}{T}t + \phi)$) with the characteristics of cytosolic H_2O_2 D_2 oscillations (peak-to-trough distance $F = 0.5$ a.u., peak-to-peak

distance $T = 24.23\,\mathrm{h}$ and $\phi = 0$) in all reactions of complex formation of Per2:Cry1 and $\mathrm{Per2^P}$:Cry1, namely in all reactions governed by the kf_{z4} and kf_{z5} parameters, as a multiplicative term. The resulting model is shown in Equations C.2.

$$
\begin{aligned}
\frac{dx1}{dt} &= sf(kf_{x1}x7 - kd_{x1}x1 - d_{x1}x1),\\
\frac{dy3}{dt} &= sf(V_{3max}\frac{1 + g(\frac{x1}{k_{t3}})^{v}}{1 + (\frac{PC}{k_{i3}})^{w}(\frac{x1}{k_{t3}})^{v} + (\frac{x1}{k_{t3}})^{v}} - d_{y3}y3),\\
\frac{dy4}{dt} &= sf(V_{4max}\frac{1 + h(\frac{x1}{k_{t4}})^{p}}{1 + (\frac{PC}{k_{i4}})^{q}(\frac{x1}{k_{t4}})^{p} + (\frac{x1}{k_{t4}})^{p}} - d_{y4}y4),\\
\frac{dz6}{dt} &= sf(k_{p3}(y3 + \mathrm{Rev}_0) - ki_{z6}z6 - d_{z6}z6),\\
\frac{dz7}{dt} &= sf(k_{p4}(y4 + \mathrm{Ror}_0) - ki_{z7}z7 - d_{z7}z7),\\
\frac{dx5}{dt} &= sf(ki_{z6}(z6 - d_{x5}x5)),\\
\frac{dx6}{dt} &= sf(ki_{z7}(z7 - d_{x6}x6)),\\
\frac{dy5}{dt} &= sf(V_{5max}\frac{1 + i(\frac{x6}{k_{t5}})^{n}}{1 + (\frac{x5}{k_{i5}})^{m} + (\frac{x6}{k_{t5}})^{n}} - d_{y5}y5),\\
\frac{dz8}{dt} &= sf(k_{p5}(y5 + \mathrm{Bmal}_0) - ki_{z8}z8 - d_{z8}z8),\\
\frac{dx7}{dt} &= sf(ki_{z8}z8 + kd_{x1}x1 - kf_{x1}x7 - d_{x7}x7),\\
\frac{dy1}{dt} &= sf(V_{1max}\frac{1 + a(\frac{x1}{k_{t1}})^{b}}{1 + (\frac{PC}{k_{i1}})^{c}(\frac{x1}{k_{t1}})^{b} + (\frac{x1}{k_{t1}})^{b}} - d_{y1}y1),\\
\frac{dy2}{dt} &= sf(V_{2max}\frac{(1 + d(\frac{x1}{k_{t2}})^{e})}{1 + (\frac{PC}{k_{i2}})^{f}(\frac{x1}{k_{t2}})^{e} + (\frac{x1}{k_{t2}})^{e}}\frac{1}{1 + (\frac{x5}{k_{i21}})^{f1}} - d_{y2}y2),\\
\frac{dz1}{dt} &= sf(k_{p2}(y2 + \mathrm{Cry}_0) + kd_{z4}z4 + kd_{z5}z5 - \mathrm{Redox}(t)kf_{z5}z1z2 - \mathrm{Redox}(t)kf_{z4}z1z3 - d_{z1}z1),\\
\frac{dz2}{dt} &= sf(k_{p1}(y1 + \mathrm{Per}_0) + kd_{z5}z5 + kdf_{z3}z3 - \mathrm{Redox}(t)kf_{z5}z1z2 - kf_{z2}z2 - d_{z2}z2),\\
\frac{dz3}{dt} &= sf(kf_{z2}z2 + kd_{z4}z4 - kdf_{z3}z3 - \mathrm{Redox}(t)kf_{z4}z1z3 - d_{z3}z3),\\
\frac{dz4}{dt} &= sf(\mathrm{Redox}(t)kf_{z4}z1z3 + ke_{x2}x2 - ki_{z4}z4 - kd_{z4}z4 - d_{z4}z4),\\
\frac{dz5}{dt} &= sf(\mathrm{Redox}(t)kf_{z5}z1z2 + ke_{x3}x3 - ki_{z5}z5 - kd_{z5}z5 - d_{z5}z5),\\
\frac{dx2}{dt} &= sf(ki_{z4}z4 - ke_{x2}x2 - d_{x2}x2),\\
\frac{dx3}{dt} &= sf(ki_{z5}z5 - ke_{x3}x3 - d_{x3}x3),\\
PC &= x2 + x3
\end{aligned}
\tag{C.2}
$$

C.1.3 Almeida model of the canonical TTFL

In order to investigate whether our findings in the Relógio model could be applied to other models of the mammalian transcriptional-translational clockwork, we chose a second ODE protein-based model that also contained Per2:Cry1 as explicit variable. This model was published by Almeida *et al.* in 2020 [233]. The equations read the following:

$$
\begin{aligned}
E_{box} &= V_E \frac{BMAL}{BMAL + k_E + (k_{Er} \cdot BMAL \cdot CRY)}, \\
RORE &= V_R \frac{ROR}{k_R + ROR} \frac{k_{Rr}^2}{k_{Rr}^2 + REV^2}, \\
D_{box} &= V_D \frac{DBP}{DBP + k_D} \frac{k_{Dr}}{k_{Dr} + E4BP4}, \\
\frac{dBMAL}{dt} &= RORE - \gamma_{bp} \cdot BMAL \cdot PERCRY, \\
\frac{dROR}{dt} &= E_{box} + RORE - \gamma_{Ror} \cdot ROR, \\
\frac{dREV}{dt} &= 2 \cdot E_{box} + D_{box} - \gamma_{Rev} \cdot REV, \\
\frac{dDBP}{dt} &= E_{box} - \gamma_{Db} \cdot DBP, \\
\frac{dE4BP4}{dt} &= 2 \cdot R_{box} - \gamma_{E4} \cdot E4BP4, \\
\frac{dCRY}{dt} &= E_{box} + 2 \cdot R_{box} - \gamma_{PC} \cdot PER \cdot CRY + \gamma_{CP} \cdot PERCRY - \gamma_C \cdot CRY, \\
\frac{dPER}{dt} &= E_{box} + D_{box} - \gamma_{PC} \cdot PER \cdot CRY + \gamma_{CP} \cdot PERCRY - \gamma_P \cdot PER, \\
\frac{dPERCRY}{dt} &= \gamma_{PC} \cdot PER \cdot CRY - \gamma_{CP} \cdot PERCRY - \gamma_{BP} \cdot BMAL \cdot PERCRY
\end{aligned}
\tag{C.3}
$$

The first three equations describe the regulation of the different clock-controlled elements (E-boxes, RORE and D-boxes) with their corresponding activators and repressors. The remaining equations describe the rates of change in clock protein concentration. The published parameter set that produces 20 h limit cycle oscillations is shown in Table C.2.

Table C.2: List of parameters of the Almeida model. Time units are given in hours and concentration units as arbitrary units. Table from [233].

Parameter	Value	Parameter	Value
V_R	44.4 h^{-1}	γ_{Ror}	2.55 h^{-1}
k_R	3.54	γ_{Rev}	0.241 h^{-1}
k_{Rr}	80.1	γ_P	0.844 h^{-1}
V_E	30.3 h^{-1}	γ_C	2.34 h^{-1}
k_E	214	γ_{Db}	0.156 h^{-1}
k_{Er}	1.24	γ_{E4}	0.295 h^{-1}
V_D	202 h^{-1}	γ_{PC}	0.191 h^{-1}
k_D	5.32	γ_{CP}	0.141 h^{-1}
k_{Dr}	94.7	γ_{BP}	2.58 h^{-1}

C.1.4 Redox regulation of the Almeida model of the canonical TTFL

In the same lines as before, we included the redox sinusoidal term (Equation 4.3, $\text{Redox}(t) = 1 + \frac{F}{2}\cos(\frac{2\pi}{T}t + \phi)$, with peak-to-trough distance $F = 0.5$ a.u., peak-to-peak distance $T = 24.23$ h and $\phi = 0$) as modulatory multiplicative signal of the Per2:Cry1 interaction. The resulting ODEs read:

$$
\begin{aligned}
E_{box} &= V_E \frac{BMAL}{BMAL + k_E + (k_{Er} \cdot BMAL \cdot CRY)}, \\
RORE &= V_R \frac{ROR}{k_R + ROR} \frac{k_{Rr}^2}{k_{Rr}^2 + REV^2}, \\
D_{box} &= V_D \frac{DBP}{DBP + k_D} \frac{k_{Dr}}{k_{Dr} + E4BP4}, \\
\frac{dBMAL}{dt} &= RORE - \gamma_{bp} \cdot BMAL \cdot PERCRY, \\
\frac{dROR}{dt} &= E_{box} + RORE - \gamma_{Ror} \cdot ROR, \\
\frac{dREV}{dt} &= 2 \cdot E_{box} + D_{box} - \gamma_{Rev} \cdot REV, \\
\frac{dDBP}{dt} &= E_{box} - \gamma_{Db} \cdot DBP, \\
\frac{dE4BP4}{dt} &= 2 \cdot R_{box} - \gamma_{E4} \cdot E4BP4, \\
\frac{dCRY}{dt} &= E_{box} + 2 \cdot R_{box} - \text{Redox}(t) \cdot \gamma_{PC} \cdot PER \cdot CRY + \gamma_{CP} \cdot PERCRY - \gamma_C \cdot CRY, \\
\frac{dPER}{dt} &= E_{box} + D_{box} - \text{Redox}(t) \cdot \gamma_{PC} \cdot PER \cdot CRY + \gamma_{CP} \cdot PERCRY - \gamma_P \cdot PER, \\
\frac{dPERCRY}{dt} &= \text{Redox}(t) \cdot \gamma_{PC} \cdot PER \cdot CRY - \gamma_{CP} \cdot PERCRY - \gamma_{BP} \cdot BMAL \cdot PERCRY
\end{aligned}
\tag{C.4}
$$

C.2 Complex nonlinear phenomena in the Almeida model

We simulated the Almeida model (using the original parameter values, Table C.2) with a sinusoidal redox modulation of the Per2:Cry1 interaction (Figure C.1). Whereas periodic redox modulation of the Per2:Cry1 complex formation in the Relógio model resulted in a 1:1 entrainment (Figure 4.3), driving the Almeida model with the same Zeitgeber input, to our surprise, produced chaotic oscillations (Figure C.1). A number of modeling studies have shown that chaotic dynamics can occur in oscillators that are driven by external periodical signals [45, 129, 310, 415, 420, 421]. Nonetheless, we analyzed whether the model displayed complex nonlinear phenomena (such as tori, chaos, etc.) in the absence of external forcing. Thus, in order to investigate whether chaotic oscillations and other complex dynamics could also occur without periodically forcing the Almeida model, we performed detailed bifurcation analyses in the unforced system. We found that different models of the mammalian circadian clock, even in the absence of external forcing, could produce chaotic and toroidal dynamics, and we published the results in [286]. In Figure C.2 we show how period doubling and chaos arose in the Almeida model upon changes in the degradation rate of Cry1 γ_C. For the

sake of the scope and length of this thesis, the detailed results are not described here. The analysis of the conditions that result in entrainment in the Almeida model driven by a periodical redox input, as well as the differences in oscillator properties between the Almeida and Relógio models, remain to be fully understood.

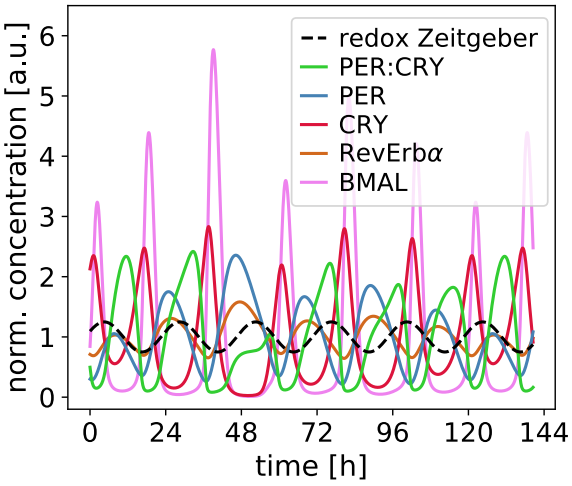

Figure C.1: Time series of the Almeida model of the transcriptional-translational mammalian clockwork regulated by a periodic redox input at the level of the Per2:Cry1 interaction. Results were obtained by numerical integration of Equations C.4 with the original model parameters (Table C.2). The redox input parameters are the following: peak-to-trough distance $F = 0.5$ a.u., $T = 24.23$ h, $\phi = 0$, determined from the D_2 oscillations (Figure 3.6). Time series were normalized to their means.

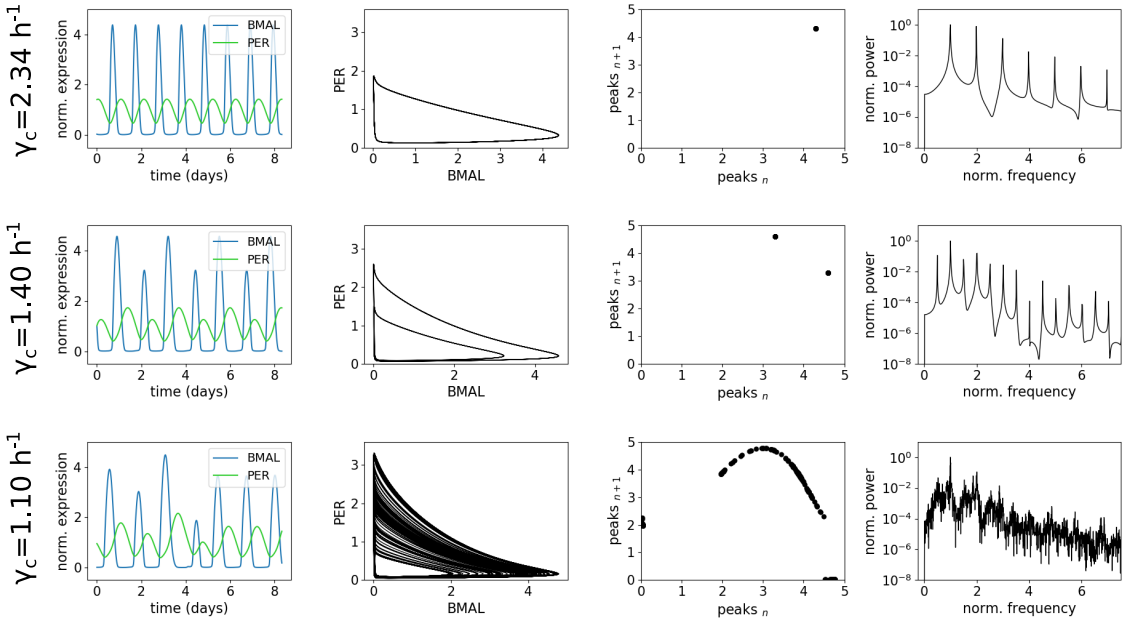

Figure C.2: Chaotic dynamics emerged in the unforced Almeida model upon changes in Cry1 degradation rate. Variations in γ_C revealed complex nonlinear phenomena in the unforced Almeida model (Equations C.3). Limit cycle (top, $\gamma_C = 2.34\,\mathrm{h}^{-1}$), period doubling (middle, $\gamma_C = 1.40\,\mathrm{h}^{-1}$), and chaos (bottom, $\gamma_C = 1.10\,\mathrm{h}^{-1}$) shown as time series, phase portraits, return maps and power spectra (from left to right respectively). Parabola-shaped return maps are a feature of chaotic dynamics. The period in the power spectra was normalized to the period with maximum power. Results were obtained by numerical integration of Equations C.3 with the parameter set from Table C.2, but with $\gamma_{Rev} = 0.4\,\mathrm{h}^{-1}$ instead of 0.241 (we changed the parameter value to tune the 20 h period from the original Almeida model to a 24 h period). Note that chaotic oscillations were not normalized to obtain a 24h peak-to-peak distance. Time series were normalized to their means. Figure from [286].

C.3 Periodic forcing of the kinetic minimal redox oscillator model

We then analyzed the TTFL-redox crosstalk in the other direction. Using the kinetic redox oscillator model (Equations 3.3), we replaced the mitochondrial H_2O_2 production parameter p from the redox model (Equations 3.3), assumed to be constant until now, by the sinusoidal term from Equation 4.3 ($\mathrm{TTFL}(t) = 1 + \frac{F}{2}\cos(\frac{2\pi}{T}t + \phi)$), as follows:

$$\begin{aligned}
\frac{dD_1}{dt} &= \mathrm{TTFL}(t) - ab\frac{D_1 R}{bR + aD_1} - dD_1, \\
\frac{dD_2}{dt} &= dD_1 - eD_2, \\
\frac{dR}{dt} &= eD_2 - qR, \\
A &= \frac{bR}{bR + aD_1}, \\
I &= 1 - A = \frac{aD_1}{bR + aD_1}
\end{aligned} \tag{C.5}$$

This way, we simulated periodical production of mitochondrial H_2O_2 D_1. Figure C.3 shows the time series of the forced system. Similar to the driven redox amplitude-phase model, we observed entrainment and a comparable amplitude expansion of D_2 oscillations to that from the driven amplitude-phase oscillator, as we expected (Figure 4.5).

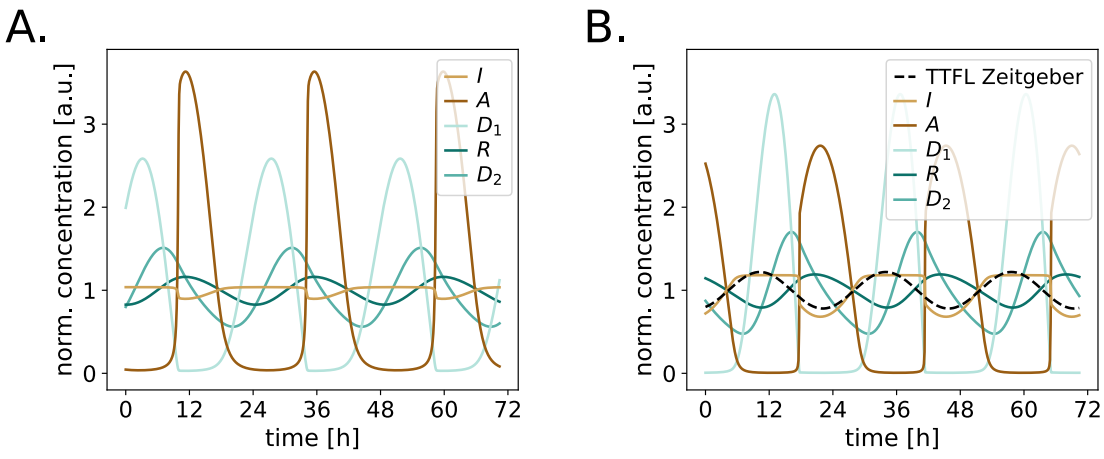

Figure C.3: Time series of the minimal kinetic redox oscillator model in the absence (A) or presence (B) of TTFL-regulated control of D_1 production. Results were obtained by numerical integration of Equations 3.3 (A) and C.5 (B) with the parameter set from Table 3.1. The TTFL input parameters used in (B) are: peak-to-trough distance $F = 0.45$ a.u., $T = 23.65$ h, $\phi = 0$, determined from the nuclear CLOCK:BMAL1 oscillations from the Relógio model. Time series were normalized to their means.

C.4 Mutual coupling of redox and TTFL systems

After having simulated unidirectional coupling, either from a periodic TTFL input to the redox oscillator or vice versa, we mutually coupled the Relógio and the kinetic core redox oscillator model in a system of 22 coupled ordinary differential equations. We assumed CLOCK:BMAL1 control of mitochondrial H_2O_2 D_1 production and D_2 modulation of the Per2:Cry1 interaction. The equations from the resulting coupled model read:

$$
\begin{aligned}
\frac{dx1}{dt} &= sf(kf_{x1}x7 - kd_{x1}x1 - d_{x1}x1),\\
\frac{dy3}{dt} &= sf(V_{3max}\frac{1+g(\frac{x1}{k_{t3}})^{v}}{1+(\frac{PC}{k_{i3}})^{w}(\frac{x1}{k_{t3}})^{v}+(\frac{x1}{k_{t3}})^{v}} - d_{y3}y3),\\
\frac{dy4}{dt} &= sf(V_{4max}\frac{1+h(\frac{x1}{k_{t4}})^{p}}{1+(\frac{PC}{k_{i4}})^{q}(\frac{x1}{k_{t4}})^{p}+(\frac{x1}{k_{t4}})^{p}} - d_{y4}y4),\\
\frac{dz6}{dt} &= sf(k_{p3}(y3+\mathrm{Rev}_0) - ki_{z6}z6 - d_{z6}z6),\\
\frac{dz7}{dt} &= sf(k_{p4}(y4+\mathrm{Ror}_0) - ki_{z7}z7 - d_{z7}z7),\\
\frac{dx5}{dt} &= sf(ki_{z6}(z6 - d_{x5}x5)),\\
\frac{dx6}{dt} &= sf(ki_{z7}(z7 - d_{x6}x6)),\\
\frac{dy5}{dt} &= sf(V_{5max}\frac{1+i(\frac{x6}{k_{t5}})^{n}}{1+(\frac{x5}{k_{i5}})^{m}+(\frac{x6}{k_{t5}})^{n}} - d_{y5}y5),\\
\frac{dz8}{dt} &= sf(k_{p5}(y5+\mathrm{Bmal}_0) - ki_{z8}z8 - d_{z8}z8),\\
\frac{dx7}{dt} &= sf(ki_{z8}z8 + kd_{x1}x1 - kf_{x1}x7 - d_{x7}x7),\\
\frac{dy1}{dt} &= sf(V_{1max}\frac{1+a(\frac{x1}{k_{t1}})^{b}}{1+(\frac{PC}{k_{i1}})^{c}(\frac{x1}{k_{t1}})^{b}+(\frac{x1}{k_{t1}})^{b}} - d_{y1}y1),\\
\frac{dy2}{dt} &= sf(V_{2max}\frac{(1+d(\frac{x1}{k_{t2}})^{e})}{1+(\frac{PC}{k_{i2}})^{f}(\frac{x1}{k_{t2}})^{e}+(\frac{x1}{k_{t2}})^{e}}\frac{1}{1+(\frac{x5}{k_{i21}})^{f1}} - d_{y2}y2),\\
\frac{dz1}{dt} &= sf(k_{p2}(y2+\mathrm{Cry}_0) + kd_{z4}z4 + kd_{z5}z5 - kf_{z5}z1z2K_2D_2 - kf_{z4}z1z3K_2D_2 - d_{z1}z1),\\
\frac{dz2}{dt} &= sf(k_{p1}(y1+\mathrm{Per}_0) + kd_{z5}z5 + kdf_{z3}z3 - kf_{z5}z1z2K_2D_2 - kf_{z2}z2 - d_{z2}z2),\\
\frac{dz3}{dt} &= sf(kf_{z2}z2 + kd_{z4}z4 - kdf_{z3}z3 - kf_{z4}z1z3K_2D_2 - d_{z3}z3),\\
\frac{dz4}{dt} &= sf(kf_{z4}z1z3K_2D_2 + ke_{x2}x2 - ki_{z4}z4 - kd_{z4}z4 - d_{z4}z4),\\
\frac{dz5}{dt} &= sf(kf_{z5}z1z2K_2D_2 + ke_{x3}x3 - ki_{z5}z5 - kd_{z5}z5 - d_{z5}z5),
\end{aligned}
\tag{C.6}
$$

$$
\begin{aligned}
\frac{dx2}{dt} &= sf(ki_{z4}z4 - ke_{x2}x2 - d_{x2}x2),\\
\frac{dx3}{dt} &= sf(ki_{z5}z5 - ke_{x3}x3 - d_{x3}x3),\\
PC &= x2 + x3,\\
\frac{dD_1}{dt} &= K_1x1 - ab\frac{D_1R}{bR + aD_1} - dD_1,\\
\frac{dD_2}{dt} &= dD_1 - eD_2,\\
\frac{dR}{dt} &= eD_2 - qR,\\
A &= \frac{bR}{bR + aD_1},\\
I &= 1 - A = \frac{aD_1}{bR + aD_1}
\end{aligned}
\tag{C.6}
$$

where $x1, x2, x3, x5, x6, x7$ represent the nuclear proteins or complexes CLOCK:BMAL1, $Per2^{P}$:Cry1 (phosphorylated Per2 in complex with Cry1), Per2:Cry1, RevErbα, Ror and BMAL1, respectively; $y1, y2, y3, y4, y5$ represent the clock transcripts *Per2, Cry1, RevErbα, Ror* and *Bmal1*, respectively; $z1, z2, z3, z4, z5, z6, z7, z8$ indicate the cytosolic clock proteins Cry1, Per2, $Per2^{P}$, $Per2^{P}$:Cry1, Per2:Cry1, RevErbα, Ror and BMAL1, respectively; PC represents the inhibitory nuclear Per2/Cry1 pool; and A, I, D_1, D_2, R represent active Prx3 (Prx3-SOH), inactive Prx3 (Prx3-SO_2H), mitochondrial H_2O_2, cytosolic H_2O_2 and mitochondrial Srx, respectively. Application of the design principles of the redox oscillator, namely fast A inactivation followed by a lengthy negative feedback loop that reactivates A, with the parameters from the kinetic redox model (Table 3.1) and from the Relógio oscillator (Table C.1) produced circadian 23.87 h limit cycle oscillations (Figure 4.7).

Bike trip to Werbellinsee

:

Publications and Distinctions

Publications

M. del Olmo, A. Kramer and H. Herzel. "A robust model for circadian redox oscillations". In: *Int J Mol Sci* 20 (2019), 2368.

I. van Soest[1], M. del Olmo[1], C. Schmal and H. Herzel. "Nonlinear phenomena in models of the circadian clock". In: *J. R. Soc. Interface* 17 (2020), 20200556.

C. H. Gabriel, M. del Olmo, A. Zehtabian, S. Reischl, H. van Dijk, B. Koller, A. Grudziecki, B. Maier, H. Ewers, H. Herzel, A. E. Granada and A. Kramer. "Live-cell imaging of circadian clock protein dynamics in CRISPR-generated knock-in cells". In: *Nat Commun* 12 (2021), 3796.

A. M. Finger, S. Jäschke, M. del Olmo, R. Hurwitz, A. E. Granada, H. Herzel and A. Kramer. "Intercellular coupling between peripheral circadian oscillators by TGF-β signaling". In: *Sci Adv* 7 (2021), eabg5174.

Conference Contributions

M. del Olmo and H. Herzel, Circadian redox oscillations, scientific talk at the Lille Chronobiology Symposium, Lille, France, 2017.

M. del Olmo, C. H. Johnson, A. Kramer and H. Herzel, Metabolic compensation in circadian clocks, scientific talk at the International Workshop on Bioinformatics and Systems Biology, Berlin, Germany, 2017.

M. del Olmo, A. Kramer and H. Herzel, Modelling redox circadian oscillations: The importance of switches, poster presentation at the EMBL Symposium: Biological Oscillators, Heidelberg, Germany, 2018.

M. del Olmo, A. Kramer and H. Herzel, Modelling redox circadian oscillations: The importance of switches, poster presentation at the IMB Workshop: Molecular Mechanisms of Circadian Clocks, Mainz, Germany, 2018.

M. del Olmo, A. Kramer and H. Herzel, Mathematical modelling of redox circadian oscillations: The importance of switches, scientific talk and poster presentation at the Timelines for Biology Conference in the Weizmann Institute, Rehovot, Israel, 2018.

M. del Olmo, A. Kramer and H. Herzel, Mathematical modelling of redox circadian oscillations: The importance of switches, poster presentation at the German Clock Club, Lübeck, Germany, 2019.

M. del Olmo, A. Kramer and H. Herzel, A robust model for circadian redox oscillations, poster presentation at the Gordon Research Conference, Casteldefells, Spain, 2019.

M. del Olmo, A. Kramer and H. Herzel, A robust model for circadian redox oscillations, scientific talk at the Summer School "Nonlinear Dynamics in the Life Sciences" in the Fields Institute, Toronto, Canada, 2019.

M. del Olmo, A. Kramer and H. Herzel, Mathematical modelling of the crosstalk between redox oscillations and the canonical circadian clockwork, poster presentation at the Society for Research on Biological Rhythms virtual conference, 2020.

Awards

FEBS Letters Poster Prize, awarded at the Timelines for Biology Conference in the Weizmann Institute, Rehovot, Israel, 2018.

Travel Award from the Fields Institute for the Summer School "Nonlinear Dynamics for the Life Sciences", Toronto, Canada, 2019.

Professional experiences

Organization of the Trainee Day at the European Biological Rhythms Society Conference in Lyon, France, 2019.

Teaching assistant in seminars from the course "Mathematische Modellierung in der quantitativen Biologie" at the Institute for Theoretical Biology, Berlin, Germany, 2019.

Organization of the German Clock Club in Berlin, Germany, 2020.

Supervision of master students, Berlin, Germany, 2018–2021.

Frankfurter Tor and Alexanderplatz

:

Acknowledgments

I would like to express my deepest gratitude to all the people and supporting institutes that made the accomplishment of this thesis possible, including the reviewers.

Above all I am deeply grateful to Prof. Dr Hanspeter Herzel and Prof. Dr. Achim Kramer for their continuous scientific and personal supervision. Their scientific honesty, insightful discussions and incomparable physical and biological intuition have kept me on track, especially in the moments when I felt more lost. They accepted me as their doctoral student and they gave me the opportunity to work on a highly interdisciplinary topic that was the perfect fit for me, combining my three greatest interests: biomedical research, numbers and oscillations (ubiquitous phenomena in music). I wish to thank Hanspeter for his patient and eminent guidance, encouragement, continuous support and advice he has provided throughout the past years (also regarding lakes, books, bike trips...). He has provided me with freedom and careful supervision in the most balanced manner. I am very grateful also to Achim, for giving me the chance to spend some time in the lab and for the careful supervision throughout the last years, especially when presenting papers or when revising manuscripts. I thank both of my supervisors for putting trust in me, pushing me and encouraging me to develop into an independent scientist and become part of the Chronobiology community. It has been a real pleasure to meet them and work with them. If this thesis is in any way readable, it is no double because of their helpful and didactic comments. But, also in this first paragraph, a huge THANK YOU in capital letters goes to my office and running mate, who became my mentor over these last years, Bharath Ananthasubramaniam, for being there to answer any question I had and for saving me from my *SOS moments*.

When your research work involves spending *some* time sitting around in an office, you better have nice office-mates and neighbors that put up with you. That said, I must thank Bharath (again), Anne, Inge, Christoph, Abhi, Nora, and former members for fruitful and not-so-fruitful discussions intertwined with cake and chitchats. I would also like to thank all ITB members for the wonderful meetings and for the relaxed working atmosphere that one always feels when walking around the corridors. A special mention must go to the ITB admins and secretaries, for their support and patience in solving all technical and bureaucratic issues. Also to Grisha, for being my first mentor in what was, at the time, a novel field to me, and that became this dissertation some years after.

In these last (almost) four years, I also got the chance to spend some time in the Kramer lab, working with Prof. Dr. Carl Johnson. A big thank you goes to Carl, for all the fun we had doing experiments together while chit-chatting about chronobiology. His constant good mood was incredibly contagious (one could even hear his laugh from the other side of the corridor!). To all the former and newer people from the Kramer lab, thanks for making going to work so easy every day.

A special thanks goes to the chronorunning team – Bharath, Bert and Anna – who have kept me (despite some struggles) more or less fit over the last years. I also can't forget the chronoladies: Manon, Müge, Anna, Teresa and Inge, without which my thesis-writing would have been much more painful. Thanks for being there with huge smiles every day and for all your moral support over the last months! To Timo, my master's companion, who has been part of my Berlin life since the very first day, thank you for our weekly lunches and for being there whenever I needed.

Many other people have been part of my life in Berlin the last years are still here. I have been lucky enough to find the most amazing family that one could ever imagine. Anna, Irene, Carla, Stefan, Brooke, Alex, Rome, Jonas, Marc, Josie, Borja and Marta – I can't imagine my life in Berlin without you or the humor that you put on everything, including in my science with the *OL model* ☺. Jordi, Mercè, Anni, although they are no longer in Berlin they have been very important cornerstones over the last years. My WG-sisters deserve a special mention. Irene and Aina, thank you for ALWAYS being there, for taking care of me in these last months of absolute stress, for the Rigaer Straße lentils, Jenga, for our living room and balcony evenings, for putting art and critical thinking in my day-to-day life... You have been my biggest support in these last months and I'm sure that writing this thesis would have been completely different without you.

And Anna, el meu miracle berlinès, this thesis is finished despite the *laptop incident*!! Friendship test, overcome! But the biggest thanks in this regard goes to Gianmarco, for finding the thesis compiling error in more than 5 files of code of thousands of lines!! Thank you as well for reading parts of this manuscript and especially for making sure that broncio-Marta was not occupying too much time in my evenings of writing this dissertation ☺. What a lucky summer school!

Para acabar, un cambio sutil al español (a ver si todavía me acuerdo de escribirlo!). Porque mi *Heimat* es y será siempre el sur. Gracias a toda mi gente de Madrid, a los que siguen allí y a los que no. Por la la alegría y la ilusión que transmitís cuando voy a visitaros o vuelvo a casa un tiempo, y por las fuerzas que me dais para volver con las pilas recargadas a Berlín. Por último, gracias a toda mi familia por su apoyo incondicional. En especial a mis tías, primas, primos, y a mis compañeros de peleas, el Payeto y la Bellaneto. Sé que no llamo demasiado, pero desde la distancia estoy siempre con vosotros. A mis padres, Cristina y Alfonso, poco les puedo decir. Mi mayor privilegio es y ha sido teneros siempre cerca. Muchísimas gracias.

Späth Arboretum, Baumschulenweg

Physiological rhythms are central to life. Mammalian behavior and metabolism are organized around the day and night by the regulated action of cell-autonomous clocks that exist throughout our bodies. At the core of this molecular clockwork are multiple coupled feedback loops that generate sustained circadian rhythms in gene expression to ultimately orchestrate mammalian physiology.

In this work we provide evidence for the role of metabolism in regulating the core clock. We present genes involved in energetic and redox pathways which we identified to be essential for the robustness of cellular timekeepers to temperature fluctuations. We developed the first computational model for circadian redox oscillations that contributes to the understanding of how cellular redox balance might adjust circadian rates in response to perturbations and convey timing information to the core molecular oscillator. Moreover, we show that our mathematical model can be coupled with prior published models of the transcriptional clockwork resulting in 1:1 entrainment.

This experimental-theoretical approach exemplifies the need of a dynamic analysis at the system level to understand complex biological processes and provides insights into how basic timekeeping mechanisms are integrated into cellular physiology. Such knowledge might highlight new ways by which functional consequences of circadian timekeeping can be explored in the context of human health and disease.

Logos Verlag Berlin

ISBN 978-3-8325-5406-4